Multiscale and Multiphysics Investigation of the Geotechnical Behaviour of Nano-Cemented Paste Backfill Plug

A thesis submitted in partial fulfilment of the requirements for the Doctorate in Philosophy degree in Civil Engineering

Submitted by

Amirreza Saremi

Under the supervision of

Prof. Mamadou Fall

Department of Civil Engineering

Faculty of Engineering

University of Ottawa

Abstract

Cemented paste backfill (CPB) technology is well-known as an excellent alternative to other, older techniques of mine waste management (e.g., surface slurry tailings dams). This technology tackles the geotechnical and environmental challenges that are associated with the traditional methods of mine waste (tailings) disposal. CPB consists of tailings, binder, water, and extra additives; the latter are used to improve the performance of CPB in various ways, such as improving mechanical or rheological properties. CPB is primarily employed for backfilling mine stopes. The process involves conveying CPB, which is produced in a ground-based mixing facility, to the underground voids, aiming to achieve three main objectives. Firstly, preventing the stopes from failing by providing sufficient mechanical strength ensuring the safety of both personnel and equipment. Secondly, increasing the mine's overall productivity by maximizing the extraction of the most ore bodies from the ground. And last, preventing hazardous elements that are present in the mine tailings from being disposed of on the ground surface which are entangled with detrimental impacts on surrounding environment.

The backfilling of a stope with CPB generally involves the following critical steps/phases. First, a retaining structure, called a barricade, is built at the draw-point base of the stope to hold the fresh CPB in place during curing and early ages. Next, a "plug" of CPB is poured a few meters above the height of the barricade to seal it. Once the CPB plug is sufficiently hardended, the main or residual pour (usually with low binder content) is continuously backfilled into the stope.

To properly fulfill the roles described above in underground mining, the CPB plug must have satisfactory geotechnical properties (e.g., mechanical strength, low pore water pressure, suction development). Furthermore, the rate of development of these geotechnical properties is of paramount importance in mine backfill operations. A faster rate of development (e.g., a faster rate of strength gain, a faster rate of pore water pressure dissipation, a faster rate of suction development) is associated with increased mine productivity, which is obviously linked to significant financial gain. The primary measure to increase the development rate of these geotechnical properties is to increase the portion of binder in CPB mixture. However, due to the

high contribution of binder content on the final cost of backfilling (up to 75%), and also environmental considerations due to carbon footprint of cement (cement production is responsible for about 7% of the global green gas generation), this method would no longer be considered as a sustainable or environmental-friendly approach. Rather than increasing the binder content, which has a substantial environmental impact due to its high cement consumption, there is an alternative approach to enhance the rate at which paste backfill of the plug gains strength. This involves incorporating different additives, such as nanoparticles. However, the geotechnical properties and behaviour of CPB plug with nanoparticles (nano-CPB) are not well understood. Therefore, in this thesis, the geotechnical properties and behavior of nano-CPB were studied experimentally at different scales (small sample and high column). In addition, the geotechnical response of nano-CPB plug subjected to multiphysical hardening conditions close to those encountered in the field was evaluated. To examine the influence of nanoparticles on the geotechnical performance of CPB, different sets of samples were prepared, each varying in nanoparticle type and dosage. This allowed the study of key geotechnical parameters that determine CPB's geotechnical behavior, including compressive strength, negative pore water pressure, and physical properties such as void ratio, porosity, and dry density. A detailed monitoring program was also implemented to investigate the evolution of these parameters and explain the geotechnical behavior of CPB containing nanoparticles. This program included monitoring of suction, electrical conductivity, and volumetric water content, along with various microstructural analyses such as thermogravimetric analysis, X-Ray diffraction, and mercury intrusion porosimetry.

The results of the initial phase of this study indicated that if nanoparticles were properly dispersed, their inclusion could enhance the geotechnical performance of CPB. The observation was that nanoparticle addition, with a dispersing agent, could enhance CPB's mechanical properties through different mechanisms such as accelerating binder hydration and the filler effect of nanoparticles. This was consistent with monitoring and microstructural analysis results, which showed that nanoparticle addition improved properties such as increased negative pore water pressure development, higher generation of hydration products, and microstructural refinement.

A pioneering aspect of this study was the formulation of a high-rise framework to simulate the curing process of a CPB column under field adapted loading condiiton. This area of inquiry had been largely uncharted in preceding studies, thereby leaving an evident knowledge deficit concerning CPB behavior under multiscale and multiphysics simulation. Utilizing this novel framework, it was recognized that the inclusion of nanoparticles in a CPB column, subjected to simulated overburden loadings, augmented various aspects of CPB's mechanical performance. A key observation was the expedited dissipation of pore water pressure at the bottom of the nanoparticle-augmented CPB column compared to the control column. Pertaining to the effect of curing stress, it was determined that CPB samples subjected to elevated levels of curing stress exhibited an increase in compressive strength. This was ascribed to several factors, notably microstructure refinement due to the effect of curing stress on void ratio, coupled with its impact on increasing the hydration reaction. This culmination led to an increase in quantity of hydration products in samples that were subjected to elevated levels of curing stress. Nonetheless, the most profound impact of curing stress was observed at the early stages of CPB, when it embodies more fluid characteristics, with the effect diminishing as the transition from a fluid to a solid state emerges within the CPB column. These findings are significantly important for optimizing the costs of backfilling while maintaining the essential geotechnical properties that guarantee the safety and stability of the backfill structures.

In the subsequent phase of this study, we extended our analysis to include additional field curing conditions, specifically non-isothermal curing temperatures, which have a profound impact on the geotechnical performance of nano modified CPB. This dissertation elucidates the comprehensive effects of field-adapted mechanical loading and non-isothermal curing temperatures on nano-CPB characteristics. Key performance indicators such as evolution of strength gain, pore water pressure, total and effective stress, and physical properties including void ratio and dry density were thoroughly examined. Findings from this study underscore the critical role of elevated field curing temperatures in enhancing CPB behavior, notably by accelerating binder hydration, which in turn significantly increases the rate of strength development, promotes pore pressure dissipation, and leads to microstructural refinement by producing more hydration products that are mainly responsible for filling the voids and provide

bonding for solid particles within CPB matrix. Moreover, it was observed that CPB columns subjected to field-adapted curing stress in conjunction with non-isothermal curing temperatures outperformed all other columns subjected to alternative curing conditions, demonstrating superior strength and stress development characteristics.

Dedication

To my beloved wife, family and friends.

Acknowledgement

First and foremost, I express my profound gratitude and reverence to Almighty God, Alhamdulillah, for endowing me with the opportunity to pursue my academic goals and for the countless blessings in my life.

This doctoral study stands on the pillars of support and contributions from numerous individuals to whom I owe my sincere appreciation and acknowledgment. I am particularly indebted to Professor Mamadou Fall, whose mentorship has been the guiding light of my Ph.D. journey. His unwavering support, insightful feedback, and enduring patience have been paramount during the course of my research and in the meticulous crafting of this thesis. His instruction has been nothing short of inspirational, and his compassion will forever be etched in my memory.

I extend my heartfelt recognition to Mr. Jean-Claude Célestin, Dr. Muslim Majeed, and Dr. Gamal Elnabelsya, whose technical expertise and sage advice have been instrumental throughout my research endeavors. Their readiness to assist has significantly contributed to the fruition of this work.

In addition, I seize this moment to convey my deepest gratitude to my colleagues and companions whose companionship, unwavering support, and assistance have been the backbone of my academic and personal journey. Among them, Mr. Amirmohammad Sabziparvar, Mr. Ali Sadeghi Jahromi, Dr. Sada Haruna, Ms. Zubaida Al-Moselly, Dr. Imad Alainachi, Mr. Mohammad Shaheen, Mr. Carlos Rosas Cabello, Mr. Abdurrahman Mohammed, and Mr. Tony Zandbelt, have been steadfast in their encouragement and assistance.

Lastly, but most importantly, my profound appreciation goes to my family—my wife, my parents, and my brother. Their unconditional love and encouragement have been the sanctuary that has empowered me to navigate and complete this scholarly voyage. The realization of this academic achievement would have been unattainable without their enduring love and belief in my aspirations.

Table of Contents

List of Figures

List of Tables

CHAPTER 1. Introduction

1.1. Background and problem statement

The mining industry holds significant financial importance for both developed and developing countries, as it plays a crucial role in driving economic indicators like GDP and employment markets. Additionally, mining provides essential resources for numerous related sub-industries. As a result, the industry's impact on the economy is substantial, contributing to the growth and development of nations. Thus, in recent decades high demands of the markets resulted in boosting the productivity of mining activities dramatically. As an illustration, mineral extraction in Canada reached a record high of $55.5 billion in 2021, which is a 20% rise from the previous year and represents a record-breaking gain (“Natural Resources Canada” 2022).

On the other hand, much like any other technical activity, mining operations encounter numerous challenges and concerns. These challenges and concerns may be broken down into two primary categories, the first of which is geotechnical considerations, and the second is environmental concerns. Mining operations in underground mines are mainly entangled with extracting ore bodies and bringing them to the ground to derive the valuable materials with different processing methods. However, main consequences of ore bodies extraction are creating massive voids in underground which increases probability of adjacent walls failure, or land subsidence, as well as producing vast amount of mine waste (tailings) (Fang and Fall 2019, 2020). Each of these hazards could result in financial loss and casualties.

Another challenge with mining activities is huge amount of mine waste produced in this type of engineering works. Many studies suggest that this huge amount of mine waste could be considered as a high potential source of environmental pollutant in case of being exposed to the surrounding environment (Ma et al. 2002, Belem et al. 2006; de Andrade Lima et al. 2008, Rico et al. 2008, Aldhafeeri and Fall, 2017; Yilmaz and Fall 2017).

Taking into account the aforementioned challenges associated with mining activities highlights the significance of a safe and environmentally sustainable technique for the disposal of the mine waste. In response to these challenges, Cemented Paste Backfill (CPB) has been developed as an

innovative approach for the underground disposal of the mine waste by utilizing the waste produced in the extraction process and returning them into the voids created underground which significantly reduces the amount of waste needed to be disposed on the surface (environmental concerns). Moreover, as the mining process penetrates further into the earth, it must be noted that backfills are mostly utilized to reinforce underground mines. Backfilling during mining guarantees that exposed pillars are adequately supported so that excavation may continue without considerable danger of collapse (Fall and Benzaazoua 2003, Belem and Benzaazoua 2008b; Cui and Fall, 2016, 2017, 2018). Furthermore, from a financial standpoint, it can assist to reduce mining cycles, hence increasing the mine's total production rate (Fall and Benzaazoua 2003, Yilmaz and Fall 2017). In this technique, tailings are blended with water and hydraulic binders such as cement, fly ash, and blast furnace slag, as well as various additives, the latter of which are primarily utilised to improve the CPB's performance such as geotechnical properties (e.g., strength gaining rate, rate of the pore water pressure dissipation, and suction increase rate) or flow ability of the paste backfill.

Due to its crucial role in ensuring the safety of personnel and equipment and maximising the mine's productivity, the rate of the development of the geotechnical properties is of utmost importance. In order to ensure the stability of the fresh CPB in the stope, it is necessary to construct a retaining wall or barrier (called barricade) made of materials such as bricks, waste rock, shotcrete, or concrete (in the draw-point at the base of the stope to hold the fresh CPB in place during curing and at early ages Figure 1-1).

Subsequently, a "plug" of CPB (CPB plug) is poured a few meters above the barricade to seal it. Once the plug has attained sufficient resistance or suitable geotechnical properties, the main pour (residual pour, Figure 1-1), typically consisting of a low binder content, is continuously backfilled into the stope. The CPB plug needs to acquire adequate strength and appropriate geotechnical properties to protect the barricade from the potential effects of the subsequent "main" pour throughout the remaining volume of the stope. Additionally, mining operations in nearby backfilled stopes should be temporarily suspended until the poured CPB plug attains the required geotechnical properties (e.g., strength, low pressure) for stability.

Once the backfill structure is deemed stable, the temporary barrier can be dismantled. It is crucial to avoid any backfill plug failure (e.g., due insufficient geotechnical performance) or barricade failure (i.e. due to CPB plug liquefaction), as it could lead to casualties and financial losses. Furthermore, minimizing stoppage time is of utmost importance to enhance mining profitability.

Increasing the dosage of binder in the CPB mix is the easiest approach to enhancing the geotechnical properties of the CPB plug and increasing the development rate of these properties, but at the expense of a large rise in carbon footprint and the ultimate cost of backfilling. Indeed, cement production is responsible for about 7% of the global green gas generation (GHG) and mine backfilling consumes a considerable amount of cement yearly. Moreover, according to Yilmaz and Fall (2017), up to 75% of the total cost of backfilling is attributable to the binder consumption. As a result, any increase in the amount of binder used will lead to a significant increase in costs, making this approach less attractive. Several mines opt for a lengthy curing period after the plug is poured, sometimes lasting several days, before proceeding with pouring the remaining fill (residual fill). However, this method substantially prolongs the mining cycles, consequently reducing the mine's overall productivity. Another method to enhance the characteristics of the plug-CPB is by employing additives that aid in the cement hydration process. In recent years, nanoparticles (NPs) have emerged as an effective supplementary additive for enhancing the performance of cementitious materials, such as concrete. However, there is a lack of comprehensive studies investigating the impact of these NP additives on the geotechnical properties and behavior of CPB and CPB plug.

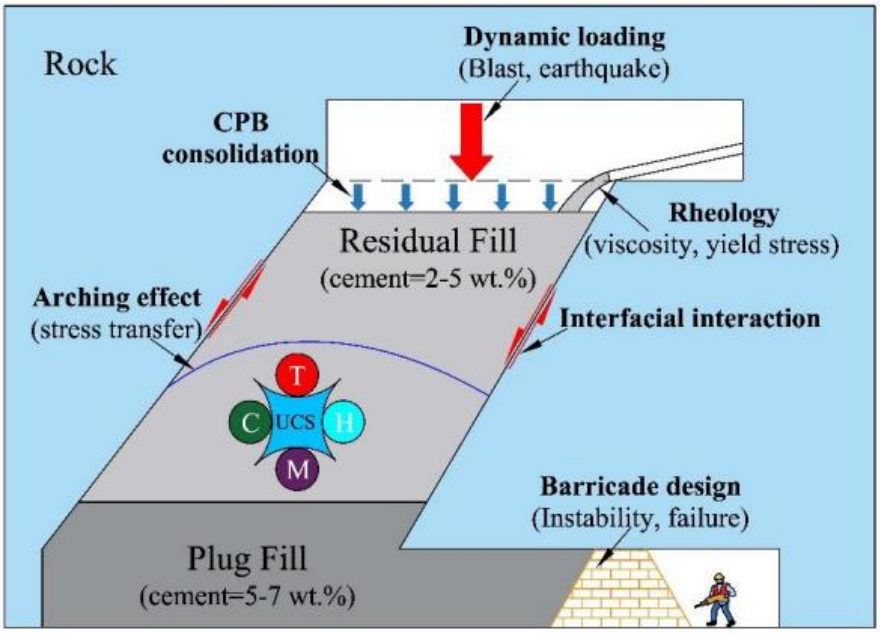

Figure 1-1. Plug and residual fill of a CPB structure (Fang 2021)

Almost all studies on the geotechnical properties of cemented paste backfill (CPB) have primarily focused on CPB without nanoparticles (NPs) (e.g., Roux et al. 2005a, Ercikdi et al. 2010, Ghirian and Fall 2013b, Wang et al. 2016, Xiu et al. 2022). Only a limited number of studies have investigated the impact of NPs on CPB. For instance, Koohestani et al. (2016) examined the effect of varying dosages of Nano-Silica on the mechanical strength of CPB. Additionally, there have been other studies that specifically examined the influence of Nano-Silica on the rheological characteristics of CPB (Roshani and Fall 2020a, 2020b). Nevertheless, a comprehensive investigation of the impact of different types of NPs on the short-term and long-term geotechnical behavior of cemented paste backfill is yet to be conducted. This includes studying factors such as strength gaining rate, suction development, pore water pressure development and pore structure development. This knowledge gap needs to be addressed to support the development of nano-CPB technology.

Furthermore, all previous studies on the use of nanoparticles in CPB have primarily focused on small laboratory samples, typically in cylindrical molds with a maximum height of 20 cm. Unfortunately, these studies overlooked the height of CPB plug in actual field conditions and the corresponding high overburden stress. Consequently, the results obtained from these small samples do not accurately reflect the behavior of nano-CPB plug in real-field scenarios. In

practice, nano-CPB plugs in the field are significantly larger and taller (up to several meters tall), and therefore experience substantial overburden pressure and stress. These external forces have a profound impact on the geotechnical response of nano-CPB plug. Surprisingly, despite the importance of understanding the field overburden loading conditions and their effects on the geotechnical properties and behavior of nano-CPB plug, there has been a lack of physical modeling using tall columns to simulate these conditions. Therefore, it is crucial to conduct a comprehensive study that thoroughly examines the impact of nanoparticles on the geotechnical properties and behaviour of CPB plug when subjected to field-simulated overburden pressure loading conditions. Additionally, in the field, CPB plug structures may be exposed to high temperatures during the curing process, primarily due to the heat generated by the hydration of the binder. The reaction between cement or binder and water releases a considerable amount of heat, which poses a challenge for large-scale CPB plug structures that can span several meters in height and width (Nasir and Fall 2009, Fall and Pokharel 2010a). As a result, the generated heat cannot dissipate rapidly, leading to significant temperature increases (which can vary depending on the type and quantity of binder used). However, no studies have specifically investigated the impact of field temperature (T) on the geotechnical properties of nano-CPB plug. Moreover, it's important to note that this field temperature (T) does not act in isolation; it is closely linked to other Multiphysics processes (such as **C**, binder hydration, mechanical processes, **M**, like stress, and hydraulic processes, **H**, like pore pressure) that collectively influence the geotechnical properties of CPB. However, no research has been conducted thus far to assess the effects of these Multiphysics processes on the geotechnical behavior of nano-CPB. Further investigation is necessary to understand the implications of field temperature (T) and its interactions with Multiphysics processes on the geotechnical properties of nano-CPB.

1.2. Objectives

This doctoral research project aims to conduct a comprehensive investigation into the geotechnical response of nano-CPB at various physical scales, while considering the field Multiphysics processes. The primary objectives of this PhD thesis are outlined below:

- Experimental investigation: The first objective is to experimentally study the effects of different types and quantities of nanoparticles on the time-dependent development of key geotechnical properties of CPB, including strength, suction development, and pore structure. This investigation will help identify the type of nanoparticle that provides the best geotechnical performance for CPB.
- Development of a fully instrumented high column nano-CPB: The second objective involves the development of a fully instrumented high column specifically designed for nano-CPB plug. This setup will enable the investigation of the geotechnical response of nano-CPB plug under curing conditions that closely mimic field conditions.
- Assessment of geotechnical response under simulated field overburden pressure: The third objective aims to assess the geotechnical response of nano-CPB plug cured under simulated field overburden pressure. This will be achieved through high-column experiments, which will provide valuable insights into the behavior and performance of nano-CPB plug in realistic field overburden conditions.
- Assessment of geotechnical response under simulated field Multiphysics processes: This objective involves evaluating the geotechnical response of nano-CPB plug under simulated field Multiphysics processes. By conducting high-column experiments, this research will investigate how nano-CPB plug performs and responds to various multiphysical processes encountered in real-world scenarios.

These objectives collectively contribute to advancing our understanding of the geotechnical behavior of nano-CPB plug, providing valuable insights for its application in practical engineering backfilling.

1.3. Research approach and methods

To meet the primary objectives of this study, a comprehensive experimental investigation has been established. Figure 1-2 depicts the detailed structure of the experimental program, which includes the following parts.

- The **first part of the research** includes the definition of the problem statement and research objectives, a thorough examination of the theoretical background and a comprehensive review of pertinent literature. These preliminary steps played a crucial role in determining the most efficient testing procedure and monitoring approaches for tracking the development of geotechnical properties in the CPB mixture as it undergoes curing under different conditions.
- The **second phase of the research** aims to examine the effects of various types of nanoparticles on the geotechnical properties of conventional small laboratory cylinders (10 cm in height) containing CPB. Specifically, we focus on parameters such as strength, pore pressure (negative pore pressure or suction), and pore structure. To ensure accurate experimental results and eliminate the influence of reactive components found in natural tailings, which could introduce uncertainties, we employed Silica tailings, also known as synthetic tailings, to create the CPB mixtures. As the most commonly used binder in mine backfill processes, we utilized Ordinary Portland Cement (OPC) type I as the primary binding agent. In order to achieve proper dispersion of the nano-particles (NPs) within the mixture and prevent their agglomeration, which hinders their contribution to the hydration process, we incorporated a polycarboxylic-ether-based superplasticizer (SP) as a dispersing agent. This SP facilitated the dispersion of the NPs. Four different types of NPs were employed to investigate their impact on the geotechnical performance of CPB. These types include Nano-SiO_2, Nano-$CaCO_3$, Nano-Fe_2O_3, and Nano-Al_2O_3. Uniaxial compressive tests (UCS) are carried out to ascertain the strength of the nano-CPBs, while suction monitoring experiments are performed to assess suction variations over time. Microstructural analyses and tests are conducted on the nano-CPB, encompassing thermal analyses such as thermogravimetry (TG) and differential thermogravimetry (DTG), as well as mercury intrusion porosimetry (MIP) and X-ray diffraction (XRD). The

results obtained in this phase make it possible to determine the type of nanoparticle that provides the CPB with the best geotechnical performance. The type of nanoparticle identified is used to prepare the nano-CPB for larger-scale testing (column experiments).

- **The third phase** consists of studying the geotechnical response of the nano-CPB plug to overburden pressure in the field, using appropriate column experiments. To achieve this objective, a fully instrumented physical model of nano-CPB plug is developed. The model enables the nano-CPB plug to be subjected to the weight of the CPB (self weight) structure in the field and to the field overburden pressure increase rate, and to monitor changes in a number of parameters, such as pore pressure, stress and progress of cement hydration. Furthermore, the effectiveness of plug CPB containing nanoparticles (NPs) is assessed by creating several sets of CPB columns, both with and without NPs, and examining their performance through monitoring experiments, mechanical and microstructural tests on samples extracted from the nano-CPB columns.
- The **fourth phase** of the study focuses on investigating the geotechnical behavior of the nano-CPB plug under various combined loadings. These loadings include the temperature during field curing (**T**), which accounts for the heat generated by the hydration of the binder. Additionally, the field overburden pressure and its rate of increase (mechanical factor, **M**) are considered, along with the chemical reactions induced by cement hydration and/or nanoparticles (chemical processes, **C** factor). To achieve the objective, the physical model developed in the previous phase is enhanced by incorporating a heating system. This system allows for the simulation and application of the field's curing temperature to the CPB plug. By subjecting the nano-CPB plug to these TMC (thermal, mechanical, chemical) conditions, the behavior of the plug is evaluated. Several sets of CPB columns are created, some with nanoparticles (NPs) and others without, to assess the impact of these conditions on the performance of the plug. Performance evaluation is conducted through monitoring experiments, as well as mechanical and microstructural tests performed on samples extracted from the nano-CPB columns.

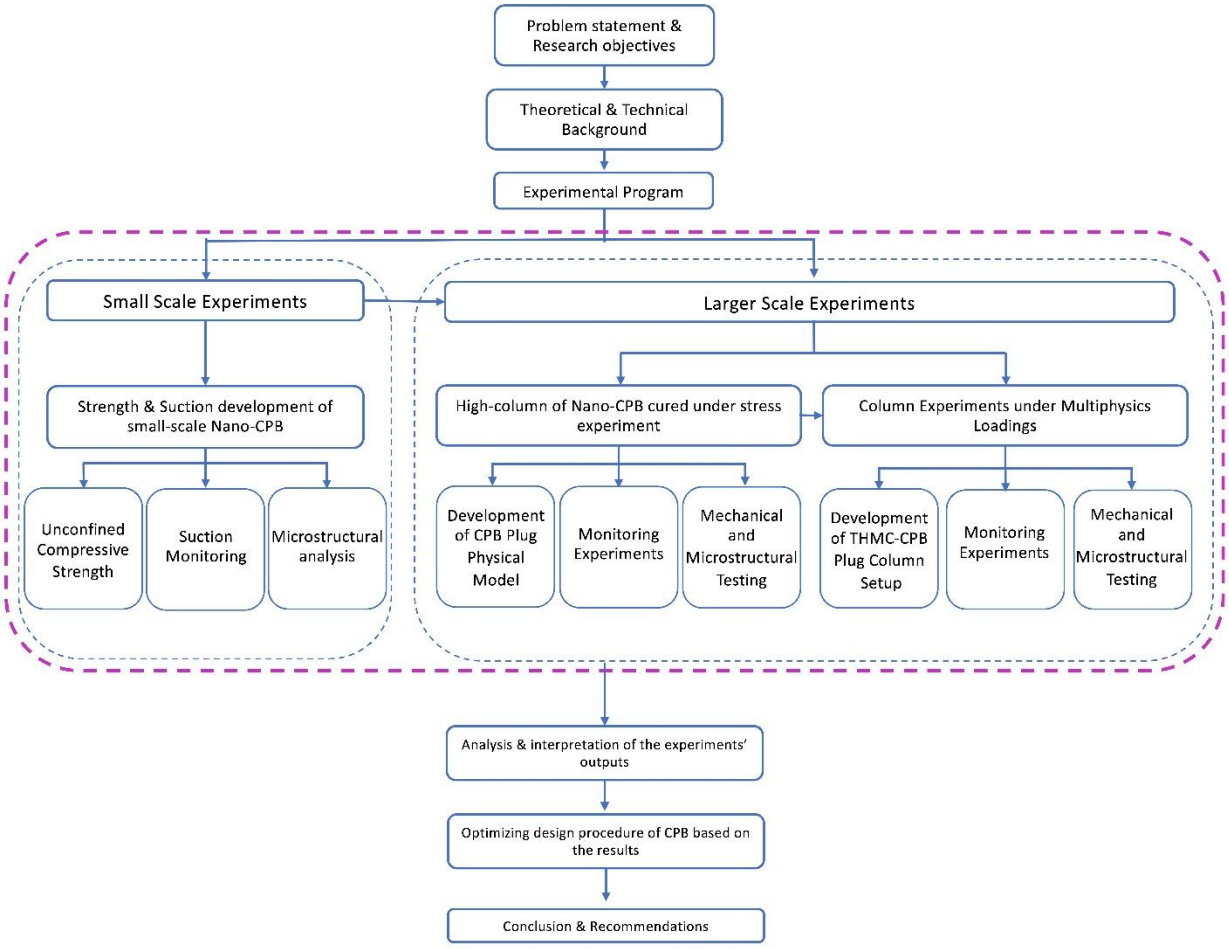

Figure 1-2. Study approach

1.4. Organization of the thesis

As seen in Figure 1-3 Thesis tasks organization, this doctoral dissertation will consist of six chapters.

The **first chapter** gives an introduction of the study by outlining the problem statement, research objectives and aims, methodology, and research approach.

In **chapter two**, a comprehensive theoretical and technical background on the principle of backfilling is covered, with an emphasis on CPB technology. This chapter describes the most important geotechnical features of CPB and the factors that influence them. In addition, this chapter provides background information on cement hydration as well as on the main Multiphysics (THMC) processes occurring in the CPB structure. The information given in this chapter is essential for a better understanding and use of the results presented in this thesis.

In chapter three, background information on nanoparticles is presented and discussed. Moreover, previous research on the application of Nanoparticles in cementitious materials, including CPB, is reviewed in this chapter to further illustrate the lack of knowledge associated with the application of these nanoparticles in CPB.

Chapter four contains the four technical papers (Technical Papers 1, 2, 3 and 4) of this doctoral research. Each paper has its own introduction, materials and methods section, findings and conclusions. The topic of each technical paper is described in Figure 1.3. Due to the fact that each paper is written individually regardless of the content of other technical papers, it should be noted that certain information is repeated in the papers and that the formatting of the papers is consistent with the publication's peer-reviewed journal.

The **fifth chapter** of this dissertation synthesises and discusses the entire results collected in compliance with the primary goals of the research.

In the **last chapter (chapter 6)**, a conclusion and suggestions for optimising the backfilling process with CPB, as well as recommendations for future studies are presented.

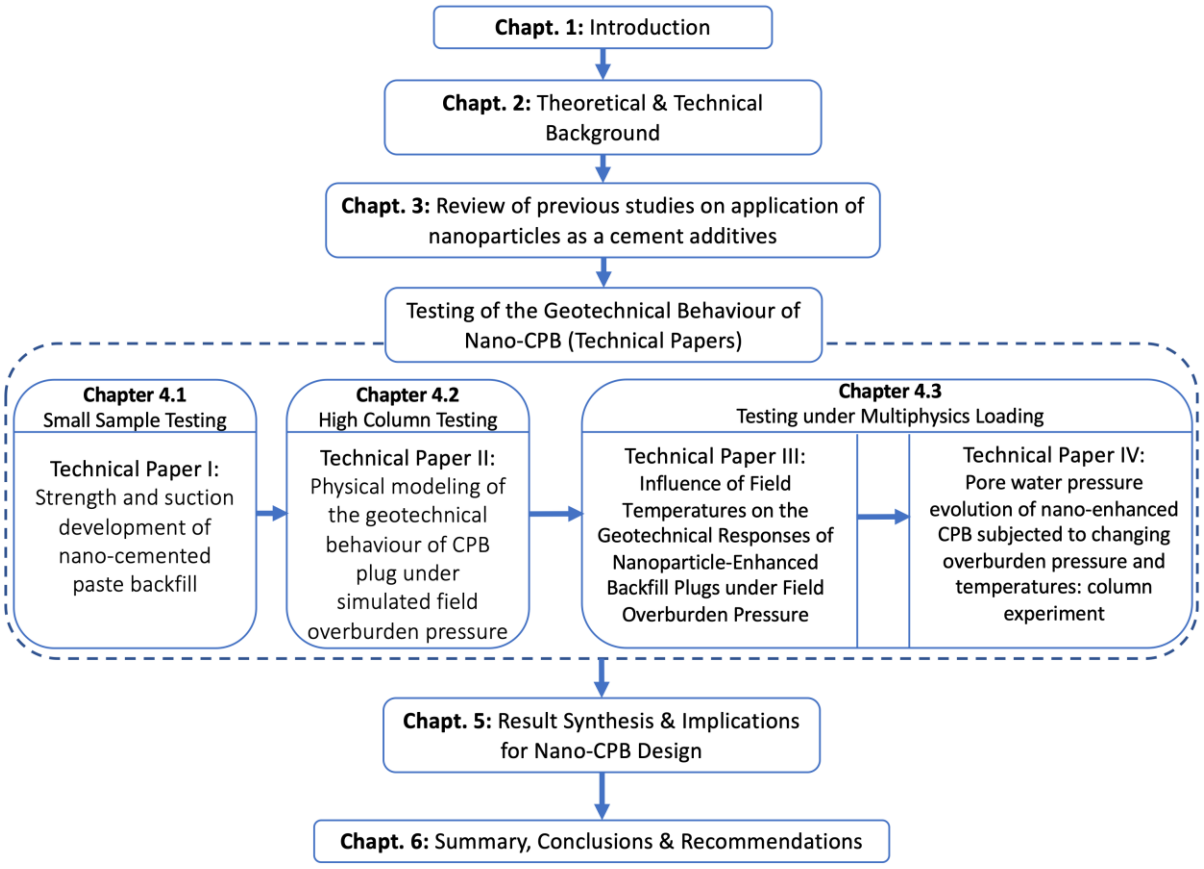

Figure 1-3 Thesis tasks organization

1.5. References

Aldhafeeri, A., and Fall, M. 2017. Sulphate induced changes in the reactivity of cemented tailings backfill. International Journal of Mineral Processing 166 (10):13-23.

de Andrade Lima, L.R.P., Bernardez, L.A., and Barbosa, L.A.D. 2008. Characterization and treatment of artisanal gold mine tailings. Journal of Hazardous Materials, 150(3): 747–753. Elsevier. doi:10.1016/J.JHAZMAT.2007.05.028.

Belem, T., and Benzaazoua, M. 2008. Design and Application of Underground Mine Paste Backfill Technology. Geotechnical and Geological Engineering, 26(2): 147–174. doi:10.1007/s10706-007-9154-3.

Belem, T., Aatar, O. El., Bussière, B., Benzaazoua, M., Fall, M., and Yilmaz, E. 2006. Self-weight consolidation of column of cemented pastefill. 7th Seminar on paste and thickened tailings, April 2006, Irlande, 13p.

Cui, L, and Fall M. 2018. Multiphysics modeling and simulation of strength development and distribution in cemented tailings backfill structures. International Journal of Concrete Structures and Materials, 12 (1): 1-22.

Cui, L, and Fall M. 2017. Modeling of pressure on retaining structures for fill mass. Tunnelling and Underground Space Technology 69:94-107.

Cui, L., and Fall, M. 2016. Multiphysics model for consolidation behaviour of cemented paste backfill. ACSE International Journal of Geomechanics 17(3): 23p; 04016077-23.

Ercikdi, B., Cihangir, F., Kesimal, A., Deveci, H., and Alp, Ì. 2010. Effect of natural pozzolans as mineral admixture on the performance of cemented-paste backfill of sulphide-rich tailings. Waste Management & Research, 28: 430–435. doi:10.1177/0734242X09351905.

Fall, M., Célestin, J.C., Pokharel, M., Touré, M. 2010. A contribution to understanding the effects of temperature on the mechanical properties of cemented mine backfill. Engineering Geology 14 (3-4): 397-413.

Fall, M., and Benzaazoua, M. 2003. Advances in predicting performance properties and cost of paste backfill. Tailings and Mine Waste,: 73–85.

Fall, M., and Pokharel, M. 2010. Coupled effects of sulphate and temperature on the strength development of cemented tailings backfills: Portland cement-paste backfill. Cement and Concrete Composites, 32(10): 819–828. Elsevier. doi:10.1016/J.CEMCONCOMP.2010.08.002.

Fang, K. 2021. Testing and multiphysics modelling of the shear behaviour of rock-cemented paste backfill interface. Université d'Ottawa/University of Ottawa.

Fang K., and Fall M. 2020. Shear behavior of the interface between rock and cemented backfill: effect of curing stress, drainage condition and backfilling rate. Rock Mechanics and Rock Engineering 53: 325–336.

Fang, K., and Fall, M. 2019. Chemically induced changes in shear behaviour of interface between rock and tailings backfill undergoing cementation. Rock Mechanics and Rock Engineering 2 (9), 3047-3062.

Ghirian, A., and Fall, M. 2013. Coupled thermo-hydro-mechanical–chemical behaviour of cemented paste backfill in column experiments. Part I: Physical, hydraulic and thermal processes and characteristics. Engineering Geology, 164: 195–207. Elsevier. doi:10.1016/J.ENGGEO.2013.01.015.

Koohestani, B., Belem, T., Koubaa, A., and Bussière, B. 2016. Experimental investigation into the compressive strength development of cemented paste backfill containing Nano-silica. Cement and Concrete Composites, 72: 180–189. Elsevier. doi:10.1016/J.CEMCONCOMP.2016.06.016.

Ma, Y., Dickinson, N.M., and Wong, M.H. 2002. Toxicity of Pb/Zn mine tailings to the earthworm Pheretima and the effects of burrowing on metal availability. Biology and Fertility of Soils, 36(1): 79–86. Springer. doi:10.1007/S00374-002-0506-0/METRICS.

Nasir, O., and Fall, M. 2009. Modeling the heat development in hydrating CPB structures. Computers and Geotechnics, 36(7): 1207–1218. Elsevier. doi:10.1016/J.COMPGEO.2009.05.008.

Natural Resources Canada. 2022. Available from https://www.nrcan.gc.ca/science-data/science-research/earth-sciences/earth-sciences-resources/earth-sciences-federal-programs/canadian-mineral-production/17722. [accessed 21 November 2022].

Programme, U.N.E. 1996. A Guide to Tailings Dams and Impoundments: Design, Construction, Use and Rehabilitation.

Rico, M., Benito, G., Salgueiro, A.R., Díez-Herrero, A., and Pereira, H.G. 2008. Reported tailings dam failures: A review of the European incidents in the worldwide context. Journal of Hazardous Materials, 152(2): 846–852. Elsevier. doi:10.1016/J.JHAZMAT.2007.07.050.

Roshani, A., and Fall, M. 2020a. Flow ability of cemented pastefill material that contains nano-silica particles. Powder Technology, 373: 289–300. doi:https://doi.org/10.1016/j.powtec.2020.06.050.

Roshani, A., and Fall, M. 2020b. Rheological properties of cemented paste backfill with nano-silica: Link to curing temperature. Cement and Concrete Composites, 114. Elsevier Ltd. doi:10.1016/J.CEMCONCOMP.2020.103785.

Roux, K. le, Bawden, W., Technology, M.G.-M., and 2005, undefined. 2005. Field properties of cemented paste backfill at the Golden Giant mine. Taylor & Francis, 114(2): 65. doi:10.1179/037178405X44557.

Wang, Y., Fall, M., and Wu, A. 2016. Initial temperature-dependence of strength development and self-desiccation in cemented paste backfill that contains sodium silicate. Cement and Concrete Composites, 67: 101–110. Elsevier. doi:10.1016/J.CEMCONCOMP.2016.01.005.

Xiu, Z., Wang, S., Ji, Y., Wang, F., and Ren, F. 2022. Experimental study on the triaxial mechanical behaviors of the Cemented Paste Backfill: Effect of curing time, drainage conditions and curing temperature. Journal of Environmental Management, 301: 113828. Academic Press. doi:10.1016/J.JENVMAN.2021.113828.

Yilmaz, E., and Fall, M. 2017. Paste tailings management. In Paste Tailings Management.

CHAPTER 2. Theorical and Technical Background

2.1. Introduction

In this chapter, the concept of backfilling and THMC (Multiphysics) processes in CPB are discussed, providing both technical and theoretical information on the subject. It's anticipated that this information will facilitate a deeper understanding of how backfilling can address issues commonly associated with traditional mine waste management methods. Following the initial discussion on the fundamental principles of backfilling, the subsequent section will offer detailed insights into the evolution of various backfilling methods, their advantages and disadvantages, and their impacts on mine waste management. The third section will present a thorough review of the different properties of Cemented Paste Backfill (CPB), a common type of backfill material used in mining operations. This will encompass a range of properties including thermal, hydraulic, mechanical, and chemical characteristics, as well as factors that can influence these properties. Furthermore, the THMC processes that occur in CPB mass will be presented and discussed. The chapter will then progress to an exploration of binder reaction, an integral process in the formation of CPB. An in-depth understanding of binder reaction is crucial as it profoundly influences the geotechnical behavior of CPB. Furthermore, the various factors that can potentially impact the hydration process, a key phase of binder reaction, will be discussed.

2.2. Backfill technology

Mining activities are entangled with the production of vast quantities of mine waste, which, given the potential dangers these wastes pose to humans and the environment, demonstrates the necessity of developing an alternative method for the conventional surface disposal approach. Surface disposal of mine waste increases the probability of environmental contamination by exposing toxic substances such as heavy metals to the surrounding environment. In addition, this waste may react with air or water to form acidic compounds, a phenomenon known as acid mine drainage (AMD) (Fall et al. 2010). CPB is a solution to these concerns, as well as the geotechnical considerations associated with the enormous openings left

by the extraction operation. This technique was initially implemented at the Bad Grund mine in Germany in the 1970s, after which it empoloyed in North America. This technology allows the industry to reuse the majority or a large quantity of the waste (tailings) generated by mining activities by transforming the tailing into CPB and then returning it to the created underground voids due to extraction process. This serves to provide mechanical support for the surrounding environment of the voids, which minimises the potential of mine roof failure by a large margin (Wu et al. 2012, 2014). Another beneficial impact of CPB is boosting the mine productivity by reducing the mining cycle (Belem et al. n.d., Abdul-Hussain and Fall 2012, Ghirian and Fall 2013a, Cui and Fall 2016a, Yilmaz and Fall 2017, Fang and Fall 2019, Haruna and Fall 2020b, Roshani and Fall 2020b).

2.2.1 Types of backfilling

There are three primary classifications for mine backfill: rock backfill, hydraulic backfill, and paste backfill. Type of mine, geometry of stopes, depth of mines, resource availability, and the cost of backfilling, which is one of the most significant considerations, all influence the selection of an appropriate backfill method (Landriault 1995, 2001).

2.2.1.1. Rock Fill

One of the first steps made to repurpose mine waste as filling material for subterranean cavities was the deployment of rock fill. This material consists primarily of waste rock generated during the extraction process and is mostly constrained by material availability. It may also be combined with tailings to achieve a more consistent grading (Ghirian 2016a). This method is considered as one of the most economical backfilling methods as there is no binder agent and at the same time the amount of waste which were disposed on the surface would be reduced. Consequently, the land used to retain the waste can be used for other purposes (Belem and Benzaazoua 2008a, Haruna 2022). However, Rock fill can be utilized either as cemented (CRF) or uncemented (URF) material, with a conventional dosage of 6% cement intended to provide the strength of the rock fill (Jian et al. 2019). The strength requirement for this application spans between 0.2 and 4.0 MPa, and its determination is contingent on parameters such as stope

dimensions, the mining methodology employed, and the duration needed for stope recovery (Hassani and Archibald 1998, Sheshpari 2015, Ghirian 2016a). The ability to regulate segregation and maintain satisfactory quality control presents a formidable challenge (Hassani, and Archibald 1998, Belem and Benzaazoua 2008a, Yilmaz and Fall 2017). Various elements, including grain size distribution, binder concentration, the geological variety of the rock, the method of placement, segregation, and the ratio of water to cement, govern the strength of the Cemented Rock Fill (CRF) (Henderson 1998, Belem and Benzaazoua 2004, Chen and Brouwers 2010a; Jian et al. 2019). Additional complexities, such as rock comminution, transportation, and the necessity for the utilization of fine materials as filler in rock backfilling, contribute to the financial burden of this approach (Landriault 1995, 2001).

2.2.1.2. Hydraulic Backfill

Hydraulic backfill constitutes a prevalent technology employed in refilling operations, where water serves as the medium for transporting materials including crushed sand, mountain sand, river sand, hydrophilic slag, and waste tailings to replenish the voids generated underground such as in stopes (Hassani and Archibald 1998, Cooke 2001). Frequently referred to as slurry backfill, this highly permeable material is characterized by a low solid density and typically comprises tailings, sand and/or rock materials amalgamated with a minor percentage of cement and water. The preparation of hydraulic backfill can be executed either on the surface or subterraneously, with subsequent transportation facilitated via borehole or pipeline distribution systems, driven by the hydraulic head generated by gravity. To expedite the elimination of surplus water, perforated drainage pipes are strategically installed within mine stopes. This particular approach employs bulkheads as a means of sealing mines, wherein a drainage system is incorporated to allow for the egress of water from the backfill within the stope. With the ascending elevation of the hydraulic fill material, there ensues an accumulation of free water on the backfill surface. This method accommodates the use of either uncemented or cemented backfill, with the non-cemented variant proving more cost-effective when waste particles are of particularly diminutive size. The primary merits of this backfilling technique lie in the simplicity of its installation and operation, the ease of supervision, the convenience of quality control, the availability of solid

components as mine waste, and the reduction in surface waste disposal (Hassani, F., and Archibald, J., 1998; Sheshpari, 2015).

2.2.1.3. Cemented Paste Backfill (CPB)

Characterized by uniformity and low permeability, Cemented Paste Backfill (CPB), also known as paste backfill, is a non-homogeneous material prepared by combining cement, water, and waste tailings, with a waste-to-solid ratio typically ranging between 70% and 85%. This engineering material has a solid density, generally between 75% and 85% by weight, compared to other backfill types. The solid components are typically milled tailings, with the binding agent and water added at a CPB plant located either at the mine's surface or underground. The fresh CPB is then transported to the underground stope via pipelines. Notably, paste backfill particles maintain their unity in static conditions, not separating into water and tailings due to the retaining effect of colloidal electrical charges. As such, the backfill preparation necessitates that at least 15% of the particles be finer than 20 microns (Grice 1998, Landriault 2001; Orejarena and Fall 2008; Roshani and Fall 2020).

CPB is optimally developed to be used in the mines where long hole open stopes are available, along with other methodologies that necessitate the use of structural fill. The design parameters of CPB structures are predominantly contingent upon factors such as durability, environmental performance, stability of barricades, and mechanical performance. In the context of CPB, there are several factors that can contribute to variations in temperature. These factors encompass friction produced between transfer pipes during the conveyance of materials, the geographical location of the mines which influences the ambient temperature, the natural gradient temperature of the earth, the heat produced by hydration processes due to the presence of hydraulic binders, and the heat generated from friction at the interface of the paste backfill and the surrounding rock (Sheshpari 2015, Yilmaz and Fall 2017, Ghirian and Fall 2017). However, some of these factors have a more crucial impact on CPB's performance, including binder hydration, which results from the presence of a hydraulic binder and is of paramount importance to the paste backfill attributes. Moreover, the curing temperature plays a critical role in either enhancing or impairing the binder hydration process. For instance, higher curing temperatures

significantly amplify the binder hydration process by markedly increasing the rate of hydration. Conversely, curing at lower temperatures diminishes the rate of binder hydration, thereby potentially affecting the structural integrity and performance of the paste backfill.

However, regarding the application of CPB, it can be stated that he principal advantages associated with the utilization of paste backfill encompass the expedited stope cycles due to an early development of mechanical strength, the optimization of ore recovery, and the enhancement of mine worker safety. Conversely, notable challenges involve the requirement for high-pressure pipeline systems for material delivery, as well as an increased demand for supervision and rigorous quality control (Brackebusch 1995, Hassani and Archibald 1998, Landriault 2001).

2.2.2 Cemented Paste Backfill Technology

2.2.2.1. Geotechnical design criteria of CPB

The transition of CPB from a hydraulic paste to a solid state signifies the onset of the hardening process and strength acquisition within CPB structures. The accrual of strength in CPB can be attributed to a myriad of factors, including cement hydration, self-desiccation (pore pressure reduction or suction development), consolidation resulting from self-weight pressure, the influence of the backfill curing temperature, and the influence of the ambient relative humidity (RH) (Galaa et al. 2011). Given the disparity in stiffness and yielding attributes between the backfill and the adjacent rock mass, a portion of the stress inherent in the backfill is transferred to the neighboring rock walls, a phenomenon known as the arching effect (Figure 2.5). Consequently, the vertical stress situated beneath the arching area is reduced compared to the overburden pressure of the backfill ($\sigma_v < \gamma h$). Certain prerequisites must be satisfied for the stability of the paste backfill structure in a designed CPB. These include (1) the capability to self-stand once its vertical faces are not reliant on any external walls, (2) the resilience to withstand both static and dynamic loads imposed by equipment traversing atop the backfill structure, (3) the capacity to bolster adjacent rock walls, thereby precluding their failure, (4) the ability to maintain stability amid ongoing undercut mining beneath the backfill structure, and (5) the

capacity to promptly develop early age strength. The unconfined compressive strength of the generated CPB, typically falling between 0.2 and 4 MPa (Revell 2000), derived from laboratory testing, constitutes the prevalent method for designing paste backfill. Nevertheless, factors such as the stability of temporary barricades, filling strategy, and backfill curing time must be considered in conjunction with the CPB's overall stability against diverse failure modes. Multiple parameters, including the dimensions and the type of temporary barricade and the load distribution at the interface of the backfill and the barricade, should be taken into account when designing temporary barricades. As for the filling strategy, a two-stage backfilling process is commonly deployed to enhance the safety of barricade stability. The first stage entails discharging the initial layer of backfill, termed plug backfill, in contact with the barricade. After the completion of the plug backfill discharge, it undergoes curing until sufficient strength is attained to bear the overburden pressure from the subsequent CPB layers. Once the plug backfill stability is ensured, the subsequent layer known as residual backfill can be deposited into the stope. This filling strategy rationale stems from the fact that having a plug backfill helps diminish the formation of intense hydrostatic pressure behind the barricades, which could lead to barricade failure and ensuing financial loss and fatalities. However, the existence of a plug backfill with a minimum strength elevates the safety level by supporting a portion of the overburden backfill and reducing the total stress exerted on the barricade. Figure 2-1. Schematic representation of backfill and its surrounding environment represents a schematic layout of the different backfill layers in a stope as well as barricade location.

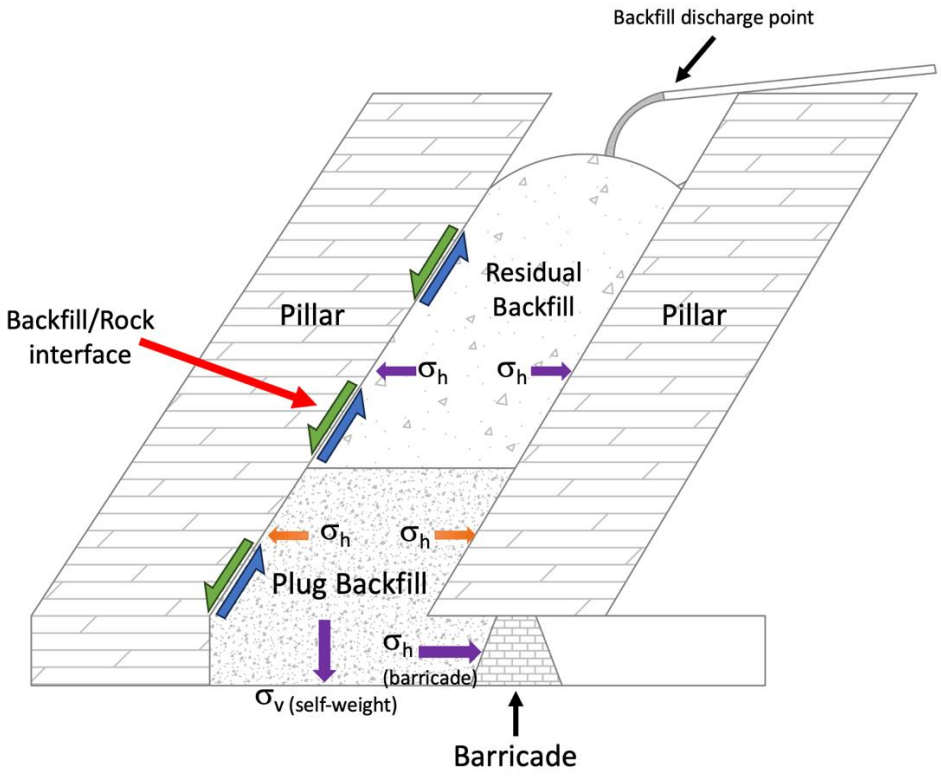

Figure 2-1. Schematic representation of backfill and its surrounding environment

2.2.2.2. Mix design and CPB preparation

The mix design of CPB holds significant importance for various reasons. Primarily, the most frequently utilized hydraulic binder in CPB preparation is ordinary cement, a material known to pose environmental risks (during cement production process) and to carry considerable costs for the backfilling process. Consequently, it is vital that the mix design be developed in such a manner that minimizes binder dosage, while maintaining key CPB properties such as the rate of early age strength gain, transportability, and durability. Beyond binder dosage, a multitude of factors influence CPB characteristics, including the content of fine particles, the water-to-cement (W/C) ratio, and final solid density (Fall et al., 2005; Yilmaz and Fall, 2017).

The tailings generated in the extraction process are typically blended with a large dosage of water, necessitating an increase in tailings concentration by reducing water dosage. This process, known as desliming, is carried out in a hydro-cyclone and yields dewatered tailings. Simultaneously, a portion of the fine tailings' particles is separated from the initial milled tailings.

It is crucial to note that a minimum content of fine particles is indispensable to maintain the consistency of the final mixture and to facilitate the transportation of fresh paste backfill.

In the Canadian mining sector, the most prevalent types of hydraulic binders employed in the backfilling process are Ordinary Portland Cement (OPC) and granulated blast-furnace slag. However, other binders, such as fly ash and pozzolans, have also been utilized.

As for the water used in the preparation of CPB, it is crucial to be mindful of the potential presence of any chemical components, such as sulphate or zinc, which could partake in the binder hydration process and subsequently detrimentally modify the CPB's mechanical behavior. Hence, conducting an analysis to ascertain the water's chemical composition prior to its usage in the mixing plant is of utmost necessity.

As previously stated, once the concentration of the initial tailings, with a variability between 35 to 60%, has achieved the minimal requirement of 75% via various dewatering methods, the tailings are then transported to a screw mixer. Within this apparatus, the tailings are combined with the predetermined quantity of binder, water, and other admixtures to create the final paste backfill mixture. This mixture is designed to exhibit specific mechanical and rheological properties such as slump, which is of vital importance in ensuring the transportability of the paste backfill. Upon production of the fresh CPB, it is then channeled into the underground voids through either a gravity-driven method, a pumping system, or a hybrid of both approaches. Figure 2-2. Flow chart of a backfill production plant provides a schematic representation of the backfill production system.

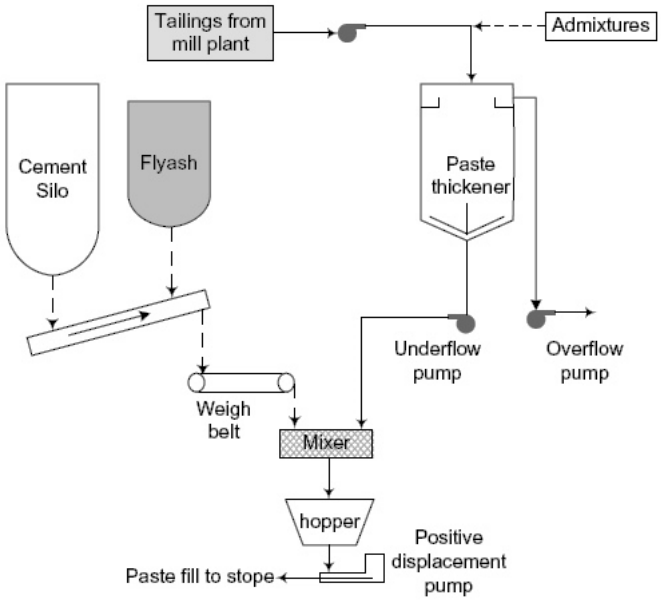

Figure 2-2. Flow chart of a backfill production plant

2.2.2.3. CPB Transportation

As noted earlier, to facilitate the transportation of the freshly produced paste backfill into the stopes, various systems such as gravity-driven, pumping, or a combination of these methods can be employed. Nevertheless, the transportability of CPB is contingent upon its rheological performance, typically determined through the measurement of CPB viscosity and shear yield stress. Precise evaluations of these properties are critical, given that designing an optimized transportation system, whether it be gravity-driven or a pumping system, is unfeasible without this information. It is worth mentioning that the viscosity and yield stress can be evaluated via indirect methods. For instance, assessing the consistency of the CPB by conducting a slump test is a prevalent practice, with the results used to extrapolate viscosity and shear yield stress values. The subsequent phase involves calculating the requisite pressure gradient for pumping systems or the maximum horizontal distance for gravity-driven systems.

Moreover, an array of factors could influence the rheological properties of fresh CPB, which can be categorized into intrinsic and extrinsic groups. Extrinsic factors include the friction coefficient at the pipe/backfill interface, ambient temperature, and the time elapsed from the plant to the stope. In contrast, intrinsic factors entail the type of binder, fine particle content, tailings particle size distribution, chemical admixtures, and water chemistry, which are accountable for

alterations in the rheological properties of fresh CPB. Consequently, it is strongly recommended to account for the impacts of these factors when designing the transportation system, to maintain an equilibrium between the pumpability of the paste and the specifications of the delivery system, such as dimensions, among other factors. Figure 2-3. Schematic view of different combination of backfill transportation system illustrates an example of delivery system in a backfill production facility.

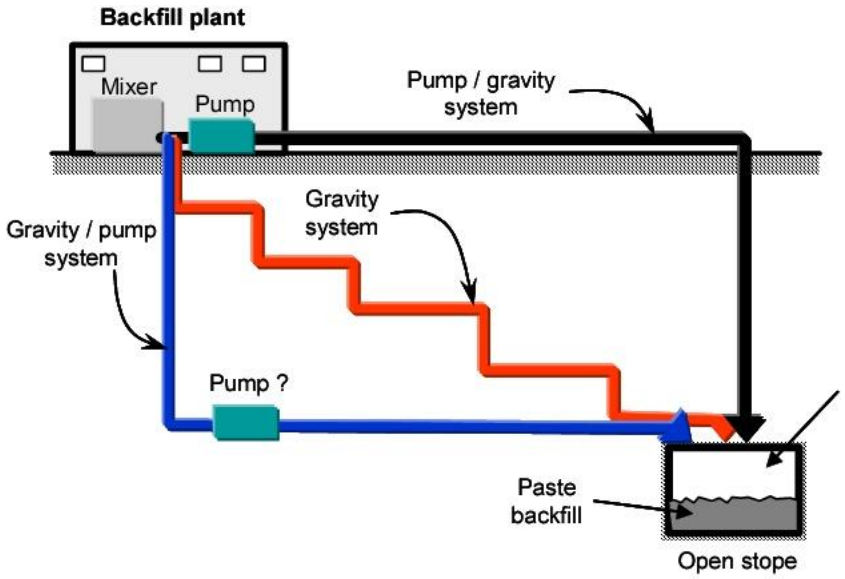

Figure 2-3. Schematic view of different combination of backfill transportation system

2.3. CPB properties

Given the intricate nature of CPB, a multitude of factors can influence its performance and properties. Furthermore, taking into account the diverse scenarios and field conditions to which paste backfill may be exposed, it becomes apparent that a thorough investigation and comprehension of these parameters and characteristics could lead to the optimization of backfill structure designs, particularly with regard to the geotechnical performance of CPB and, more significantly, from a financial perspective. Accordingly, this section will provide a review of the various properties of CPB such as physical, mechanical, chemical, thermal, hydraulic, and the potential factors that influence these parameters.

2.3.1 Physical properties

The geotechnical performance of a paste backfill structure is profoundly influenced by the physical characteristics of the CPB matrix, which can be defined by physical properties like void ratio (or porosity), bulk unit weight, and degree of saturation. Therefore, understanding the evolution of these parameters during the curing cycle can result in more precise predictions of CPB's geotechnical behavior. Various in-situ or laboratory methods must be considered to examine these parameters. Numerous studies have been conducted to explore the evolution of CPB's physical properties throughout its curing period. However, compared to laboratory research, there are fewer reports on the in-situ investigation of CPB physical properties. This knowledge gap mainly arises from the challenges associated with in-situ data extraction, which often make it unfeasible to gather such data. For instance, to collect samples and data from a backfilled mine stope, all mining activities must be halted until a sufficient number of samples are gathered, or in many cases, it's nearly impossible to access the backfilled stopes for sampling. Furthermore, the safety concerns and the range of instrumentation needed to gather representative data elucidate why there is limited data on in-situ studies regarding the evolution of physical properties of CPB (Roux et al. 2002, Ghirian 2016b).

In light of the above, Roux et al., (2005) study on-site monitoring of the physical properties of CPB revealed a progression in these properties as the CPB's curing cycle progressed. For instance, a 90-day field surveillance indicated a void ratio fluctuating between 1.1 and 1.4, while the degree of saturation ranged from 79% to 100%. Relative to their earlier in-situ studies on CPB's physical properties, a follow-up study was conducted under laboratory conditions to draw comparisons between the field and laboratory results. Their findings suggested that the void ratio values derived from field tests were 20% higher than those procured in the lab, and the unit weight of the field samples was 10% lower than its laboratory counterparts. They've stated that this progression in evolution of physical properties could be attributed to different factors and mechanisms that occur during backfill curing cycle such as self-weight consolidation, stress regime redistribution, chemical impacts of binder hydration process, and tailings physical characteristics.

In a separate experimental investigation led by Belem et al., (2006), the team aimed to recreate more authentic conditions in their laboratory procedures by observing the evolution of a column of CPB's physical properties over a 91-day curing period, mirroring the conditions of previous studies. They cured their column under two distinct scenarios: drained and undrained conditions. It was observed that in the undrained scenario, depending on the height at which the samples were taken, the void ratio and degree of saturation oscillated between 0.85-0.97 and 83% to 94% respectively. Conversely, these variances for the drained condition were reported between 0.77-0.91 for the void ratio and 75% to 93% for the degree of saturation.

Ghirian & Fall (2013) advanced their investigation by widening their research scope to the evolution of Thermal, Hydraulic, Mechanical, and Chemical (THMC) processes in a column of CPB. They inferred that the mechanical behavior of CPB, as represented by the outcomes of uniaxial compressive strength (UCS) tests, is heavily influenced by both the stage of the curing cycle and the sample's location within the column. In their study, the upper surface of the columns was exposed to the surrounding environment, resulting in a semi-drained condition. They consequently highlighted three main findings:

1. The physical properties of the CPB column, such as the void ratio, are highly time-dependent parameters mainly associated with THMC processes such as binder hydration, self-desiccation-induced negative pore pressure, internal and external heat sources, and self-weight pressure.
2. Negative pore water pressure or decrease in degree of saturation induced by the hydration progression's water consumption plays a pivotal role in the evolution of the CPB column's mechanical properties.
3. They reported that thermal factors such as heat generated due to the hydration reaction should be considered another crucial factor that could alter CPB properties because of its impact on the negative pore water pressure rate and acceleration of binder reactions, both of which lead to the enhancement of the CPB's mechanical performance.

Another critical factor responsible for governing the mechanical performance of CPB is binder type. Considering the key role of hydration products in providing the bonding between tailings particles and filler role of precipitated hydration products, the importance of studying the impact

of binder type on the mechanical performance of CPB becomes more obvious. Consequently, Yilmaz et al., (2009) undertook a research project to examine how the binder content impacted the physical properties of both consolidated and unconsolidated CPB columns. Their insights into how binder dosage modifies the CPB's physical properties showed that any increment in the binder concentration could lead to minor or substantial changes in a variety of physical attributes. For instance, they reported that for an unconsolidated column, porosity dropped from 0.47 to 0.42, while the degree of saturation exhibited a decrease from 97% to 90%. Conversely, for the consolidated condition, it was noted that samples cured under applied pressure initially had a void ratio of 0.45 at the onset of the curing period, while at the end of the curing phase (28 days), the recorded void ratio was 0.41. Similarly, the degree of saturation under this condition indicated a reduction from 94% at the start to 80% at the end of the curing process. These observations can be tied to the idea that an increase in binder content directly leads to more precipitation of hydration products. In simpler terms, a higher binder dosage results in a more intense development of negative pore water pressure within the CPB, promoting the formation of a denser microstructure.

2.3.2 Mechanical characteristics

The central focus pertaining to the mechanical performance of CPB is its structural stability throughout the course of its existence. As such, every element with potential to affect the mechanical performance necessitates thorough examination during the design phase. In the wake of CPB's introduction, a substantial academic endeavor has been devoted to researching the influence of a plethora of factors on the mechanical properties of CPB.

The most widely accepted method of evaluating the mechanical resilience of CPB within the industry context is through the application of Unconfined Compressive Strength (UCS) test (Fall et al. 2005; Belem and Benzaazoua 2008c). Nonetheless, there exist other direct methods for gauging the mechanical resilience of CPB, including the triaxial test (Roux et al. 2005a, Simms and Grabinsky 2009), and others such as the direct shear test (Rankine and Sivakugan 2007). These methods are utilized to determine stress-strain graphs, shear strength, and associated parameters such as the friction angle and cohesion. In parallel to these direct methods, several

studies have considered indirect techniques of determining the mechanical properties of CPB, encompassing ultrasonic wave measurements or shear wave velocity (Klein et al. 2006, Diez d'Aux 2008, Ercikdi et al. 2014, Yilmaz et al. 2014, Xu et al. 2016, Yan et al. 2020). The acquisition of strength properties is viewed as a preliminary step towards evaluating the stability of the backfill structure. The challenge of stability escalates when dealing with backfill structures with unsupported faces, necessitating the backfill structure to be self-stable (Li and Aubertin 2012, 2014, Zhang et al. 2021, 2022, Qi et al. 2022).

Past research has revealed that the friction angle of the CPB tends to reduce during the curing phase and continues to decrease over the long term (Rankine and Sivakugan 2007, Bawden et al. 2011, Xiu et al. 2022). This behavior is believed to be as a result of various mechanisms occurring during the curing period and the lifespan of the backfill structure, including self-desiccation development, hydration progression, and water evaporationWith respect to cohesion, numerous studies have concluded that this parameter significantly increases with the curing period and higher binder content (Edward Pierce and Ontario 1999, Xiu et al. 2022). Observations indicate that cohesion may exhibit a steady increment in its value, reaching up to 1500 kPa, in tandem with the progression of the curing duration. However, this increase in the cohesion is critically contingent on the type and dosage of binder, along with other physical properties of CPB such as the content of fine particles (Belem et al. 2000). Ghirian and Fall (2013) performed a column experiment, investigating the evolution of physical properties of the CPB within a column. They deduced that under a drained condition, where water evaporation and loss could transpire, the friction angle at the column's midpoint remained relatively unaltered. Yet, a decrease in this parameter was noted at the top and base of the column, attributable to the impact of drainage and water evaporation.

In their research, the effects of curing under pressure were not scrutinized. Therefore, in a subsequent study, they designed a pressure cell enabling them to cure a small cylindrical CPB sample (with a height of 30cm and a diameter of 15cm) under externally applied pressure. This simulated the impact of the self-weight of CPB and other overburden pressure, such as the loads exerted due to equipment transportation or the load of the ground's overlying layer. Their findings mirrored previous observations, with no significant changes in the friction angle.

However, for cohesion, it was demonstrated that curing under applied pressure could prompt a more robust development of cohesion. This is due to the fact that applied pressure resulted in a higher generation of hydration products that facilitate the bonding between solid particles (Ghirian and Fall, 2016).

As previously mentioned, the CPB design procedure is highly dependent on the results of the UCS test. Therefore, numerous studies have investigated the effect of different parameters on the UCS results of CPB. Due to the nature of strength growing in CPB, several factors have a key role such as binder type/content, negative pore water pressure development, temperature, physical and chemical characteristics of CPB main ingredients, applied pressure, drainage, etc.

It is of significance to underscore that the characteristics of tailings are instrumental in directing the strength development of the backfill mixture. Properties of tailings, encompassing mineralogy, chemical characteristics, and particle size distribution, hold the potential to either obstruct or hasten the strengthening rate. For instance, the use of sulphide-rich tailings could potentially lead to a decline in early age and long-term strength of paste backfill depending on the concentration of the sulphate components, attributable to the phenomenon termed as sulphate attack (Fall et al. 2004, Kesimal et al. 2005a, Ercikdi et al. 2009, 2010, Fall and Pokharel 2010b). In this context, it is important to note that the existence of high volume of sulphide components is detrimental to the precipitated hydration products, like calcium silicate hydrate (C-S-H), which facilitate the bonding between the tailing's particles. The absorption of sulphate by C-S-H and subsequent reaction result in the production of an expansive material, termed ettringite. This can potentially contribute to the development of microcracks within the CPB structure, thereby adversely impacting the mechanical performance of CPB (Benzaazoua et al. 2002, Kesimal et al. 2005a, Liu et al. 2020).

Another factor of substantial importance concerning the strength development of CPB is the fineness of tailings. Many researches has been devoted to studying the effect of utilizing different particle size distributions, concentrating on the percentage of the fine particle portion. The consensus among these studies is that the fineness of tailings can significantly influence the strength of CPB through various mechanisms such as pore structure refinement and acceleration of binder consumption. Both these mechanisms contribute to a higher packing density and

stronger bonding between the solid particles (Fall et al. 2005b, Fall and Pokharel 2010b, Ke et al. 2015, 2016, Qiu et al. 2020, Al-Moselly et al. 2022a). As previously elucidated, the enhancement discerned in the Unconfined Compressive Strength (UCS) results, attributable to the influence of fineness, adheres to an optimal value. Exceeding this optimal value of fineness could prove counterproductive and potentially deleterious. This particular behavior can be interpreted by acknowledging that until the optimal value is reached, any increase in the proportion of fine particles contributes to reducing the void ratio and achieving a higher packing density. This in turn facilitates the positive amplification of shear stress transmission within the CPB matrix. Nevertheless, once this optimal value is surpassed, the larger particles, which are inherently equipped to shoulder a significant segment of the exerted loads, are supplanted by fine particles possessing a diminished load-bearing capacity (Fall et al. 2004, 2005b).

An additional critical factor concerning the strength development of CPB is the curing temperature. It has been validated that the curing temperature can significantly alter the mechanical performance of the CPB, by modifying the microstructure and amplifying the self-desiccation phenomenon. A study conducted by Fang and Fall (2018), investigating the effect of curing temperature on the shear behavior of the backfill/rock interface, unveiled that curing CPB under elevated temperatures could expedite the hydration process and amplify the negative pore-water pressure development. Figure 2.4 illustrates the results of suction development monitoring in CPB samples cured under different curing temperatures. As can be seen in this figure sample cured at a higher curing temperature developed more intense negative pore pressure compared to the samples cured at a lower curing temperature which represents a faster hydration process that resulted in faster pore water pressure dissipation.

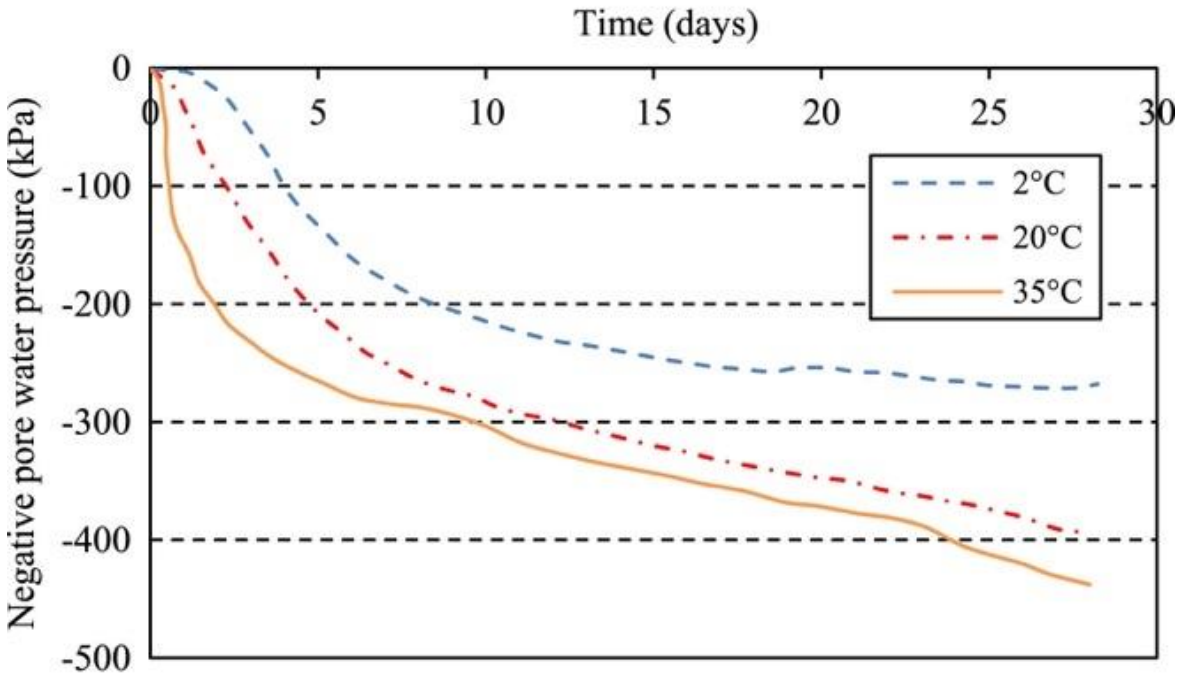

Figure 2-4. Impact of various curing temperatures on the suction development of CPB samples (Fang and Fall 2018b)

In a separate study executed by Chen et al. (2021), which focused on the coupled effect of temperature and curing stress on the mechanical properties of CPB, it was concluded that both the curing stress and curing temperature could potentially enhance the UCS results of CPB. This could be rationalized by the notion that each of these factors could hasten the binder hydration process, culminating in a higher yield of hydration products and micro-pore refinement. Fall and Pokharel (2010) delved into the impacts of curing temperature and sulphate contents on the mechanical performance of CPB. They tested a multitude of CPB samples under diverse curing temperatures (0 °C, 25 °C, 20 °C, 35 °C, and 50 °C) and varying sulphate dosages (0, 5000, 15,000, and 25,000 ppm) over a period of 28 days. Their findings suggest that the coupled effect of sulphate and curing temperature could either be beneficial or detrimental to the strength development of CPB, contingent on the sulphate dosage and curing temperature. For instance, it was observed that samples cured with the inclusion of sulphate up to a concentration of 1500ppm and cured at temperatures exceeding 20 °C manifested higher UCS results compared to those prepared with a higher dosage of sulphate. This behavior can be interpreted by

considering that the introduction of sulphate into the hydration process under high curing temperatures results in the formation of weak calcium silicate hydrate (C-S-H) compounds due to the absorption of sulphate ions by C-S-H.

2.3.3 Hydraulic characteristics

The hydraulic characteristics of CPB are mainly characterized by the evolution of pore water pressure -which may either be in negative (suction) or positive pressure- and hydraulic conductivity. With respect to the significance of pore water pressure, it can be posited that key aspects of the backfilling process such as the stability of temporary barricades, dynamic stability of the CPB in situations involving seismic loadings like a blast or earthquake, and the effective stress regime distribution could be influenced by the evolution of pore water pressure within the backfill structure. Concerning hydraulic conductivity, several critical attributes of Cemented Paste Backfill (CPB) in its early stages are highly dependent on the evolution of hydraulic conductivity. These attributes include behavior during the consolidation process, workability, and transportability prior to its placement in the designated stopes. Nonetheless, it should be underscored that the unsaturated hydraulic conductivity of CPB has of great importance in determining the environmental performance of the CPB. This includes assessing potential risks like acid rock drainage (ARD) or determining the velocity of groundwater seepage in backfill structure and/or at the interface between CPB and adjacent rock masses. Furthermore, it is crucial to maintain a precise understanding of the leakage potential of CPB, particularly considering scenarios where the CPB comprises harmful components such as heavy metals' ions, which could exacerbate the risk of groundwater contamination (Fourie 2009, Ercikdi et al. 2017). As emphasized previously, precise comprehension of the evolution of pore water pressure is essential in facilitating cost-effective design strategies and augmenting the safety measures associated with retaining structures like temporary barricades. The stability of such barricades is predicated on the widely-accepted understanding that, subsequent to the emplacement of fresh CPB behind the barricades, substantial positive hydrostatic pressure amasses which, in instances of flawed design or construction, can culminate in barricade collapse and ensuing complications (Helinski et al. 2007).

The extant body of literature has conducted experimental studies to gain a more sophisticated understanding of the mechanisms that precipitate the development of both negative and positive pore-water pressures. There have also been efforts to elucidate the influence of a variety of internal and external factors on the rate at which self-desiccation develops. These include binder type and content, curing temperature, and tailings mineralogy as internal factors, and curing stress, filling rate, and drainage feasibility as external factors.

For instance, Li and Fall (2016) undertook experimental research to evaluate the impact of various sulphate concentrations on the self-desiccation progression within CPB. Their findings suggest that the presence of sulphate could potentially impede the rate at which early age strength develops. This is attributable to the downstream effects of a diminished binder hydration process, which in turn stymies the development of self-desiccation in the early curing stages.

Similarly, Chen et al. (2022) probed the impact of curing stress on the suction development within CPB, concluding that there exists a direct relationship between the degree of microstructure refinement and the intensity of suction development. Observational evidence indicated that curing the CPB under pressure substantially refined the microstructure of the investigated samples, thereby yielding samples with lower porosity. In these samples, a more pronounced negative pore-water pressure was observed, thus substantiating the beneficial influence of curing stress.

Further, experimental research conducted by Wang et al. (2016) examined the effect of sodium silicate on the strength and suction development of CPB. Their findings suggest that the initial temperature exerts a critical influence on not only the rate at which strength is gained, but also on the development of self-desiccation. They noted that samples cured under elevated initial temperatures demonstrated more intensified suction at their early age. This can be attributed to the fact that higher temperatures directly contribute to the acceleration of the hydration process.

2.3.4 Thermal characteristics

The thermal properties of CPB can be delineated into two categories. The first encapsulates inherent properties such as thermal conductivity, while the second covers extrinsic factors like

the heat generated during binder hydration and the temperature used for curing. One significant reason to scrutinize these thermal characteristics relates to thermal expansion. The various components of the CPB mixture may each expand differently in response to heat. If not correctly accommodated, this differential expansion can introduce stresses into the backfill structure as temperature varies, potentially leading to structural deficiencies such as cracking. Furthermore, the curing process of CPB, which is exothermic - it emits heat - requires careful management. Inappropriate heat dissipation can elevate the CPB's temperature, thereby affecting its curing process. Excessive heat can precipitate premature solidification or even lead to cracking, while insufficient heat can retard the process or result in incomplete curing. A comprehensive understanding of the thermal characteristics thus facilitates effective oversight of the curing process. Lastly, a thorough understanding of CPB's thermal characteristics is paramount for evaluating its environmental implications. If, for instance, the backfill material experiences significant heating during the curing process, this could potentially impact the surrounding ecology, particularly in cold regions. Furthermore, it has been proposed that the thermal curing conditions of CPB exert a substantial influence on the development of factors critical to its environmental impacts, particularly hydraulic conductivity. Hence, assessing the thermal responses of CPB is essential for understanding its broader environmental footprint.

Several studies have been undertaken to explore how various parameters can affect the thermal conductivity of paste backfill. One notable study, conducted by Célestin and Fall in 2009, examined how factors such as the main ingredients of CPB, curing time, temperature, and degree of saturation could influence the thermal characteristics of the material.

Their observations highlighted that the mineralogy of the tailings could significantly affect the thermal conductivity of the CPB. For instance, if the tailings primarily consist of quartz minerals, the resulting CPB may exhibit higher thermal conductivity. The research also revealed that the particle size distribution of the tailings could markedly alter the CPB's thermal conductivity. The utilization of coarser tailings tends to increase thermal conductivity compared to CPB composed of finer particles. This phenomenon can be explained by the fact that an increase in fine particle content disrupts the uniformity of particle size distribution, leading to a decrease in the CPB's

packing density. Essentially, higher fine particle content corresponds to increased porosity within the CPB mixture, which may not be adequately filled by the hydration products.

Furthermore, they observed that higher curing temperatures could decrease the thermal conductivity of the CPB. This could be attributed to the fact that elevated temperatures quicken the water consumption through the acceleration of the hydration process. Consequently, water, which has a higher thermal conductivity, is replaced by air, which has lower thermal conductivity. However, the researchers concluded that certain mix parameters, such as the water-to-cement (W/C) ratio, binder type and content (maintaining a constant slump), and sulphate content, seem to have negligible or minor effects on the thermal conductivity of the CPB.

Cui and Fall, (2016) carried out a study to assess the impact of curing stress, initial temperature, and drainage conditions on the thermal properties of CPB. Consistent with earlier studies, they observed an inverse relationship between the initial temperature and the thermal conductivity of the CPB. Interestingly, they found that CPB samples cured under applied pressure exhibited lower thermal conductivity. This phenomenon could be attributed to the rearrangement of solid particles in the CPB microstructure leading to a reduction in pore space, which consequently increased the volumetric water content.

Additionally, their study revealed that CPB samples cured in a drained condition displayed a consistent decrease in thermal conductivity throughout the curing cycle. This could be rationalized by the fact that in a drained system, air takes the place of water in the pores as the curing cycle progresses. This replacement process inevitably decreases the thermal conductivity, given that air has lower thermal conductivity compared to water.

2.4. Binder reaction

Having discussed a variety of CPB characteristics and the impact of various elements such as internal and external factors on CPB performance, it becomes evident that the binder hydration process plays an important role in determining CPB's behavior in various respects. Consequently, the succeeding section will delve deeper into the nature of the binder used in paste backfill formulation and factors that shape the hydration process.

The primary reason for incorporating a binder agent in paste backfill preparation is to address the lack of adhesion between solid particles and the substantial volume of water present in the initial mixture. Thus, a binder agent is incorporated into the mixture to promote interparticle bonding, which is essential to sustain mechanical strength. Moreover, the binder agent alleviates issues associated with the large volume of water in several ways, including water consumption for hydration process progression and initiation of the self-desiccation mechanism in CPB.

Ordinary Portland Cement (OPC) is often the preferred hydraulic binder for CPB mixture preparation due to its wide availability and accessibility. Nevertheless, other pozzolanic materials, including blast furnace slag or pulverized fly ash (PFA), can be incorporated as partial substitutes for OPC with the intention of lowering the overall backfilling expense (Weaver and Luka 1970, Aylmer 1973, Benzaazoua et al. 2004, Kesimal et al. 2005b). As previously highlighted, the incorporation of a binder, a distinguishing feature of CPB compared to earlier backfilling techniques, enhances the mechanical performance, which primarily hinges on internal friction and cohesion of final mixture (Hassani et al. 2007, Abdul-Hussain and Fall 2012).

2.4.1 OPC hydration process

To appreciate how the inclusion of a binder enhances the mechanical strength of CPB, it is critical to comprehend the chemical processes occurring during hydration. Ordinary cement contains diverse components, notably clinkers and gypsum (3-7 wt%). Produced in the process of Portland cement creation, clinker serves as an intermediary material. Gypsum is added to modulate the initial setting time of the resulting compound. Nevertheless, the chemical behavior of cement is best understood by exploring the components of clinker, which predominantly contains silicates and aluminates as outlined below (Alizadeh 2009):

1. Silicates:
   - Tricalcium silicate or alite (C_3S, 26% to 53%)
   - Dicalcium silicate or belite (C_2S, 16% to 54%)
2. Aluminates:
   - Tricalcium aluminate (C_3A, 3% to 15%)
   - Tetracalcium alumina ferrite (C_4AF, 8% to 12%)

On contact with water, these clinker components hydrate, leading to the formation of three primary cement hydration products as detailed below:

- Calcium Silicate Hydrate (C-S-H): This product, derived from the hydration of C3S and C2S, is chiefly accountable for the compressive strength and durability of the hydrated cement paste. Resistant to most environmental conditions, C-S-H can degrade when exposed to acid attack or sulfate ions. This exposure may alter the C-S-H structure and lead to gypsum or ettringite formation, thereby causing material expansion and cracking. C-S-H contributes about 60% to the total volume of hydration products (Allen et al. 2007, Alizadeh 2009).
- Calcium Hydroxide (CH): As a by-product of calcium silicates, CH takes the second place in the total hydration product volume, contributing 20%. Characterized by thin to large hexagonal sheets, this element helps to develop strength in cementitious materials (Double 1983).
- Calcium Sulphoaluminate or Ettringite (AF): Resulting from the reaction between gypsum and the aluminate components of clinker, ettringite assumes a needle-like shape. While highly reactive with sulfate—potentially leading to the development of cracks in the hydrated cement paste—ettringite does not contribute to strength development. However, it plays a role in regulating the setting process in cementitious materials (Double 1983).

Ghirian (2016b) offered a visual representation of the Portland cement hydration process, as shown in Figure 2-5. schematic representation of Portland cement hydration process It's worth noting that the size of the boxes in this figure corresponds to the volume of the respective hydration products.

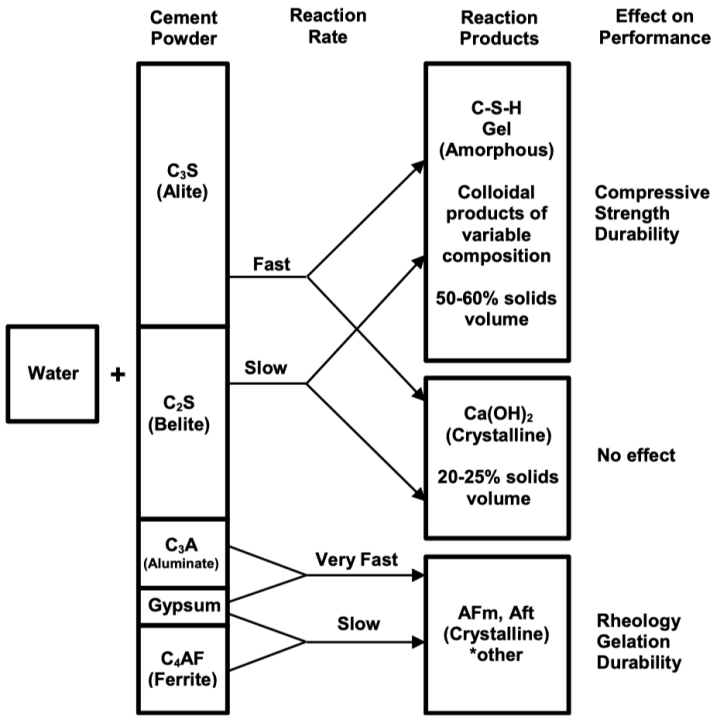

Figure 2-5. schematic representation of Portland cement hydration process (Ghirian 2016b)

2.4.2 Binder hydration characteristics

The hydration of cement is identified as an exothermic chemical process. This denotes that it produces heat during the reaction, which occurs between the solid unhydrated cement and the liquid phase (water) (Swaddiwudhipong et al. 2002, Chen and Brouwers 2010b, Bullard et al. 2011, Winter 2012). Given the substantial amount of heat generated during this reaction, it's imperative to understand the impact of this thermal output on the resultant products' physical and chemical properties. The total heat produced, also known as the "heat of hydration," can be quantified as the cumulative heat generated by each individual component involved in the hydration reaction. This summation can be mathematically represented as:

$$Q\ sum = Q_{C3S} + Q_{C2S} + Q_{C3A} + QC4AF \quad \text{(Eq. 2.1)}$$

Swaddiwudhipong et al. (2002), evaluated the heat generation corresponding to the hydration of each constituent of cement. Based on their findings, the heat evolved during cement hydration is:

- C_3A :1340 (kJ/kg)

- C_3S :502 (kJ/kg)
- C_4AF :419 (kJ/kg)
- C_2S :260 (kJ/kg)

Earlier research delineated the cement hydration reaction into five discernible phases, which include: initial reaction (blending), induction (dormant period), acceleration (hardening), deceleration (cooling), and densification. These stages are graphically depicted in Figure 2-6. different stages of cement hydration process (Bullard et al. 2011).

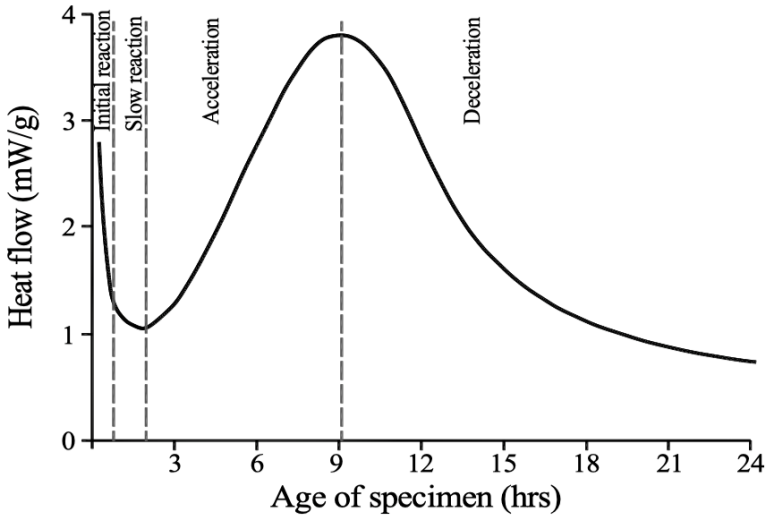

Figure 2-6. different stages of cement hydration process (Bullard et al. 2011)

1. Initial reaction: This is the stage that begins the moment dry cement particles come into contact with water. The aluminate compounds and gypsum begin to dissolve at this point, and this dissolution is the primary cause of the substantial heat emitted during this phase. Another crucial aspect of this stage is the release of several ions into the water-based medium, including sodium (Na), potassium (K), calcium (Ca), hydroxide (OH), and sulfate (SO4). Typically, this phase endures for approximately 30 minutes.
2. Induction: During this phase of hydration which also known as dormant period, calcium silicate compounds including C3S and C2S begin their reaction, leading primarily to the formation of calcium silicate hydrate gel, or C-S-H gel. Simultaneously, gypsum and C3A also react, producing ettringite. Notably, the C-S-H gel and ettringite form a sort of barrier around the C_3S and C_3A particles, which accounts for the slowed pace of hydration

following this stage, as the free contact surface of C_3S and C_3A with the liquid medium becomes reduced. The induction phase generally spans from around 30 minutes to 4 hours and no significant heat release is expected for this phase.

3. Acceleration: Also referred to as the hardening phase, this stage is chiefly responsible for the main strength and hardening development. This occurs due to a dramatic increase in the generation of C-S-H gel and ettringite, caused by the breaking of the formed coating layer around unhydrated particles due to excess pressure. As a result, a substantial amount of heat is released during this phase, mainly due to the reaction of C3A and gypsum, and later, C_3A and ettringite. During this hydration period, a refinement in the pore structure is anticipated due to the highest production of hydration products. This phase typically lasts between 2 to 17 hours.
4. Deceleration: Similar to earlier stages, the creation of hydration products persists in this phase, but at a significantly slower rate. This is due to the limited access of water to unhydrated cement grains caused by the formation of C-H and C-S-H gel around cement particles. Also, unstable ettringite compounds produced in previous stages have an opportunity to transform into more stable monosulphate compounds. In terms of heat release, the highest heat release occurs during this stage, but a sharp decrease is expected due to the significant drop in the production rate of hydration products. This step lasts around 24 to 48 hours.
5. Densification: This is the final stage where the remaining C_3S and C_2S continue to react with water, but at much slower rates. This reaction happens through diffusion and can continue for several years, as long as the conditions for the reaction exist. As the reaction progresses, hydration products fill up the available pores. This leads to refinement of the pores, resulting in reduced permeability and porosity, while improving the mechanical strength of the cement paste.

2.5. Coupled effect of Thermo-Hydraulic-Mechanical-Chemical (THMC) processes on geotechnical behavior of CPB

In this section a comprehensive review on the interconnected effect of Multiphysics processes on the geotechnical performance of CPB is provided. To achieve this goal, the most important processes that occur during the early and advanced ages of CPB curing time will be discussed.

2.5.1 Introduction

The integrated framework of Thermal, Hydraulic, Mechanical, and Chemical (THMC) coupled processes provides a robust perspective to examine the intricate and intertwined behaviors of porous media, such as soil and cementitious materials, including concrete and CPB. Porous materials are defined by their labyrinthine structure of interconnected pores and voids, potentially filled with singular or mixed fluids, including air, water, or oil. A salient characteristic of such materials is their permeability, permitting fluid to penetrate one face of the material and exit through another. The THMC coupled processes are an essential aspect of porous material characterization, where thermal processes can instigate expansion or contraction, modifying the material state. Hydrological processes concern the fluid dynamics within the material's pore spaces, mechanical processes study the material's response to applied loads or stresses, and chemical processes focus on potential reactions within the material or between the material and its environment.

The comprehension of these intertwined THMC processes is fundamental in any study of porous material behavior. Each of these processes can act upon and be influenced by the others, engendering a complex matrix of interactions that dictate the material's macroscopic behavior. For instance, in the case of concrete, the heat evolution during the hydration process, a chemical phenomenon, can instigate thermal expansion and thus influence the material's mechanical properties. Similarly, the soil's hydraulic conductivity, a hydrological attribute, can affect its mechanical stability and its response to thermal variations.

A comprehensive understanding and careful consideration of these THMC coupled processes are indispensable for accurate predictions of material performance under a diversity of conditions. Any deficiency in this understanding may lead to erroneous predictions, possibly culminating in disastrous failures. This becomes crucial in the domain of geotechnical engineering, where such knowledge is vital in evaluating the stability of infrastructural elements like dams, levees, and subterranean tunnels. In the context of waste management, the exploration of THMC processes in cemented paste backfill is crucial for predicting the long-term containment and stability of hazardous substances. Hence, the consideration of these interdependent processes is essential for the safe and dependable utilization of porous materials.

2.5.2 Effect of Coupled THMC processes on CPB

In a coupled system, it's important to understand that individual processes are interlinked and can greatly influence one another. A clear illustration of this can be seen in the geotechnical behavior of cemented paste backfill (CPB) applied in mining stopes (Ghirian 2016b). Here, the primary processes at play—thermal (T), hydraulic (H), mechanical (M), and chemical (C) factors—are not isolated occurrences but parts of a complex, interconnected system. Consequently, to gain a precise understanding of the system's behavior, it is crucial not to consider these factors as independent variables, but as interacting elements within a larger, synergistic framework. The influence of each process on the others is not always uniform, with the extent and direction of this influence varying significantly. In some instances, these interactions can be rather weak, whereas in other situations, they might be remarkably strong. This variation in interaction strength is a significant consideration in the study of such systems. Particularly noteworthy are the strong interactions, which can substantially control the geotechnical performance of backfill structures. Consequently, an in-depth understanding of these coupled processes and the way they interact is fundamental to the study of materials such as CPB. This comprehensive approach ensures that the intricate dynamics at play within these systems are accurately represented, thereby providing valuable insights for the sustainable and safe utilization of these materials in geotechnical applications.

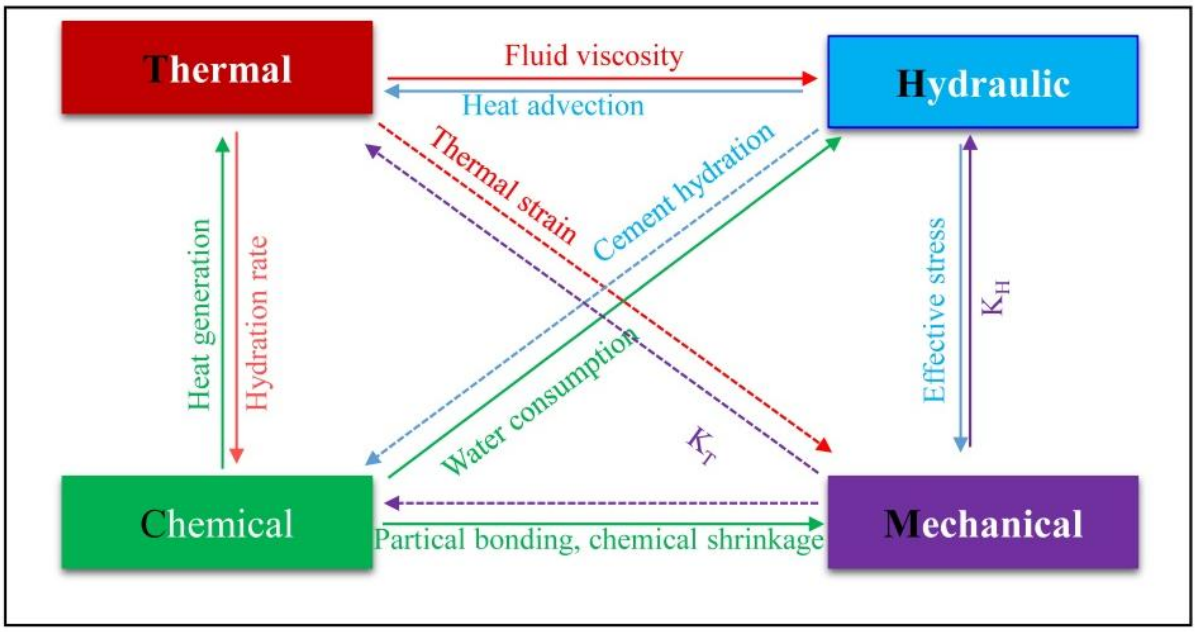

Figure 2-7. Interactions between multiphysics processes (KH: hydraulic conductivity; KT: thermal conductivity (Fang 2021)

Figure 2-7 provides a conceptual depiction of the intertwined processes that govern the performance of CPB. With regard to the thermal process, which was previously discussed, in this chapter, it is worth noting that both intrinsic and extrinsic heat sources are integral to the CPB system. Factors such as the heat generated through the hydration of the binder, heat exchange at the interface between CPB and the surrounding rock masses, and temperature fluctuations induced by the percolation of groundwater into the CPB structure collectively account for the variations in temperature observed within CPB. These elements of thermal variation have been corroborated by several studies, confirming their essential roles in the comprehensive thermal behaviour of CPB (Nasir and Fall 2010, Cui and Fall 2016b, Fang and Fall 2018a).

When considering the hydraulic processes influencing CPB, three key processes are of paramount importance: the consumption of pore water due to binder hydration (Al-Moselly et al. 2022a), the drainage and evaporation of water at the interface between CPB and the surrounding environment such as barricades or other exposed surfaces (Ghirian and Fall 2013b), and the gradient of pore water flow brought about by gravitational forces (Cui 2017).

In the realm of mechanical processes, a variety of factors contribute to the mechanical performance of the CPB structure. For instance, factors such as chemical shrinkage as a result of

binder hydration and thermal deformation due to various heat sources are known to cause mechanical deformation. The same applies to mechanical stresses applied to the CPB mass due to its own weight and/or in situ stresses such as those induced by the closing of rock walls. This deformation subsequently results in the redistribution of stress/strain and causes alterations to the microstructure of the CPB structure (Cui 2017).

Lastly, within the framework of chemical processes, binder hydration is identified as a critical factor governing the behavior of CPB. This exothermic reaction primarily consumes pore water, leading to the generation of hydration products, causing changes in the microstructure of the CPB mass and inducing chemical shrinkage. This process thus plays a significant role in the overall performance of CPB.

Ghirian (2016) comprehensive study underscores the impact of THMC processes on CPB behavior. A focal point of the study was the interplay of these processes and their collective impact. Its findings about the effect of different processes on CPB behavior are summarized as follows:

Effects of Thermal Processes:

- Impact on hydraulic characteristics:
    1. Temperature increases after fresh CPB placement, mainly due to binder hydration. Higher temperatures increase the rate of chemical reactions, including hydration, which in turn releases heat.
    2. This increase potentially signifies the development of negative pore water pressure and higher pore water dissipation rates. The heat can cause water to vaporize, leading to a reduction in pore water pressure.
    3. High temperature can decrease water flowability within the CPB structure due to the production of more hydration products that refine the structure's micropores and decrease overall porosity. More hydration products are produced as the rate of hydration reaction is accelerated under higher temperatures. These products fill in the micropores, reducing the overall porosity and subsequently the water flowability.
- Impact on mechanical characteristics:
    1. Curing CPB under higher temperatures results in the generation of more binder hydration products. This is because the rate of chemical reactions, including hydration, increases with temperature.

2. This leads to a denser microstructure and finer pores in the CPB. More hydration products fill in the pores, making the structure denser.
3. The refined micropores enable the CPB to evenly distribute shear stress, enhancing its mechanical strength. A denser structure with finer pores can more effectively transfer stress throughout the material.

- Impact on chemical characteristics:
    1. Higher curing temperatures can speed up the hydration process, potentially altering the concentration of ions in the CPB's pore fluid. With a faster hydration process, the chemical equilibrium within the pore fluid can change, possibly leading to shifts in ion concentration.

Effect of Hydraulic Processes:

- Impact on thermal characteristics:
    1. Hydraulic properties, such as degree of saturation, can influence thermal properties like thermal conductivity. Water has higher thermal conductivity than air, so when water in the pores is replaced by air due to hydration, thermal conductivity decreases.
    2. Progression of binder hydration initiates a desaturation process that, as it progresses, replaces pore water with air, thus reducing the CPB's thermal conductivity. This happens because the water consumed in the hydration process is replaced by air, which has lower thermal conductivity.
- Impact on mechanical characteristics:
    1. Development of negative pore water pressure due to self-desiccation strongly impacts the strength development of CPB. The reduction in pore water pressure can increase the effective stress in the material, thus increasing its strength.
    2. Evaporation could cause microcrack development, leading to weak planes in the CPB's microstructure and reducing its mechanical strength. As water evaporates, it can leave voids that turn into microcracks, reducing the mechanical strength of the material.
- Impact on chemical characteristics:
    1. Hydraulic processes such as water drainage or self-desiccation can increase ion concentrations due to the dilution effect. When water is drained from the material, the remaining pore water becomes more concentrated with ions.

Effect of Mechanical Processes:

- Impact on thermal characteristics:
    1. No significant coupling effect of mechanical processes on thermal characteristics of CPB was observed in the study.
- Impact on hydraulic characteristics:
    1. Mechanical processes like consolidation due to CPB's self-weight or externally applied pressure can significantly influence the hydraulic characteristics of CPB. These processes can squeeze water out of the material, reducing pore water pressure.
    2. Such processes reduce pore water pressure in drained curing conditions, leading to an increase in effective stress and enhanced mechanical strength. With less pore water pressure, the effective stress (total stress minus pore water pressure) increases, leading to enhanced strength.
    3. The increased stress refines the CPB's microstructure by reducing overall porosity. Increased stress can cause the material to compact, reducing its porosity.
    4. However, higher mechanical pressures can lead to the development of local microcracks, enhancing water flowability within the CPB structure. These microcracks can act as channels for water flow, improving the flowability.
- Impact on chemical characteristics:
    1. Unlike other cementitious materials such as concrete, where high levels of curing stress can accelerate hydration progression, it was concluded that in realistic mining operations, the lower levels of applied stress on the paste backfill structure don't significantly alter the chemical characteristics of CPB. This is because the level of stress applied in these conditions is not enough to significantly increase the rate of hydration reactions.

Effect of Chemical Processes:

- Impact on thermal characteristics:
    1. Cement hydration, as an exothermic reaction, generates heat after the emplacement of CPB. This heat generation significantly influences the geotechnical behavior of CPB because it can increase the material's temperature, which can in turn impact other properties such as hydration rate and water vaporization.
- Impact on hydraulic characteristics:
    1. The chemical reaction of binder hydration directly impacts the hydraulic properties of CPB, such as hydraulic conductivity. As hydration progresses, more hydration products, like calcium silicate hydrate (C-S-H), precipitate and fill the

voids, refining the microstructure of the CPB. This process of refinement makes the pores finer, reducing the ability of water to flow through the CPB structure.

- Impact on mechanical characteristics:
    1. The progression of cement hydration primarily contributes to the development of mechanical strength in the CPB. The precipitation of hydration products provides bonding between the solid particles of the CPB structure, enhancing its cohesion strength. As these products fill the voids and bind particles together, the material becomes stronger and more resistant to deformation.

2.6. Conclusion

In this chapter, the focus is on CPB as a forward-thinking and environmentally friendly method for managing mine waste, a notable shift from traditional practices. This chapter investigates the distinct characteristics of CPB - spanning thermal, hydraulic, mechanical, to chemical aspects, illustrating its comprehensive application. Emphasizing precision in the formulation, preparation, and delivery of CPB, the text highlights its critical role in backfill performance. The interplay of diverse processes within CPB, crucial in shaping the geotechnical behavior of backfills, is insightfully discussed, illustrating CPB's transformative potential in mining. This analysis not only informs current practices but also directs future research, advocating for an environmentally responsible and safer mining activities. This analysis is crucial for guiding future advancements in CPB technology.

2.7. References

Abdul-Hussain, N., & Fall, M. (2012). Thermo-hydro-mechanical behaviour of sodium silicate-cemented paste tailings in column experiments. Tunnelling and Underground Space Technology, 29, 85–93. https://doi.org/10.1016/J.TUST.2012.01.004

Alizadeh, R. A. (2009). Nanostructure and engineering properties of basic and modified calcium-silicate-hydrate systems. University of Ottawa (Canada).

Allen, A. J., Thomas, J. J., & Jennings, H. M. (2007). Composition and density of nanoscale calcium–silicate–hydrate in cement. Nature Materials 2007 6:4, 6(4), 311–316. https://doi.org/10.1038/nmat1871

Al-Moselly, Z., Fall, M., & Haruna, S. (2022). Further insight into the strength development of cemented paste backfill materials containing polycarboxylate ether-based superplasticizer. Journal of Building Engineering, 47, 103859. https://doi.org/10.1016/J.JOBE.2021.103859

Aylmer, F. L. (1973). Cement properties related to the behaviour of cemented fill. Proceedings Jubilee Symposium on Mine Filling, Mount Isa, North West Queensland Branch, The AusIMM, August, 59–63.

Bawden, W. F., Thompson, B. D., & Grabinsky, M. W. (2011). In-situ Monitoring of Cemented Paste Backfill. 45th US Rock Mechanics/Geomechanics Symposium.

Belem, T., & Benzaazoua, M. (2004). An overview on the use of paste backfill technology as a ground support method in cut-and-fill mines. Proceedings of the Ground Support in Mining Underground Construction, Perth, Australia, 28–30.

Belem, T., & Benzaazoua, M. (2008a). Design and application of underground mine paste backfill technology. Geotechnical and Geological Engineering, 26(2), 147–174. https://doi.org/10.1007/S10706-007-9154-3

Belem, T., & Benzaazoua, M. (2008b). Design and Application of Underground Mine Paste Backfill Technology. Geotechnical and Geological Engineering, 26(2), 147–174. https://doi.org/10.1007/s10706-007-9154-3

Belem, T., Benzaazoua, M., & Bussière, B. (2000). Mechanical behaviour of cemented paste backfill. Proceedings of 53rd Candadian Geotechnical Conference.

Belem, T., El Aatar, O., Bussière, B., Benzaazoua, M., Fall, M., & Yilmaz, E. (2006). Characterisation of self-weight consolidated paste backfill. Paste 2006: Proceedings of the Ninth International Seminar on Paste and Thickened Tailings, 333–345.

Belem, T., in, M. B.-P. of the G. S., & 2004, undefined. (n.d.). An overview on the use of paste backfill technology as a ground support method in cut-and-fill mines. Academia.Edu. Retrieved January 16, 2023, from https://www.academia.edu/download/61761696/Ground_Support_in_Mining_and_Underground_Construction_220200112-89736-dhymt9.pdf#page=1220

Benzaazoua, M., Belem, T., & Bussière, B. (2002). Chemical factors that influence the performance of mine sulphidic paste backfill. Cement and Concrete Research, 32(7), 1133–1144. https://doi.org/10.1016/S0008-8846(02)00752-4

Benzaazoua, M., Fall, M., & Belem, T. (2004). A contribution to understanding the hardening process of cemented pastefill. Minerals Engineering, 17(2), 141–152. https://doi.org/10.1016/J.MINENG.2003.10.022

Brackebusch, F. W. (1995). Basics of paste backfill systems. International Journal of Rock Mechanics and Mining Sciences and Geomechanics Abstracts, 3(32), 122A.

Bullard, J. W., Jennings, H. M., Livingston, R. A., Nonat, A., Scherer, G. W., Schweitzer, J. S., Scrivener, K. L., & Thomas, J. J. (2011). Mechanisms of cement hydration. Cement and Concrete Research, 41(12), 1208–1223. https://doi.org/10.1016/J.CEMCONRES.2010.09.011

Célestin, J. C. H., & Fall, M. (2009). Thermal conductivity of cemented paste backfill material and factors affecting it. Http://Dx.Doi.Org/10.1080/17480930902731943, 23(4), 274–290. https://doi.org/10.1080/17480930902731943

Chen, S. man, Yilmaz, E., Wang, W., & Wang, Y. ming. (2022). Curing stress effect on stability, microstructure, matric suction and electrical conductivity of cementitious tailings backfills. Construction and Building Materials, 360, 129601. https://doi.org/10.1016/J.CONBUILDMAT.2022.129601

Chen, S., Wu, A., Wang, Y., & Wang, W. (2021). Coupled effects of curing stress and curing temperature on mechanical and physical properties of cemented paste backfill. Construction and Building Materials, 273, 121746. https://doi.org/10.1016/J.CONBUILDMAT.2020.121746

Chen, W., & Brouwers, H. J. H. (2010a). Alkali binding in hydrated Portland cement paste. Cement and Concrete Research, 40(5), 716–722. https://doi.org/10.1016/j.cemconres.2009.12.007

Chen, W., & Brouwers, H. J. H. (2010b). Alkali binding in hydrated Portland cement paste. Cement and Concrete Research, 40(5), 716–722. https://doi.org/10.1016/J.CEMCONRES.2009.12.007

Cooke, R. (2001). Design procedure for hydraulic backfill distribution systems. Journal of the Southern African Institute of Mining and Metallurgy, 101(2), 97–102.

Cui, L. (2017). Multiphysics modeling and simulation of the behavior of cemented tailings backfill. Université d'Ottawa/University of Ottawa.

Cui, L., & Fall, M. (2016a). Mechanical and thermal properties of cemented tailings materials at early ages: Influence of initial temperature, curing stress and drainage conditions. Construction and Building Materials, 125, 553–563. https://doi.org/10.1016/J.CONBUILDMAT.2016.08.080

Cui, L., & Fall, M. (2016b). Mechanical and thermal properties of cemented tailings materials at early ages: Influence of initial temperature, curing stress and drainage conditions. Construction and Building Materials, 125, 553–563. https://doi.org/10.1016/J.CONBUILDMAT.2016.08.080

Diez d'Aux, M. (2008). Ultrasonic wave measurement through cement paste backfill.

Double, D. D. (1983). New developments in understanding the chemistry of cement hydration. Philosophical Transactions of the Royal Society of London. Series A, Mathematical and Physical Sciences, 310(1511), 53–66.

Edward Pierce, M., & Ontario, K. (1999). Laboratory and numerical analysis of the strength and deformation behaviour of paste backfill. https://library-archives.canada.ca/eng/services/services-libraries/theses/Pages/item.aspx?idNumber=46581329

Ercikdi, B., Cihangir, F., Kesimal, A., & Deveci, H. (2017). Practical importance of tailings for cemented paste backfill. Paste Tailings Management, 7–32. https://doi.org/10.1007/978-3-319-39682-8_2/TABLES/7

Ercikdi, B., Cihangir, F., Kesimal, A., Deveci, H., & Alp, Ì. (2010). Effect of natural pozzolans as mineral admixture on the performance of cemented-paste backfill of sulphide-rich tailings. Waste Management & Research, 28, 430–435. https://doi.org/10.1177/0734242X09351905

Ercikdi, B., Kesimal, A., Cihangir, F., Deveci, H., & Alp, I. (2009). Cemented paste backfill of sulphide-rich tailings: Importance of binder type and dosage. Cement and Concrete Composites, 31(4), 268–274. https://doi.org/10.1016/J.CEMCONCOMP.2009.01.008

Ercikdi, B., Yilmaz, T., & Külekci, G. (2014). Strength and ultrasonic properties of cemented paste backfill. Ultrasonics, 54(1), 195–204. https://doi.org/10.1016/J.ULTRAS.2013.04.013

Fall, M., Benzaazoua, M., & Ouellet, S. (2004). Effect of tailings properties on paste backfill performance. Proceedings of the 8th International Symposia on Mining with Backfill, Beijing, China, 193–202.

Fall, M., Benzaazoua, M., & Ouellet, S. (2005). Experimental characterization of the influence of tailings fineness and density on the quality of cemented paste backfill. Minerals Engineering, 18(1), 41–44. https://doi.org/10.1016/j.mineng.2004.05.012

Fall, M., Célestin, J.C., and Sen, H.F 2010. Potential use of polymer-pastefill as waste containment barrier materials. Journal of Waste Management 30: 2570-2578.

Fall, M., & Pokharel, M. (2010a). Coupled effects of sulphate and temperature on the strength development of cemented tailings backfills: Portland cement-paste backfill. Cement and Concrete Composites, 32(10), 819–828. https://doi.org/10.1016/J.CEMCONCOMP.2010.08.002

Fall, M., & Pokharel, M. (2010b). Coupled effects of sulphate and temperature on the strength development of cemented tailings backfills: Portland cement-paste backfill. Cement and Concrete Composites, 32(10), 819–828. https://doi.org/10.1016/J.CEMCONCOMP.2010.08.002

Fang, K. (2021). Testing and multiphysics modelling of the shear behaviour of rock-cemented paste backfill interface. Université d'Ottawa/University of Ottawa.

Fang, K., & Fall, M. (2018a). Effects of curing temperature on shear behaviour of cemented paste backfill-rock interface. International Journal of Rock Mechanics and Mining Sciences, 112, 184–192. https://doi.org/10.1016/J.IJRMMS.2018.10.024

Fang, K., & Fall, M. (2018b). Effects of curing temperature on shear behaviour of cemented paste backfill-rock interface. International Journal of Rock Mechanics and Mining Sciences, 112(June), 184–192. https://doi.org/10.1016/j.ijrmms.2018.10.024

Fang, K., & Fall, M. (2019). Shear Behavior of the Interface Between Rock and Cemented Backfill: Effect of Curing Stress, Drainage Condition and Backfilling Rate. Rock Mechanics and Rock Engineering, 53(1), 325–336. https://doi.org/10.1007/s00603-019-01909-2

Fourie, A. (2009). Preventing catastrophic failures and mitigating environmental impacts of tailings storage facilities. PROEPS, 1, 1067–1071. https://doi.org/10.1016/j.proeps.2009.09.164

Galaa, A. M., Thompson, B. D., Grabinsky, M. W., & Bawden, W. F. (2011). Characterizing stiffness development in hydrating mine backfill using ultrasonic wave measurements. Canadian Geotechnical Journal, 48(8), 1174–1187.

Ghirian, A. (2016a). Coupled Thermo-Hydro-Mechanical-Chemical (THMC) Processes in Cemented Tailings Backfill Structures and Implications for their Engineering Design. https://doi.org/10.20381/RUOR-5763

Ghirian, A. (2016b). Coupled thermo-hydro-mechanical-chemical (THMC) processes in cemented tailings backfill structures and implications for their engineering design. https://ruor.uottawa.ca/handle/10393/34605

Ghirian, A., & Fall, M. (2013a). Coupled thermo-hydro-mechanical-chemical behaviour of cemented paste backfill in column experiments. Part I: Physical, hydraulic and thermal processes and characteristics. Engineering Geology, 164, 195–207. https://doi.org/10.1016/J.ENGGEO.2013.01.015

Ghirian, A., & Fall, M. (2013b). Coupled thermo-hydro-mechanical–chemical behaviour of cemented paste backfill in column experiments. Part I: Physical, hydraulic and thermal processes and characteristics. Engineering Geology, 164, 195–207. https://doi.org/10.1016/J.ENGGEO.2013.01.015

Ghirian, A., & Fall, M. (2016). Strength evolution and deformation behaviour of cemented paste backfill at early ages: Effect of curing stress, filling strategy and drainage. International Journal of Mining Science and Technology, 26(5), 809–817. https://doi.org/10.1016/J.IJMST.2016.05.039

Ghirian, A., & Fall, M. (2017). Properties of cemented paste backfill. Paste Tailings Management, 59–109. https://doi.org/10.1007/978-3-319-39682-8_4/FIGURES/50

Grice, T. (1998). Underground mining with backfill. 2nd Annual Summit œ Mine Tailings Disposal Systems, Brisbane, Nov, 24–25.

Haruna, S. (2022). Effect of Superplasticizer on the Performance Properties of Cemented Paste Backfill at Different Curing Temperatures. https://doi.org/10.20381/RUOR-28427

Haruna, S., & Fall, M. (2020). Time- and temperature-dependent rheological properties of cemented paste backfill that contains superplasticizer. Powder Technology, 360, 731–740. https://doi.org/10.1016/J.POWTEC.2019.09.025

Hassani, F., Archibald, J. (1998). Mine Fill Hand Book.

Hassani, F., Razavi, S. M., & Isagon, I. (2007). A study of physical and mechanical behaviour of gelfill. CIM Bulletin, 2(5), 1–7.

Helinski, M., Fourie, A., Fahey, M., & Ismail, M. (2007). Assessment of the self-desiccation process in cemented mine backfills. Canadian Geotechnical Journal, 44(10), 1148–1156. https://doi.org/10.1139/T07-051/ASSET/IMAGES/LARGE/T07-051F9.JPEG

Henderson, A. (1998). The implementation of paste fill at the Henty gold mine. Proc. Minefill'98, 299–304.

Jiang, H. Fall, M., Li, Y., and Han J. 2019. An experimental study on compressive behaviour of cemented rockfill. Construction and Building Materials 213:10-19.

Ke, X., Hou, H., Zhou, M., Wang, Y., & Zhou, X. (2015). Effect of particle gradation on properties of fresh and hardened cemented paste backfill. Construction and Building Materials, 96, 378–382. https://doi.org/10.1016/J.CONBUILDMAT.2015.08.057

Ke, X., Zhou, X., Wang, X., Wang, T., Hou, H., & Zhou, M. (2016). Effect of tailings fineness on the pore structure development of cemented paste backfill. Construction and Building Materials, 126, 345–350. https://doi.org/10.1016/J.CONBUILDMAT.2016.09.052

Kesimal, A., Yilmaz, E., Ercikdi, B., Alp, I., & Deveci, H. (2005a). Effect of properties of tailings and binder on the short-and long-term strength and stability of cemented paste backfill. Materials Letters, 59(28), 3703–3709. https://doi.org/10.1016/J.MATLET.2005.06.042

Kesimal, A., Yilmaz, E., Ercikdi, B., Alp, I., & Deveci, H. (2005b). Effect of properties of tailings and binder on the short-and long-term strength and stability of cemented paste backfill. Materials Letters, 59(28), 3703–3709. https://doi.org/10.1016/J.MATLET.2005.06.042

Klein, K., journal, D. S.-C. geotechnical, & 2006, undefined. (2006). Effect of specimen composition on the strength development in cemented paste backfill. Cdnsciencepub.Com, 43(3), 310–324. https://doi.org/10.1139/T06-005

Landriault, D. (1995). Paste backfill mix design for Canadian underground hard rock mining. 97th Annual General Meeting of CIM. Rock Mechanics and Strata Control Session. Halifax, Nova Scotia, 238–239.

Landriault, D. (2001). Backfill in underground mining. Underground Mining Methods: Engineering Fundamentals and International Case Studies, 601–614.

le Roux, K. A., Bawden, W. F., & Grabinsky, M. W. F. (2002). Comparison of the material properties of in situ and laboratory prepared cemented paste backfill. Annual Conference, BC, Canada, 201–209.

Li, L., & Aubertin, M. (2012). A modified solution to assess the required strength of exposed backfill in mine stopes. Canadian Geotechnical Journal, 49(8), 994–1002. https://doi.org/10.1139/T2012-056/ASSET/IMAGES/T2012-056IEQ81.GIF

Li, L., & Aubertin, M. (2014). An improved method to assess the required strength of cemented backfill in underground stopes with an open face. International Journal of Mining Science and Technology, 24(4), 549–558.

Li, W., & Fall, M. (2016). Sulphate effect on the early age strength and self-desiccation of cemented paste backfill. Construction and Building Materials, 106, 296–304. https://doi.org/10.1016/J.CONBUILDMAT.2015.12.124

Liu, L., Xin, J., Huan, C., Qi, C., Zhou, W., & Song, K. I. I. L. (2020). Pore and strength characteristics of cemented paste backfill using sulphide tailings: Effect of sulphur content. Construction and Building Materials, 237, 117452. https://doi.org/10.1016/J.CONBUILDMAT.2019.117452

Nasir, O., & Fall, M. (2010). Coupling binder hydration, temperature and compressive strength development of underground cemented paste backfill at early ages. Tunnelling and Underground Space Technology, 25(1), 9–20. https://doi.org/https://doi.org/10.1016/j.tust.2009.07.008.

Orejarena, L., and Fall, M., 2008. Mechanical response of a mine composite material to extreme heat load. Bulletin of Engineering Geology and Environment 67(3):387-396.

Qi, C., Guo, L., Wu, Y., Zhang, Q., & Chen, Q. (2022). Stability Evaluation of Layered Backfill Considering Filling Interval, Backfill Strength and Creep Behavior. Minerals, 12(2), 271. https://doi.org/10.3390/MIN12020271/S1

Qiu, J., Guo, Z., Yang, L., Jiang, H., & Zhao, Y. (2020). Effect of tailings fineness on flow, strength, ultrasonic and microstructure characteristics of cemented paste backfill. Construction and Building Materials, 263, 120645. https://doi.org/10.1016/J.CONBUILDMAT.2020.120645

Rankine, R. M., & Sivakugan, N. (2007). Geotechnical properties of cemented paste backfill from Cannington Mine, Australia. Geotechnical and Geological Engineering, 25(4), 383–393. https://doi.org/10.1007/S10706-006-9104-5

Revell, M. (2000). Cannington backfill taking the pig out of paste. Paste Technology Seminar, 1–12.

Roshani, A., & Fall, M. (2020). Rheological properties of cemented paste backfill with nano-silica: Link to curing temperature. Cement and Concrete Composites, 114. https://doi.org/10.1016/J.CEMCONCOMP.2020.103785

Roux, K. le, Bawden, W., Technology, M. G.-M., & 2005, undefined. (2005a). Field properties of cemented paste backfill at the Golden Giant mine. Taylor & Francis, 114(2), 65. https://doi.org/10.1179/037178405X44557

Roux, K. le, Bawden, W., Technology, M. G.-M., & 2005, undefined. (2005b). Field properties of cemented paste backfill at the Golden Giant mine. Taylor & Francis, 114(2), 65. https://doi.org/10.1179/037178405X44557

Sheshpari, M. (2015). A review of underground mine backfilling methods with emphasis on cemented paste backfill. Electronic Journal of Geotechnical Engineering, 20(13), 5183–5208.

Simms, P., & Grabinsky, M. (2009). Direct measurement of matric suction in triaxial tests on early-age cemented paste backfill. Canadian Geotechnical Journal, 46(1), 93–101. https://doi.org/10.1139/T08-098

Swaddiwudhipong, S., Chen, D., & Zhang, M. H. (2002). Simulation of the exothermic hydration process of Portland cement. Advances in Cement Research, 14(2), 61–69. https://doi.org/10.1680/ADCR.2002.14.2.61/ASSET/IMAGES/SMALL/ADCR14-061-F6.GIF

Wang, Y., Fall, M., & Wu, A. (2016). Initial temperature-dependence of strength development and self-desiccation in cemented paste backfill that contains sodium silicate. Cement and Concrete Composites, 67, 101–110. https://doi.org/10.1016/J.CEMCONCOMP.2016.01.005

Weaver, W. S., & Luka, R. (1970). Laboratory studies of cement-stabilized mine tailings. Can. Min. Metall. Bull, 64(701), 988–1001.

Winter, N. B. (2012). Understanding cement: An introduction to cement production, cement hydration and deleterious processes in concrete. (No Title).

Wu, D., Fall, M., and Cai, S-J, 2012. Coupled modeling of temperature distribution and evolution in cemented tailings backfill structures that contains mineral admixtures. Journal of Geotechnical and Geological Engineering 30(4): 935-961.

Wu, D., Fall, M., and Cai, S-J, 2014. Numerical modelling of thermally and hydraulically coupled processes in hydrating tailings backfill columns. International Journal of Mining, Reclamation and Environment 28(3):173-199.

Xiu, Z., Wang, S., Ji, Y., Wang, F., & Ren, F. (2022). Experimental study on the triaxial mechanical behaviors of the Cemented Paste Backfill: Effect of curing time, drainage conditions and curing temperature. Journal of Environmental Management, 301, 113828. https://doi.org/10.1016/J.JENVMAN.2021.113828

Xu, S., Suorineni, F. T., Li, K., & Li, Y. (2016). Evaluation of the strength and ultrasonic properties of foam-cemented paste backfill. Https://Doi.Org/10.1080/17480930.2016.1215782, 31(8), 544–557. https://doi.org/10.1080/17480930.2016.1215782

Yan, B., Zhu, W., Hou, C., Yilmaz, E., & Saadat, M. (2020). Characterization of early age behavior of cemented paste backfill through the magnitude and frequency spectrum of ultrasonic P-wave. Construction and Building Materials, 249, 118733. https://doi.org/10.1016/J.CONBUILDMAT.2020.118733

Yilmaz, E., Benzaazoua, M., Belem, T., & Bussière, B. (2009). Effect of curing under pressure on compressive strength development of cemented paste backfill. Minerals Engineering, 22(9–10), 772–785.

Yilmaz, E., & Fall, M. (2017). Paste tailings management. In Paste Tailings Management. https://doi.org/10.1007/978-3-319-39682-8

Yilmaz, T., Ercikdi, B., Karaman, K., & Külekçi, G. (2014). Assessment of strength properties of cemented paste backfill by ultrasonic pulse velocity test. Ultrasonics, 54(5), 1386–1394. https://doi.org/10.1016/J.ULTRAS.2014.02.012

Zhang, M., He, H., Jin, X., Qu, Y., & Guo, H. (2021). Research on Key Factors Influencing Surface Subsidence of Paste Backfilling Mining in Thick Coal Seam of Deep Mine. Advances in Civil Engineering, 2021. https://doi.org/10.1155/2021/6634331

Zhang, Q. ;, Yang, K. ;, Zhang, J. ;, Wang, Q. ;, Yuan, L. ;, Shi, Z. ;, Xu, X., Zhang, Q., Yang, K., Zhang, J., Wang, Q., Yuan, L., Shi, Z., & Xu, X. (2022). A Theoretical Model of Roof Self-Stability in Solid Backfilling Mining and Its Engineering Verification. Applied Sciences 2022, Vol. 12, Page 12114, 12(23), 12114. https://doi.org/10.3390/APP12231211

CHAPTER 3. Background on Nanoparticles and Review of Previous Studies on Nanoparticles in Cementitious Materials

3.1. Introduction

As mentioned earlier, different chemical admixtures have a long history of being used to modify various properties of cementitious materials like concrete or cemented paste backfill. Typically, these admixtures are used to enhance characteristics such as mechanical strength, durability, workability, and cost-efficiency by reducing the cement content while maintaining necessary attributes. Recently, there has been increased interest in studying the effects of nanoparticles (NPs) as additives in cementitious materials, due to their unique traits such as their extremely high specific surface area (SSA) and reactivity. These traits offer the potential to improve both the mechanical and physical properties of concrete and paste backfill, common types of cementitious materials used in construction. Moreover, the use of NPs would result in the decrease of the amount of Portland cement used in cementitious materials, such as CPB, thereby improving their carbon footprint.

NPs are identified as particles with dimensions ranging from 1 to 100 nanometers in at least two out of three dimensions (Lewinski et al. 2008). Their extremely small size imparts them with the ability to react in chemical reactions very quickly, as their high SSA values mean that they have a larger contact area available for engaging in chemical reactions.

When it comes to cement-related materials, NPs can modify different properties in various ways. If a uniform dispersion of NPs can be achieved in a cement hydration reaction, NPs can serve as nucleation sites to accelerate the hydration process. Additionally, a refinement in pore structure can be expected, as NPs can be used as fillers to occupy the voids between cement particles. This leads to a denser structure or matrix of the hardened cemented material and immobilization of pore water pressure. Another notable effect of NPs on the performance of materials related to cement is the reduction in initial setting time. This is primarily due to the accelerating impact of NPs during the early stages of the hydration process (Hakamy et al., 2015; Liu et al., 2012; Oey et al., 2013; Sanchez & Sobolev, 2010; Singh et al., 2013; K. Wang et al., 2014).

In the subsequent subsections, detailed discussions will be provided about four distinct types of nanoparticles: nano-silica (SiO_2), nano-limestone ($CaCO_3$), nano-iron (Fe_2O_3), and nano-alumina (Al_2O_3). The potential applications and implications of these nanoparticles for modifying materials related to cement will be explored.

3.2. Nano-Silica

In addition to the mechanisms already mentioned related to the modifications made by NPs, other studies have suggested that the addition of NPs can also alter the chemical characteristics of the hydration process. For example, research conducted by (Thomas et al., 2009) explored the impact of adding nano-silica to the hydration process. They discovered that, in the presence of these nanoparticles, extra calcium silicate hydrate (C-S-H) particles were created on the surface of the nanoparticles due to an early pozzolanic reaction, influenced by the nanoparticles acting as nucleation seeds for the hydration products. Shih et al. (2006) examined the effects of liquid nano-silica on the microstructural and material properties of Portland cement. They prepared various samples with different nanoparticle dosages and tested them at four different curing times. Their findings demonstrated that the addition of 0.6 wt% of nanoparticles by the weight of cement displayed the best overall performance compared to other samples with varying nanoparticle dosages. They observed a 43.8% increase in compressive strength in the samples with the optimal concentration of nanoparticles compared to the control sample. Through different analysis methods such as Nuclear Magnetic Resonance(NMR), Brunauer-Emmett-Teller (BET), and Mercury Intrusion Porosimetry (MIP) tests, they found that the cement paste mixed with nanoparticles developed a denser and more stable structure compared to the pure OPC paste. Jo et al. (2007) conducted an experimental program to study the characteristics of cement mortars blended with nano-silica and compare the performance of cement paste with nano-silica and silica fume. In their microstructural analysis, they found that samples prepared with the addition of nano-SiO_2 produced a significant amount of C-S-H, resulting in denser and more compact concentrations of hydration products compared to the pure samples. They also noted a decrease in the number of calcium hydroxide crystals, due to the presence of nanoparticles, which indicates the formation of a greater amount of C-S-H compounds.

Furthermore, by tracking the heat of hydration, they found that the maximum heat released during the early stages of cement pastes was highest in samples mixed with the addition of nanoparticles, releasing 245.5 J/g of heat. In contrast, samples mixed with silica fume and control samples released 235.7 J/g and 231.1 J/g, respectively. They also measured the quantity of hydration products to better correlate their observations. They observed that, after 7 days, the remaining amount of $Ca(OH)_2$ in the cement paste was 4.06% for cement paste with nanoparticles, 6.09% for cement paste with silica fume, and 8.89% for control samples. This supports the idea that the pozzolanic reaction was more intense with the addition of nano-silica, resulting in more C-S-H and a denser microstructure.

Nano-silica's synthesis involves several sophisticated techniques, with the precipitation method, sol-gel process, vaporization, and biological approaches being the most prominent (Quercia and Brouwers 2010). Industrially, the precipitation method is favored for its scalability. It involves a meticulous reaction where sodium silicate interacts with a mineral acid, such as sulfuric acid, to produce silica gel. This gel is then processed—washed, dried, and finely ground—to yield nanoparticles of silica. The manipulation of reaction parameters, including pH, temperature, and reactant concentrations, allows precise control over the particle dimensions and physical properties (Sobolev et al. 2006).

Turning to the sol-gel process, this technique begins with the dissolution of sodium silicate or organometallic precursors like tetraethyl orthosilicate (TEOS) into a suitable solvent. This addition triggers a pH shift, setting the stage for the transformation of the initial sol into a gel (a matrix entwining both liquid and solid states) (Quercia and Brouwers 2010). The gel's maturation process, followed by controlled drying and heating, produces nano-silica with custom-tailored porosity and particle size. Notably, the sol-gel method is advantageous for its ability to engineer silica nanoparticles with designated surface modifications and to construct materials with precise porous architectures, suitable for a wide array of applications.

While the beneficial impact of nano-silica on the compressive strength and microstructure of cement paste is promising, some research indicates that the addition of nano-silica may negatively affect the workability of the cement paste, largely due to its high specific surface area (SSA)(Sobolev et al. 2006). To address this issue, Kawashima et al. (2013) experimented with

partially replacing the Ordinary Portland Cement (OPC) with fly ash, a pozzolanic material known to enhance the workability of cementitious materials. This approach intended to balance the benefits of each supplementary material, with nano-silica improving the mechanical performance of the cement paste and fly ash enhancing its workability.

Another distinguishing aspect of their study was the extended curing time for the samples, intended to provide a clearer understanding of the impact of nano-silica on the long-term strength of the cement paste. The results demonstrated that the addition of nanoparticles significantly improved the early age strength of the cement mortars. However, for more advanced ages, such as 3 months, no significant difference in strength development was observed compared to the control sample.

The researchers suggested that the explanation for this behavior might be that fly ash particles are unable to hydrate at later ages due to a lack of sufficient calcium hydroxide ($Ca(OH)_2$) compounds and lower calcium-to-silica (Ca/Si) hydrates, which act as a hydration barrier surrounding the fly ash particle surfaces. Both of these factors are considered to be consequences of the intense hydration of nano-silica in the early curing stage.

Koohestani et al. (2016) pioneered the use of nano-silica in paste backfill materials, utilizing Tetraethyl-Orthosilicate (TEOS) and Tetramethyl-Orthosilicate (TMOS) as the foundational elements in producing nano-silica. The development of nanoparticles using these precursors fundamentally involves the sol-gel process. This intricate process begins with a precursor solution, known as a 'sol,' which then undergoes hydrolysis.

During hydrolysis, the sol experiences a transformation and eventually converts into an inorganic solid, more commonly referred to as a 'silica gel.' This transformation is not a simple phase change, but rather it occurs through a process of inorganic polymerization, often described as condensation. In this method, the small molecules of the sol interact, bond, and grow into large polymer networks, leading to the formation of the inorganic solid or silica gel. Therefore, the sol-gel process presents a mechanism for controlling the growth of nanoparticles. Figure 3-1. a) Chemical presentation of hydrolysis reaction of TEOS, b) Pozzolanic reaction of TEOS and CH represents a schematic representation of chemical reaction for producing nano-silica using TEOS precursor.

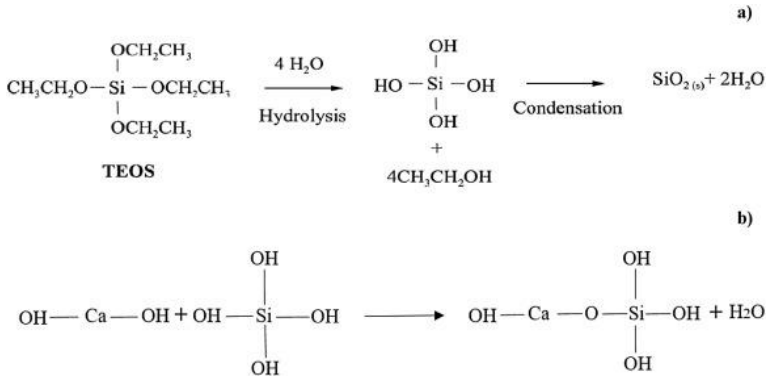

Figure 3-1. a) Chemical presentation of hydrolysis reaction of TEOS, b) Pozzolanic reaction of TEOS and CH

In this experimental project, CPB samples were prepared using two distinct types of binder: Ordinary Portland Cement (OPC) and slag-cement. They also varied the Tetraethyl-Orthosilicate (TEOS) dosages, ranging from 0.7 to 14 wt.% of the binder. To mitigate the potential issue of nanoparticle agglomeration, they employed an ether-based Polycarboxylate superplasticizer (PCS). All the CPB samples underwent a 28-day curing process, with testing carried out at multiple intervals - on the 3rd, 7th, 14th, and 28th day of curing.

They conducted an array of tests to scrutinize the impact of TEOS-PCS on the CPB's mechanical performance. This included tests for Unconfined Compressive Strength (UCS), slump height measurement, differential thermogravimetric analysis (DTG), and monitoring the progression of gravimetric water.

Their findings showed that the addition of TEOS, coupled with the presence of PCS, could significantly bolster the compressive strength development of the CPB during the early stages of curing. This is primarily due to the various beneficial mechanisms that nano-silica introduces mentioned above, thereby enhancing the CPB's mechanical performance. Figure 3-2 illustrates the UCS testing results of CPB samples prepared with varying TEOS dosages.

The DTG results further substantiated the presence of a higher volume of produced Calcium-Silicate-Hydrate (C-S-H), owing to the contribution of nano-silica in the hydration process. Interestingly, they also discovered that samples prepared with a lower binder content showcased a more substantial improvement in strength development compared to those with a higher binder content. However, the underlying reason behind this observation remains unclear. Figure

3-3 highlights the improvement in UCS values for samples prepared with different binder dosages.

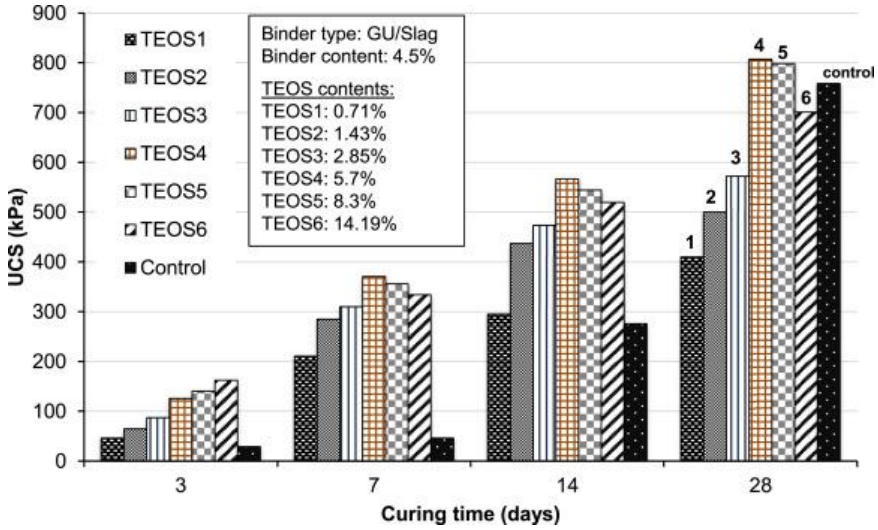

Figure 3-2. Effect of different TEOS dosage on strength development of CPB (Koohestani et al. 2016)

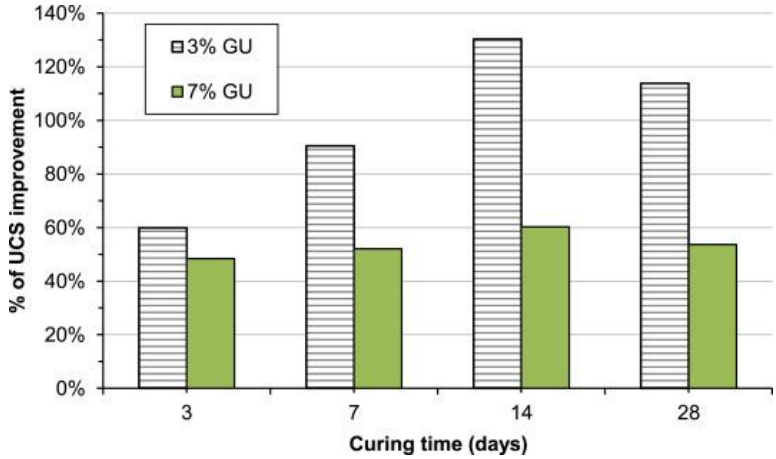

Figure 3-3. Impact of different dosage of binder on UCS values improvement of CPB samples (Koohestani et al. 2016)

3.3. Nano-calcium carbonate

Limestone, widely used as a supplementary cementitious material in the construction industry, can significantly improve various aspects of cementitious materials properties. It is naturally present in the form of different minerals like calcite, aragonite, vaterite, and amorphous calcium carbonate (Wang et al. 2018, Cao et al. 2019).

The production of nano-calcium carbonate encompasses various methods, such as precipitation, emulsion, mechanical, polymerization, and biological processes (Fadia et al. 2021). The precipitation method, which is widely adopted for nano-calcium carbonate synthesis, entails generating CO_3^{-2} ions by either dissolving CO_2 in water or by the slow hydrolysis of compounds such as ammonium carbonate or dimethyl carbonate under alkaline conditions. This approach, highlighted by Groboillot et al. (1994), is renowned for its simplicity and does not require additives, relying instead on the straightforward mixing of supersaturated sodium carbonate (Na_2CO_3) and calcium chloride ($CaCl_2$) solutions to synthesize naked calcium carbonate micro-particles.

Carbonation stands out as another prevalent method for producing nano-calcium carbonate on a large scale (Fadia et al. 2021). This process involves introducing CO_2 gas into slaked lime ($Ca(OH)_2$), leading to the formation of $CaCO_3$ particles. As described by Fadia et al. (2021), the carbonation method predominantly yields rhombohedral and cubic calcite crystals. Notably, the synthesis of the calcite phase remains stable against variations such as high pressure, minor temperature changes, and the presence of polymers and surfactants, underscoring the robustness of this synthesis technique.

Similar to nano-silica, prior research has demonstrated that limestone can enhance the characteristics of cementitious materials through two primary mechanisms: the filler effect and the chemical reaction. However, it is worth noting that the filler effect involves a combination of specific sub-mechanisms, including the filler effect itself, the nucleation effect, and the dilution effect.

3.3.1 Filler effect

The filler effect of limestone is largely determined by its particle size distribution. This property has a direct impact on the packing density of cement mortar or concrete. When limestone powder with a finer particle size than cement grains is used, the packing density of the final mortar mixture can be increased compared to a scenario where limestone powder is of the same or larger size than cement grains (Cao et al. 2019). Previous studies have shown that the use of nano-calcium carbonate in ultra-high performance concrete (UHPC) improves compressive

strength and reduces flowability. This happens because the fine grains of nano-limestone fill the gaps between cement grains and aggregates (Li et al. 2015a). A decrease in flowability could be due to the large specific surface area of the nano-limestone, requiring more water to cover its particles.

3.3.2 Nucleation effect

Numerous researchers have established that limestone can provide nucleation sites for hydration products, accelerating the hydration process), and enhancing the degree of cement hydration (Cyr et al. 2006, Camiletti et al. 2013, Cao et al. 2019, Benkirane et al. 2023). However, the nucleation effect is highly dependent on particle size. Hence, it can be expected that nano-limestone, due to its smaller size, would provide more nucleation sites for hydration products compared to its coarse-grained counterpart (Li et al. 2015b)

3.3.3 Dilution effect

When nano-limestone is used as an additive in concrete, the "dilution effect" refers to the reduction in cement quantity for a given volume of concrete. Since limestone doesn't have pozzolanic characteristics, partially substituting cement with nano-limestone could make more free water available for cement grain reaction, increasing the degree of cement hydration (Cyr et al. 2006, Deschner et al. 2012, Scrivener et al. 2015). However, as nano-limestone is not as reactive as cement, this substitution might slow down the overall rate of cement hydration, leading to slower setting time and initial strength development. While nano-limestone is typically less reactive than cement, it can engage in secondary, pozzolanic reactions with the free lime (calcium hydroxide) released by cement hydration, contributing to long-term strength development and concrete durability, albeit more slowly than cement hydration.

3.3.4 Chemical effect

The chemical effect of limestone depends significantly on its particle size distribution and the amount of available alumina in the hydration medium. Incorporating nano-limestone can modify

the physical properties of Calcium Silicate Hydrate (C-S-H) by altering its morphology into shorter and thicker C-S-H fibers (Nehdi et al., 1996).

Wang et al., (2018) concluded that integrating nano-calcium accelerates cement grain hydration by increasing the C_3S reaction rate and the heat of hydration. Furthermore, the addition of nano-calcium elevates the degree of cement hydration, subsequently increasing the amount of C-S-H and Calcium Hydroxide (CH) during the early curing stages. However, no significant changes were observed during the advanced curing stages. According to their findings, incorporating nano-calcium significantly refines the microstructure of cement mortar, primarily through the nucleation and filler effects.

Sato et al. (2010) carried out a comprehensive study analyzing the impact of the particle size distribution and concentration of nano-calcium on the hydration reaction of cement. Their findings revealed that nano-calcium particles could enhance the rate of the hydration process, particularly during the induction period. This is when Tricalcium Silicate (C_3S), a key component of cement, begins to undergo hydration, a process significantly expedited by the nucleation characteristic of nano-calcium carbonate. They further noted that a higher concentration of nano-calcium tends to have a more pronounced impact on increasing the hydration rate (Sato and Beaudoin, 2015; Sato and Diallo, 2010). These findings align well with the research conducted by Wu et al. (2016). As depicted in Figure 3-4, the inclusion of different doses of nano-calcium particles led to a reduction in the dormant period. They explained this phenomenon by noting that nano-calcium possesses the ability to absorb calcium ions present in the hydration medium. As a result of this absorption, the concentration of calcium ions surrounding the C_3S decreases, which directly accelerates the hydration of C_3S.

In addition, the carbonate ions dissolved in the hydration medium due to the presence of nano-calcium can potentially react with Tricalcium Aluminate (C_3A), leading to the formation of monocarboaluminates (Wu et al. 2016). Finally, they noted that introducing nano-calcium could lead to the formation of a greater quantity of Calcium Silicate Hydrate (C-S-H) and calcium hydroxide ($Ca(OH)_2$). This occurs as a result of the reaction between nano-calcium and C3S, which could clarify the quicker and more intense release of hydration heat, as illustrated in Figure 3-4.

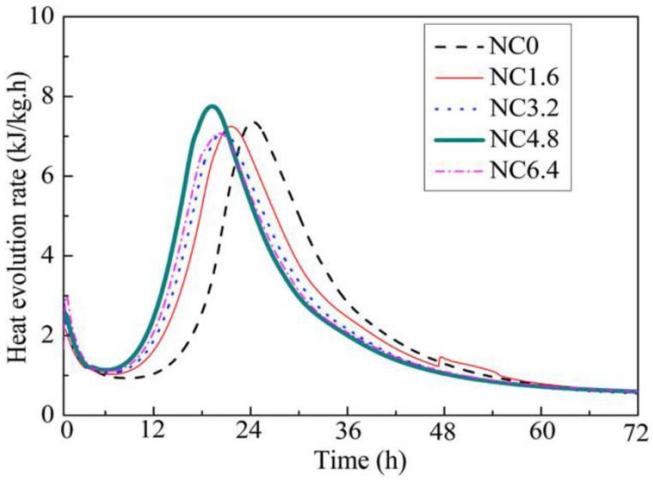

Figure 3-4. Effect of different dosage of nano-calcium on heat release of hydration reaction (Wu et al. 2016)

In a distinct study led by Xiaoyan et al. (2012), the researchers reported that the addition of nano-calcium did not significantly alter the water content required to maintain the consistency of the paste when compared to instances where nanoparticles were not incorporated into the paste. The team attributed this behavior to the filler effect of nano-calcium, which fills the pores around the cement grains, effectively immobilizing the free water that helps to maintain the consistency of the paste. However, it's also noted that due to the large surface area of the nanoparticles, a higher dosage of water content is needed to activate them and reap their beneficial effects. Therefore, while the addition of nano-calcium may not change the consistency of the paste mixture, it might adversely impact the transportability and workability of the final cement paste. Xiaoyan et al. also confirmed that the introduction of nano-calcium led to a shortened initial and final setting time due to an accelerated rate of hydration process, a mechanism mentioned previously. Moreover, when they tested the flexural strength of cement paste blended with nano-calcium, they reported a strength increase in all samples treated with nano-calcium. The significance of this increase in strength at the early age of curing was especially pronounced for the samples with a higher dosage of nanoparticles. In conclusion, after considering all aspects of the mechanical performance of cement pastes studied, they determined that the optimal dosage of nano-calcium is 1%, which enhanced all the studied mechanical indices of tested samples, such as compressive strength, flexural strength, and shrinkage.

In a different research effort, Camiletti et al. (2013) examined the influence of both micro and nano-limestone on the early-age properties of ultra-high-performance concrete (UHPC) subjected to various thermal loadings (10, 20 °C). They discovered that nano-limestone could accelerate the hydration process due to its promising nucleation and filler effects. The researchers also stated that the addition of both forms of limestone, micro and nano-particles, could increase the flowability of the UHPC, depending on the content of the nanoparticles. The team observed that the addition of a nanoparticle dosage less than 5% could increase the flowability of the UHPC by 30%. However, raising the nanoparticle content between 5 to 15% negatively impacted the UHPC's flowability by reducing it up to 54%. This behavior was explained by the fact that a lower dosage of nanoparticles could facilitate the movement of cement grains, while a higher dosage would significantly increase the water content required to thoroughly wet the nanoparticles, due to their exceptionally high specific surface area.

Regarding the setting time, they stated that regardless of the curing time, the setting time significantly reduced in the case of adding both forms of calcium carbonate. More specifically, samples prepared with an addition of 5% nano-calcium had the shortest setting time compared to other samples with different nanoparticle dosages and the control sample cured at both curing temperatures.

In terms of the development of compressive strength, the team found that in both of the studied temperatures, samples prepared with the addition of nano-calcium at a dosage of 5% exhibited the best performance among all other samples. This was due to the microstructural refinement brought about by the promising filler effect and the increase in hydration products caused by the additional nucleation sites provided by the nanoparticles. However, at the higher temperature, the lack of available space for the growth of hydration products inhibited the continuation of the accelerated hydration caused by the presence of nanoparticles.

3.4. Nano-alumina

Nano-alumina is another nanomaterial frequently utilized as an additive within the cement and concrete industry. The fabrication of nano-alumina encompasses both mechanical and chemical approaches. Mechanical techniques include mechanical ball milling, laser ablation, and

flame synthesis, while chemical methods cover hydrothermal synthesis, vapor-phase reactions, co-precipitation, combustion processes, sol-gel techniques, and the leaching of kaolin (Thiruchitrambalam et al. 2004, Tok et al. 2006, Rogojan et al. 2011, Isfahani et al. 2012).

Among these, the sol-gel process is distinguished as the most prevalent method for nano-alumina production (Behera et al. 2016). This technique involves forming a network of oxides through a polycondensation reaction of molecular precursors. Its advantages include the ability to yield pure, homogeneous nano-alumina powders without the requirement for high-temperature conditions. However, the sol-gel method is not without its challenges, as highlighted by Behera et al. (2016). It incurs a higher cost due to the need for specialized storage facilities and necessitates a meticulously controlled transformation system to ensure the quality of the final product.

A variety of studies have delved into the impact of nano-alumina, a type of nanomaterial, on the behavior and performance of cement mortars and concrete (Said et al. 2019, 2020, Alomayri 2019a, Matalkah et al. 2022). These research initiatives have underlined that nano-alumina may be a positive addition to cement, owing to its unique properties such as a high surface area, excellent thermal stability, and distinctive mechanical traits. Through these investigations, it's been established that nano-alumina has the potential to significantly improve the mechanical strength and durability of cement and concrete, acting as a filler to bolster the material's structure.

Beyond traditional cementitious materials, nano-alumina has found applications in the rapidly evolving geopolymer industry (Chindaprasirt et al. 2012a, Phoo-ngernkham et al. 2014, Nazari and Sanjayan 2015, Alomayri 2019b). Certain research findings indicate that introducing nano-alumina to geopolymeric binders, specifically those with high calcium content, can accelerate the setting process. However, it's important to note that this faster setting time does not seem to correspond with an increase in compressive strength, a crucial factor in the durability of the material (Chindaprasirt et al. 2012b).

In their pioneering work, Campillo et al. (2007) embarked on a study to examine the effect of nano-alumina on the early-age strength of belite cement. While belite cement is recognized for its satisfactory long-term mechanical performance, concerns about its strength in the early stages

have led to certain limitations on its industrial use. To address this issue, the researchers investigated the possibility of using nano-alumina as a supplement. They tested two types of nano-alumina: agglomerated dry alumina (ADA) and colloidal alumina (CA) that was dispersed in a water solution.

Their research concluded that the introduction of nano-alumina can have a beneficial impact on the strength of the cement samples, particularly in the early stages of curing. The samples that incorporated CA nano-alumina exhibited greater strength than those with ADA and the control samples. This was attributed to the smaller particle size of the nanomaterials in the CA nano-alumina, which seemed to have a more significant effect on the cement's strength. While the addition of nano-alumina did not significantly alter the overall porosity (the total volume of empty spaces), the researchers observed a notable change in pore sizes, which became smaller as a result of the nano-alumina addition.

In a separate study, Li et al. (2006) conducted an in-depth investigation into the effect of nano-alumina on reinforced cement composites. Their research findings indicated that the inclusion of nano-alumina led to an increase in the elasticity, or ability to return to its original shape after being deformed, of the cement mortars. The researchers also found a direct correlation between the amount of nano-alumina used and the resulting elasticity: higher nano-alumina dosages resulted in greater elasticity. Figure 3-5. provides a visual representation of these findings, displaying the results of their measurements of the cement's elastic modulus, a measure of a material's resistance to being deformed when a force is applied.

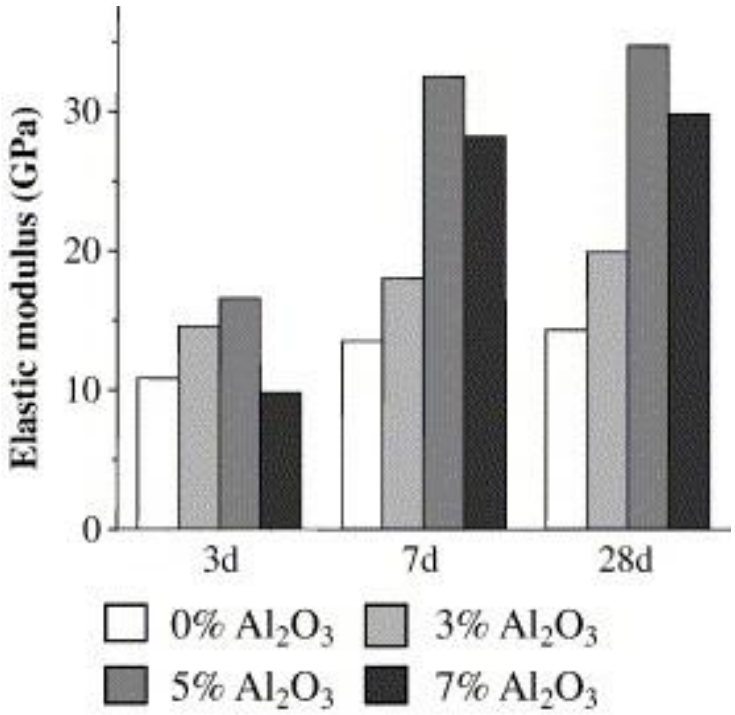

Figure 3-5. effect of nano-alumina on the evolution of elastic modulus of cement mortars (Li et al. 2006)

When it came to the compressive strength of the studied samples, the researchers noted that the incorporation of nano-alumina did not lead to a marked improvement in this property. Even more, in certain instances, the samples mixed with nano-alumina exhibited a lower development of compressive strength compared to the standard mortar mix, as depicted in Figure 3-6.

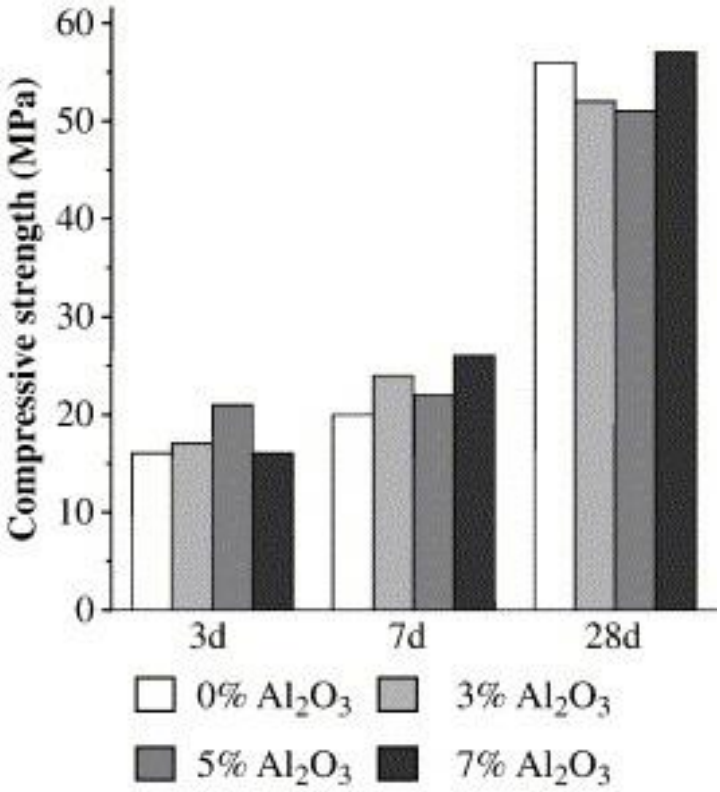

Figure 3-6. Evolution of compressive strength in cement mortars subject to addition of nano-alumina (Li et al. 2006)

3.5. Nano-iron oxide

Nano-iron oxide is widely employed in the construction industry as a supplementary cementitious material (SCM), intended to enhance various properties of cement mortars and concrete. Nazari et al. (2010) explored the effects of substituting a portion of cement with nano-iron oxide particles and concluded that an increase in nano-iron oxide dosage correspondingly increased the strength of the concrete samples tested. Optimal strength gains were recorded with a 1% replacement of cement by nano-iron oxide particles. However, this enhancement in mechanical strength was counterbalanced by a reduction in concrete workability. The study attributed this phenomenon primarily to the swift consumption of calcium hydroxide ($Ca(OH)_2$) produced during the hydration of Portland cement, particularly at early stages, due to the high reactivity of nano- Fe_2O_3 particles. Consequently, cement hydration is expedited, and a greater volume of reaction products is formed. Additionally, nano- Fe_2O_3 particles improve the particle

packing density in the cement blend, leading to a decrease in the volume of larger pores within the cement paste.

Yazdi et al. (2011) also examined the influence of nano-iron oxide on the morphological properties and microstructure of cement mortar. They found that the addition of 1% and 3% nano-iron oxide notably improved mechanical characteristics like strength. Microstructural analyses of the samples indicated that nano-iron oxide particles acted as a filler material, diminishing the size of large $Ca(OH)_2$ crystals and yielding denser, more compact hydrate products such as calcium silicate hydrate (C-S-H) and calcium hydroxide (CH).

Furthermore, Seifan et al. (2022) assessed nano-iron oxide particles' effects on the workability, strength, and absorption rate of cement mortar containing fly ash. Their findings suggest that nano-iron oxide enhances the mechanical properties of cement mortars through various mechanisms, including a more significant filling effect and a pronounced impact on cement hydration.

Despite the considerable research on nano-iron oxide's impact on concrete and cement mortars, few studies have examined its effect on the geotechnical performance of Cemented Paste Backfill (CPB). Consequently, this study aims to bridge this gap by investigating the influence of nano-iron oxide on CPB behavior.

3.6. Conclusions

The literature review presented above indicates that almost all the previous on the impact of nanoparticles on the properties of cementitious materials focussed on conventional concrete or mortar materials. Since concrete and mortar are different from CPB the results related to concrete and mortar are not directly applicable to CPB. Moreover, only limited studies were carried out on the effect of nano-silica particles on strength and microstructure of CPB which concluded that addition of NPs could potentially enhance the studied CPB's parameters. However, these ignored the effects of nano-silica particles on relevant engineering properties of CPB, such as pore water pressure evolution, self-desiccation. Moreover, no previous studies have addressed the impact of other types of nanoparticles, such nano-carbonates, nano-iron and nano-alumina, on key engineering properties of CPB (e.g., strength, microstructural properties,

pore water pressure, self-desiccation). In addition, from this literature review, it is clear that no previous investigations have examined the geotechnical behaviour of CPB plug enhanced with nanoparticles by using column experiments. The effects of field curing conditions, such as field vertical stresses and non-isothermal temperature conditions on geotechnical behaviour and performance of CPB plug with nanoparticles have not been studied . Consequently, they are research gaps and needs to be addressed.

3.7. References

Alomayri, T. (2019a). Experimental study of the microstructural and mechanical properties of geopolymer paste with nano material (Al2O3). Journal of Building Engineering, 25, 100788. https://doi.org/10.1016/J.JOBE.2019.100788

Alomayri, T. (2019b). Experimental study of the microstructural and mechanical properties of geopolymer paste with nano material (Al2O3). Journal of Building Engineering, 25, 100788. https://doi.org/10.1016/J.JOBE.2019.100788

Camiletti, J., Soliman, A. M., & Nehdi, M. L. (2013). Effects of nano- and micro-limestone addition on early-age properties of ultra-high-performance concrete. Materials and Structures/Materiaux et Constructions, 46(6), 881–898. https://doi.org/10.1617/S11527-012-9940-0/FIGURES/17

Campillo, I., Guerrero, A., Dolado, J. S., Porro, A., Ibáñez, J. A., & Goñi, S. (2007). Improvement of initial mechanical strength by nanoalumina in belite cements. Materials Letters, 61(8–9), 1889–1892. https://doi.org/10.1016/J.MATLET.2006.07.150

Cao, M., Ming, X., He, K., Li, L., & Shen, S. (2019). Effect of Macro-, Micro- and Nano-Calcium Carbonate on Properties of Cementitious Composites—A Review. Materials 2019, Vol. 12, Page 781, 12(5), 781. https://doi.org/10.3390/MA12050781

Chindaprasirt, P., De Silva, P., Sagoe-Crentsil, K., & Hanjitsuwan, S. (2012a). Effect of SiO 2 and Al 2O 3on the setting and hardening of high calcium fly ash-based geopolymer systems. Journal of Materials Science, 47(12), 4876–4883. https://doi.org/10.1007/S10853-012-6353-Y/TABLES/4

Chindaprasirt, P., De Silva, P., Sagoe-Crentsil, K., & Hanjitsuwan, S. (2012b). Effect of SiO 2 and Al 2O 3on the setting and hardening of high calcium fly ash-based geopolymer systems. Journal of Materials Science, 47(12), 4876–4883. https://doi.org/10.1007/S10853-012-6353-Y/TABLES/4

Cyr, M., Lawrence, P., & Ringot, E. (2006). Efficiency of mineral admixtures in mortars: Quantification of the physical and chemical effects of fine admixtures in relation with compressive strength. Cement and Concrete Research, 36(2), 264–277. https://doi.org/10.1016/J.CEMCONRES.2005.07.001

Deschner, F., Winnefeld, F., Lothenbach, B., Seufert, S., Schwesig, P., Dittrich, S., Goetz-Neunhoeffer, F., & Neubauer, J. (2012). Hydration of Portland cement with high replacement by siliceous fly ash. https://doi.org/10.1016/j.cemconres.2012.06.009

Hakamy, A., Shaikh, F. U. A., & Low, I. M. (2015). Characteristics of nanoclay and calcined nanoclay-cement nanocomposites. Composites Part B: Engineering, 78, 174–184.

Jo, B. W., Kim, C. H., Tae, G. ho, & Park, J. Bin. (2007). Characteristics of cement mortar with nano-SiO2 particles. Construction and Building Materials, 21(6), 1351–1355. https://doi.org/10.1016/J.CONBUILDMAT.2005.12.020

Kawashima, S., Hou, P., Corr, D. J., & Shah, S. P. (2013). Modification of cement-based materials with nanoparticles. Cement and Concrete Composites, 36(1), 8–15. https://doi.org/10.1016/J.CEMCONCOMP.2012.06.012

Koohestani, B., Belem, T., Koubaa, A., & Bussière, B. (2016). Experimental investigation into the compressive strength development of cemented paste backfill containing Nano-silica. Cement and Concrete Composites, 72, 180–189. https://doi.org/10.1016/J.CEMCONCOMP.2016.06.016

Lewinski, N., Colvin, V., & Drezek, R. (2008). Cytotoxicity of nanopartides. Small, 4(1), 26–49. https://doi.org/10.1002/SMLL.200700595

Li, W., Huang, Z., Zu, T., Shi, C., Duan, W. H., & Shah, S. P. (2015a). Influence of Nanolimestone on the Hydration, Mechanical Strength, and Autogenous Shrinkage of Ultrahigh-Performance Concrete. Journal of Materials in Civil Engineering, 28(1), 04015068. https://doi.org/10.1061/(ASCE)MT.1943-5533.0001327

Li, W., Huang, Z., Zu, T., Shi, C., Duan, W. H., & Shah, S. P. (2015b). Influence of Nanolimestone on the Hydration, Mechanical Strength, and Autogenous Shrinkage of Ultrahigh-Performance Concrete. Journal of Materials in Civil Engineering, 28(1), 04015068. https://doi.org/10.1061/(ASCE)MT.1943-5533.0001327

Li, Z., Wang, H., He, S., Lu, Y., & Wang, M. (2006). Investigations on the preparation and mechanical properties of the nano-alumina reinforced cement composite. Materials Letters, 60(3), 356–359. https://doi.org/10.1016/J.MATLET.2005.08.061

Liu, X., Chen, L., Liu, A., & Wang, X. (2012). Effect of nano-CaCO3 on properties of cement paste. Energy Procedia, 16, 991–996.

Matalkah, F., Ababneh, A., & Aqel, R. (2022). Effects of nanomaterials on mechanical properties, durability characteristics and microstructural features of alkali-activated binders: A comprehensive review. Construction and Building Materials, 336, 127545. https://doi.org/10.1016/J.CONBUILDMAT.2022.127545

Nazari, A., & Sanjayan, J. G. (2015). Hybrid effects of alumina and silica nanoparticles on water absorption of geopolymers: Application of Taguchi approach. Measurement, 60, 240–246. https://doi.org/10.1016/J.MEASUREMENT.2014.10.004

Nehdi, M., Mindess, S., & Altcin, P.-C. (1996). PII SOOOg-g846(96)00071-3 OPTIMIZATION OF HIGH STRENGTH LIMESTONE FILLER CEMENT MORTARS. Cement and Concrete Research, 26(6), 883–893.

Oey, T., Kumar, A., Bullard, J. W., Neithalath, N., & Sant, G. (2013). The Filler Effect: The Influence of Filler Content and Surface Area on Cementitious Reaction Rates. Journal of the American Ceramic Society, 96(6), 1978–1990. https://doi.org/10.1111/JACE.12264

Phoo-ngernkham, T., Chindaprasirt, P., Sata, V., Hanjitsuwan, S., & Hatanaka, S. (2014). The effect of adding nano-SiO2 and nano-Al2O3 on properties of high calcium fly ash geopolymer cured at ambient temperature. Materials & Design, 55, 58–65. https://doi.org/10.1016/J.MATDES.2013.09.049

Said, S., Mikhail, S., & Riad, M. (2019). Recent progress in preparations and applications of meso-porous alumina. Materials Science for Energy Technologies, 2(2), 288–297. https://doi.org/10.1016/J.MSET.2019.02.005

Said, S., Mikhail, S., & Riad, M. (2020). Recent processes for the production of alumina nano-particles. Materials Science for Energy Technologies, 3, 344–363. https://doi.org/10.1016/J.MSET.2020.02.001

Sanchez, F., & Sobolev, K. (2010). Nanotechnology in concrete–a review. Construction and Building Materials, 24(11), 2060–2071.

Sato, T., & Beaudoin, J. J. (2015). Effect of nano-CaCO3 on hydration of cement containing supplementary cementitious materials. Https://Doi.Org/10.1680/Adcr.9.00016, 23(1), 33–43. https://doi.org/10.1680/ADCR.9.00016

Sato, T., & Diallo, F. (2010). Seeding effect of nano-CaCO3 on the hydration of tricalcium silicate. Transportation Research Record, 2141(1), 61–67.

Scrivener, K. L., Lothenbach, B., De Belie, N., Gruyaert, E., Skibsted, J., Snellings, R., & Vollpracht, A. (2015). TC 238-SCM: hydration and microstructure of concrete with SCMs: State of the art on methods to determine degree of reaction of SCMs. Materials and Structures/Materiaux et Constructions, 48(4), 835–862. https://doi.org/10.1617/S11527-015-0527-4/FIGURES/21

Shih, J. Y., Chang, T. P., & Hsiao, T. C. (2006). Effect of nanosilica on characterization of Portland cement composite. Materials Science and Engineering: A, 424(1–2), 266–274. https://doi.org/10.1016/J.MSEA.2006.03.010

Singh, L. P., Karade, S. R., Bhattacharyya, S. K., Yousuf, M. M., & Ahalawat, S. (2013). Beneficial role of nanosilica in cement based materials–A review. Construction and Building Materials, 47, 1069–1077.

Sobolev, K., Flores, I., Hermosillo, R., & Torres-Martínez, L. M. (2006). Nanomaterials and nanotechnology for high-performance cement composites. Proceedings of ACI Session on Nanotechnology of Concrete: Recent Developments and Future Perspectives, 7, 93–120.

Thomas, J. J., Jennings, H. M., & Chen, J. J. (2009). Influence of nucleation seeding on the hydration mechanisms of tricalcium silicate and cement. Journal of Physical Chemistry C, 113(11), 4327–4334. https://doi.org/10.1021/JP809811W

Wang, D., Shi, C., Farzadnia, N., Shi, Z., Jia, H., & Ou, Z. (2018). A review on use of limestone powder in cement-based materials: Mechanism, hydration and microstructures.

Construction and Building Materials, 181, 659–672. https://doi.org/10.1016/J.CONBUILDMAT.2018.06.075

Wang, K., Tanesi, J., & Ardani, A. (2014). Effects of nanomaterials on the hydration kinetics and rheology of Portland cement pastes.

Wu, Z., Shi, C., Khayat, K. H., & Wan, S. (2016). Effects of different nanomaterials on hardening and performance of ultra-high strength concrete (UHSC). Cement and Concrete Composites, 70, 24–34. https://doi.org/10.1016/J.CEMCONCOMP.2016.03.003

Xiaoyan, L., Ch, L., Aihua, L., & Xinrui, W. (2012). Effect of Nano-CaCO3 on Properties of Cement Paste. Energy Procedia, 16(2012), 991–996.

CHAPTER 4. Technical Paper I: Strength and suction development of nano-cemented paste tailings materials

Published in Cleaner Materials Journals, Volume 8, June 2023, 100190

https://doi.org/10.1016/j.clema.2023.100190

Amirreza Saremi, Mamadou Fall

4.1. Abstract

This paper presents an experimental study of the strength and suction development of cemented paste backfill (CPB), which is an innovative cementitious construction material for mining (made by recycling mine waste into a construction material) and modified with nanoparticle (NP) additives. The effects of different amounts of four types of NP additives, including nano-silica (SiO_2), nano-calcium carbonate ($CaCO_3$), nano-iron oxide (Fe_2O_3), and nano-aluminum oxide (Al_2O_3), on the key engineering properties of CPB are investigated. An ether-based polycarboxylate superplasticizer (SP) is added to the backfill to help the NPs to better disperse in the mixture. Ordinary Portland cement is used as the binder in the CPB mixture. Uniaxial compressive tests (UCS) are conducted to determine the strength of the CPB, while suction monitoring experiments are performed to evaluate changes in suction with time. To understand the effects of the NP additives, different microstructural analyses and tests, including thermal analyses (thermogravimetry (TG), differential thermogravimetry (DTG)), mercury intrusion porosimetry (MIP), and X-ray diffraction (XRD) are conducted on the nano-CPB and the cement paste of nano-CPB. The results indicate that the addition of NP additives in the absence of SP results in lower strength due to high likelihood of agglomeration. In contrast, samples with SP and NP additives show a higher UCS and more suction than the control sample at the early ages of curing. It has been observed that the addition of NP additives results in the generation of more hydration products which enhance the interparticle friction and packing density of the CPB structure. Higher strength is obtained by increasing the SP content (0.25%) with the same NP content (1%). Enhancement of the strength of CPB and increase in suction, particularly at early

ages, can have great importance in speeding up the mining cycle and thus increasing mining productivity, which is obviously associated with financial benefits to the mine.

Keywords: cemented paste backfill; silica tailings; mine; nanoparticles; strength; suction, cement additives.

4.2. Introduction

The mining industry is a critical part of economic development in most developed and developing nations. The demand for important minerals has increased dramatically during the last several decades, which has necessitated the extraction of more ore bodies from the earth. Mining operations create a significant quantity of tailings in extracting and processing minerals from the ore bodies. Surface disposal of tailings, the most frequently used technique of storing mine waste, is potentially hazardous to the environment in many ways. First, due to high water content of tailings and difficulties in construction, typical tailings impoundments are susceptible to geotechnical failures (for e.g., liquefaction failure, dam collapse, foundation failure) that often have significant consequences (e.g., casualties, financial loss, social and environmental impacts). Second, from an environmental perspective, the surface disposal of tailings increases the risk of environmental contamination by exposing dangerous components, such as heavy metals and acidic components, to the environment(Yilmaz and Fall 2017). Therefore, it has become necessary to find another technique to manage mine wastes more effectively.

Backfilling has been proposed as a more environmentally friendly tailings management technique and widely used in underground mines globally. Backfilling is the process of returning a significant quantity of the mine waste (e.g., tailings) into the underground mine cavities or stopes (Yilmaz et al. 2004, Fall and Benzaazoua 2005, Sivakugan et al. 2006). In recent years, cemented paste backfilling has become one of the most innovative techniques in mine backfilling. Typically cemented paste backfill (CPB) is a mixture of tailings (75-85 wt %), hydraulic binder (3-9 wt % of total dry paste weight) and water (Yilmaz and Fall 2017).

The mechanical strength of cemented paste backfill (CPB) is intrinsically linked to its mechanical stability. A CPB with a high mechanical strength offers better ground support and improves the overall safety of underground mining operations. Consequently, the rate at which CPB gains mechanical strength is equally important, as it determines the efficiency and productivity of the mining process. A faster strength-gaining rate allows for quicker re-entry of the mine workers into the backfilled areas after a mined stope is backfilled with the CPB, optimizing the work schedule, and minimizing potential delays which these factors can be considered critical factors for productivity of the mine from financial point of view. Additionally, a rapid strength-gaining

rate contributes to a more effective management of mine tailings and supports environmentally sustainable mining practices by ensuring the timely and secure containment of the tailings material. The uniaxial compressive strength (UCS) of CPB is often used to assess the mechanical stability. Once the CPB is placed into the stopes, mining around the stopes is stopped until the CPB attains the required strength to ensure stability. Therefore, the rate of increase of the strength of the CPB has a significant impact on mining productivity. To increase mining efficiency, the curing time of the CPB must be reduced. In other words, the strength increases in the early stages of curing should be as fast as possible. Furthermore, the stability of the CPB structure is crucial, since collapse of a CPB structure can have serious consequences such as injury to workers and fatalities, and damage to equipment. Therefore, the rate of strength increase of CPB is an important design consideration.

Self-desiccation due to water consumption during cement hydration is another important performance consideration of CPB (Li and Fall 2018). Self-desiccation results in a decrease of the pore water pressure and/or the development of matric suction in the CPB, which is advantageous for the early-age strength development with increase in effective stress in the backfill structure. Consequently, self-desiccation reduces the likelihood of liquefaction of the CPB material. Higher strength at the early stages of curing of the CPB and shorter time between mining cycles are beneficial in the improvement of mine productivity.

Increasing the amount of binder/cement in the CPB will result in more cement hydration products and acceleration of the self-desiccation process which is one of the more practical approaches to reduce the time required for higher strength in the early stages of curing (Fall et al. 2008). However, increasing binder content to enhance strength will increase cost since the binder accounts for up to 75 percent of the final cost of CPB production (Fall and Benzaazoua 2003). Furthermore, more cement consumption increases carbon dioxide emissions in the production of cement which emits a large quantity of greenhouse gases that cause more environmental concerns (Palla et al. 2017). Due to these concerns, finding an alternative approach to increase the rate of increase of the strength of CPB becomes important.

Since cement is one of the most widely used construction materials, many studies have been carried out to increase the strength and improve the mechanical properties of concrete at the

early stages of curing with chemical admixtures or additives. Due to significant advancements in nanotechnology in recent years, nanomaterials have been used to enhance the properties of concrete in construction. For example, Oltulu and Şahin (2013) investigated the effects of NP additives, including nano-silica (SiO_2), nano-iron oxide (Fe_2O_3), and nano-aluminum oxide (Al_2O_3) on the compressive strength of cement mortar. They found that adding NP additives lead to an increase of the compressive strength of cement mortar. Ltifi et al. (2011) investigated the effect of nano-SiO_2 on the behaviour of cement mortar and observed an increase in the compressive strength of the mortar. Nazari and Riahi (2011) experimentally investigated the influence of nano-Al_2O_3 on the compressive strength of conventional concrete and found that by partly substituting ordinary Portland cement (OPC) with nano-Al_2O_3, the compressive strength of concrete is increased.

It should be noted that due to high potential of agglomeration in Nano-scale materials, utilization of a proper dispersing agent is required. The addition of superplasticizers to cemented paste backfill (CPB) has a profound impact on its performance, leading to substantial enhancements in various properties. When added to the CPB mixture, superplasticizers greatly reduce its yield stress and viscosity, regardless of the type of tailings used(Lothenbach et al. 2007, Zhang et al. 2015). This reduction is most effective when using a specific proportion, as indicated by the study. Additionally, the inclusion of superplasticizers results in a notable increase in the unconfined compressive strength (UCS) of the CPB. This improved strength is primarily attributed to the superplasticizer's ability to enhance cement hydration through ionic diffusion and self-consolidation of solid particles. Moreover, the polycarboxylate ether-based superplasticizer contributes to better environmental performance of the CPB by lowering its hydraulic conductivity and reactivity. This reduction can be ascribed to the superplasticizer's influence on particle mobility, cement hydration, and its interaction with other chemical compounds found in the tailings (Haruna and Fall 2020a, 2020b, Al-Moselly et al. 2022b, Haruna 2022).

These findings show that studies on adding NP additives to CPB is a worthwhile undertaking. In contrast to studies carried out on concrete, NP additives have seldom been used in CPB, and the impact of the nano-additives on the mechanical performance of CPB is not well understood or known. In addition, no research has been conducted on the suction and self-desiccation

development of nano-modified CPB (nano-CPB). In this experimental study, the effects of different amounts of four types of nano-particles (NPs), i.e,. including nano-silica (SiO_2), nano-calcium carbonate ($CaCO_3$), nano-iron oxide (Fe_2O_3), and nano-aluminum oxide (Al_2O_3) on the mechanical strength and suction of CPB are examined.

4.3. Experimental program

4.3.1 Materials

4.3.1.1. Tailings

In this work, silica tailings (STs) are used as synthetic tailings. STs are made of 99.8 percent quartz which is the major mineral in the tailings from Canadian hard rock mines (Fall et al. 2010a). The purpose of using STs is to reduce material variability and uncertainty in the test results due to the presence of reactive minerals in natural tailings. These minerals can react with the binder during the hydration process of CPB, which makes it difficult to interpret and analyze the test results. The STs used in this study have almost the same particle size distribution as those of natural tailings, which are based on tailings from nine hard rock mines in Eastern Canada, see

Figure 4-1.

Table 4-1 includes the physical parameters of the tailings used in this experiment, in addition to their mineral composition.

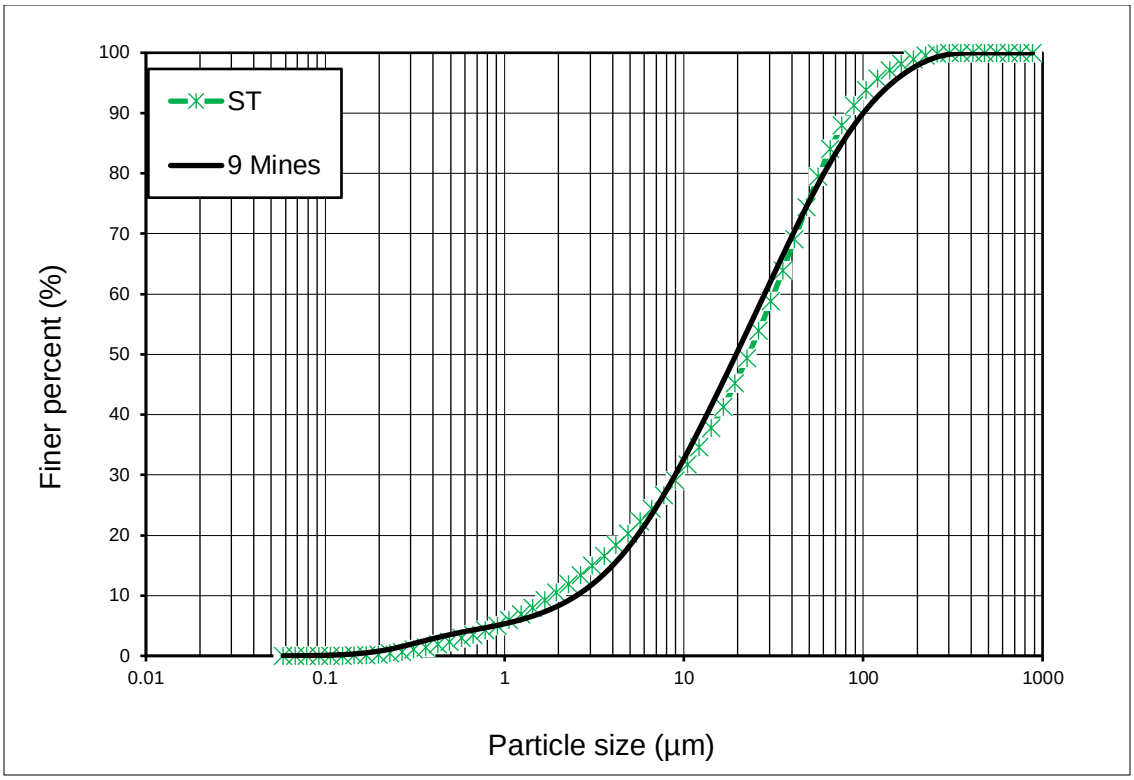

Figure 4-1 Grain size distribution of the silica tailings (ST) and average grain size distribution of tailings from nine mines in Eastern Canada

Table 4-1. Physical properties of tailings used in experiment.

Properties	G_s	D_{10}	D_{30}	D_{50}	D_{60}
Unit	-	µm	µm	µm	µm
ST	2.7	1.9	9.0	22.5	31.5
Average of 9 types of tailings	2.9	1.8	9.1	20.0	30.8

G_s: specific gravity;

4.3.1.2. Nanoparticles

In this study, four types of NP additives are used: to prepare the needed CPB samples. NPs include Nano-Calcium carbonate (CaCO3), Nano-Iron oxide (Fe2O3), Nano-Aluminium oxide (Al2O3) and Nano-Silica (SiO2). Regarding Nano-silica, Tetraethyl-Orthosilicate (TEOS), the manufacturing precursor of nano-SiO2, was used. Dow Corning, Inc. supplied the TEOS under the brand name XIAMETER® OFS-6697 silane. TEOS was used as a colloid which resulted in enhanced nano- SiO2 particle dispersion in the CPB mixture (Thomas et al. 2009b). Table 4-2 lists the physical and chemical characteristics of the NP additives.

The CPB samples were made with different amounts of NP additives - 0%, 1%, and 3%, which depended on the amount of cement binder.

Table 4-2 Chemical and physical specifications of nanoparticles used.

Nano-SiO_2		
	Appearance	Clear liquid
	SiO_2 (%)	>99
	Particle size (nm)	<12
	Specific surface area (m^2/g)	350
	pH	6-8
	Bulk density (g/cm^3)	<0.10
	Cost (per 120 mL)	$120
Nano-$CaCO_3$		
	Appearance	White powder
	$CaCO_3$ (%)	≥98
	Particle size (nm)	20–50
	Specific surface area (m^2/g)	40-80
	pH	8-10
	Bulk density (g/cm^3)	2-3

	Cost (per 100 g)	$59
Nano-Fe_2O_3		
	Appearance	Red brown
	Fe_2O_3	≥98
	Particle size (nm)	20-40
	Specific surface area (m^2/g)	40–60
	pH	5-7
	Bulk density (g/cm^3)	1.2
	Cost (per 100 g)	$159
Nano-Al_2O_3		
	Appearance	White powder
	Al_2O_3	≥99
	Particle size (nm)	<50
	Specific surface area (m^2/g)	>40
	pH	7
	Bulk density (g/cm^3)	1.5
	Cost (per 100 g)	$98

Data obtained from suppliers.

4.3.1.3. Cement and mixing water

The basic binding agent used in this research is Portland cement Type I (PCI) which is the most common type of cement used in CPB. Table 4-3 lists the chemical and physical characteristics of the PCI.

Table 4-3 Chemical and physical properties of PCI

Element	PCI (%)
SO_3	3.82
Fe_2O_3	2.70

Al_2O_3	4.53
SiO_2	18.03
CaO	62.82
MgO	2.65
(Relative Density)	3.1

4.3.1.4. Superplasticizer

According to Roshani & Fall, (2020a), the addition of NP additives to CPB considerably reduces the flowability of CBP by increasing the yield stress and viscosity of the mixture as a result of multiple processes (e.g., generation of more cement hydration products, increased water demand). In addition, higher water consumption has been noted due to more cement hydration products, such as calcium silicate hydrate (C-S-H). In addition, NP additives are extremely prone to forming agglomerated particles, which inhibit the cement hydration process (Shaikh and Supit 2016) and subsequently affect the mechanical performance of CPB. To address these concerns, many samples in this investigation are made with the addition of an SP, since it has been shown that superplasticizer (SP) improves the flowability of the CPB by lowering the yield stress (Roshani and Fall 2020a) and also enhancing NP dispersion. In the process of preparing the CPB samples, multiple sets of samples, including a control set (pure CPB, i.e., CPB without NP additives) and different nano-CPB sets, were made with the addition of Master Glenium 7500 concrete admixture (Master G; Badische Andilin und Soda Fabrik (BASF)) as the SPf ("MasterGlenium 7500 | Master Builders Solutions" n.d.).

4.3.2 Specimen preparation and mix proportions

Different sets of nano-CPB samples were prepared to investigate the effects of the different types of NP additives on the properties of the CPB with different types of binders. Further details about the CPB mix design are given in Table 4-4. To prepare the CPB samples, the tailings and binder were added to a mixer and mixed for 3 minutes to obtain a uniform dry mixture of cement and tailings. However, adding NP additives directly into the mixer results in weak and unhydrated

NPs due to agglomeration, which occupy the voids between the CPB particles and reduce the mechanical strength of the CPB (Senff et al. 2009, Quercia et al. 2012a). This problem is attributed to the high reactivity of NPs and high Van der Waals forces between the NPs, which in turn causes the NPs to more readily agglomerate than other pozzolanic materials. To remedy this problem, the additives were first added into the water and mixed for at least five minutes and then the solution was added into the dry mixture of tailings-cement and mixed for 15 minutes. For the samples that contained SP, water and SP were first mixed together for 1 minute, and then the NP additives were added and mixed for another 3 minutes. Afterwards, this was added to the mixture of tailings and binder. After adequate mixing, the fresh CPB was poured into cylindrical molds with a diameter of 5 cm and a height of 10 cm for UCS testing at different curing times. To remove any air bubbles trapped in the CPB, the samples were shaken for 1 minute after poured into the molds. Finally, they were placed in a temperature-controlled container until testing occurred.

Table 4-4 Summary of the mix composition of the prepared nano-CPB specimens

Sample name	Binder content (%)	PCI in the binder (%)	SP content (%)	W/C ratio	NP contents (%)	NP type
Effect of curing time and nano-particle content						
PCI- CPB	4.5	100	0	7.8	0	None
PCI-CPB-NS	4.5	100	0	7.8	1	NS
PCI-CP-NC	4.5	100	0	7.8	1	NC
PCI-CPB-NF	4.5	100	0	7.8	1	NF
PCI-CPB-NA	4.5	100	0	7.8	1	NA
Effect of curing time and SP content						
PCI- CPB	4.5	100	0.125	7.8	0	None
PCI- CPB-NS	4.5	100	0.125	7.8	1	NS
PCI- CPB-NC	4.5	100	0.125	7.8	1	NC
PCI- CPB-NF	4.5	100	0.125	7.8	1	NF

PCI-CPB-NA	4.5	100	0.125	7.8	1	NA
PCI- CPB	4.5	100	0.25	7.8	0	None
PCI- CPB-NS	4.5	100	0.25	7.8	1	NS
PCI- CPB-NC	4.5	100	0.25	7.8	1	NC
PCI- CPB-NF	4.5	100	0.25	7.8	1	NF
PCI-CPB-NA	4.5	100	0.25	7.8	1	NA

PCI, Portland cement type I; W/C ratio, mass of water divided by the mass of binder. Binder Content = Mass of binderx100/ (Mass of dry tailings + Mass of binder); -NS: Nano-silica particles; NC: Nano-$CaCO_3$ particles; NF: Nano-Fe_2O_3 particles; and NA: Nano-Al_2O_3 particles.

4.3.3 Test methods and monitoring program

4.3.3.1. Unconfined compressive strength test

The compressive strength of each CPB sample was determined in accordance with ASTM – C39. After a specific curing time (12 hours, and 1, 3, 7, and 28 days), the specimens were removed from the molds and placed in an automated mechanical press that applied a vertical load at a rate of 1.0 mm/min. The ultimate stress at which the specimens fail can be determined by recording the compressive stress imposed onto them. Each test was conducted on at least two identical specimens to ensure the repeatability of the test results.

4.3.3.2. Microstructural analysis

To obtain more information about the changes in the CPB microstructure due to the cement hydration process in the presence of NP additives and different curing conditions, various microstructural analyses or tests, including thermal analysis (thermogravimetry (TG), differential thermogravimetry (DTG)), mercury intrusion porosimetry (MIP), and XRD were conducted on the CPB or cement paste of CPB with or without the NP additives. In order to prepare samples for the XRD and TG/DTG tests, cement paste samples (w/c =1), prepared in the same manner as the CPB samples described above, were completely dried in an oven at 45 °C for 4 days to ensure the evaporation of the free water. Then, they were grounded into powder. At this stage, TG/DTG

analyses were conducted with a thermogravimetric analyzer SDT 2960 simultaneous DSC-TGA. The specimens were heated at a rate of 10°C/min up to the maximum temperature of 1000°C under a nitrogen (N_2) atmosphere at a rate of 100 mL/min. The XRD tests were performed by using a Rigaku Ultima IV diffractometer, which is equipped with cross beam optics, and tests were done at a beam voltage of 40 kV and current of 44 mA. The MIP tests were performed on dried CPB samples by using a Micromeritics AutoPore III 9420 mercury porosimeter.

4.3.3.3. Monitoring program

To gain better insights into the NP reaction process with the binder, which is responsible for changing the mechanical characteristics of the CPB, a 5TE electrical conductivity (EC) sensor for monitoring the EC, temperature, and volumetric water content (VWC) was used, which has an accuracy of ±10% for the EC, ±3% for the VWC, and ±1°C for temperature measurements. The sensor was placed in the center of each CPB sample and connected to a data logger to record the measured value. The EC was measured by applying an alternating current between two electrodes placed in the sensor and determining the electrical resistance between them. Variation of the EC in a cement-based material is a practical indicator of the ion transfer through a material caused by the chemical progression of cement hydration (Ghirian and Fall 2017). In addition to the 5TE sensor, an MPS-6 dielectric water potential sensor was used to monitor the suction in the CPB samples with and without NP additives. This sensor has an accuracy of ±10% to measure the suction under an operational range of -9 kPa to -100 kPa. In order to monitor each of these properties, the CPB samples were contained in a cylindrical mold with a diameter of 10 cm and a height of 20 cm.

4.4. Results and discussion

4.4.1 Suction development in nano-CPB

Figure 4-2. Changes in negative pore water pressure (matric suction) for nano-CPB samples blended with 1% dosage of different types of NPs and 0.125% of SP (NP: nano-particles; SP: superplasticizer) depicts the effect of adding NP additives on the development of suction in the

nano-CPB samples. As shown, the suction of all of the CPB samples steadily increases with curing time regardless of the presence or lack of NP additives. This is due to the progression of the cement hydration process (precipitation of hydration products such C-S-H, calcium hydroxide (C-H), and ettringite), which consumes water with increase in curing time. This progression is confirmed by the results presented in Figure 4-3, which illustrates the results of the thermal analyses (e.g., TG/DTG) conducted on cement paste cured for different times (7 and 28 days). The results can be interpreted as an indication of hydration advancement as a function of curing time. As observed, three significant decomposition peaks in the DTG diagrams correspond with the rapid weight loss found in the TG analysis. The first peak or rapid weight loss between 80°C and 120°C is associated with the decomposition of the hydration products, including C-S-H, gypsum and ettringite, and water evaporation (Nonnet et al. 1999, Haiqiang et al. 2016). The next peak observed between 400°C and 500°C is attributed to the disintegration of CH, and the last peak between 650°C and 700°C refers to dehydration of calcite (Pane and Hansen 2005, Fall et al. 2010b). A comparison of the endothermic peaks identified in the thermal analysis result shows that the cement paste that was subjected to a curing cycle of 28 days generates more cement hydration products than that cured for 7 days. In other words, more hydration products are formed in the 7- and 28-day specimens, i.e., the cement products generated increases as the curing time is increased. Therefore, it can be inferred that the negative pore water pressure (suction) increases as hydration progresses owing to the fact that a larger volume of water will be consumed due to the precipitation of more hydration products.

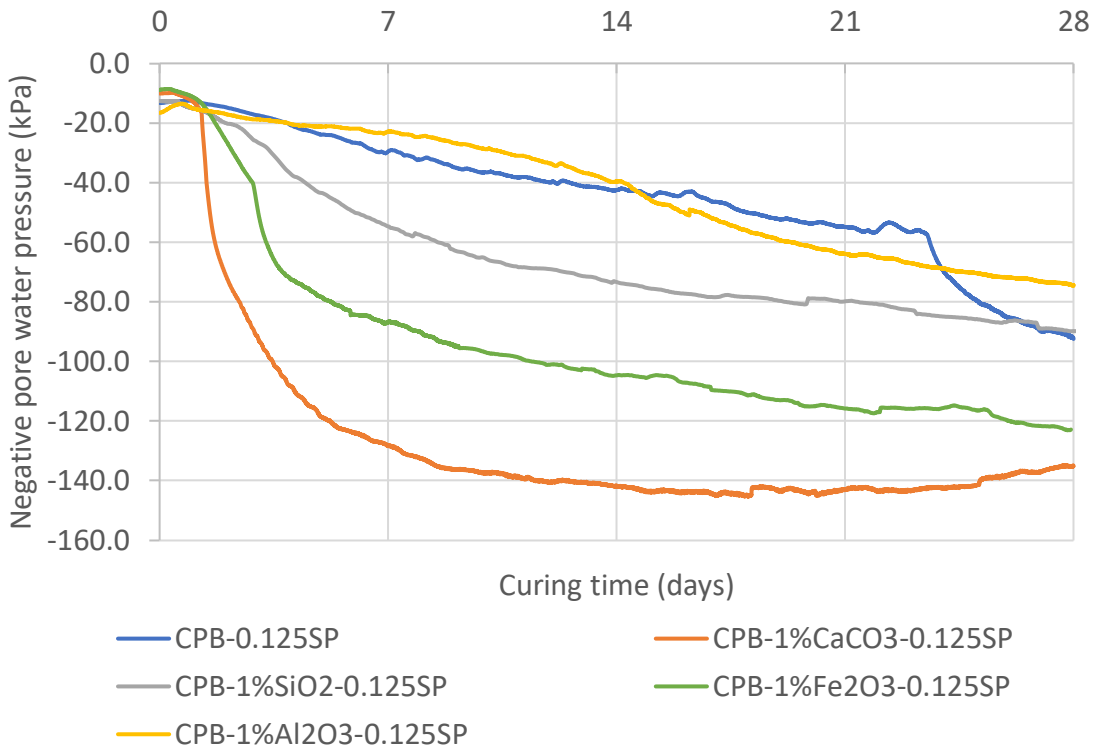

Figure 4-2. Changes in negative pore water pressure (matric suction) for nano-CPB samples blended with 1% dosage of different types of NPs and 0.125% of SP (NP: nano-particles; SP: superplasticizer)

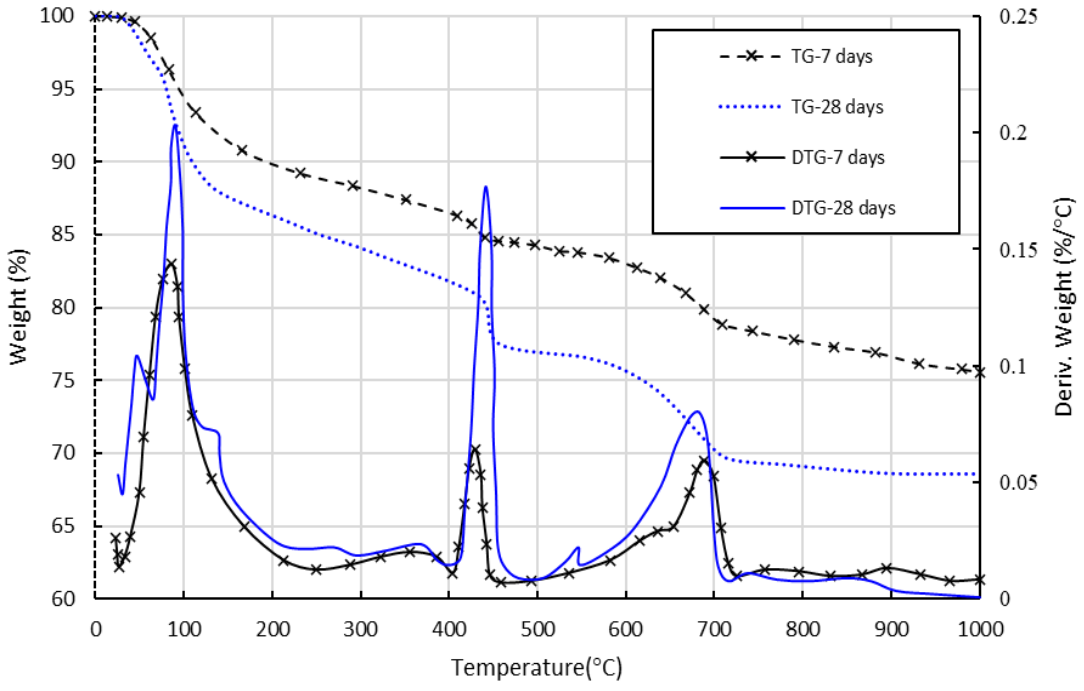

Figure 4-3. TG/DTG analyses of cemented paste of CPB samples cured for 7 and 28 days (20°C)

Furthermore, it is also evident from Figure 4-2 that aside from the nano-CPB sample with nano-Al_2O_3, the other CPB samples with NP additives show a much higher suction value (more intense self-desiccation). In other words, nano-SiO_2, nano-$CaCO_3$ and nano-Fe_2O_3 significantly impact the self-desiccation or suction development in CPB, whereas the impact of nano-Al_2O_3, is insignificant. This significant impact of the aforementioned NP additives on the suction development in CPB is related to the fact that the NPs, nano-silica (SiO_2), nano-calcium carbonate ($CaCO_3$) and nano-iron oxide (Fe_2O_3), enhance the cement hydration process, thus resulting in the generation of more cement hydration products (Ghirian and Fall 2013a). This is obviously associated with the consumption of more pore water, i.e., decreasing the pore water pressure or increasing the suction. This explanation is experimentally supported by the results of TG/DTG analyses performed on the cement paste samples with or without the different NP additives as shown in Figure 4-4, which indicate that the samples with the NPs, nano-silica (SiO_2), nano-calcium carbonate ($CaCO_3$) or nano-iron oxide (Fe_2O_3), have more hydration products as evidenced by their higher endothermic peaks or weight loss observed in the temperature range of 100°- 150°C. Figure 4-4 presents the TG/DTG analysis results on cement paste specimens with a 1% of different NP additives and 0.125% of SP. The cement paste mixed with nano-$CaCO_3$ or nano-Fe_2O_3 show higher peaks between 100°C and 180°C in comparison to the control sample and nano-Al_2O_3 specimen. These findings suggest that nano-CPBs with nano-$CaCO_3$, nano-Fe_2O_3, and nano-SiO_2 produce more C-S-H gel and ettringite, which is consistent with the suction monitoring results in Figure 4-2. This figure also shows that the CPB sample with nano-$CaCO_3$ exhibits the highest rate of suction development, which is in agreement with the DT/DTG results in Figure 4-4 that show the cement paste modified with nano-$CaCO_3$ has the highest endothermic peaks and weights loss in the temperature range of 100°- 150°C, which indicate more hydration products and obviously associated with the consumption of more pore water or higher and more rapid suction development. However, according to Figure 4-4, the addition of nano-Al_2O_3 does not significantly change the quantity of hydration products generated, which is consistent with the results of suction monitoring in Figure 4-2 as well as the findings in Barbhuiya et al. [23]. These researchers concluded that adding nano-Al_2O_3 does not increase the compressive strength of cement mortar at the early ages of curing (7 days).

Moreover, the order of suction development in the nano-CPB samples with different types of NP additives (Figure 4-2) is consistent with the thermal analysis in Figure 4-4. In other words, samples with more hydration products as shown in the TG/DTG curve have higher suction or more rapid development of desiccation. Having said that, the observed order of suction in the nano-CPB samples is as follows: nano-CPB-$CaCO_3$> nano-CPB-Fe_2O_3> nano-CPB-SiO_2> nano-CPB-Al_2O_3≈ control sample. This indicates that the addition of the NP additives nano-$CaCO_3$, nano-Fe_2O_3, or nano-SiO_2, to CPB enhances the cement hydration reaction, which directly affects the pore water consumption and suction development in the CPB mass, and refinement of the nano-CPB microstructure. The observed decrease in negative pore water pressure (suction) of the cemented paste backfill containing nano calcium carbonate specimen after 28 days, as compared to its values at 14 and 21 days, may be due to several factors. Although an increase in curing time generally results in the formation of more hydration products and consumption of water, other factors could contribute to this observation could be the effect of secondary reactions, changes in microstructure, self-desiccation, and measurement uncertainty.

Over time, secondary reactions like pozzolanic reactions may occur, which involve the consumption of calcium hydroxide and the formation of additional calcium silicate hydrate (C-S-H) gel. This could result in the liberation of some water molecules, causing a decrease in negative pore water pressure (Mehta and Monteiro 2014). As the curing process progresses, the microstructure of the cemented paste backfill can change. These changes could lead to the formation of more capillary pores or the modification of existing pore sizes, which could affect the pore water pressure. The cement hydration process could lead to self-desiccation due to the water molecules being trapped within the hydration products. In some cases, as the hydration progresses, some of the trapped water may be released and reintroduced into the pore network, reducing the negative pore water pressure. Lastly, experimental errors and inaccuracies in measuring the pore water pressure could also contribute to the observed decrease after 28 days. Regarding the secondary reactions, Pozzolanic reactions involve the reaction between pozzolanic materials and calcium hydroxide ($Ca(OH)_2$) produced during the cement hydration process. In the case of cemented paste backfill containing nano calcium carbonate, the nano calcium carbonate could potentially serve as a pozzolanic material, depending on its specific properties and

composition. Pozzolanic materials are generally characterized by their high content of silica (SiO_2), alumina (Al_2O_3), and/or iron oxide (Fe_2O_3), which are reactive in the presence of calcium hydroxide. When a pozzolanic reaction occurs, these materials react with calcium hydroxide to form additional calcium silicate hydrate (C-S-H) gel, which is a crucial component of the cement paste matrix responsible for strength development. As the pozzolanic reaction consumes calcium hydroxide and forms additional C-S-H gel, the process could result in the liberation of some water molecules previously bound to the calcium hydroxide. This released water could then be reintroduced into the pore network of the cemented paste backfill, causing a decrease in the negative pore water pressure after a certain curing period (in this case, after 28 days).

It's important to note that the extent and rate of pozzolanic reactions depend on several factors, including the nature of the pozzolanic material, its specific surface area, and its reactivity. The environmental conditions, such as temperature and humidity, can also influence the rate of pozzolanic reactions (Taylor 1997, Mehta and Monteiro 2014).

These findings have significant practical implications. A key objective in any mining operation is to increase or maintain high productivity for financial gain and competitiveness. Therefore, a rapid-mining cycle is an important target in underground mining operations. In mine backfilling operations, a primary obstacle to a rapid-mining cycle is the risk of failure of the backfilled structures at the early ages due to liquefaction. Since the build-up of pore water pressure during undrained static or cyclic loading is the underlying reason that leads to CPB liquefaction, any mechanism that can eliminate or reduce this increase of pore water pressure will increase the liquefaction resistance of the CPB mass and thus accelerate the mining cycle. Thus, from the findings presented above, it can be concluded that the addition of the NP additives such as nano-$CaCO_3$, nano-Fe_2O_3, or nano -SiO_2 increases the liquefaction resistance of the CPB structure and thus increases the mining-cycle.

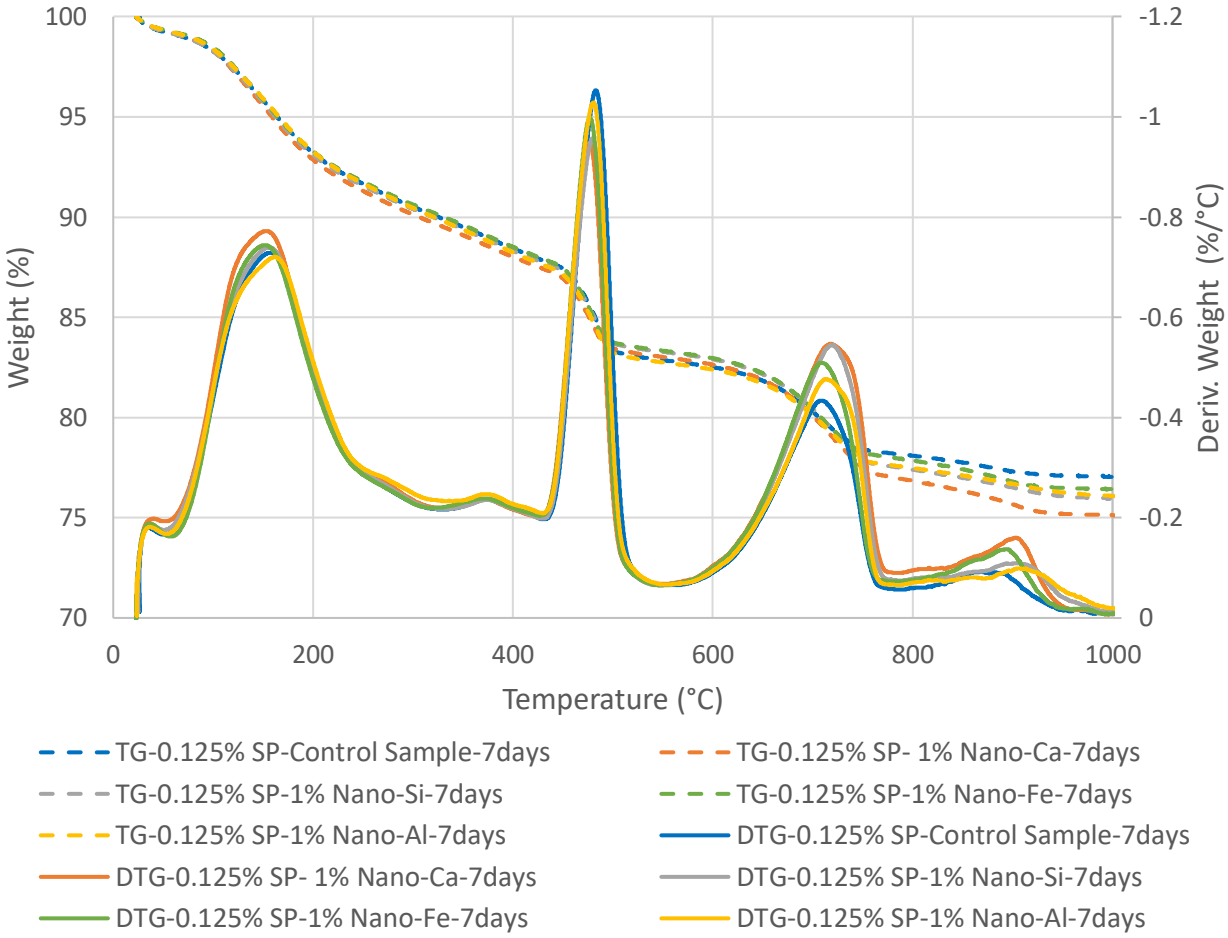

Figure 4-4. Effect of different types of NP additives on thermal analysis results of cement paste cured for 7 days

4.4.2 Effect of nanoparticle additive on strength development of Nano-CPB

Figure 4-5 illustrates the development of the strength of CPB samples with 1% NP additive in absence of any dispersing agent (SP) with curing time. All of the samples demonstrate a continuous increase in strength with curing time due to the progression of cement hydration (Taylor 1966, Puertas et al. 2000, Tariq and Yanful 2013).

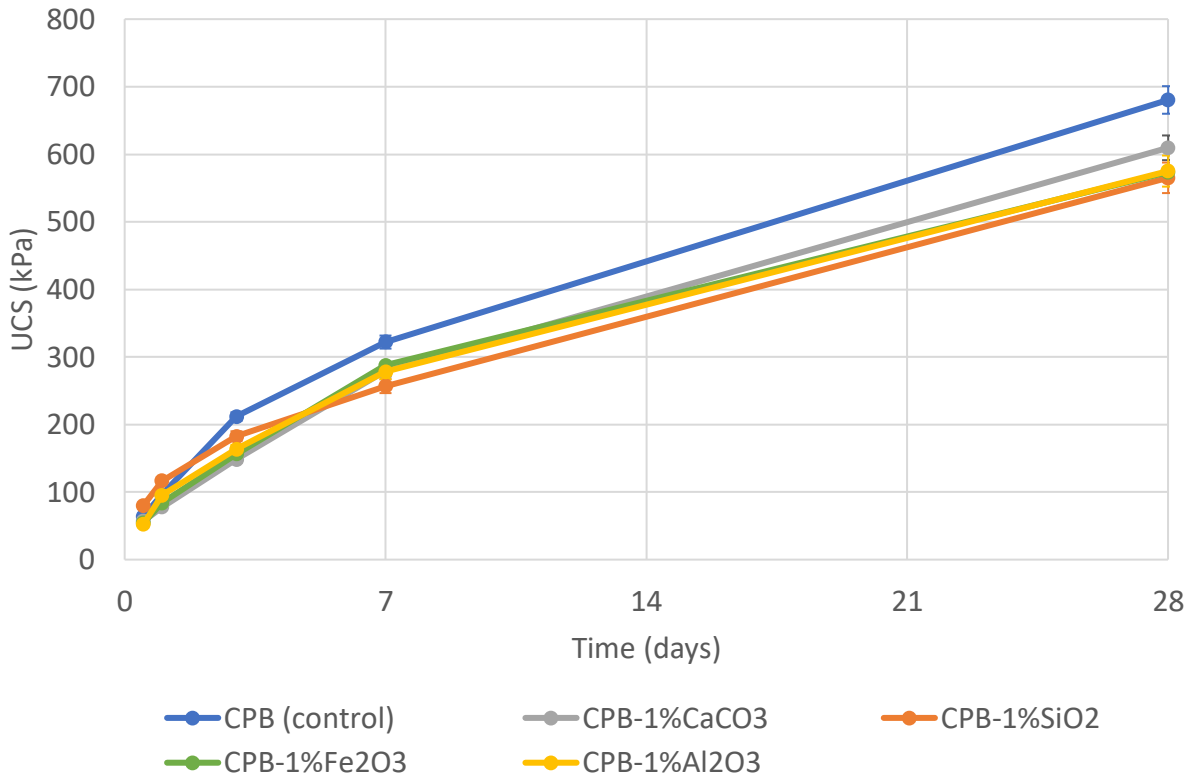

Figure 4-5. Development of compressive strength of CPB samples with different types of NP additives and without SP

Three essential factors explain the continuous increase in strength. First, as cement hydration progresses throughout the curing process, more hydration products are generated, which is shown in Figure 4-4 and discussed earlier, thus increasing the bonding (cementation) between the tailings particles, and consequently, increasing the UCS of the CPB. Second, as observed in Figure 4-6, consumption of pore water owing to cement hydration results in a decrease of the water content. From this graph, the progression of hydration causes the volumetric water content of the CPB sample to continuously decrease over the curing cycle. Lower content or higher suction is usually associated with a lower strength of the porous medium or cementitious material (Zhang et al. n.d., Yilmaz and Fall 2017). Finally, pore structure refinement induced by the aforementioned mechanisms (e.g., changes in suction and precipitation of hydration products) transforms the fresh CPB from its soft stage to a dense and hardened material with diminished pore size and void ratio. The findings of the MIP tests carried out on two identical CPB samples cured for different ages (7 and 28 days), as shown in Figure 4-7, provide evidence of pore

refinement. The CPB sample cured for 28 days has lower cumulative pore volume (lower void ratio) compared to the 7-day sample owing to more precipitated hydration products that fill the pores.

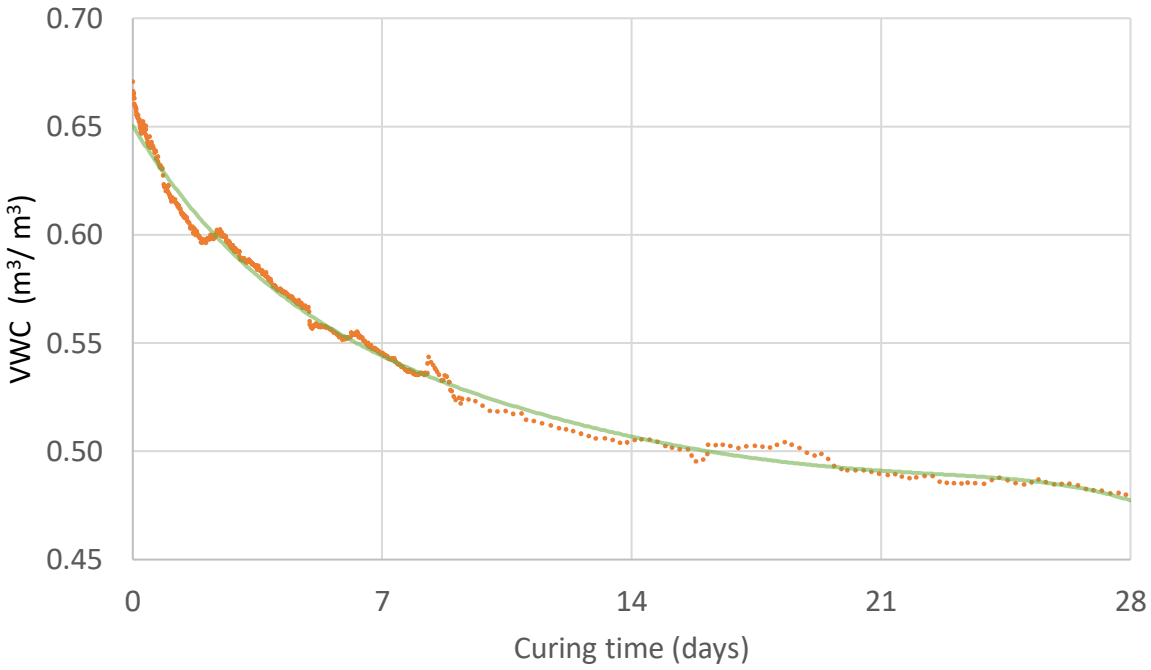

Figure 4-6. Changes in volumetric water content of CPB with curing time

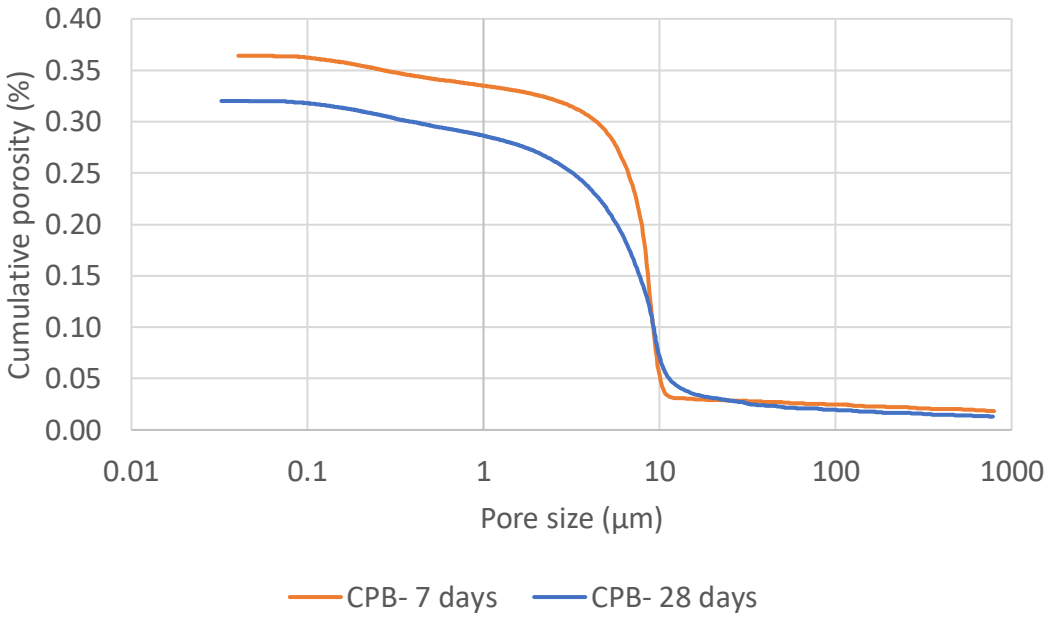

Figure 4-7. Changes in total pore refinement of CPB with curing time

The results of the UCS testing also show that, except for the first 24 hours when the strength of the backfill samples with and without NP additives is relatively similar, the strength of the former is lower than the latter for all curing times. For example, after 28 days, the UCS of the control sample is 680 kPa, which is the highest measured strength whereas the sample with 1% nano-Al_2O_3 has the lowest strength of 565 kPa. This could be due to the agglomeration of NPs. Compared with the particles of the same material but larger in size, the predominant forces that act on the NPs are interparticle forces, such as van der Waals and electrostatic forces, whereas gravity is the dominant force for the same material with a larger particle size (Quercia et al. 2012b). Thus, the attraction forces of the electric charges on the surface of the NPs prevent them from dispersing uniformly, forming agglomerated particles in the mixture. Note that improper dispersion of NPs adversely affects the mechanical characteristics of the cementitious materials or CPB in two different ways. First, the rate of reactivity of the agglomerated NPs is much lower than individual NPs due to the lower specific surface area (SSA) of the agglomerated particles compared to NPs; therefore, fewer NPs contribute to cement hydration, thus resulting in less hydration products generated at the end of the curing (Siang Ng et al. 2020). Second, in the absence of the uniform dispersion of NPs, the filler effect of NPs that enhances the packing

density by filling the micropores of the mixture will not be feasible (Liu et al. 2012b, Shaikh and Supit 2015).

To solve the observed problem caused by the agglomeration of NPs on the compressive strength of the nano-CPB samples, there is the need to add a dispersing agent to the nano-CPB agent. Polycarboxylate-based SPs have the most effective performance in dispersing NPs, according to Kim et al. (2018) who examined the impact of several kinds of SPs on the dispersion of nanomaterials in cementitious materials. As a result, the second group of nano-CPB samples, which were mixed with 1% NP additives, received a dose of 0.125% SP. This addition of SP enhances the dispersion of the NPs in the CPB mixture, and ultimately refines the pore structure of the hardened nano-CPB. This refinement is supported by the results of the MIP test performed on two distinct nano-CPB samples with varying dosages of SP (Figure 4-8). In contrast to the nano-sample prepared with SP, as in Figure 4-8, the nano-CPB sample prepared without SP has a higher total pore volume and larger pore size, thus supporting the presence of agglomerated masses of NPs that do not fill the pores. However, the samples prepared with SP have smaller pores, which proves that enhanced NP dispersion facilitates the filling action of the NPs.

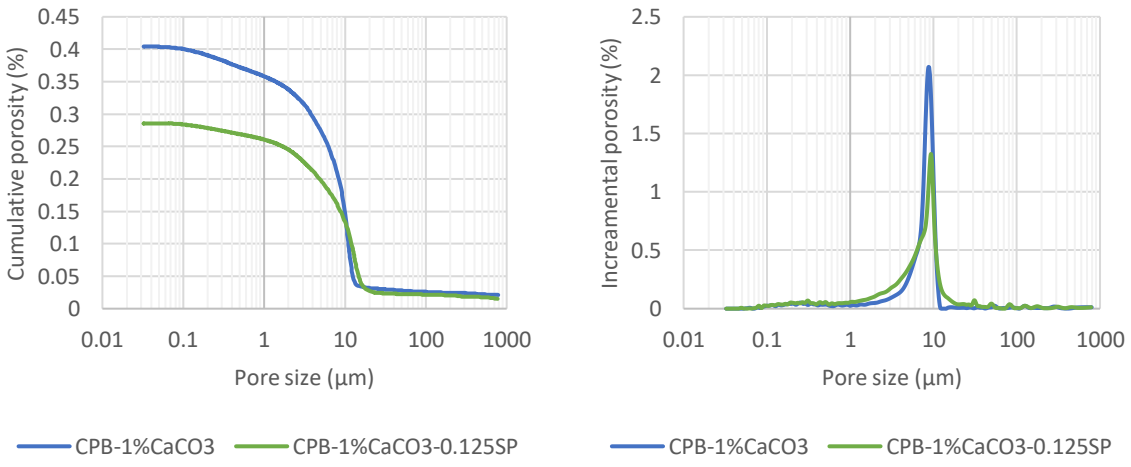

a) Cumulative pore volume b) Pore distribution

Figure 4-8. Effect of SP on the pore structure of nano-CaCO3-CPB

The UCS test results of the nano-CPB samples blended with 0.125% SP are shown in Figure 4-9. As expected, the samples with 0.125% SP and 1% NP additive show higher strength in comparison

to the samples without SP (Figure 4-5). This increase can be explained by the dispersion effect of the repulsive forces that act on the CPB solid particles and NPs formed by addition of SP which facilitate the contribution of NPs to the hydration reaction and also uniformly distributes NPs through the cementitious medium as supported by the MIP test results in Figure 4-8.

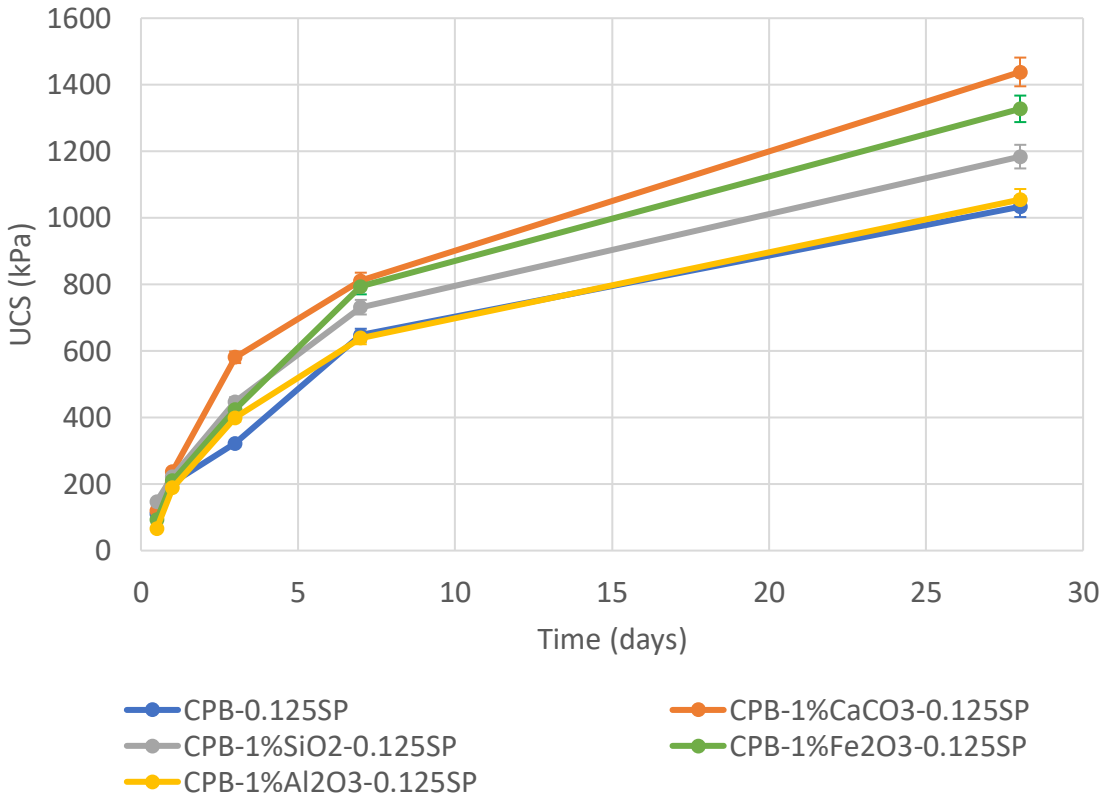

Figure 4-9. Strength development of nano-CPB samples with 0.125% SP

The sequence of the strength increase in the samples shown in Figure 4-8 is consistent with the pattern of the suction monitoring detailed in Section 3.3.1. Based on this arrangement, CPB samples with nano-$CaCO_3$, nano-Fe_2O_3 and nano-SiO_2 show higher strength than the control sample, whereas the strength of CPB modified with nano-Al_2O_3 is similar to that of the control sample. The effect of nano-$CaCO_3$ on the strength of CPB with SP is consistent with those obtained by other studies that assess the impact of nano-$CaCO_3$ on concrete and/or mortar. For example, (Kadri and Duval 2002, Camiletti et al. 2013a, Hefni and Ali 2021)) examined the effect of partial substitution of cement with nano-$CaCO_3$ and found potential enhancement of the

mechanical performance of concrete and the cement paste. The NP additive induced strength increase can be explained by two main mechanisms.

The first mechanism is the filler effect of the NP additives (nano-$CaCO_3$, nano-FeO_3, nano-SiO_2) which results in a higher packing density of the final backfill material; thus, a smaller void ratio and denser microstructure are obtained, which obviously means higher strength of the backfill material (Fall et al. 2008, Yilmaz and Fall 2017). The MIP test results conducted on the nano-CPB samples confirm the refinement of the pore structure of the CPB, as presented in Figure 4-10. Among the other nano-CPB samples and control samples, the nano-CPB with $CaCO_3$ has the lowest cumulative porosity, followed by the nano-FeO_3 and nano-SiO_2 specimens, which is in good agreement with the fact the nano- $CaCO_3$ samples have the highest strength, followed by the nano-FeO_3 and nano-SiO_2 samples. However, as compared to the control sample, the addition of Al_2O_3 does not refine the pore structure of the CPB, which is consistent with the findings of the suction and strength development discussed earlier.

Second, the active contribution of the NP additives to the hydration reaction leads to the generation of more hydration products due to the acceleration of the nucleation during the hydration process (Kadri and Duval 2002, Camiletti et al. 2013a). Roshani & Fall, (2020b) stated that adding NPs results in numerous nucleation sites, which facilitates the consumption of main cement components such as C_3S, C_2S, C_3A, and C_4AF. To better demonstrate the logic behind this enhancement of NPs in hydration reactions, note that at the early ages (<12 hr) of cement hydration reaction in the absence of any NPs, the concentration of main ions that are part of the hydration reaction including Ca^{2+},SiO_4^{2-}, and SO_4^{2-}, increases up to a threshold that is over the saturation point, or the critical nucleation concentration. After this threshold is reached, the stable hydrate phases start to nucleate; in other words, the precipitation of hydration products would start after this concentration is obtained, followed by a continuous decrease in the concentration of these ions (Keller et al. 2010, Reches 2018). However, it has been observed that in cement hydration reactions where there are NPs, the precipitation of the hydration products starts right after the concentration of ions passes the saturation limit which means the time gap needed to reach critical nucleation concentration will be eliminated. Finally, by reducing the time required to start the precipitation of hydration products, the addition of NP additives results in

the acceleration of the hydration process. In addition, the contribution of NPs to the hydration process can be discussed from the point of view of pozzolanic reactivity. As mentioned in Roshani & Fall, (2020a), the pozzolanic activity of nano-SiO_2 (as the studied NP) plays a critical role in modifying the hydration process. In this study, the pozzolanic activity of the studied NPs (e.g., nano-SiO_2) increases the amount of produced C-S-H at the expense of the consuming CH reacting with the added NPs. Another factor that should be noted is that the enhancement of NPs in the hydration process is the chemical modification of the produced C-S-H. Based on the studies conducted by Gaitero et al. (2006, 2009), the addition of nano-SiO_2 results in producing more stiff C-S-H compounds that exhibit better mechanical performance in comparison with that produced in the absence of any NPs. The results obtained in this study confirm the mechanical improvements due to the addition of NP additives and presence of more hydration products. The thermal analysis results conducted on the cement paste of nano-CPB prepared with water/cement = 1 presented earlier (e.g., Figure 4-4) have consistently more hydration products due to the nano-$CaCO_3$ compared to the other nano-CPB and control samples.

However, as Figure 4-9 shows, the nano-CPB sample modified with nano-Al_2O_3 does not show any significant strength improvement compared with the control sample. Other experimental results obtained in this study also confirm the null effect of this type of NP additive in the hydration process. The thermal analysis (e.g., Figure 4-4) shows that the nano-CPB sample made with nano-Al_2O_3 does not show a considerable difference in amount of hydration products. Barbhuiya et al., (2014) conducted an experimental study on the effect of nano-Al_2O_3 on cement paste. One of their findings is that the addition of nano-Al_2O_3 does not lead to the development of any new crystalline phases at the early ages of the cement paste. This finding is consistent with the results of the different microstructural and mechanical tests in this article. That is, the addition of nano-Al_2O_3 does not change the pattern of suction development, quantity of hydration products, and strength development.

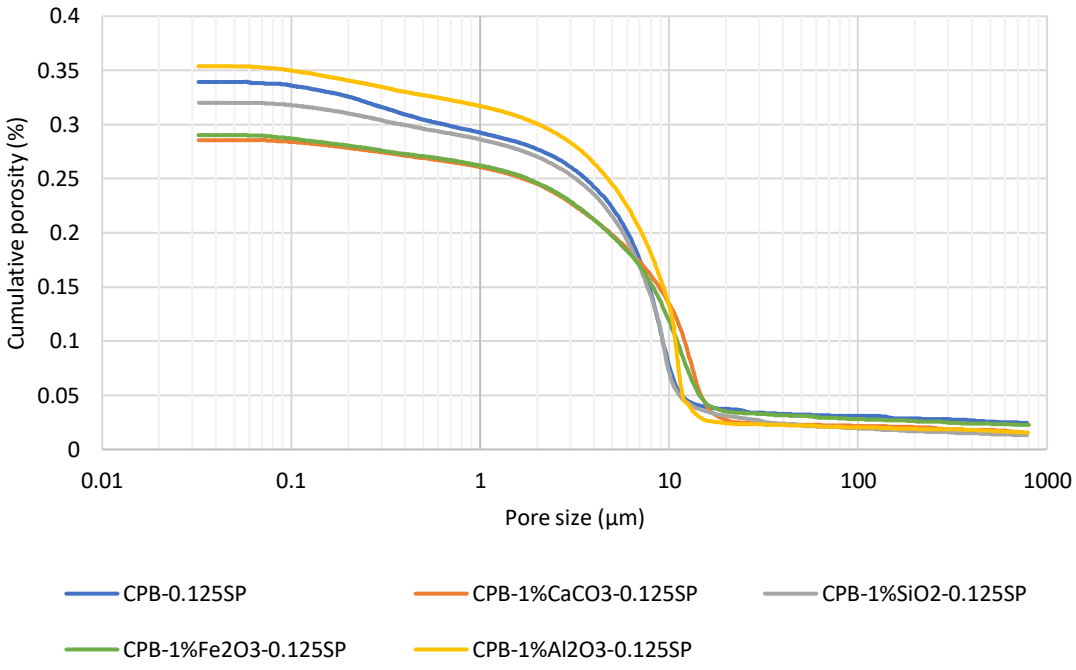

Figure 4-10. Impact of NPs on pore size distribution of nano-CPB samples mixed with 0.125% of SP

Furthermore, it can be seen from Figure 4-9 that the incorporation of NP additives counteracts the inhibiting action of the SP on the development of the strength of the CPB samples at the early ages. According to Haruna and Fall (2020) who examined the impact of SP on the compressive strength of CPB, the addition of SP delays the hydration process, which inhibits the development of strength of CPB at an early age. Monitoring the electrical conductivity (EC) of the studied nano-CPB samples showed supporting evidence of the benefits of NP additives for cement hydration that compensate for the retarding effect of SP. Any changes in the concentration of ions in the pore water of the paste backfill due to cement hydration can be monitored by measuring the variation in the EC values of the paste backfill (Thottarath 2010, Ghirian and Fall 2013a, Yilmaz and Fall 2017). According to Levita et al. (2000), the first peak in the EC graph in cementitious media represents the moment at which the cement paste begins to transition to the solid phase. Thus, less time for a sample to reach its first EC peak means an anticipated higher early age strength. Moreover, since the size of the capillary pores in a porous medium directly affects the EC of the medium -as it restricts the flow of ions- it can be stated that increasing the tortuosity of the backfill microstructure by filling the pores with hydration products results in the decline of

the EC of the paste backfill (Puertas et al. 2000). Having said that, lower EC values are correlated with a CPB with a smaller void ratio or higher packing density. According to Figure 4-11, nano-CPB with $CaCO_3$ reaches its first peak earlier than the other nano-CPB and control samples, which is consistent with the highest strength observed for CPB with $CaCO_3$ in the UCS test. Additionally, nano-CPB with $CaCO_3$ shows the lowest EC compared to the other samples after 11 days, which is consistent with the results of the thermal analysis presented in Figure 4-4 on the generation of more hydration products and more intensified suction development.

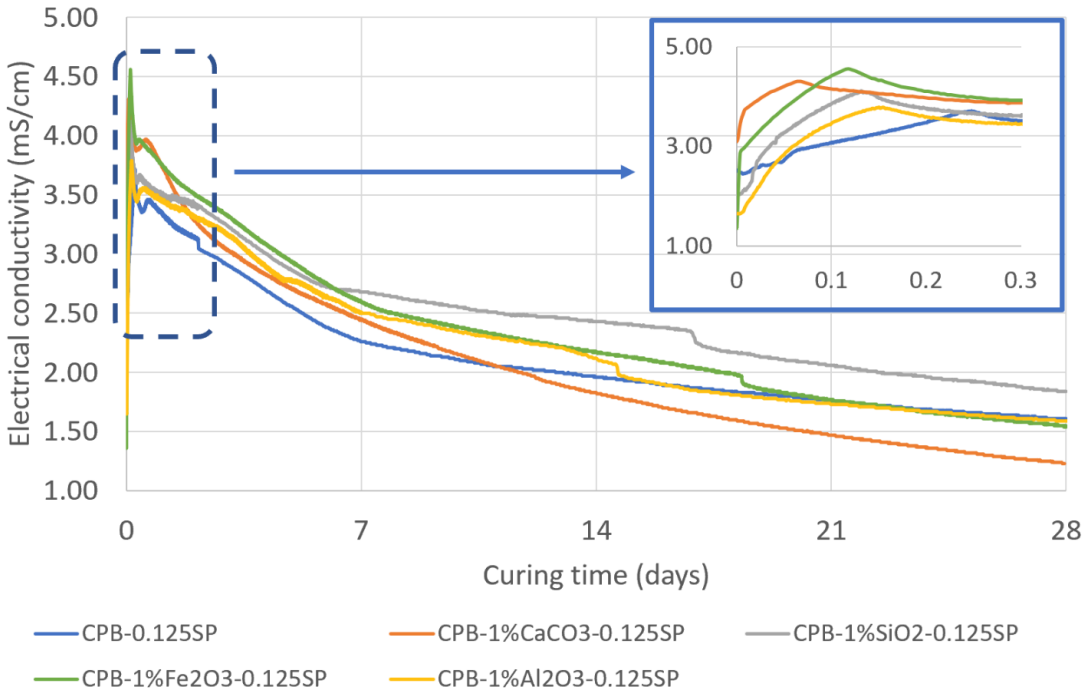

Figure 4-11. Changes in EC of nano-CPB samples prepared with 1% NPs and 0.125% of SP

The increase in the amount of cementitious products due to the presence of NPs is illustrated by the XRD analysis which was performed on cement paste with and without nano-$CaCO_3$ as shown in Figure 4-12. It can be observed that cement paste blended with nano-$CaCO_3$ and cured for 7 days shows more hydration products compared to the control sample cured under similar conditions. For example, the intensity (e.g., CPS) of C-S-H in the cement paste mixed with $CaCO_3$ at 32.16° at 2θ is 367, while the control sample is 363 at 2θ. The intensity of CH for the sample with nano-$CaCO_3$ is 1993 at 18.06°, whereas for the control sample, it is 1862 at 2θ.

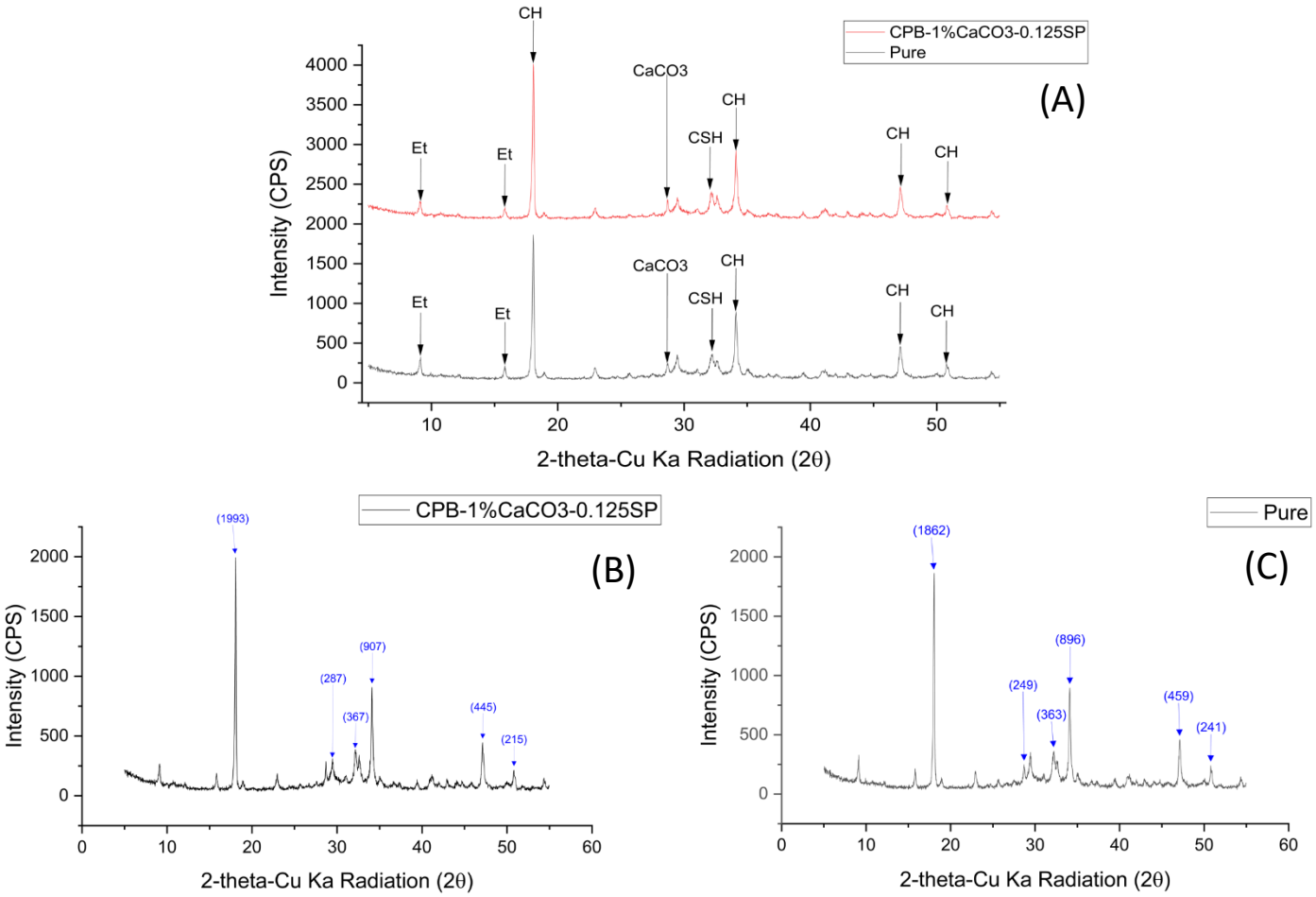

Figure 4-12. Effect of addition of nano-CaCO3 on the XRD analysis result on 7 day cement paste. A) full range results of both samples B) detailed intensity of nano-CPB with nano-CaCO3 C) detailed intensity of control sample

4.4.3 Effect of superplasticizer content on the strength development of Nano-CPB

In backfilling practices, various amounts or proportions (often 0.0 to 0.3%) of SP can be added to the CPB during preparation to improve its flowability. However, the objective is to use the smallest amount possible of SP to avoid a significant increase in the cost of the CPB. As a result and following the findings on the crucial effect of SP on the dispersion of NPs in a CPB mixture, the impact of different doses of SP (i.e., 0%, 0.125%, and 0.25%) on the development of strength of the nano-CPB samples were examined, and the obtained results can be seen in Figure 4-5, Figure 4-9, and Figure 4-13. These figure show that all of the nano-CPB and control samples, regardless whether there is SP, show a constant trend of increase in strength with time, which is due to the development of the binder agent hydration. Based on these figures, it can be stated

that the nano-CPB samples with higher contents of SP have a higher UCS when the samples are at least one day. Note that testing samples with 0.25% of SP at the 12th hour after mixing is not possible (Figure 4-13), owing to the lack of minimum strength acquisition which takes place in the first 12 hours. This behaviour can be explained by the increased influence of the repulsive forces produced by the presence of the high dosage of SP that acts on the solid particles of the CPB mixture, including the tailing particles, NPs, and cement. This factor is the main reason for delaying the initial setting time of CPB and thereby retarding the hydration process (Šiler et al. 2014). However, after 24 hours, a sharp and continuous increase in strength development was observed for all of the studied samples with 0.25% of SP. This observed higher strength of nano-CPBs with higher SP content could be attributed to the fact that more SP promotes better dispersion of the NPs in the backfill mixture, thus increasing the filler effect of the NPs and their impact on cement hydration processes (enhances binding effect). Both phenomena lead to the refinement of the pore structure of the nano-CPB, which contributes to the increase in UCS. Moreover, previous studies on the effect of SP on the mechanical and rheological performances of CPB, such as Haruna and Fall (2020a, 2020b) and Al-Moselly et al. (2022) conclude that an increase of SP in CPB leads to the refinement of its microstructure. The impact of the higher dosage of SP on pore structure refinement of the nano-CPB sample can be seen in the result of the MIP test conducted on two nano-CPB samples with different SP contents (e.g., 0.125% and 0.25%), as shown in Figure 4-14. The nano-CPB sample with 0.25% of SP exhibits a denser pore structure compared to the nano-CPB sample with less SP (i.e., 0.125% of SP), which explains for favorable effect of a higher content of SP on the mechanical performance of nano-CPB samples.

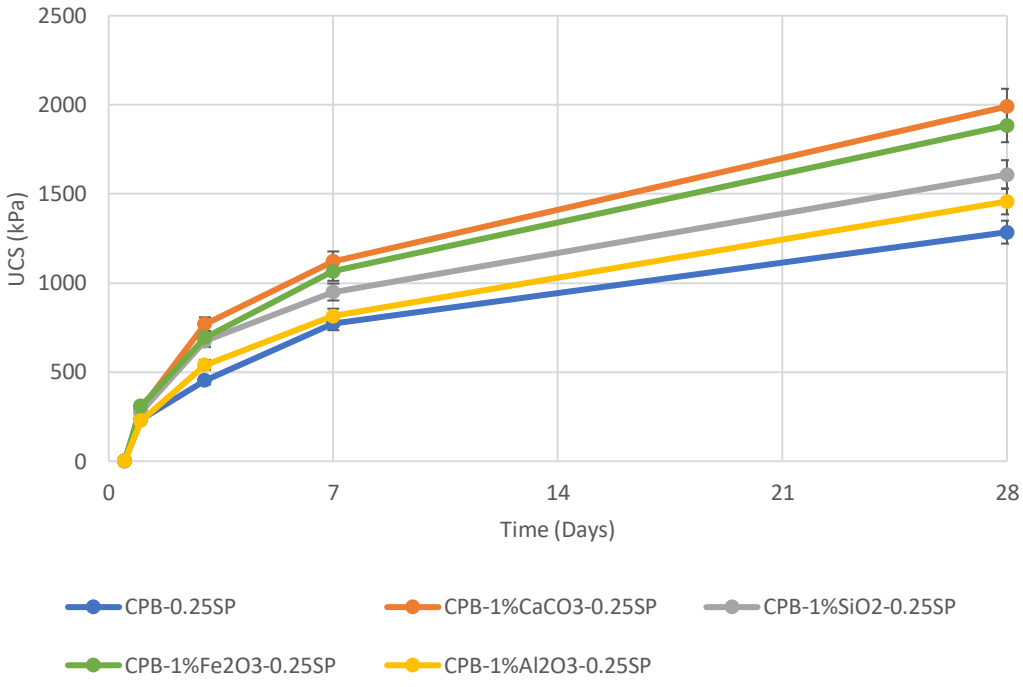

Figure 4-13 Effect of superplasticizer content the strength development of CPB with 1% nano-particle and a dosage of 0.25% of SP

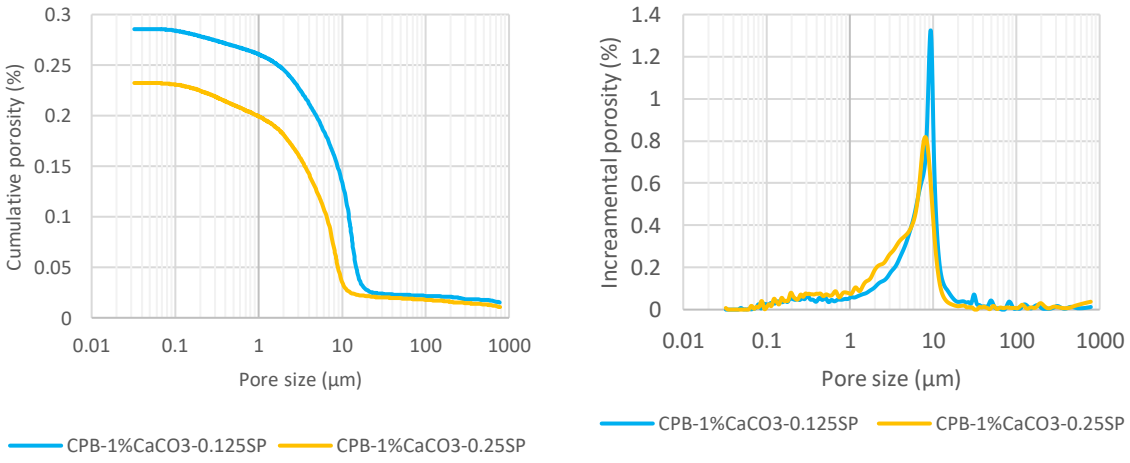

a) Cumulative pore volume b) Pore distribution

Figure 4-14. Results of MIP test for effect of different dosages of SP on the pore structure of the nano-CPB sample

4.5. Summary and conclusion

In this article, the effect of introducing different types of NP additives on the development of the strength of CPB and rate of suction development, the two most important performance variables at the early ages of the CPB, is explored. A polycarboxylate ether-based SP is utilized as the dispersing agent to help distribute the NPs efficiently. Different microstructural tests and monitoring programs are implemented to further explain the results obtained in the UCS tests conducted on CPB samples mixed with NP additives. The main outcomes of this study based on the results observed in the experiment are summarized as follows:

- Regardless whether NP additives are added, the rate of the strength and suction development in the CPB shows an increase over the period of the curing cycle.
- Depending on the presence of an effective dispersing agent in the CPB mixture, the addition of NP additives can enhance the mechanical performance of CPB or adversely diminish the strength gain rate.
- CPB samples prepared with proper dispersion of NPs including nano-$CaCO_3$, nano-Fe_2O_3, and nano-SiO_2 exhibit higher strength and suction values than the control sample and the sample mixed with nano-Al_2O_3.
- An increase in SP results in significant improvement in rate of the strength development of nano-CPB due to increased contribution of SP in hydration reactions, thus resulting in the generation of more hydration products and a higher degree of NP dispersion.
- Among the tested NP additives, nano-$CaCO_3$ has the best overall impact on the mechanical properties of CPB owing to the formation of a denser microstructure as well as more bonding products. Thereby, the highest UCS values and higher negative pore water pressure are attained compared to the other types of NP additives and control samples.

4.6. References

Al-Moselly, Z., Fall, M., and Haruna, S. 2022. Further insight into the strength development of cemented paste backfill materials containing polycarboxylate ether-based superplasticizer. Journal of Building Engineering, 47: 103859. Elsevier. doi:10.1016/J.JOBE.2021.103859.

Barbhuiya, S., Mukherjee, S., and Nikraz, H. 2014. Effects of nano-Al2O3 on early-age microstructural properties of cement paste. Construction and Building Materials, 52: 189–193. Elsevier. doi:10.1016/J.CONBUILDMAT.2013.11.010.

Camiletti, J., Soliman, A.M., and Nehdi, M.L. 2013. Effect of nano-calcium carbonate on early-age properties of ultrahigh-performance concrete. Magazine of Concrete Research, 65(5): 297–307. doi:10.1680/MACR.12.00015.

Fall, M., and Benzaazoua, M. 2003. Advances in predicting performance properties and cost of paste backfill. Tailings and Mine Waste,: 73–85.

Fall, M., and Benzaazoua, M. 2005. Modeling the effect of sulphate on strength development of paste backfill and binder mixture optimization. Cement and Concrete Research,. doi:10.1016/j.cemconres.2004.05.020.

Fall, M., Benzaazoua, M., and Saa, E.G. 2008. Mix proportioning of underground cemented tailings backfill. Tunnelling and Underground Space Technology, 23(1): 80–90. Pergamon. doi:10.1016/j.tust.2006.08.005.

Fall, M., Célestin, J.C., Pokharel, M., and Touré, M. 2010a. A contribution to understanding the effects of curing temperature on the mechanical properties of mine cemented tailings backfill. Engineering Geology, 114(3): 397–413. doi:https://doi.org/10.1016/j.enggeo.2010.05.016.

Fall, M., Célestin, J.C., Pokharel, M., and Touré, M. 2010b. A contribution to understanding the effects of curing temperature on the mechanical properties of mine cemented tailings backfill. Engineering Geology, 114(3–4): 397–413. Elsevier. doi:10.1016/J.ENGGEO.2010.05.016.

Gaitero, J.J., de Ibarra, Y.S., Erkizia, E., and Campillo, I. 2006. Silica nanoparticle addition to control the calcium-leaching in cement-based materials. physica status solidi (a), 203(6): 1313–1318. John Wiley & Sons, Ltd. doi:10.1002/PSSA.200566168.

Gaitero, J.J., Zhu, W., and Campillo, I. 2009. Multi-scale Study of Calcium Leaching in Cement Pastes with Silica Nanoparticles. Nanotechnology in Construction 3,: 193–198. Springer, Berlin, Heidelberg. doi:10.1007/978-3-642-00980-8_26.

Ghirian, A., and Fall, M. 2013. Coupled thermo-hydro-mechanical-chemical behaviour of cemented paste backfill in column experiments. Part I: Physical, hydraulic and thermal processes and characteristics. Engineering Geology, 164: 195–207. doi:10.1016/J.ENGGEO.2013.01.015.

Ghirian, A., and Fall, M. 2017. Properties of cemented paste backfill. Paste Tailings Management,: 59–109. Springer International Publishing. doi:10.1007/978-3-319-39682-8_4/FIGURES/50.

Haiqiang, J., Fall, M., and Cui, L. 2016. Yield stress of cemented paste backfill in sub-zero environments: Experimental results. Minerals Engineering, 92: 141–150. Pergamon. doi:10.1016/J.MINENG.2016.03.014.

Haruna, S. 2022. Effect of Superplasticizer on the Performance Properties of Cemented Paste Backfill at Different Curing Temperatures. Université d'Ottawa / University of Ottawa. doi:10.20381/RUOR-28427.

Haruna, S., and Fall, M. 2020a. Strength development of cemented tailings materials containing polycarboxylate ether-based superplasticizer: experimental results on the effect of time and temperature. https://doi.org/10.1139/cjce-2019-0809, 48(4): 429–442. NRC Research Press 1840 Woodward Drive, Suite 1, Ottawa, ON K2C 0P7 . doi:10.1139/CJCE-2019-0809.

Haruna, S., and Fall, M. 2020b. Time- and temperature-dependent rheological properties of cemented paste backfill that contains superplasticizer. Powder Technology, 360: 731–740. Elsevier. doi:10.1016/J.POWTEC.2019.09.025.

Hefni, M., and Ali, M.A. 2021. The Potential to Replace Cement with Nano-Calcium Carbonate and Natural Pozzolans in Cemented Mine Backfill. doi:10.1155/2021/5574761.

Kadri, E.H., and Duval, R. 2002. Effect of Ultrafine Particles on Heat of Hydration of Cement Mortars. Materials Journal, 99(2): 138–142. doi:10.14359/11705.

Keller, A.A., Wang, H., Zhou, D., Lenihan, H.S., Cherr, G., Cardinale, B.J., Miller, R., and Zhaoxia, J.I. 2010. Stability and aggregation of metal oxide nanoparticles in natural aqueous

matrices. Environmental Science and Technology, 44(6): 1962–1967. American Chemical Society. doi:10.1021/ES902987D/SUPPL_FILE/ES902987D_SI_001.PDF.

Kim, G.M., Nam, I.W., Yoon, H.N., and Lee, H.K. 2018. Effect of superplasticizer type and siliceous materials on the dispersion of carbon nanotube in cementitious composites. Composite Structures, 185: 264–272. Elsevier Ltd. doi:10.1016/J.COMPSTRUCT.2017.11.011.

Levita, G., Marchetti, A., Gallone, G., Princigallo, A., and Guerrini, G.L. 2000. Electrical properties of fluidified Portland cement mixes in the early stage of hydration. Cement and Concrete Research, 30(6): 923–930. Pergamon. doi:10.1016/S0008-8846(00)00282-9.

Li, W., and Fall, M. 2018. Strength and self-desiccation of slag-cemented paste backfill at early ages: Link to initial sulphate concentration. Cement and Concrete Composites, 89: 160–168. doi:https://doi.org/10.1016/j.cemconcomp.2017.09.019.

Liu, X., Chen, L., Liu, A., and Wang, X. 2012. Effect of Nano-CaCO3 on Properties of Cement Paste. Energy Procedia, 16(PART B): 991–996. Elsevier. doi:10.1016/J.EGYPRO.2012.01.158.

Lothenbach, B., Winnefeld, F., and Figi, R. 2007. The influence of superplasticizers on the hydration of Portland cement. Empa, Dübendorf, Switzerland,.

Ltifi, Guefrech, A., Mounanga, P., and Khelidj, A. 2011. Experimental study of the effect of addition of nano-silica on the behaviour of cement mortars Mounir. Procedia Engineering, 10: 900–905. doi:https://doi.org/10.1016/j.proeng.2011.04.148.

MasterGlenium 7500 | Master Builders Solutions. (n.d.). Available from https://www.master-builders-solutions.com/en-us/products/concrete-admixtures/water-reducers/water-reducers-high-range/masterglenium-7500. [accessed 14 April 2023].

Mehta, P., and Monteiro, P. 2014. Concrete: microstructure, properties, and materials.

Nazari, A., and Riahi, S. 2011. Improvement compressive strength of concrete in different curing media by Al2O3 nanoparticles. Materials Science and Engineering: A, 528(3): 1183–1191. doi:https://doi.org/10.1016/j.msea.2010.09.098.

Nonnet, E., Lequeux, N., and Boch, P. 1999. Elastic properties of high alumina cement castables from room temperature to 1600°C. Journal of the European Ceramic Society, 19(8): 1575–1583. Elsevier. doi:10.1016/S0955-2219(98)00255-6.

Oltulu, M., and Şahin, R. 2013. Effect of nano-SiO2, nano-Al2O3 and nano-Fe2O3 powders on compressive strengths and capillary water absorption of cement mortar containing fly ash: A comparative study. Energy and Buildings, 58: 292–301. doi:https://doi.org/10.1016/j.enbuild.2012.12.014.

Palla, R., Karade, S.R., Mishra, G., Sharma, U., and Singh, L.P. 2017. High strength sustainable concrete using silica nanoparticles. Construction and Building Materials, 138: 285–295. doi:https://doi.org/10.1016/j.conbuildmat.2017.01.129.

Pane, I., and Hansen, W. 2005. Investigation of blended cement hydration by isothermal calorimetry and thermal analysis. Cement and Concrete Research, 35(6): 1155–1164. Pergamon. doi:10.1016/J.CEMCONRES.2004.10.027.

Puertas, F., Martínez-Ramírez, S., Alonso, S., and Vázquez, T. 2000. Alkali-activated fly ash/slag cements: Strength behaviour and hydration products. Cement and Concrete Research, 30(10): 1625–1632. Pergamon. doi:10.1016/S0008-8846(00)00298-2.

Quercia, G., Hüsken, G., and Brouwers, H.J.H. 2012a. Water demand of amorphous nano silica and its impact on the workability of cement paste. Cement and Concrete Research, 42(2): 344–357. doi:https://doi.org/10.1016/j.cemconres.2011.10.008.

Quercia, G., Hüsken, G., and Brouwers, H.J.H. 2012b. Water demand of amorphous nano silica and its impact on the workability of cement paste. Cement and Concrete Research, 42(2): 344–357. Pergamon. doi:10.1016/J.CEMCONRES.2011.10.008.

Reches, Y. 2018. Nanoparticles as concrete additives: Review and perspectives. Construction and Building Materials, 175: 483–495. Elsevier Ltd. doi:10.1016/J.CONBUILDMAT.2018.04.214.

Roshani, A., and Fall, M. 2020a. Flow ability of cemented pastefill material that contains nano-silica particles. Powder Technology, 373: 289–300. doi:https://doi.org/10.1016/j.powtec.2020.06.050.

Roshani, A., and Fall, M. 2020b. Rheological properties of cemented paste backfill with nano-silica: Link to curing temperature. Cement and Concrete Composites, 114. Elsevier Ltd. doi:10.1016/J.CEMCONCOMP.2020.103785.

Senff, L., Labrincha, J.A., Ferreira, V.M., Hotza, D., and Repette, W.L. 2009. Effect of nano-silica on rheology and fresh properties of cement pastes and mortars. Construction and Building Materials, 23(7): 2487–2491. doi:https://doi.org/10.1016/j.conbuildmat.2009.02.005.

Shaikh, F.U.A., and Supit, S.W.M. 2015. Effects of Superplasticizer Types and Mixing Methods of Nanoparticles on Compressive Strengths of Cement Pastes. Journal of Materials in Civil Engineering, 28(2): 06015008. American Society of Civil Engineers. doi:10.1061/(ASCE)MT.1943-5533.0001373.

Shaikh, F.U.A., and Supit, S.W.M. 2016. Effects of Superplasticizer Types and Mixing Methods of Nanoparticles on Compressive Strengths of Cement Pastes. Journal of Materials in Civil Engineering, 28(2): 06015008. American Society of Civil Engineers. doi:10.1061/(ASCE)MT.1943-5533.0001373.

Siang Ng, D., Paul, S.C., Anggraini, V., Kong, S.Y., Qureshi, T.S., Rodriguez, C.R., Liu, Q. feng, and Šavija, B. 2020. Influence of SiO2, TiO2 and Fe2O3 nanoparticles on the properties of fly ash blended cement mortars. Construction and Building Materials, 258. Elsevier Ltd. doi:10.1016/J.CONBUILDMAT.2020.119627.

Šiler, P., Kolářová, I., Krátký, J., Havlica, J., and Brandštetr, J. 2014. Influence of superplasticizers on the course of Portland cement hydration. Chemical Papers, 68(1): 90–97. De Gruyter. doi:10.2478/S11696-013-0413-X/MACHINEREADABLECITATION/RIS.

Sivakugan, N., Rankine, R.M., Rankine, K.J., and Rankine, K.S. 2006. Geotechnical considerations in mine backfilling in Australia. Journal of Cleaner Production,. doi:10.1016/j.jclepro.2004.06.007.

Tariq, A., and Yanful, E.K. 2013. A review of binders used in cemented paste tailings for underground and surface disposal practices. Journal of Environmental Management, 131: 138–149. Academic Press. doi:10.1016/J.JENVMAN.2013.09.039.

Taylor, H. 1966. Chemistry of cements.

Taylor, H.F.W. 1997. Cement chemistry.

Thomas, J.J., Jennings, H.M., and Chen, J.J. 2009. Influence of Nucleation Seeding on the Hydration Mechanisms of Tricalcium Silicate and Cement. The Journal of Physical Chemistry C, 113(11): 4327–4334. American Chemical Society. doi:10.1021/jp809811w.

Thottarath, S. 2010. Electromagnetic characterization of cemented paste backfill in the field and laboratory.

Yilmaz, E., and Fall, M. 2017. Paste tailings management. In Paste Tailings Management.

Yilmaz, E., Kesimal, A., and Ercidi, B. 2004. Strength development of paste backfill simples at Long term using different binders. In Proceedings of 8th symposium MineFill04, China.

Zhang, Y.-R., Kong, X.-M., Lu, Z.-B., Lu, Z.-C., and Hou, S.-S. 2015. Effects of the charge characteristics of polycarboxylate superplasticizers on the adsorption and the retardation in cement pastes. Cement and Concrete Research, **67**: 184–196. doi:https://doi.org/10.1016/j.cemconres.2014.10.004.

CHAPTER 5. Technical Paper II: Physical modeling of the geotechnical behaviour of cemented backfill plug with and without nanoparticles under simulated field overburden pressure

Amirreza Saremi, Mamadou Fall
Department of Civil Engineering, University of Ottawa, Canada

(Submited)

5.1. Abstract

This research article investigates the geotechnical responses of cemented paste backfill (CPB) plugs both with and without nanoparticles (NPs), specifically nano-calcium carbonate (nano-$CaCO_3$). The study considers the effects of realistic field overburden pressures on the CPB plugs, analyzing parameters such as strength development, pore water pressure evolution, total stress evolution, and pore structure changes. To accurately simulate field conditions, a novel physical model equipped with various sensors and a mechanical loading system was developed, considering factors like backfill height and backfilling rate. Monitoring experiments, along with mechanical and microstructural tests, were conducted using the physical model to assess the geotechnical characteristics of the CPB plugs under realistic vertical mechanical loading conditions. The study's key findings revealed that the addition of NPs significantly enhances the strength and strength-gaining rate of CPB plugs compared to control samples. This improvement is attributed to several mechanisms, including the filler effect of NPs, acceleration of the hydration process, and the generation of more hydration products. Furthermore, curing CPB plugs under field overburden pressures was observed to lead to enhanced mechanical properties, primarily due to pore structure refinement (lower void ratio/porosity), faster pore water dissipation, and accelerated hydration progress. However, as the CPB hardens and gains strength, the impact of applied vertical stress (overburden pressure) weakens, particularly in comparison to the initial stages. Notably, CPB plugs with NPs experienced a lower and faster decrease in the pore water pressure and total stresses compared to those without NPs. These findings have significant implications for designing higher-performance CPB plugs while enhancing the sustainability of backfilling and mining operations. The study contributes valuable insights into optimizing the utilization of nanotechnology in geotechnical engineering applications.

Keywords: tailings; cemented paste backfill; nanoparticles; geotechnical; plug; physical model

5.2. Introduction

The mining industry faces significant challenges in balancing the need to increase productivity, improve safety and the growing demand for environmentally responsible practices. Cemented Paste Backfill (CPB), a mixture of tailings, cement, water, and sometimes additives, has emerged as a key solution to address these challenges, as it offers both operational and environmental benefits. The use of CPB not only provides ground support and facilitates the disposal of mine waste (tailings), but also enhances the stability of underground excavations, reduces surface subsidence, improve mine productivity, and minimizes the environmental footprint of mining operations [2, 15, 31]. From an environmental perspective, the surface disposal of mine wastes, such as tailings, can have significant detrimental effects on the surrounding ecosystem. Tailings often contain harmful constituents, including heavy metals and acidic components, which can pose serious risks when disposed of on the ground surface. The potential for these contaminants to leach into the soil, water, and atmosphere raises significant concerns regarding the long-term environmental and public health consequences of such practices. Moreover, from a geotechnical standpoint, the formation of underground cavities as a result of mining activities presents additional challenges. These voids can undermine the structural integrity of the terrain, increasing the likelihood of ground subsidence and subsequent damage to infrastructure, property, and the natural landscape. These voids can also affect mining safety and productivity. Addressing these interconnected environmental and geotechnical issues is essential for promoting responsible and sustainable mining practices that minimize the negative impacts on both the environment and the safety of mining operations [8, 9, 13, 14, 16, 18, 21].

Typically, mined stopes are filled with two distinct layers of paste backfill material. Initially, a retaining structure known as a barricade is constructed at the base of the stope to secure the fresh CPB in place during the curing process and in its early stages (Figure 5-1). Subsequently, the first layer of CPB, known as “plug” of CPB (CPB plug), is poured into the stope, followed by the second layer called residual backfill (Figure 5-1). The primary differences between plug and residual backfill lie in the binder dosage and the height of these layers. Concerning binder

content, CPB plug generally contains a higher dosage due to its crucial functions. Firstly, it provides sufficient structural support to withstand overburden pressure from the residual backfill and its self-weight. This, in turn, helps to alleviate excess pressure on the temporary barricade at the draw point. Secondly, plug prevents the failure and collapse of adjacent walls, thereby ensuring underground mine excavation stability [30]. The height of CPB plug is typically much lower than that of residual backfill for two key reasons. Firstly, the higher binder dosage in CPB plug makes any unnecessary increase in height economically undesirable, as it significantly raises backfilling costs. Secondly, before introducing residual backfill, the plug layer must achieve the minimum strength needed or suitable geotechnical properties to remain mechanically stable. This necessitates a pause in the backfilling process until the minimum curing time for the CPB plug is reached. Consequently, any increase in the height of plug would extend the required curing time, delaying the backfilling process, which has a detrimental impact on mine productivity [1, 10, 31].

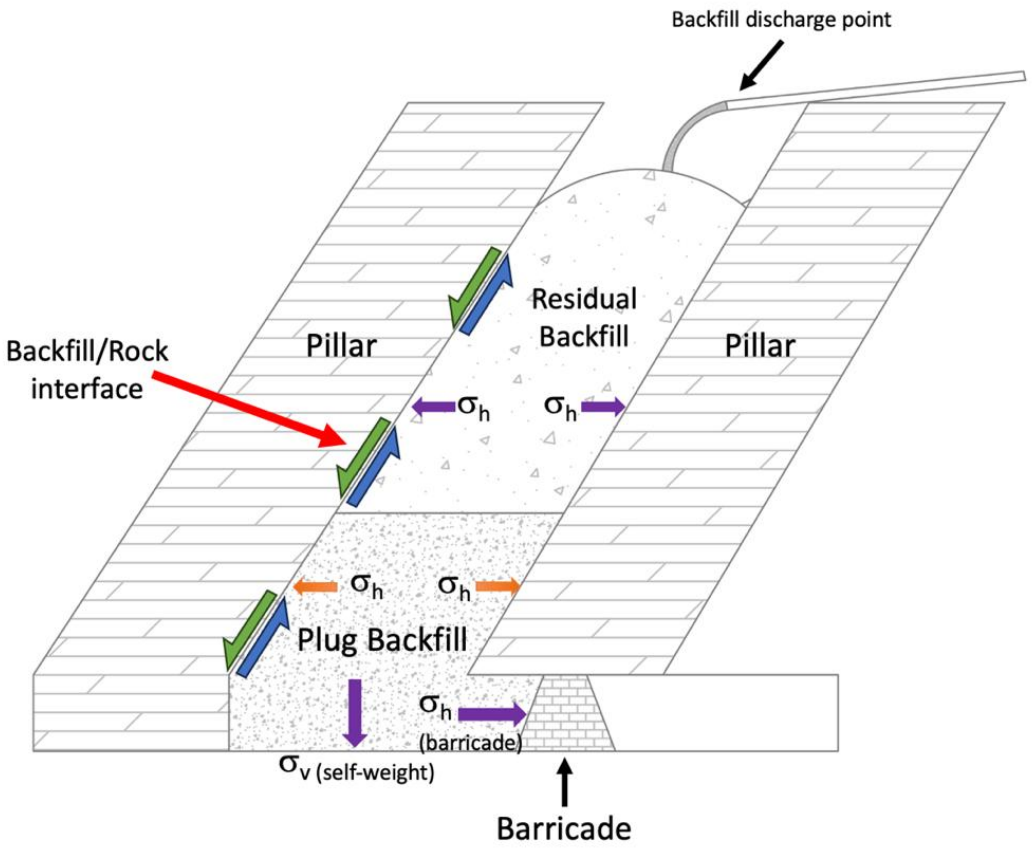

Figure 5-1. Schematic representation of a backfilled mine stope, illustrating the interaction between the plug of cemented paste backfill, residual backfill, and the surrounding rock masses

As a result, proper geotechnical design of CPB plug is of paramount importance for ensuring the safety and efficiency of mining operations. The plug structure must exhibit mechanical stability, which entails gaining strength and geotechnical properties to support its own weight, to withstand external loads to which it is exposed, and to protect the barricade from potential effects during the subsequent "main" pour (residual backfill) throughout the remaining volume of the stope, as presented in Figure 5-1. Critical geotechnical properties or behaviors required to evaluate the geotechnical performance of the CPB plug include strength development, pore water pressure dissipation rate, rate of suction increase and total stress evolution in the CPB plug. The CPB strength serves as a crucial parameter for evaluating the mechanical stability of the plug structure. Additionally, pore water pressure plays a significant role in influencing both the liquefaction potential of the CPB plug and its overall strength, as well as the total stress

exerted on the barricade. Notably, the development of suction within the plug not only enhances its strength but also significantly diminishes its liquefaction potential and reduces the pressure on the barricade. In addition, understanding the total stress within the plug becomes essential in accurately assessing the total stress applied to the barricades [10].

It is crucial to avoid any CPB plug failure or barricade failure, as it could lead to casualties and financial losses. Moreover, it is vital to minimize stoppage time to enhance overall mining profitability. This can be achieved by either reducing the strength-gaining period of the CPB plug or accelerating the development of its suitable geotechnical properties. By focusing on optimizing the CPB plug's geotechnical performance and expediting its mechanically stabilization process, mining operations can minimize downtime, increase productivity, and ensure safer and more profitable mining practices.

One common approach utilized in backfilling operations to improve the geotechnical properties of the CPB plug and expedite the development rate of its geotechnical characteristics (e.g., strength, suction, dissipation of pore water pressure) involves increasing the amount of binder in the CPB mix formulation, typically cement. This adjustment leads to the production of more cement hydration products, which play a crucial role in enhancing the strength of CPB [6], as well as in faster dissipation of pore water pressure or a higher rate of suction development due to water consumption by cement hydration (self-desiccation process). While this method positively impacts the geotechnical performance of CPB, it comes with a notable drawback – a substantial increase in the overall cost of backfilling. The binder, which constitutes a significant portion of the CPB cost, can account for up to 75% of the final expenses [31]. Moreover, the use of cement in the industry has raised environmental concerns due to its substantial contribution to carbon dioxide emissions [19]. Considering the growing emphasis on sustainable practices, it is essential to explore alternative solutions that strike a balance between geotechnical performance and environmental impact. Moreover, several mines opt for a lengthy curing period after the plug is poured, sometimes lasting several days, before proceeding with pouring the remaining fill (residual fill). However, this method substantially prolongs the mining cycles, consequently reducing the mine's overall productivity.

To overcome the aforementioned challenges related to enhancing the geotechnical properties of CPB plugs and accelerating their development rate, researchers and practitioners are actively investigating diverse strategies. Among these, a promising and emerging approach involves the use of additives to facilitate the cement hydration process. In recent years, nanoparticles (NPs) have emerged as an effective supplementary additive for enhancing the performance of cementitious materials, such as concrete. By incorporating these nano-sized particles into the CPB plug, it would be possible to improve its geotechnical properties and speed up their development rate. This innovative approach holds great promise in addressing the environmental concerns linked to the use of Portland cement, ultimately paving the way for more sustainable and efficient underground mining operations. However, comprehensive studies on the impact of these NP additives on the geotechnical properties and behavior of CPB plug are lacking. Additionally, there has been no exploration of the geotechnical behavior of CPB containing nanoparticles under field vertical stress (overburden pressure) loading conditions.

To bridge this knowledge gap, our study aims to investigate the geotechnical behavior of plug CPB, both with and without nanoparticles, under various overburden pressure loading conditions that mirror real-world practices. A carefully developed and designed physical model will be employed to simulate a CPB plug, incorporating vertical stress loading conditions to mimic field overburden pressure scenarios. Within this experimental setup, we will evaluate several critical geotechnical parameters that significantly influence the stability of the plug CPB structure and barricade. These parameters include strength, pore water pressure, and stress distribution within the CPB plug. By closely examining these factors, our research aims to offer valuable insights into the performance of CPB plugs, contributing to the optimization of CPB design for enhanced safety, sustainability, and efficiency in underground mining applications. Ultimately, this investigation holds the potential to advance knowledge in the field and promote sustainable mining practices, reducing the environmental impact of traditional Portland cement usage.

5.3. Materials, Physical Model and Methods

5.3.1 Materials

5.3.1.1. Tailings

To eliminate any uncertainties related to reactive and acidic components existing in natural tailings, synthetic silica tailings (ST) have been used in this study. As shown in Table 5-1, the mineralogical composition of ST illustrates that quartz, the most frequent mineral in tailings from Canadian hard rock mines, is the predominant mineral (up to 99.8% of ST weight) of ST, which is a non-reactive mineral. The physical properties of the used tailings and the average of 9 mines located in the eastern part of Canada are given in Table 5-2.

Table 5-1.Mineralogical composition of the tailings used.

Tailings	Mineral											
	Quartz	Albite	Dolomite	Calcite	Chlorite	Magnetite	Pyrite	Talc	Pyrrhotite	Spinel	Others	Total
ST (wt.%)	99.8	-	-	-	-	-	-	-	-	-	0.2	100.0

ST: silica tailings; wt.: weight.

Table 5-2. Physical properties of the tailings used.

Element	G_s	D_{10}	D_{30}	D_{50}	D_{60}
Unit	-	µm	µm	µm	µm
ST	2.7	1.9	9.0	22.5	31.5
Average of 9 types of tailings	-	1.8	9.1	20.0	30.8

G_s: specific gravity

5.3.1.2. Nanoparticles

According to the findings of the research that was carried out by Saremi and Fall [25] on the effects of various types of nanoparticles on the suction and mechanical strength development of cemented paste backfill material, it was found that nano-calcium carbonate (nano-$CaCO_3$) significantly enhances the mechanical strength of CPB at its early age due to different mechanisms. These mechanisms include providing more nucleation sites for hydration reaction, which results in higher generation of hydration products including calcium silicate hydrates (C-S-H), calcium silica (C-H), and ettringite which provide the bonding between tailings particles. In addition, it has been determined that the incorporation of nano-$CaCO_3$ into the paste backfill significantly increases the packing density of the material. This is accomplished through the formation of a more compact microstructure, which is brought about by the coupled effect of a greater quantity of hydration products and the filler effect of nano-$CaCO_3$. For the reasons mentioned above nano-$CaCO_3$ particles were used as nanoparticles in this study. The physical properties of the nano- calcium carbonate is given in Table 5-3.

Table 5-3. Chemical and physical specifications of the nano-calcium carbonate used

Nano-$CaCO_3$	
Appearance	White powder
$CaCO_3$ (%)	≥98
HCl insoluble (%)	≤0.1
Particle size (nm)	20–50
Fe (%)	≤0.08
Mn (%)	≤0.006

5.3.1.3. Cement and mixing water

In order to prepare the CPB mixture, Ordinary PCI (general use Portland cement, e.g., type GU) has been used, which is the most common type of binder for producing backfill mixture in the field operations. In this study, tap water has been used to be mixed with other ingredients of the CPB. In order to prevent agglomeration of nano-particles due to their high Van der Waals interparticle forces and high specific surface area (SSA), a polycarboxylate ether-based

superplasticizer that has been proved to address this issue [20, 26], was used to help nanoparticles disperse uniformly throughout the CPB mixture.

5.3.2 Mix Proportioning and Specimen Preparation

In this experimental program, two different types of CPB mixtures have been prepared, including a control sample, which is CPB without nanoparticles, and a CPB sample that contains nanoparticles. To prepare CPB, the weighted amount of ST and PCI were mixed for 5 minutes in a mechanical mixer, then the solution of nanoparticles, superplasticizer, and water has been added to the mixer. This stage of mixing ran for another 10 minutes to obtain a homogenous mixture. The full details about the composition of the prepared specimens are given in Table 5-4. After the mixing process is completed, the CPB is poured into the column. The total duration of the filling process is approximately 10 minutes.

Table 5-4. Summary of the mix composition of the prepared CPB specimen and control specimen

Sample nomenclature	Binder Content (%)	SP (%)	Tailings type	W/C ratio	NP. (%)	NP, type	Curing Temp (ºC)	Solid Content (%)
PCI- CPB (control)	4.5	0.125	ST	7.8	0	None	20	74
PCI- CPB-NC	4.5	0.125	ST	7.8	1	NC	20	74

PCI, Portland cement type I; ST, silica tailings; W/C ratio, mass of water divided by the mass of binder. NP (%) = Mass of nanoparticlex100/Mass of dry tailings; Binder Content = Mass of binderx100/ (Mass of dry tailings + Mass of binder); NC, Nano-Calcium Carbonate, Solid Content (%) = (Mass of solid/Mass of the whole CPB); SP: superplasticizer content

5.3.3 Physical model and monitoring

Creating a realistic experimental setting that mimics a CPB plug was essential to address the objectives of this research. It must also be able to generate the mine stope filling sequences and support the external overburden pressure that stands in for the self-weight pressure caused by the backfill mass. The developed setup should also allow for the tracing of key CPB features over time, such as pore-water pressure and self-desiccation changes brought on by the cement hydration process, and stress distribution/redistribution brought on by the weight of the CPB

itself and external applied pressure. Figure 5-2 depicts the experimental setup that was designed and created in light of the aforementioned needs. Aluminum was chosen as the primary material for the structure for a number of reasons, with its great tensile strength being the most significant. This characteristic makes it an appropriate material for constructing the CPB plug structure, since it assures the column can endure the high pressure necessary during the curing process. The use of aluminum in the CPB's framework not only improves its safety and dependability, but also decreases the column's overall weight, making it easier to maneuver and move.

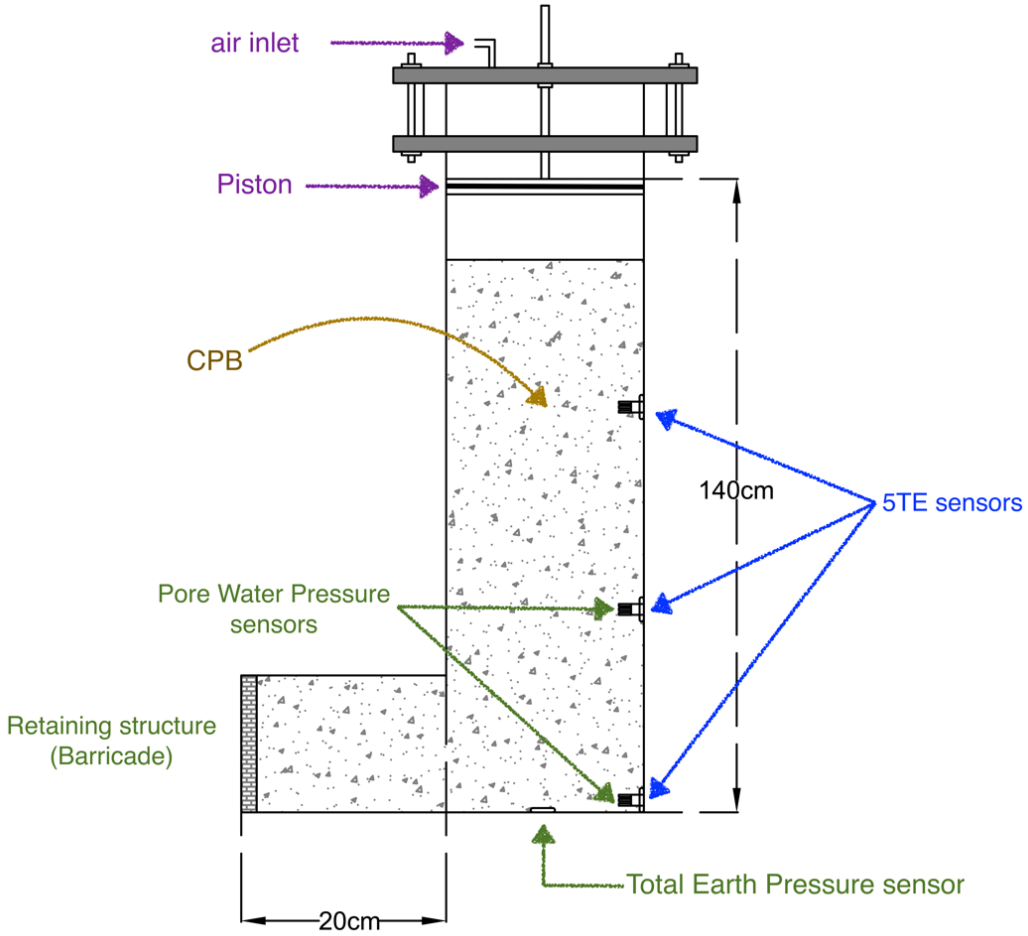

Figure 5-2. Schematic diagram of the developed plug model and details of sensors

Furthermore, the absence of friction between the CPB and the wall of the model, owing to the smooth surface of the aluminum, prevents the arching effect from being mobilized, which helps to eliminate the impact of the arching effect on the mechanical performance of the CPB column,

which was beyond the scope of this study. CPB column has a 20 x 20 cm cross-section and a height of 1.4 m. The horizontal component of the model which represents the drift of the stope has a same cross-section as the column with a length of 30 cm. Figure 5-3 depicts the schematic diagram of the developed physical model.

Due to inherent physical limitations, constructing a column of the entire CPB structure (including plug and residual backfill) with real field dimensions, which can reach up to 150 meters in height or 60 meters in width, for simulating the pressure that can be applied to the CPB plug in the field is currently infeasible. This limitation is primarily attributed to the substantial size of the plug and the residual backfill involved. To surmount this challenge, a mechanical air pressure system has been meticulously implemented to effectively apply the required vertical load, mimicking the overburden pressure, in real field conditions (refer to Figure 5-2). This approach allows us to replicate the desired pressure scenario without the need for a physically unattainable column. The pressure system consists of an axial piston propelled by air pressure. This piston is positioned atop the modeled plug to create the stope backfilling load on the CPB plug and barricade. The adoption of a mechanical air pressure system permits a realistic simulation of field conditions, guaranteeing that the CPB and barricade are subjected to the same stress as they would be in a real mine.

Figure 5-3 illustrates the external pressure application on the column, which has been imposed to simulate the equivalent height of the backfill structure. As can be seen the duration of pouring CPB has been assumed to be a period of three days. At the starting point, to obtain a more realistic simulation of the self-weight pressure, the external pressure was gradually increased every three hours in the first twelve hours after discharging the backfill. Afterwards, the pressure increased every 24 hours up to 600 kPa, equivalent to a 34.8-m high CPB structure in the field, if arching effect is neglected or insignificant. The equivalent height of the backfill has been calculated based on the bulk unit weight of 17.2 kN/m^3 for the CPB.

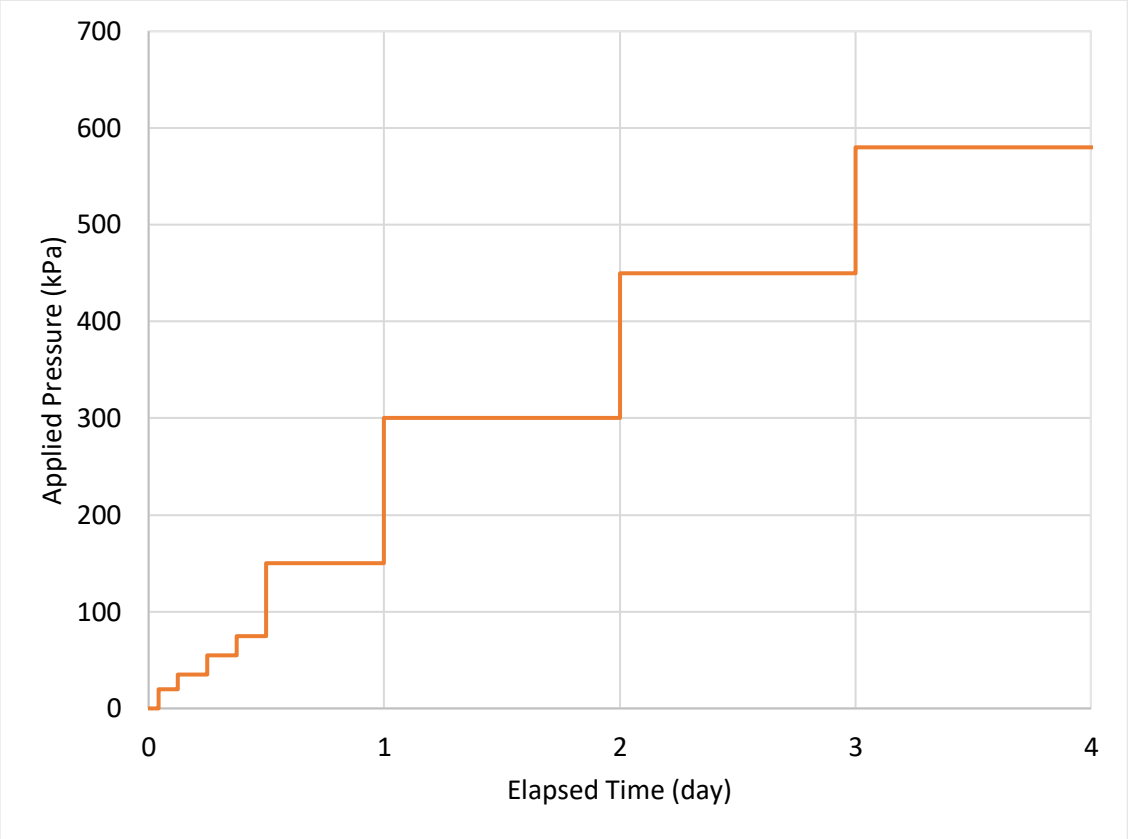

Figure 5-3. Scheme of adapted loading pattern that simulates the backfilling of a stope with 34.8m of height

In order to efficiently monitor the pressure at different sections and heights of the CPB plug column, two distinct strain gauge transducers detecting pressure have been placed in the model. These sensors are essential for comprehending the performance of the paste backfill and its capacity to sustain field loads and pressures. The major function of these sensors is to determine the total and effective stress of the paste backfill by measuring the pore water pressure and total earth pressure at various parts of the CPB column. The first class of sensors consists of mini-pore water pressure gauges, which can measure a maximum pressure of 1 MPa with an accuracy of 0.3% (Figure 5-2). Similarly, another DMTY total earth pressure sensor has been installed at the base of the column, in order to measure the total stresses acting on the CPB. These sensors provide an extensive image of the stress distribution within the CPB and the barricade's capacity to avoid instability and collapse. Table 5-5 provides more detailed information about these sensors, including their specifications.

Table 5-5. Detailed specifications of earth pressure and pore water pressure sensors used in the model

Sensor	Total earth pressure sensor	Pore water pressure sensor
Manufacture	Dan street Nanjing Electronic Technology Co.	
Model Type	DMTY	DMKY
Capacity	1 MPa	1 MPa
Accuracy	±0.3%	±0.3%
Output signal	0 to 5V	0 to 5V

A data collection system made by Xi'an Yima Opto-electrical Technology Co. is linked to the pore water pressure and earth pressure sensors, as well as a computer. This allows for the data that is collected by the strain gauges and strain sensors to be captured and analyzed. This system has the capability to record and analyze data gathered by up to 40 strain gauges and strain sensors concurrently, which provides a thorough insight of the performance of the CPB and barricade under a variety of loading circumstances.

In order to gain a deeper understanding of the interaction between nanoparticles and the binder, which significantly impacts the mechanical properties of CPB, a 5TE electrical conductivity (EC) sensor is employed for monitoring EC, temperature, and volumetric water content (VWC). This high-precision sensor offers an accuracy of ±10% for EC measurements, ±3% for VWC, and ±1°C for temperature readings. The sensor is strategically positioned at the center of each CPB sample and connected to a data logger for continuous data recording. EC is assessed by applying an alternating current between a pair of electrodes within the sensor and measuring the resulting electrical resistance. Fluctuations in EC serve as a practical indicator of ion transfer within cement-based materials, which is driven by the chemical progression of cement hydration.

5.3.4 Tests for determination of strength, microstructure and physical properties

5.3.4.1. Unconfined compressive strength (UCS) test

The ASTM-C109 standard was followed to determine the compressive strength of each CPB sample. The column was dismantled after a specific curing time (1, 3, 7, and 28 days), and various cores were taken from different sections of the CPB using a coring machine. The cores were then cut into multiple samples according to the standards. Subsequently, an automated mechanical press applied a vertical load to each sample at a speed of 1.0 mm/min to determine the ultimate

stress at which the specimens failed. To ensure the repeatability of test results, at least two identical specimens were used for each test.

5.3.4.2. Microstructural analysis and determination of physical properties

Several microstructural analyses and physical tests were performed to gain a better understanding of how the presence of NPs and different curing conditions affects the cement hydration and the evolution of CPB pore structure or physical properties (void ratio, porosity, dry density).

Thermal analyses (thermogravimetry (TG), differential thermogravimetry (DTG)) were carried out on CPB cement pastes with and without nanoparticles to gain a better insight into the cement hydration products formed in the CPB material. To prepare samples for TG/DTG testing, cement paste samples (with a w/c ratio of 1) were dried in an oven at 45°C for four days to ensure complete evaporation of free water. The samples were then reduced to powder and analyzed using an SDT 2960 thermogravimetric analyzer (simultaneous DSC-TGA). Samples were heated at a rate of 10°C/min to a maximum temperature of 1000°C in an N2 atmosphere at a rate of 100 ml/min.

In order to determine the physical properties of CPB, an extensive series of tests was conducted on samples obtained at various column heights and at different curing times. The sampling was achieved using a coring tool. These samples were then subjected to specific gravity determination using relevant standards, such as ASTM D854, which outlines the procedure for measuring the specific gravity of soil solids by water pycnometer. By measuring the specific gravity, the particle density of the CPB samples can be determined, which is an essential component for calculating the void ratio. Next, the bulk density of the samples was measured by filling a known volume container with the dried CPB material and subsequently calculating the mass per unit volume. With the bulk density and particle density values obtained, the total porosity of the samples could be calculated using the formula: $n = 1 - (\rho_b / \rho_p)$ where ρ_b is the bulk density (kg/cm^3) and ρ_p is the specific gravity (kg/cm^3). Finally, the void ratio was derived from the total porosity, using the formula: $e = n / (1 - n)$.

5.4. Results and discussion

5.4.1 Pore water pressure evolution

The results of pore water pressure monitoring at different sections in both the nano-CPB and control columns are illustrated in Figure 5-4. A noticeable decrease in pore water pressure is observed over the curing period for both columns, which can be ascribed to the effects of the cement hydration process. This process influences the pore water pressure in two distinct manners. Firstly, as hydration progresses, it consumes pore water to generate various hydration products, such as calcium silicate hydrates, ettringite, and others [2]. Secondly, the pore matrix refinement resulting from the hydration process (Figure 5-8 a, b) leads to the entrapment of pore water within the pore structure. Consequently, this impedes the interconnection of pore water molecules, further contributing to the reduction in pore water pressure [3].

Moreover, Figure 5-4 shows that both columns exhibited similar pore water pressure at the very beginning of their curing time, however pore water pressure in the column prepared with the addition of nanoparticles dissipated at a faster rate during the curing time, which can be explained by the effect of nanoparticles in different manners. First of all, the nano-calcium carbonate particles can act as nucleation sites, promoting the formation of hydration products such as calcium silicate hydrates (C-S-H) and calcium aluminate hydrates (C-A-H). This accelerated hydration reaction consumes more pore water, leading to a reduction in pore water pressure [25]. Results of thermal analysis (TG/DTG) presented in Figure 5-9 support this statement. According to this analysis, cement paste mixed with nano-calcium carbonate underwent greater weight loss during thermal analysis, corresponding to higher peak values, each of which represents the generation of different hydration products. Therefore, higher degree of weight loss or higher values in the associated peaks means existence of more hydration products in the cement paste sample. As an example, the peak observed in the range of 80°C and 120°C is associated with the decomposition of the hydration products, including C-S-H, gypsum and ettringite, and water evaporation [11]. While the peak observed in the range of 400°C and 500°C is attributed to the disintegration of CH, and the last peak between 650°C and 700°C refers to dehydration of calcite [7, 10]. In other words, as nano-calcium carbonate particles are

incorporated into the cement matrix, they can contribute to pore matrix refinement by forming additional hydration products and occupying the voids in the pore structure. This refinement can lead to the entrapment of pore water within the pore structure, which further impedes the interconnection of pore water molecules and contributes to the reduction in pore water pressure.

The other factor that results in development of lower pore water pressure due to addition of nanoparticles is improved particle packing of the CPB microstructure. The fine size of nano-calcium carbonate particles can improve the packing density of the cement matrix, filling the voids between larger particles [4, 5, 12, 24]. This improved packing results in a more refined pore structure, reducing the overall volume of pore water and thereby lowering the pore water pressure. This nanoparticle induced refined of the pore structure is consistent with the results of evolution of void ratio and porosity of CPB without and with nano-calcium carbonate particles presented in Figure 5-8 (a) and (b), respectively. These figures show that the void ratio or porosity of CPBs with nano-calcium carbonate particles is smaller than that without nanoparticles.

The findings presented above suggest that CPB plugs containing the nanoparticles studied will dissipate their excess pore water pressure faster than those containing no nanoparticles. Faster dissipation of excess pore water pressure more rapidly improves the liquefaction resistance of the plug structure and more rapidly decreases the total stress applied to the barricade. In other words, this can result in faster barricade opening, which has a significant impact on mine productivity.

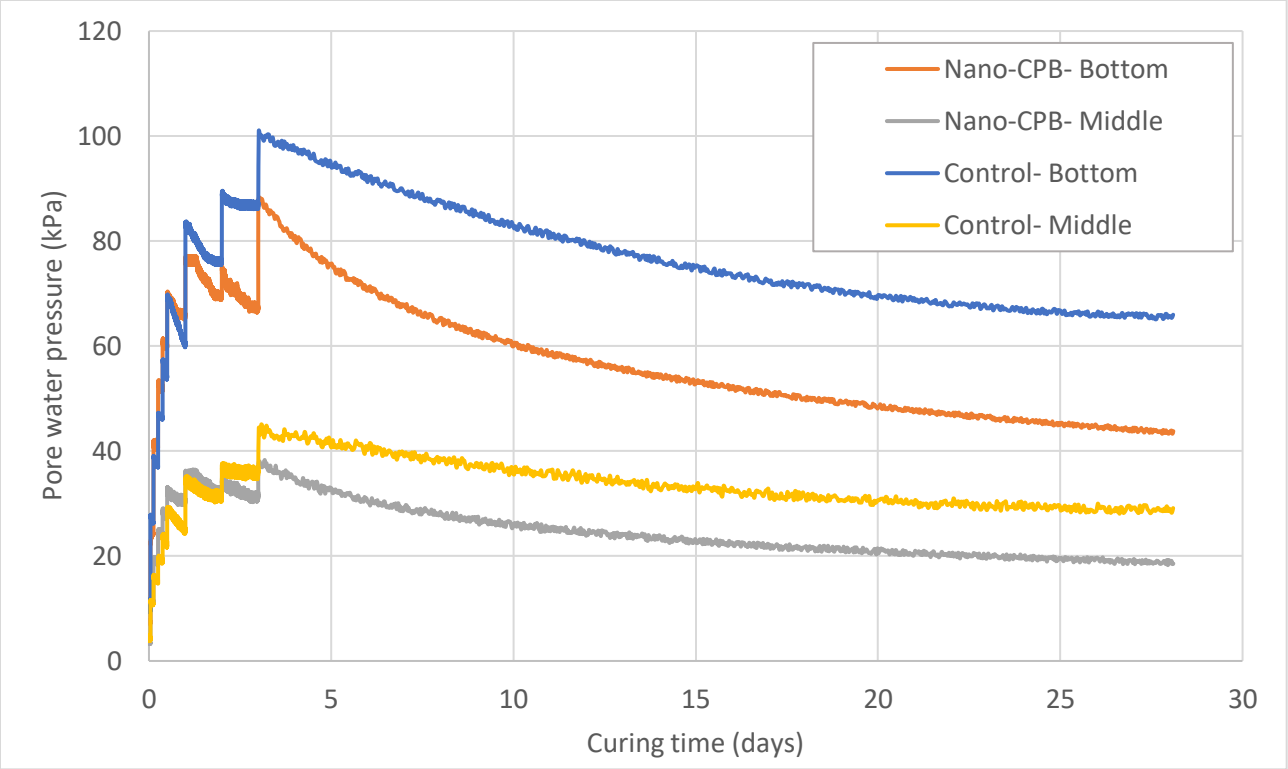

Figure 5-4. Evolution of pore water pressure at different heights of the CPB columns during curing (Bottom or base = 10 cm high in the column; Middle = 50 cm high)

5.4.2 Evolution of Unconfined Compressive Strength (UCS)

Figure 5-5 illustrates the evolution of the compressive strength of the CPB at different depths in the CPB columns with curing time. This figure shows that whether the CPB contains nanoparticles or not, there is an overall increase in the strength of the CPB with time at all depths. This increase is attributed to progress of the binder hydration and its subsequent effect on the enhancement of the cohesion of the CPB material, which is obviously associated with strength increase of CPB [8].

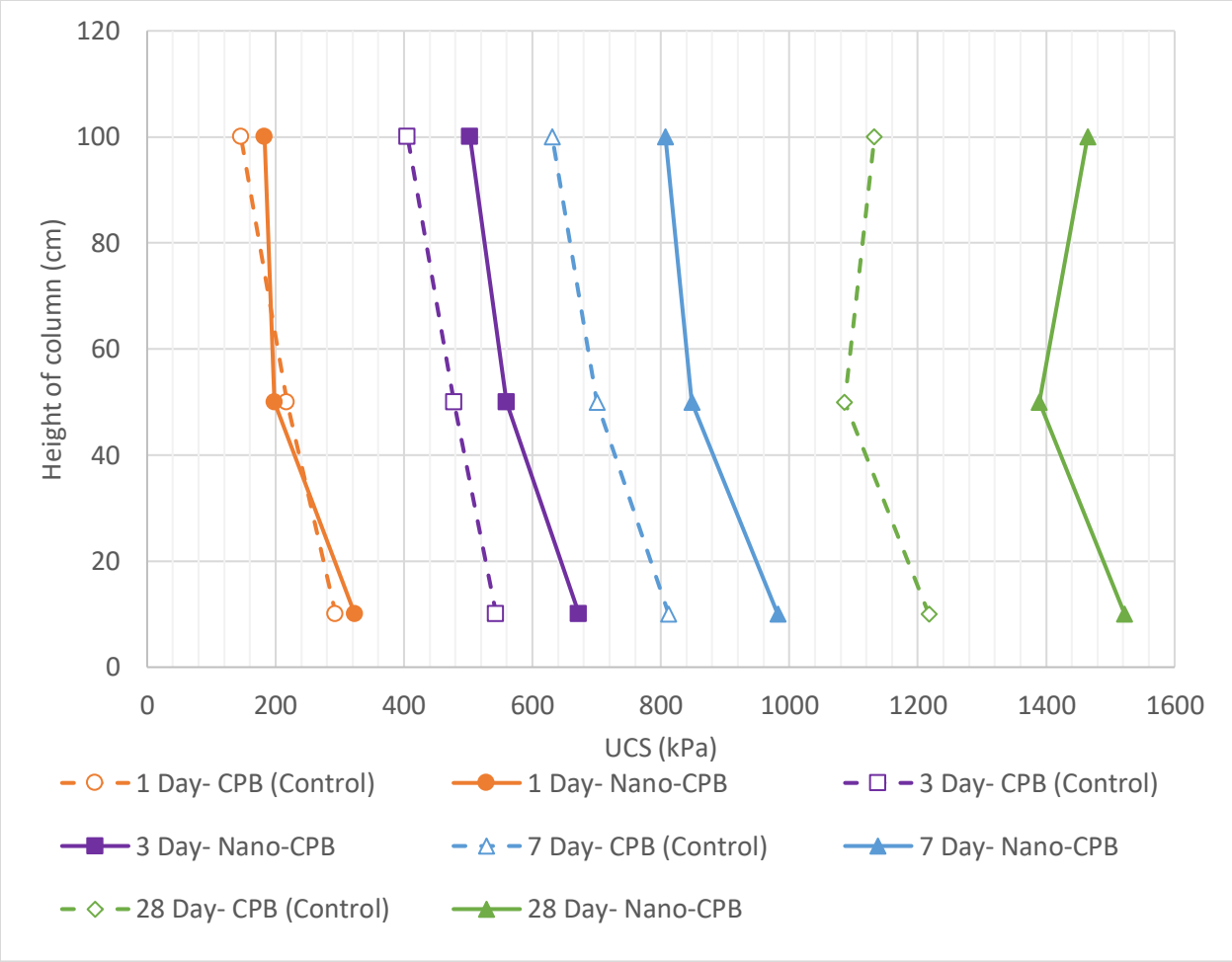

Figure 5-5. Evolution of compressive strength at different sections along with the curing cycle for control and nano-CPB column

This time-dependent progress of cement hydration is supported by the results of TG/DTG results presented in

Figure 5-6. This figure depicts the results of thermal analysis on a cement paste cured for two different curing times. The first sample was cured for seven days, and the second sample was cured for 28 days. The thermal analysis of Portland cement paste indicates that it decomposes in three separate phases at various temperatures [29]. The first stage, which occurs between 80°C and 120°C, is marked by rapid weight loss due to the decomposition of hydration products such as C-S-H, gypsum, ettringite, and the water's evaporation. The second peak, seen between 400 and 500 degrees Celsius, is caused by the disintegration of calcium hydroxide (CH), whereas the

third peak, visible between 650 and 700 degrees Celsius, is caused by the dehydration of calcite. Comparing the endothermic peaks shown in

Figure 5-6 demonstrates that the cement paste subjected to a 28-day curing cycle produces more cement hydration products, including calcium silicate hydrate, calcium hydroxide, and ettringite than cement paste exposed to a 7-day curing cycle. Hence, a longer curing time results in a larger amount of hydration products.

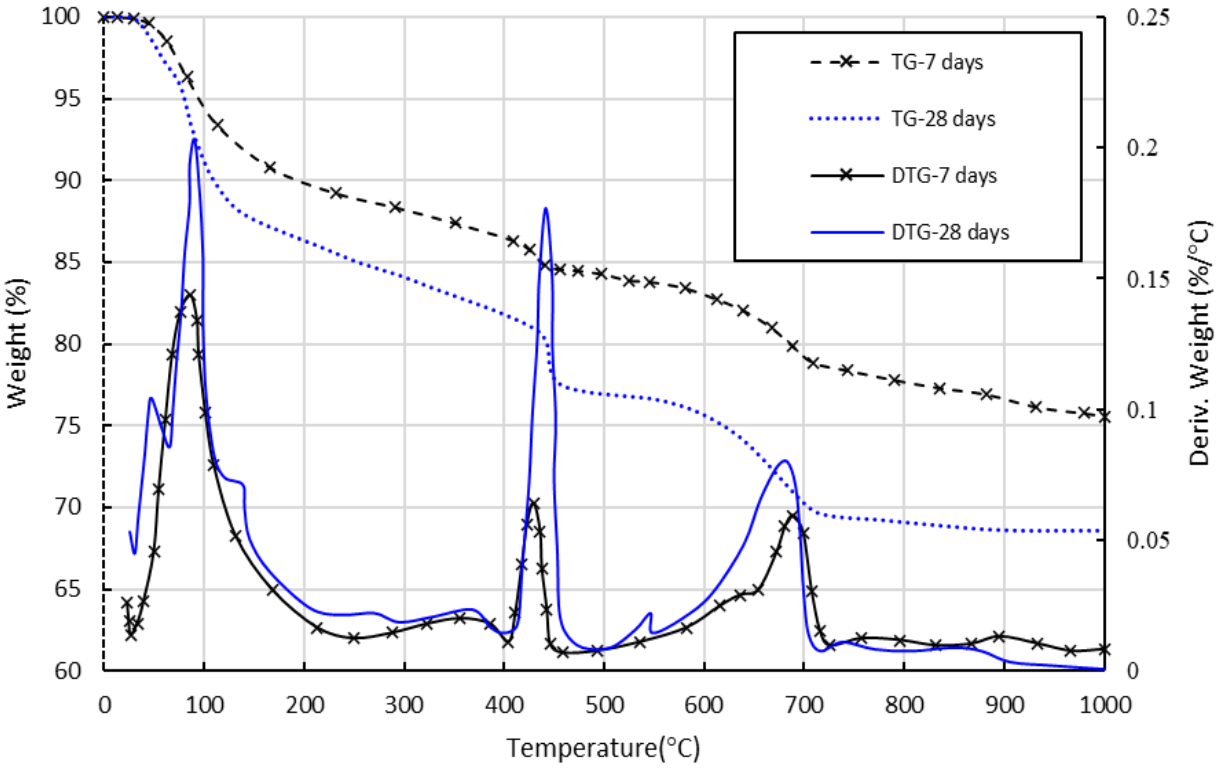

Figure 5-6. TG/DTG analyses results for cemented paste samples after 7 and 28 days of curing.

In addition, Figure 5-5 clearly depicts that the strength development of the CPB plug is also a function of the depth regardless of the content in nanoparticles. The CPB sample acquired from the base of the column (i.e., 10 cm high) displays higher strength during the early phases of the curing. For example, after one day of curing, the UCS measurements of the samples obtained from the bottom of the control column were, respectively, 35% and 100% higher than those from the middle (i.e., 50 cm high) and top (i.e., 100 cm high) of the column. Thus, it can be concluded that the rate of strength growth for samples obtained from the base of the CPB structure was

much greater than that of samples collected from the middle and top of the column during the initial phases of CPB. In other words, at early ages, the rate of strength development is faster in the lower part of the CPB plug than in its upper part. Nevertheless, as the curing period progresses, this pattern reverses, and the strength growth rate for samples taken from the top of the column becomes greater than that for samples obtained from the bottom. For instance, in the control column, samples cured for 28 days exhibited an 80% increase in strength compared to those cured for seven days at the top of the column. Comparatively, this rate was roughly 49% for samples obtained at the column's base.

This behavior can be explained by considering the effect of pressure gradient effect on the CPB mechanical properties. Considering the fluid nature of the fresh CPB at its early age and the weight of the paste above, the pressure exerted on the paste at the base of the CPB column is the greatest. This high pressure leads the CPB material to become less porous and denser, resulting in increased cementation and strength. Consequently, samples selected from the bottom of the column have higher UCS values on average. In contrast, as the column rises in height, the pressure drops, and the CPB becomes less dense and more porous. Figure 5-8 demonstrates the outcomes of void ratio and porosity measurements throughout the curing period. As evidenced in this figure, CPB displayed greater void ratios and porosity in the upper sections of the column compared to samples obtained from the base, which corroborates the observed results for the UCS testing.

Moreover, upon examination of the electrical conductivity (EC) monitoring results illustrated in Figure 5-7, a discernible trend emerges in the rate of strength gain. Ghirian and Fall [10] investigation posits that curing CPB under stress may give rise to a greater quantity of hydration products, such as calcium silicate hydrate (C-S-H). This compound is primarily responsible for facilitating bonding between tailings particles, thereby directly influencing the CPB's electrical conductivity. In essence, increased pressure applied to the CPB corresponds to reduced EC values. The EC monitoring outcomes presented in Figure 5-7 corroborate this observation. As demonstrated, the CPB's lower EC at the column base throughout the curing period, compared to the upper sections, can be ascribed to the combined impact of self-weight, external pressure, and the generation of additional hydration products. Consequently, this results in a decrease in

interconnected capillary pores and an increase in the CPB matrix's tortuosity. Furthermore, during the CPB column's initial stages, the middle section of the CPB column exhibits lower EC than the top section. This phenomenon can be elucidated by the accelerated CPB hardening process, driven by the rapid generation of hydration products due to self-weight and applied pressure. In other words, at early ages, the CPB in the column's bottom and middle sections harden more quickly than the top section.

The measurements of void ratio and dry density for samples extracted from various column sections or depths at different curing times, as depicted in Figure 5-8, substantiate the observed compressive strength and EC monitoring findings. In the early stages of CPB development, lower void ratio and porosity values are observed at the column's base, while porosity increases with height. This phenomenon can primarily be attributed to the pressure gradient engendered by the CPB's self-weight and applied pressure. However, after a certain period, the rate of change in void ratio values and porosity for the column's lower levels decelerates compared to the higher levels where the applied pressure is more proximal. As a result, by the end of the curing period, CPB samples procured from the column's upper-level exhibit lower void ratios, reduced porosity, and heightened dry density relative to samples obtained from the middle levels of the column.

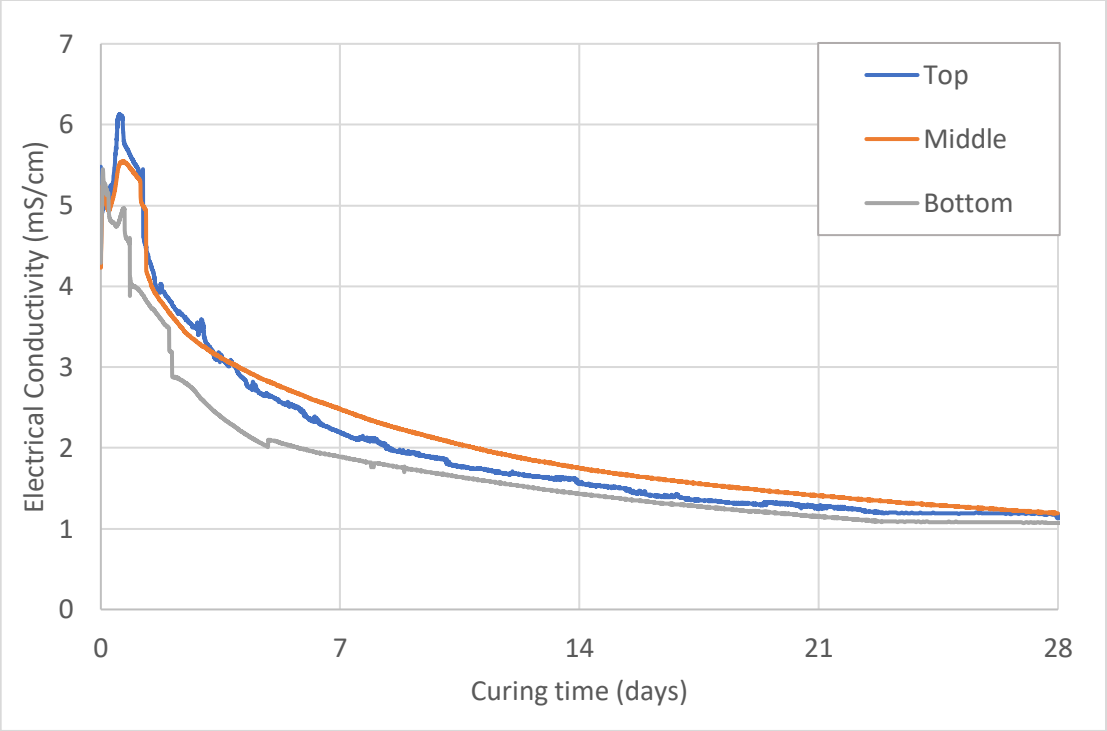

Figure 5-7. Evolution of EC at different sections of the CPB column along with the curing cycle (Bottom or base = 10 cm high in the column; Middle = 50 cm high; Top = 100 cm high)

Furthermore, Figure 5-5 indicates the addition of nanoparticles to CPB plug affects its strength development. However, the magnitude of the impact is a function of the curing time. Upon evaluating the unconfined compressive strength (UCS) test results for both the control column (CPB without nano-particles) and the nano-CPB (nano-cemented paste backfill) column, as depicted in Figure 5-5, it becomes evident that during the initial phase of CPB maturation, there is no significant discrepancy between the two columns. Nonetheless, with the progression of the curing duration, the nano-CPB column demonstrates a markedly superior strength relative to the control column. For instance, after a seven-day curing period, nano-CPB specimens obtained from the column's base exhibited a 20% increase in strength compared to equivalent samples from the control column. This observed enhancement in mechanical properties can be ascribed to a combination of microstructural processes taking place within the nano-CPB matrix, including particle dispersion and filler effects, nucleation and accelerated hydration, as well as pozzolanic reactions [22, 23] as discussed below.

Particle dispersion and filler effect can be explained by the advantageous effects of the nano-scale size and high specific surface area (SSA) of nano-$CaCO_3$ particles, which, when combined with a suitable dispersing agent such as an ether-based polycarboxylate superplasticizer (SP), enables the nanoparticles (NPs) to disperse uniformly throughout the CPB matrix. This uniform distribution results in a firmly packed microstructure, which leads to the CPB mixture having lower porosity and better strength. The results presented in Figure 5-8 demonstrate the remarkable impact of NPs on the microstructure of CPB. As it can be seen in Figure 5-8, the nano-$CaCO_3$ particles perform the function of a filler, effectively bridging the spaces between the bigger tailing particles and strengthening the bonding between individual particles. The measured void ratio and porosity unequivocally confirm the efficacy of NPs in impacting these CPB's properties. Specifically, the incorporation of NPs into the CPB recipe yielded a remarkable 12% reduction in void ratio at the bottom of the nano-CPB column compared to the control column after seven days of curing. This observation underscores the profound impact of NPs on the microstructural properties of CPB and highlights the potential of NPs as a valuable additive for CPB formulation.
For nucleation and hydration acceleration, it can be said that the addition of nano-$CaCO_3$ has been shown to accelerate the hydration process of CPB materials [25]. This occurs because the nanoparticles provide additional nucleation sites for the formation of hydration products, such as calcium silicate hydrate (C-S-H) and calcium hydroxide ($Ca(OH)_2$). These products occupy the space between cement particles, effectively increasing the density and strength of the CPB matrix. As previously discussed in the evolution of pore water pressure, the addition of nano-calcium carbonate is shown to significantly increase the generation of hydration products. This effect is clearly evident in Figure 5-9, which displays the results of thermal analysis on two distinct cement paste samples - one of which was prepared by mixing the cement with NPs, while the other served as a control (i.e., has no NPs). The analysis clearly shows that the nano-cement paste exhibited a substantially higher weight loss, which is directly associated with the decomposition of various hydration products such as C-S-H. These findings provide strong evidence of the efficacy of nano-calcium carbonate in promoting the formation of hydration products and suggest its potential as a key additive for improving the performance of cementitious materials.

Regarding the Pozzolanic reaction, the nano-$CaCO_3$ particles can also participate in pozzolanic reactions with the cementitious material. In these reactions, the calcium hydroxide produced during cement hydration reacts with the nano calcium carbonate to form additional C-S-H gel. This further contributes to the densification and strength enhancement of the CPB matrix [24]

The findings presented in this section indicate that incorporating nano-$CaCO_3$ particles into the CPB mixtures accelerates the strength development of nano-CPB plugs, leading to the attainment of the required mechanical stability more rapidly compared to CPB plugs without nano-$CaCO_3$ particles.

(a)

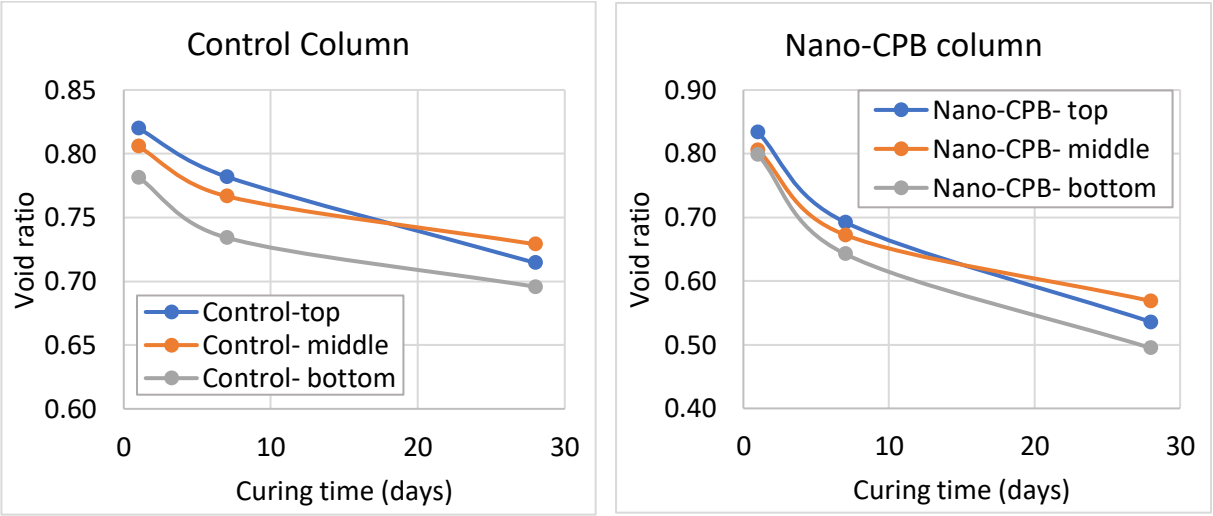
Control Column
Void ratio
0.85
0.80
0.75
0.70
0.65
0.60
0
10
20
30
Curing time (days)
Control-top
Control- middle
Control- bottom
Nano-CPB column
Void ratio
0.90
0.80
0.70
0.60
0.50
0.40
0
10
20
30
Curing time (days)
Nano-CPB- top
Nano-CPB- middle
Nano-CPB- bottom

(b)

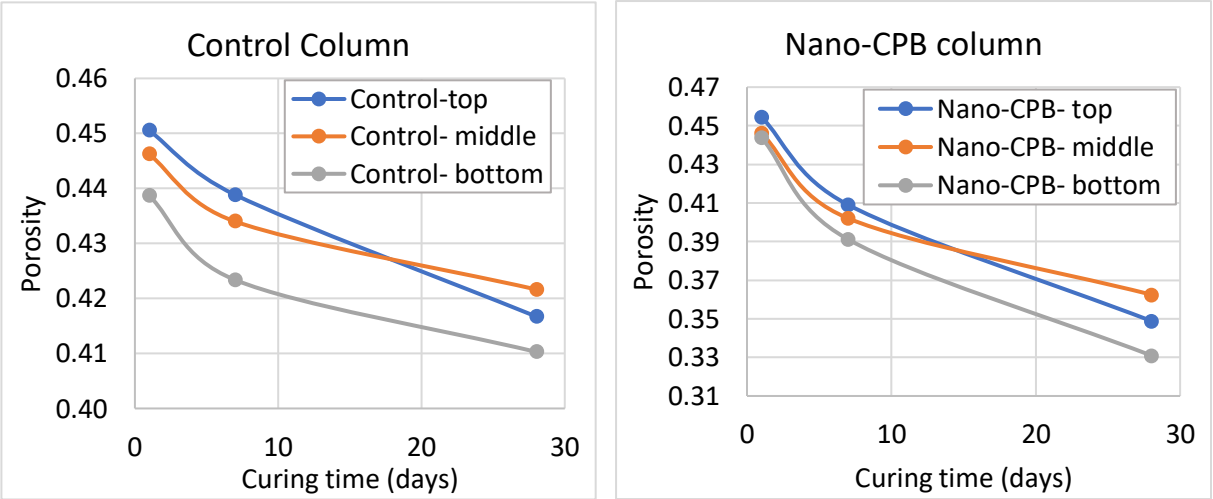
Control Column
Porosity
0.46
0.45
0.44
0.43
0.42
0.41
0.40
0
10
20
30
Curing time (days)
Control-top
Control- middle
Control- bottom
Nano-CPB column
Porosity
0.47
0.45
0.43
0.41
0.39
0.37
0.35
0.33
0.31
0
10
20
30
Curing time (days)
Nano-CPB- top
Nano-CPB- middle
Nano-CPB- bottom

(c)

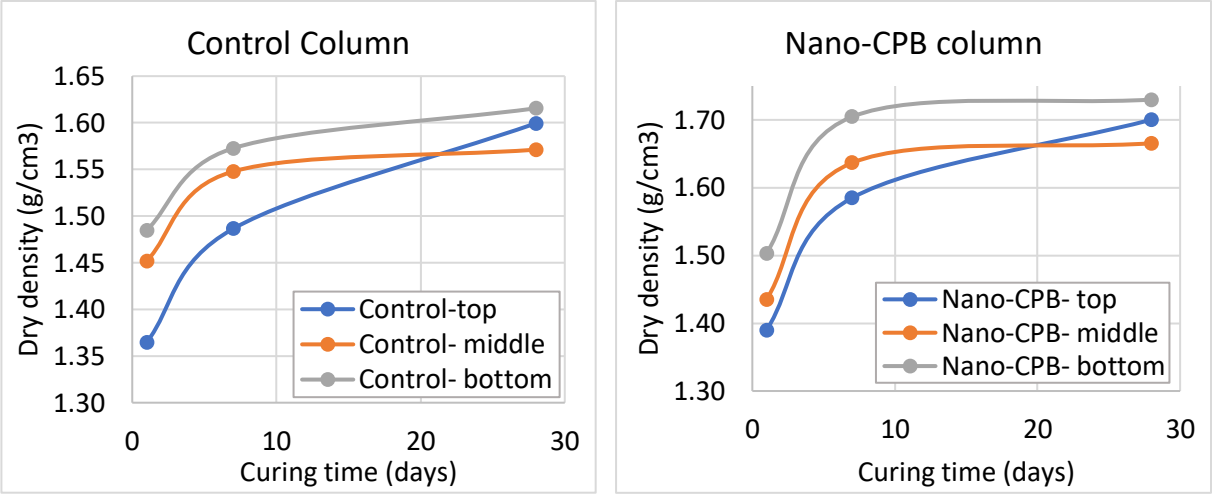

Figure 5-8. Evolution of physical properties at different height of the control and Nano-CPB column: (a) void ratio; (b) porosity; (c) dry density.

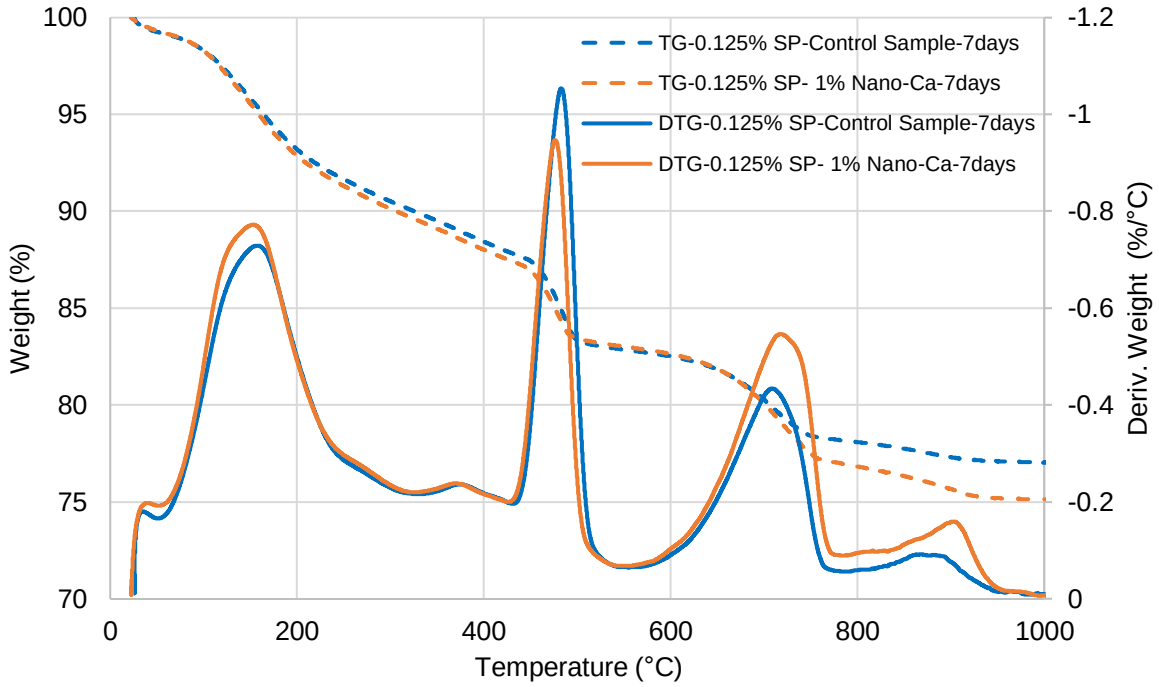

Figure 5-9.Thermal analysis results of 7-day-old cement pastes with and without nano-CaCO3 particles

5.4.3 Evolution of total stress

Figure 5-10 elucidates the temporal progression of total stress at the base of the control and Nano-CPB columns as a function of curing time. It is evident that, in the initial phase of the CPB curing period (up to 1 day), the total stress at their lowest points is approximately equal to or

slightly exceeds the externally imposed pressure applied to their top. This means that initially, whether the CPB contains nanoparticles or not, the pressures increase hydrostatically. This phenomenon can be elucidated by considering the role of the superplasticizer, which causes CPB to exhibit fluid-like properties during the early stages of curing due to its influence on the rheological properties of the material. Consequently, the total stress at the column's base comprises not only the self-weight of the CPB, but also the applied pressure, thereby accounting for the higher stress values detected by the sensors. Prior research has demonstrated that, during the early stages of curing, pore water pressure constitutes the principal component of total stress, implying that the effective stress of CPB is negligible at this juncture [9, 27, 28]. This is a critical observation, as it underscores the significance of pore water pressure in the overall stress distribution.

Furthermore, Figure 5-10 shows that the hydrostatic stress increase at the bottom of the backfill column stopped earlier in the CPB column with nanoparticles than in that without nanoparticles. In other words, the CPB plug with nanoparticles starts to gain shear strength earlier than the CPB without nanoparticles. This is an important finding that has significant practical implications, as it would mean that CPB plug with nanoparticles would allow for earlier opening of the barricade. The latter is a key target in mine backfilling and mining, as it accelerates mining cycles and thus mine productivity.

In addition, from Figure 5-11 it can be seen, as the curing process progresses, a subtle decrease in the observed total stress is discernible. Furthermore, this decrease is faster and more significant for CPB with nanoparticles. According to the investigation conducted by [17], this diminution in total stress is primarily correlated with the dissipation of pore water pressure due to self-desiccation (pore water consumption by cement hydration), which, in turn, affects the mechanical properties (strength) of the CPB. This dissipation of pore water pressure is faster in the CPB with nanoparticles since the nanoparticles enhance the cement hydration (i.e., the self-desiccation) as previously demonstrated. This dissipation of pore water pressure is experimentally demonstrated by the results of monitoring of volumetric water content presented in Figure 5-11. Indications of pore water dissipation can be detected by examining the volumetric water content of the CPB. This figure reveals that both CPB columns exhibit a decline

in their volumetric water content, which can be ascribed to the advancement of cement hydration. This process plays a pivotal role in the development of the CPB' strength and thus mechanical stability [1] Notably, the Nano-CPB column, which was prepared with the incorporation of nanoparticles (NPs), displays a more rapid rate of volumetric water content dissipation compared to its control counterpart. This finding suggests that the presence of NPs expedites the hydration process, potentially leading to enhanced mechanical properties and more efficient utilization of the CPB. The accelerated hydration progress would also result in a shorter time to achieve the desired CPB plug design strength, thus enabling more rapid backfilling and reduced overall project timelines.

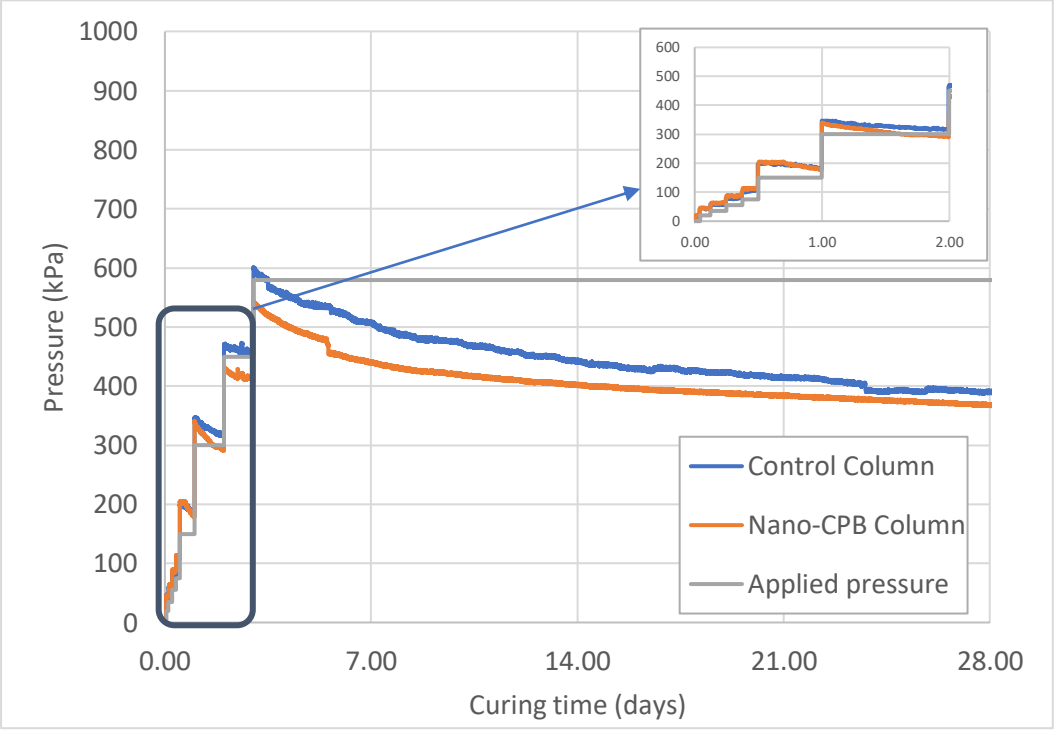

Figure 5-10. Changes in total stress at the bottom of the column versus the applied external pressure

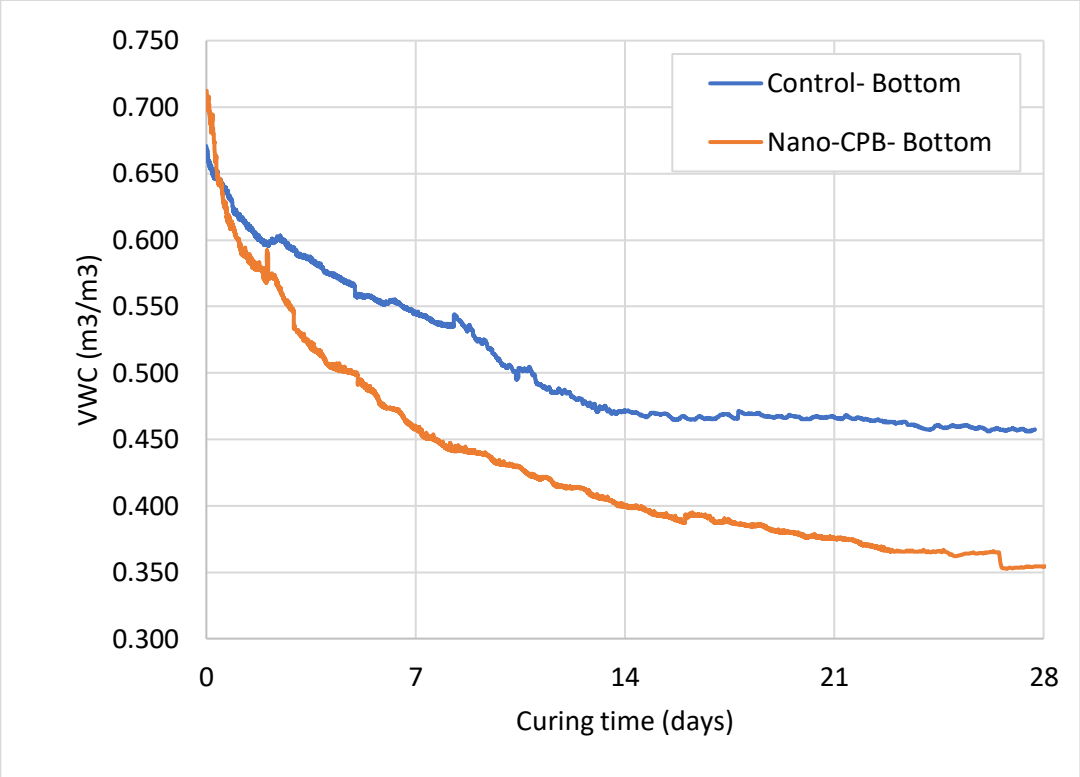

Figure 5-11. Changes in volumetric water content of different CPB columns

5.5. Summary and conclusions

The objective of this experimental study was to investigate the geotechnical behavior of a CPB plug, both with and without nano-calcium carbonate particles, under simulated field overpressure loading conditions. To accomplish this, a physical CPB plug model was developed and equipped with various sensors, along with a mechanical loading system. To mimic realistic field conditions of overburden pressure and backfilling rates, air pressure was applied to the top of the CPB column. Samples were extracted from different sections of the column (top, middle, and bottom) at various curing times (1, 3, 7, and 28 days). These samples were subjected to uniaxial compressive strength (UCS) and microstructural tests to assess the CPB's compressive strength and microstructure. Moreover, several key properties of the CPB plug, such as electrical conductivity, pore water pressure, total earth pressure, and volumetric water content, were continuously monitored using the integrated sensors.

Based on the comprehensive investigation of the experimental results, several key conclusions can be drawn regarding the geotechnical performance of CPB plugs with and without nanoparticles:

- The strength development of CPB plugs is influenced by their depth within the column, with samples at the bottom displaying higher strength than those in the middle and upper parts. This behavior is attributed to the pressure gradient's effect on refining the pore structure of CPB. The higher overburden pressure at the bottom causes greater compaction, as evidenced by void ratio and porosity measurements.
- The incorporation of nanoparticles into CPB significantly improves both its strength and the rate at which strength is gained, irrespective of the depth. The presence of nanoparticles impacts the cement hydration process and pore structure refinement. Thermal analysis and volumetric water content monitoring demonstrate increased hydration product generation (e.g., calcium silicate hydrate and ettringite) and faster dissipation of pore water pressure due to accelerated hydration. Moreover, void ratio, porosity, and dry density measurements confirm the formation of a finer and denser CPB material with nanoparticle addition.
- CPB plugs containing nanoparticles exhibit faster dissipation of pore water pressure compared to those without nanoparticles. This is mainly attributed to enhanced self-desiccation of CPB and refinement of its pore structure, resulting from the nanoparticles' beneficial impact on cement hydration.
- The nano-CPB column experiences a lower total earth pressure and faster rate of total pressure decrease during curing compared to the control column. This is due to the positive effects of nanoparticles on CPB's properties, accelerating the hydration process and refining its physical structure. Consequently, faster pore water pressure dissipation leads to a quicker reduction in total earth pressure at the bottom of the column.
- The observed faster dissipation of pore water and total earth pressure, along with the higher strength and strength increase with nanoparticles, hold significant practical importance. Lower total pressure on the barricades enhances safety and reduces design

costs. Faster achievement of the required mechanical stability of the plug increases overall mine productivity while ensuring workplace safety.

- This study provides valuable insights into the geotechnical behavior of CPB plugs, particularly when incorporating nano-calcium carbonate particles and simulating field overpressure loading conditions. The findings highlight the positive effects of nanoparticles on CPB plug geotechnical performance, suggesting their potential application as additives in backfill material as well as the need to assess its economic feasibility. In order to assess the economic feasibility of incorporating nanoparticles into the CPB and its potential impact on productivity, a comprehensive cost-benefit analysis should be conducted. This analysis will evaluate the benefits derived from enhanced mine cycle efficiency resulting from nanoparticle usage, juxtaposed against the costs involved in acquiring or producing the nanoparticles. Additionally, it should be important to take environmental factors into account during this evaluation, such as the reduction in the use of environmentally taxing materials like Portland cement.

Acknowledgements

The authors would like to acknowledge the financial support from the Natural Sciences and Engineering Research Council (NSERC) of Canada.

Data availability

Some or all data, models, or code that support the findings of this study are available from the corresponding author upon reasonable request.

Declaration of interests

The authors declare that they have no known competing financial or non-financial interests or personal relationships that could have appeared to influence the work reported in this paper.

5.6. References

1. Abdul-Hussain N, Fall M (2012) Thermo-hydro-mechanical behaviour of sodium silicate-cemented paste tailings in column experiments. Tunnelling and Underground Space Technology 29:85–93. doi: 10.1016/J.TUST.2012.01.004
2. Alainachi I, Fall M, Majeed M (2022) Behaviour of Backfill Undergoing Cementation Under Cyclic Loading. Geotechnical and Geological Engineering 40:4735–4759. doi: 10.1007/S10706-022-02181-Y/FIGURES/19
3. Al-Moselly Z, Fall M, Haruna S (2022) Further insight into the strength development of cemented paste backfill materials containing polycarboxylate ether-based superplasticizer. Journal of Building Engineering 47:103859. doi: 10.1016/J.JOBE.2021.103859
4. Camiletti J, Soliman AM, Nehdi ML (2013) Effect of nano-calcium carbonate on early-age properties of ultrahigh-performance concrete. Magazine of Concrete Research 65:297–307. doi: 10.1680/MACR.12.00015
5. Cao M, Ming X, He K, Li L, Shen S (2019) Effect of Macro-, Micro- and Nano-Calcium Carbonate on Properties of Cementitious Composites—A Review. Materials 2019, Vol 12, Page 781 12:781. doi: 10.3390/MA12050781
6. Fall M, Benzaazoua M, Saa EG (2008) Mix proportioning of underground cemented tailings backfill. Tunnelling and Underground Space Technology 23:80–90. doi: 10.1016/j.tust.2006.08.005
7. Fall M, Célestin JC, Pokharel M, Touré M (2010) A contribution to understanding the effects of curing temperature on the mechanical properties of mine cemented tailings backfill. Eng Geol 114:397–413. doi: 10.1016/J.ENGGEO.2010.05.016
8. Fang K, Fall M (2019) Shear Behavior of the Interface Between Rock and Cemented Backfill: Effect of Curing Stress, Drainage Condition and Backfilling Rate. Rock Mech Rock Eng 53:325–336. doi: 10.1007/s00603-019-01909-2
9. Ghirian A, Fall M (2013) Coupled thermo-hydro-mechanical-chemical behaviour of cemented paste backfill in column experiments. Part I: Physical, hydraulic and thermal

processes and characteristics. Eng Geol 164:195–207. doi: 10.1016/J.ENGGEO.2013.01.015

10. Ghirian A, Fall M (2016) Strength evolution and deformation behaviour of cemented paste backfill at early ages: Effect of curing stress, filling strategy and drainage. Int J Min Sci Technol 26:809–817. doi: 10.1016/J.IJMST.2016.05.039
11. Haiqiang J, Fall M, Cui L (2016) Yield stress of cemented paste backfill in sub-zero environments: Experimental results. Miner Eng 92:141–150. doi: 10.1016/J.MINENG.2016.03.014
12. Hefni M, Ali MA (2021) The Potential to Replace Cement with Nano-Calcium Carbonate and Natural Pozzolans in Cemented Mine Backfill. doi: 10.1155/2021/5574761
13. Jones H, Boger D V. (2012) Sustainability and Waste Management in the Resource Industries. Ind Eng Chem Res 51:10057–10065. doi: 10.1021/IE202963Z
14. Landriault D (1995) Paste backfill mix design for Canadian underground hard rock mining. In: 97th Annual General Meeting of CIM. Rock Mechanics and Strata Control Session. Halifax, Nova Scotia. pp 238–239
15. Nasir O, Fall M (2009) Modeling the heat development in hydrating CPB structures. Comput Geotech 36:1207–1218. doi: 10.1016/J.COMPGEO.2009.05.008
16. Nasir O, Fall M (2010) Coupling binder hydration, temperature and compressive strength development of underground cemented paste backfill at early ages. Tunnelling and Underground Space Technology 25:9–20. doi: https://doi.org/10.1016/j.tust.2009.07.008
17. Nujaim M, Belem T, Giraud A (2020) Experimental Tests on a Small-Scale Model of a Mine Stope to Study the Behavior of Waste Rock Barricades during Backfilling. Minerals 2020, Vol 10, Page 941 10:941. doi: 10.3390/MIN10110941
18. Öhlander B, Chatwin T, Alakangas L (2012) Management of Sulfide-Bearing Waste, a Challenge for the Mining Industry. Minerals 2012, Vol 2, Pages 1-10 2:1–10. doi: 10.3390/MIN2010001
19. Palla R, Karade SR, Mishra G, Sharma U, Singh LP (2017) High strength sustainable concrete using silica nanoparticles. Constr Build Mater 138:285–295. doi: https://doi.org/10.1016/j.conbuildmat.2017.01.129

20. Quercia G, Hüsken G, Brouwers HJH (2012) Water demand of amorphous nano silica and its impact on the workability of cement paste. Cem Concr Res 42:344–357. doi: 10.1016/J.CEMCONRES.2011.10.008
21. Ritcey GM (2005) Tailings management in gold plants. Hydrometallurgy 78:3–20. doi: 10.1016/J.HYDROMET.2005.01.001
22. Roshani A, Fall M (2020) Rheological properties of cemented paste backfill with nano-silica: Link to curing temperature. Cem Concr Compos 114. doi: 10.1016/J.CEMCONCOMP.2020.103785
23. Roshani A, Fall M (2020) Flow ability of cemented pastefill material that contains nano-silica particles. Powder Technol 373:289–300. doi: https://doi.org/10.1016/j.powtec.2020.06.050
24. Sanchez F, Sobolev K (2010) Nanotechnology in concrete–a review. Constr Build Mater 24:2060–2071
25. Saremi A, Fall M (2023) Strength and suction development of nano-cemented paste tailings materials. Cleaner Materials 100190. doi: 10.1016/J.CLEMA.2023.100190
26. Senff L, Labrincha JA, Ferreira VM, Hotza D, Repette WL (2009) Effect of nano-silica on rheology and fresh properties of cement pastes and mortars. Constr Build Mater 23:2487–2491. doi: https://doi.org/10.1016/j.conbuildmat.2009.02.005
27. Shahsavari M, Grabinsky M (2015) Mine backfill pore water pressure dissipation: numerical predictions and field measurements. Proceedings of GeoQuébec, Québec city, Canada 1–8
28. Shahsavari M, Grabinsky M (2016) Pore Water Pressure Variations in Cemented Paste Backfilled Stopes. 331–342. doi: 10.1061/9780784480137.033
29. Taylor HFW (1997) Cement chemistry. Thomas Telford London
30. Yilmaz E, Belem T, Benzaazoua M (2015) Specimen size effect on strength behavior of cemented paste backfills subjected to different placement conditions. Eng Geol 185:52–62. doi: 10.1016/J.ENGGEO.2014.11.015
31. Yilmaz E, Fall M (2017) Paste tailings management

CHAPTER 6. Technical Paper III: Influence of Field Temperatures on the Geotechnical Responses of Nanoparticle-Enhanced Backfill Plugs under Field Overburden Pressure: Insights from Column Experiments

Amirreza Saremi, Mamadou Fall

(submitted)

6.1. Abstract

In this research, the geotechnical performance of cemented paste backfill (CPB) plug, enhanced with nano-calcium carbonate (Nano-$CaCO_3$), was examined under simulated field conditions, incorporating factors like field mechanical overburden pressure and non-isothermal field curing temperatures. For this purpose, a novel curing framework was developed and built, empowering the curing of CPB columns under simulated field conditions and facilitating real-time monitoring through integrated sensors at varied column heights. The temporal variations in geotechnical parameters such as compressive strength, pore water pressure, and total stress alongside physical traits including void ratio, porosity, and dry density in these nano-augmented backfills was assessed via column experiments. The results elucidate that the individual impact of field curing conditions, nanoparticle (NP) presence, and their coupled effects profoundly impact CPB plug performance in terms of increasing strength acquisition rates, pore water pressure dissipation rates, total stress dissipation, arching effect and fostering microstructural enhancements such as CPB pore refinement. The underlying mechanisms are attributed to the beneficial roles of NPs in CPB performance, spanning the filler effects, hydration acceleration, and augmented hydration product generation. Moreover, the study underscores the pivotal role of field non-isothermal curing in bolstering mechanical attributes, refining physical properties, and hastening pore pressure and total stress dissipation rates resulting from accelerated cement hydration. Notably, the CPB column, enriched with 1% NPs and subjected to field thermal and mechanical curing conditions, emerged as the top-performing CPB plug. The results of this investigation are of paramount importance in improving the stability of backfilled plugs, optimizing the design of underground backfill structures, reducing backfill costs, and enhancing overall mine productivity.

Keywords: cemented paste backfill; tailings; mine; geotechnical; plug; underground cavity

6.2. Introduction

The role of mining activities in augmenting economic systems through sustainable growth is integral, underpinning their crucial significance. Nonetheless, like any industrial activity, mining is not without its challenges, most notably the substantial quantity of mine waste, termed 'tailings', generated during the extraction process (Fall et al. 2010). Given the magnitude of the environmental implications associated with tailings, a myriad of techniques have evolved to effectively manage this waste. Among these techniques, Cemented Paste Backfill (CPB) has emerged as a contemporary method for tailing management, exhibiting distinct advantages over traditional methods such as surface deposition (Wu et al. 2012). These advantages include land recovery, enhancement of mine productivity, and a pronounced reduction in the likelihood of environmental contamination (Orejarena and Fall 2008; Sheshpari 2015).

CPB, an engineered mixture, primarily comprises tailings (70-85% solids), a hydraulic binder agent, water, and various admixtures when applicable (Belem et al. 2006; Wu et al. 2014; Haruna and Fall 2020). Once the CPB constituents are amalgamated at the processing plant to yield the fresh CPB, it can be conveyed by gravity and/or a pumping system to fill the excavated voids or 'stopes'. This innovative approach allows a significant portion of the mine waste generated through mining processes to be reintroduced to the mine. Consequently, less mine waste needs to be stored on the surface, thereby minimizing the potential for contact between the surrounding environment and hazardous waste and consequently decreasing the possibilities of contamination. Furthermore, in the context of underground mines, there is a need for a vertical support structure - typically referred to as a 'pillar' - between two excavated stopes to mitigate the risk of roof failure or mine burst (Sheshpari 2015, Sui et al. 2015, Cui and Fall 2016, Ghirian 2016). This requirement, from an economic perspective, renders the process of ore recovery suboptimal, as the pillar cannot be processed. This scenario underscores another advantageous role of CPB: by backfilling the stopes, there is no need to leave a pillar for mine safety, which subsequently leads to increased productivity of the mining operations. Hence, CPB presents a multifaceted solution, addressing both environmental and economic challenges inherent in mining activities.

Given the paramount importance of safety in mining operations, the role of CPB as a robust safety barrier capable of withstanding a variety of overburden pressures, including the self-weight of the CPB, is highly consequential. Consequently, the mechanical performance of the CPB, governed by a myriad of factors such as the binder content, tailings particle size, and other field-related parameters, becomes a focal point of concern (Yilmaz and Fall 2017). It is imperative that the structural integrity of the CPB is sufficient to forestall any potential failure due to the application of these aforementioned loads.

Typically, mined stopes are filled with two distinct layers of fresh paste backfill material: a plug and a residual fill or main (final) pour, as illustrated in Figure 6-1. Initially, a barricade, a retaining structure several meters high, is constructed at the stope's base to secure the fresh CPB in place during the curing process and its early stages (Figure 6-1). Subsequently, the first layer of CPB, referred to as the "plug" (CPB plug), is poured into the stope, extending a few meters above the undercut brow. This is followed by the second layer, known as the residual backfill (main pour). The commencement of the main or final pour should only occur once the plug has gained sufficient strength or is mechanically stable to prevent failure under the load applied by the residual fill. In essence, a plug with satisfactory mechanical performance or stability is crucial to ensuring the safety of mine workers and the success of the mine backfilling process. Furthermore, from a productivity perspective, the rate at which the plug gains strength or mechanical stability is of significant importance due to its pivotal role in reducing the suspension time of mining operations after the initial layer of fresh CPB (plug) is deposited into a stope (Li and Fall 2016). This necessary suspension time allows the plug, situated behind temporary barricades, to attain the minimum strength required or mechanical stability for ensuring the stability of the CPB structure. Hence, any modifications that expedite the strength-gaining or mechanical stability-gain rate of the CPB plug are advantageous, as they positively impact the productivity rate of the mine. Achieving this minimizes the suspension time required between each mining cycle, enhancing overall operational efficiency. Moreover, a plug with a high strength gain rate or excellent mechanical performance can facilitate the implementation of continuous pouring in CPB operations. Continuous pouring of CPB significantly enhances underground mining efficiency

by reducing stope cycle time and simplifying logistics. This streamlined approach is associated with substantial financial gains for the mine.

The critical parameter for assessing the mechanical stability of the plug structure is the CPB strength. However, pore water pressure within the backfill mass is another significant factor influencing both the liquefaction potential of the CPB plug and its overall strength, as well as the total stress exerted on the barricade. In essence, a comprehensive understanding of strength development, pore pressure evolution, and total stress within the plug is crucial for accurately evaluating the mechanical stability of the plug and, consequently, the stability of the barricade.

Considering the paramount significance of the mechanical performance and stability of the CPB plug for ensuring the safety of mine workers, enhancing mine productivity, facilitating successful backfill operations, and bolstering the financial gains for the mine, researchers have dedicated considerable effort towards finding and advancing methods to enhance the plug's mechanical capabilities and stability. Particularly, the focus has been on expediting its strength gain rate to maximize efficiency and safety in mining operations. A pragmatic approach to enhancing the mechanical strength and stability of CPB involves the augmentation of binder dosage, which is typically ordinary Portland cement. This strategy results in the formation of superior bonding between tailings particles, and consequently, an optimized transmission of shear stress within the CPB structure can be anticipated. However, this strength enhancement is not without its trade-off, as it engenders a substantial increase in the final cost of backfilling. Given that the contribution of binder to the overall cost of backfilling is estimated to be around 70%, the economic implications of this method are decidedly significant (Yilmaz and Fall 2017, Sagade 2023). Moreover, the use of Portland cement negatively impacts the environmental footprint of the mine, since the production of Portland cement significantly contributes to the generation of greenhouse gas, globally. For these reasons, the researchers have been looking for alternative methods to improve the mechanical stability of CPB plugs.

One of the most effective strategies for modifying the mechanical properties of cementitious materials involves the application of various chemical and/or mineral additives aimed at adjusting distinct attributes of these materials. With the advent of nanotechnology, an extensive array of nano-scale additives has been effectively integrated with concrete - the most prevalent

cementitious material in the construction industry. These nano-additives have demonstrably improved the mechanical performance of concrete (Sanchez and Sobolev 2010, Oey et al. 2013, Wang et al. 2014, Ren et al. 2021), enhancing aspects such as durability, compressive strength, and workability. Given the cementitious nature of CPB, certain studies (e.g., Koohestani et al. 2016, Roshani and Fall 2020a,b, Benkirane et al. 2023, Saremi and Fall 2023) have corroborated the beneficial impacts of NPs as supplementary additives blended with the primary ingredients of CPB. The integration of such NPs has resulted in a notable enhancement in the mechanical performance of CPB, yielding improvements in areas like compressive strength, strength-gaining rate, pore water pressure dissipation rate, and microstructure refinement (Saremi and Fall 2023). Thus, these findings elucidate the potential of nanotechnology in offering effective and efficacious solutions for enhancing the mechanical performance of CPB plug.

As elucidated earlier, a myriad of field variables have the capacity to impact the performance of CPB plug structures. Among these variables, CPB mass self-weight (overburden pressure) and thermal loading in underground mines are of paramount importance. CPB structures typically consist of sizable high-rise (several tens of meters in height) geotechnical formations. The considerable mass of CPB imposes significant time-dependent total pressure and stress within the plug, crucially affecting the development of CPB strength (Saremi and Fall 2023). Thermal loading can affect the mechanical performance of CPB structures in several ways, such as modifying the rate of the cement hydration process, which manifests its effects on the quantity of produced hydration products, or instigating changes in the pore water pressure dissipation rate. Each of these factors could lead to significant alterations in the performance of the backfill structure (Nasir and Fall 2010, Walske et al. 2016, Wang et al. 2016, Jiang et al. 2020, Xu et al. 2021). For instance, a faster dissipation of pore water pressure could curtail the required suspension time necessary for the CPB plug to acquire sufficient strength to ensure the stability of the backfill structure (Wang et al. 2016, Tian and Fall 2021). Thermal loads imposed on a backfill structure emanate from different sources, which can be categorized as internal and external. Internal sources can be elucidated by considering the heat generated by the hydration reaction of the binder (Figure 6-1). External sources, on the other hand, encompass the heat released by surrounding rock masses (Figure 1), such as rock temperatures in deep mines, heat

generated by sulfidic rock masses, or climatic heat to which CPB structures are subjected during their lifespan (Yilmaz and Fall 2017).

However, to date, while a limited number of studies have been conducted on the effect of overburden pressure or backfill self-weight on the mechanical behavior of CPB plugs (e.g., Saremi and Fall 2023), there have been no studies on the influence of field CPB thermal loading on the geotechnical performance (e.g., strength development, pore water pressure evolution, total stress) of a CPB plug subjected to realistic field vertical stress (overburden pressure) loadings. It is crucial to understand how the combined effect of field curing temperatures and overburden pressure, along with the presence of NPs as an admixture, modifies the geotechnical behavior of CPB plug. This insight is fundamental for the design of more cost-effective or sustainable backfill plug materials, since in the field the CPB plug is simultaneously subjected to mechanical loads form the overburden pressure of the backfill mass and to the field non-isothermal curing conditions of the backfill structure.

As a result, this experimental investigation aims to examine the effects of field thermal loading on the geotechnical behaviour a column of CPB with nano-calcium carbonate under simulated field overburden pressure. The study focuses on examining its influence on the mechanical strength of the CPB column as well as tracing the evolution of total stress, and pore water pressure, which are also critical geotechnical design parameters.

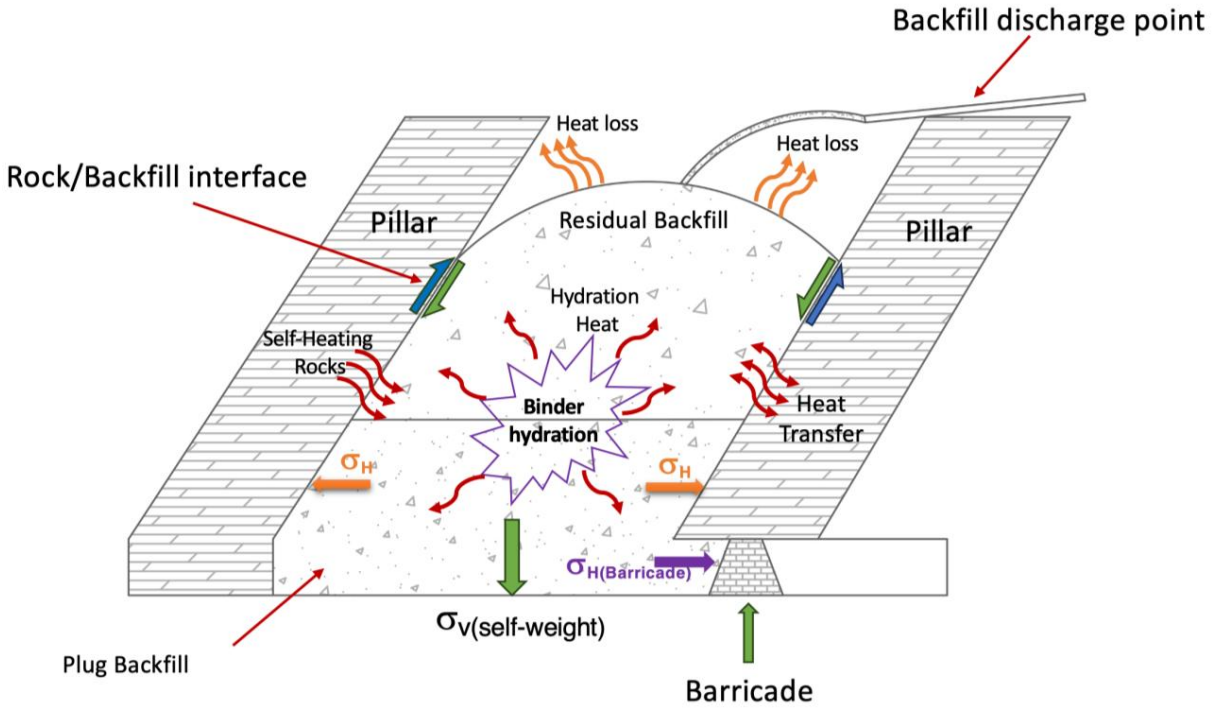

Figure 6-1. Schematic representation of a backfilled mine underground cavity (stope), illustrating the thermal interaction between the plug of cemented paste backfill, residual backfill, and the surrounding rock masses.

6.3. Experimental program

6.3.1 CPB ingredients

6.3.1.1. Tailings

For the preparation of the CPB mixture in this study, a synthetic type of silica tailings (ST) has been utilized. The rationale for employing this particular type of tailings hinges on two primary factors. Firstly, its particle size distribution (PSD) closely mirrors the average particle size distribution of tailings generated from nine mines located in the eastern region of Canada (as shown in Figure 6-2). Secondly, the non-reactive nature of the ST - attributable to its primary composition of 99.8 wt.% quartz - plays a crucial role in mitigating any undesirable chemical reactions that could impede the hydration process, which could affect the interpretation of the results and introduce uncertainties in the results. Consequently, ST can facilitate a controlled

environment conducive for the hydration process of the binder and chemical admixtures. The physical and chemical properties of the ST used in this study are delineated in Table 6-1 and Table 6-2, respectively.

Table 6-1. Mineralogical composition of the tailings used

Tailings	Mineral											
	Quartz	Albite	Dolomite	Calcite	Chlorite	Magnetite	Pyrite	Talc	Pyrrhotite	Spinel	Others	Total
ST (wt.%)	99.8	-	-	-	-	-	-	-	-	-	0.2	100.0

ST: silica tailings; wt.: weight.

Table 6-2. Physical properties of used tailing

Element	G_s	D_{10} (µm)	D_{30}(µm)	D_{50}(µm)	D_{60}(µm)
ST	2.7	1.9	9.0	22.5	31.5
Average of 9 types of tailings	-	1.8	9.1	20.0	30.8

G_s: specific gravity.

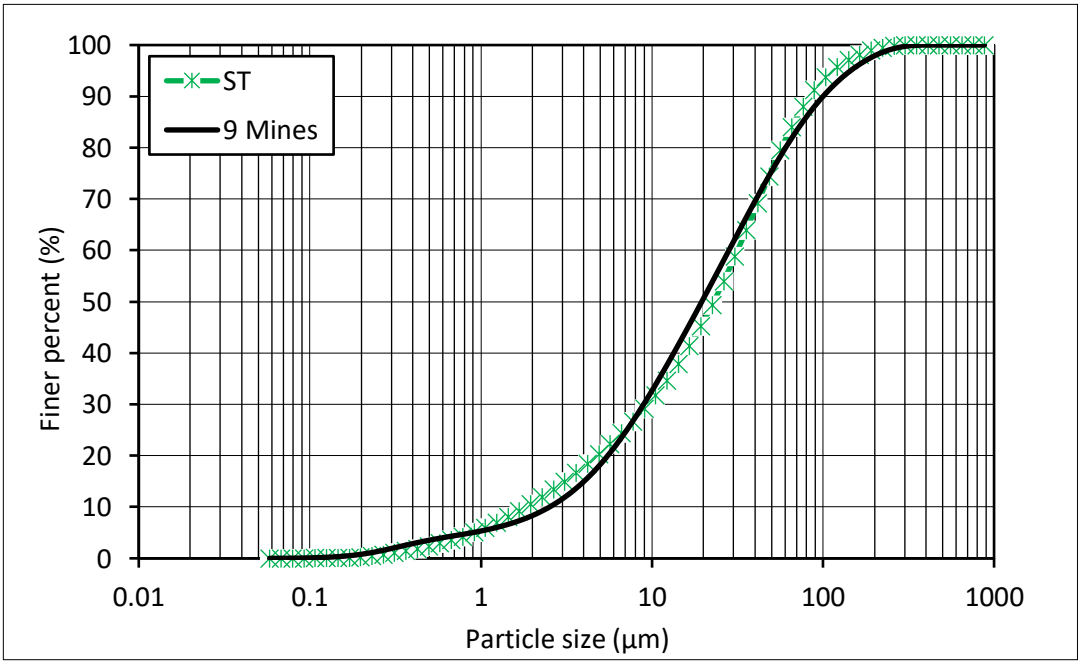

Figure 6-2. Comparative Analysis of Grain Size Distribution: Silica Tailings (ST) vs Average Grain Size Distribution from Nine Eastern Canadian Mines

6.3.1.2. Nanoparticles

In this study, nano-calcium carbonate has been incorporated into the CPB blend following its observed advantageous impact on enhancing various mechanical properties of CPB. These enhancements, as detailed in previous studies on small CPB samples (e.g., Roshani and Fall 2020a, Benkirane et al. 2023a, Saremi and Fall 2023) include increased negative pore water pressure (suction), heightened compressive strength, and refined microstructure. The observed improvements in the mechanical performance of CPB can be accounted for by various mechanisms induced by the presence of NPs (e.g., Koohestani et al. 2016, Roshani and Fall 2020b, Saremi and Fall 2023). The first mechanism involves the contribution of NPs to the hydration process, providing an abundance of nucleation sites. This results in elevated amounts of hydration products and an accelerated hydration reaction. Both of these factors ultimately converge to produce a more resistant backfill material in a timely manner. The second mechanism pertains to the filler effect of NPs, contributing to the microstructural refinement of the backfill material. This is achieved by filling the micro pores within the CPB material, resulting in a denser backfill microstructure. Consequently, this facilitates better transmission of shear stress and, therefore, an elevated compressive strength is expected for the backfill. Such microstructural refinement can be ascribed to the generation of larger amounts of precipitated hydration products and the presence of unreacted NPs capable of filling the voids. Moreover, previous studies (e.g., Koohestani et al. 2016, Roshani and Fall 2020b, Benkirane et al. 2023b, Saremi and Fall 2023) on the effect of different type of NPs (e.g., nano-silica (SiO_2), nano-calcium carbonate ($CaCO_3$), nano-iron oxide (Fe_2O_3), and nano-aluminum oxide (Al_2O_3)) on CPB properties have shown that nano-calcium carbonate (Nano-$CaCO_3$) has the most significant impact on the strength development of small CPB samples. Thus, these studies underscore the potential of nano-calcium carbonate as a promising additive for optimizing the performance of CPB. More detailed information about the physical properties and chemical characteristics of the NP used in this study, Nano-$CaCO_3$, is presented in Table 6-3.

Table 6-3. Chemical and physical specifications of the nano-calcium carbonate used.

Nano-$CaCO_3$

Appearance	White powder
$CaCO_3$ (%)	≥98
HCl insoluble (%)	≤0.1
Particle size (nm)	20–50
Fe (%)	≤0.08
Mn (%)	≤0.006

6.3.1.3. Binder, water, and superplasticizer

The Ordinary Portland cement type I (general use Portland cement, e.g., type GU) was chosen as the hydraulic binder for this study due to its common usage in the backfilling practices around the industry. General characteristics of Portland cement type I (PCI) are provided in Table 6-4.

Table 6-4. chemical properties of PCI cement used

Type of binder	MgO (%)	CaO (%)	SiO_2 (%)	Al_2O_3 (%)	Fe_2O_3 (%)	SO_3 (%)	Relative density	Specific surface (m^2/g)
PCI	2.65	62.82	18.03	4.53	2.70	3.82	3.10	1.30

To avert the introduction of undesired chemicals into the binder hydration process that could potentially alter both the hydration products and the rate of hydration, tap water has been judiciously chosen for combination with the principal ingredients of the CPB. Additionally, given the high proclivity for nanoparticle (NP) agglomeration owing to their strong interparticle forces, the presence of an effective dispersing agent is essential to neutralize these forces and facilitate uniform dispersion within the mixture. Without this, agglomerated NPs would be unable to actively participate in the hydration process and fail to fulfill their function as filler material within the micro voids (Oey et al. 2013, Kong et al. 2013). In addressing this challenge, a polycarboxylate ether-based superplasticizer (MasterGlenium 7500), proven to be an efficacious dispersing agent for NPs, was employed at a constant dosage. This ensures uniform distribution of the NPs within the fresh CPB mixture, thus optimizing the hydration process and enhancing the structural integrity of the CPB.

6.3.2 CPB preparation and mix proportioning

In order to compose the fresh CPB mixture, an initial dry mix was formulated, comprising the required quantity of tailings and PCI. This mixture was processed for five minutes within a concrete mixer. Subsequently, the precise dosage of superplasticizer and NPs were incorporated into the water, stirring continuously for three minutes to secure a homogeneous final solution. In the following stage, the derived solution was added to the dry mix of PCI and tailings, instigating the final stage of mixing, which endured for ten minutes. The product of this concluding step is the fresh CPB mixture.

Of note, in order to gain an incisive understanding of the impact of NPs on the behavior of the CPB column, a control column was also prepared. This involved the creation of fresh CPB using the same mix proportioning, but without the addition of NPs. More comprehensive information concerning the composition of the CPB columns can be found in Table 6-5. Upon the completion of the mixing procedure, the columns were filled with the resultant fresh CPB mixture.

Table 6-5. Mix composition of the prepared nano-CPB column and control column

Sample nomenclature	Binder Content (%)	PCI in the Binder (%)	SP (%)	W/C ratio	NP content (%)	NP type	Solid Content (%)
PCI- CPB (control)	4.5	100	0.125	7.8	0	None	74
PCI- CPB-NC	4.5	100	0.125	7.8	1	NC	74

PCI, Portland cement type I; ST, silica tailings; W/C ratio, mass of water divided by the mass of binder. NP. Content (%) = Mass of NPx100/Mass of binder; Binder Content = Mass of binderx100/ (Mass of dry tailings + Mass of binder); NC, Nano-Calcium Carbonate, Solid Content (%) = (Mass of solid/Mass of the whole CPB)

6.3.3 Developed column set up and monitoring program

Figure 6-3 provides a schematic representation of the physical model devised to simulate the more realistic CPB field conditions, such as the mechanical and thermal loading exerted on backfill plug masses during deposition and post-deposition. The physical model includes fully instrumented columns equipped with a thermal and mechanical loading system. The thermal loading system enables to apply to the CPB column curing temperatures that the CPB mass is subjected in the field, whereas the mechanical loading system enables to cure the CPB under

vertical stresses induced by the self-weight of the CPB during its deposition and curing in the field. The constructed columns were fabricated using aluminum sheets, a design choice that endowed the column with the capacity to bear the mechanical load applied via the air-driven piston.

The thermal conductivity of aluminum emerged as another pivotal factor in the design process, allowing for the proper transfer and uniform distribution of external heat generated by the heating system throughout the column during the curing process. To supply this external heat, the columns were enveloped with a heating element tape, manufactured by Omega Sensing Solutions ULC, which possesses the capability to generate heat up to 760 ºC. This heating element equipped with a controller enables to mimic any temperature profiles or non-isothermal curing conditions to which a CPB mass can be subjected in the field. In an effort to retain this generated heat, an additional layer of a glass wool blanket, with a thickness of 100mm, was employed. This layer serves dual purposes: it aids in mitigating heat loss and also diminishes heat transfer with the surrounding environment. This design helps in creating a controlled, realistic environment to better understand the effects of field thermal loading conditions on the geotechnical response of CPB structure. In this study, the non-isothermal curing condition or temperature profile applied to the CPB columns during their curing is shown in Figure 6-4. This temperature profile (non-isothermal) represents the time-dependent temperature development in the lower part (plug) of a CPB mass in the field, as described in (Nasir and Fall 2009). The point at which the temperature was measured was located at 2.5 m above the bottom of a backfill structure with a dimension of 20 m for height and 10 m as width (Nasir and Fall 2009). Figure 6-4 also show the temperature profile of CPB column cured under constant (isothermal) room temperature (20◦C) for comparison purpose.

As it can be seen in Figure 6-3, the developed column is benefiting an air driven piston (mechanical loading system) which enables curing the CPB under vertical stresses. The main purpose of implementing such a system was to be able to study the behavior of CPB plug under the actual self-weight load that a backfill structure experiences in the field. Having said that, Figure 6-5 represents the stress loading pattern applied on the top of the CPB column during curing. The maximum pressure applied to the column is 600 kPa which is equivalent to 34.8 m of

a backfill structure (considering 17.2 kN/m^3 for the CPB's bulk density). However, to maintain a realistic condition the applied pressure was gradually increased to simulate the gradual filling process of the mine cavity or stope.

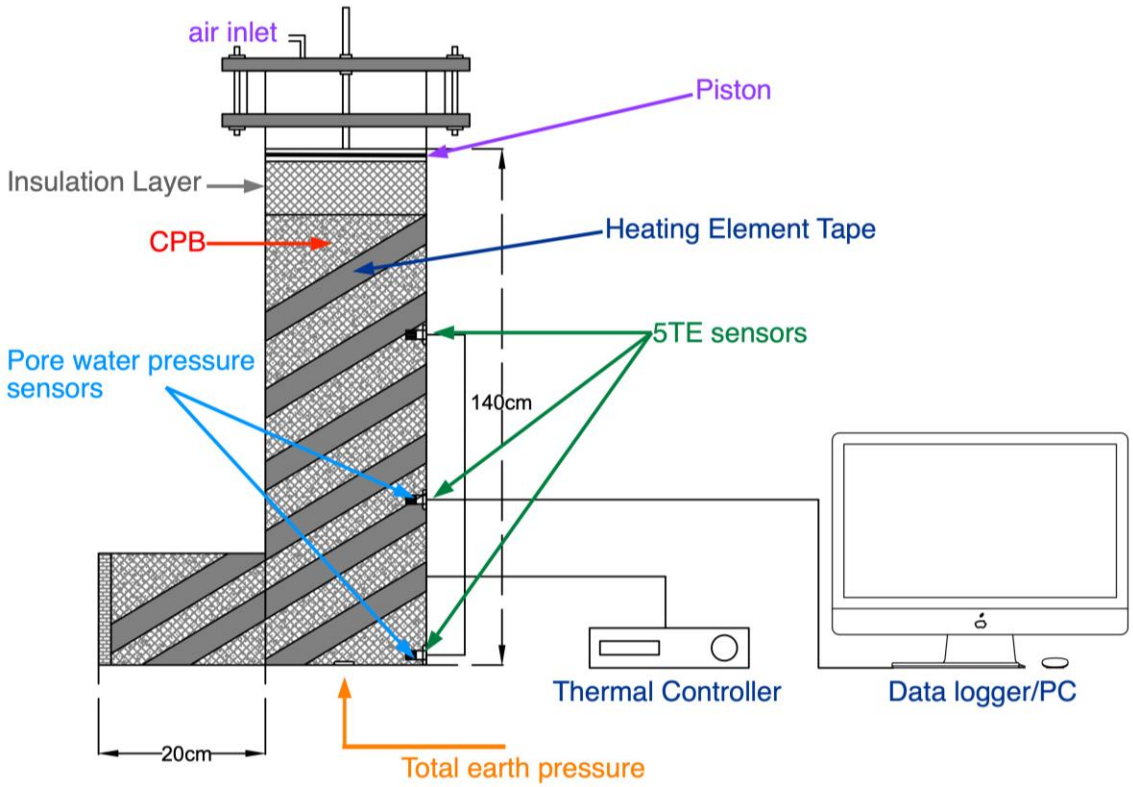

Figure 6-3. Schematic illustration of the developed plug backfill physical model and details of sensors deployed for monitoring purposes

To procure the requisite samples for a range of laboratory examinations at specific curing times (e.g., 1, 3, 7, and 28 days), an initial step involved dismantling the insulation layers and the heating elements tapes. Following these measures, cores were strategically retrieved from specific elevations (10, 50, and 100 cm from the base) within the column. Access to these cores was achieved by opening both the front and small rear windows of the column, after which the CPB was precisely drilled using a handheld saw. This extraction process was expedited and completed within a 2-hour timeframe, with the obtained cores promptly secured in sealed bags. This precautionary measure was taken to mitigate any potential moisture loss and oxidation. Finally, these large cores were cut and shaped to fit the standards for different testing procedures. Following these preparatory steps, a series of laboratory tests were performed on

the CPB cores. These examinations included the measurement of unconfined compressive strength (UCS), void ratio, dry density, and porosity as well as microstructural analyses (e.g., MIP tests). Such systematic testing protocols ensured a comprehensive assessment of the CPB core's properties under different curing conditions.

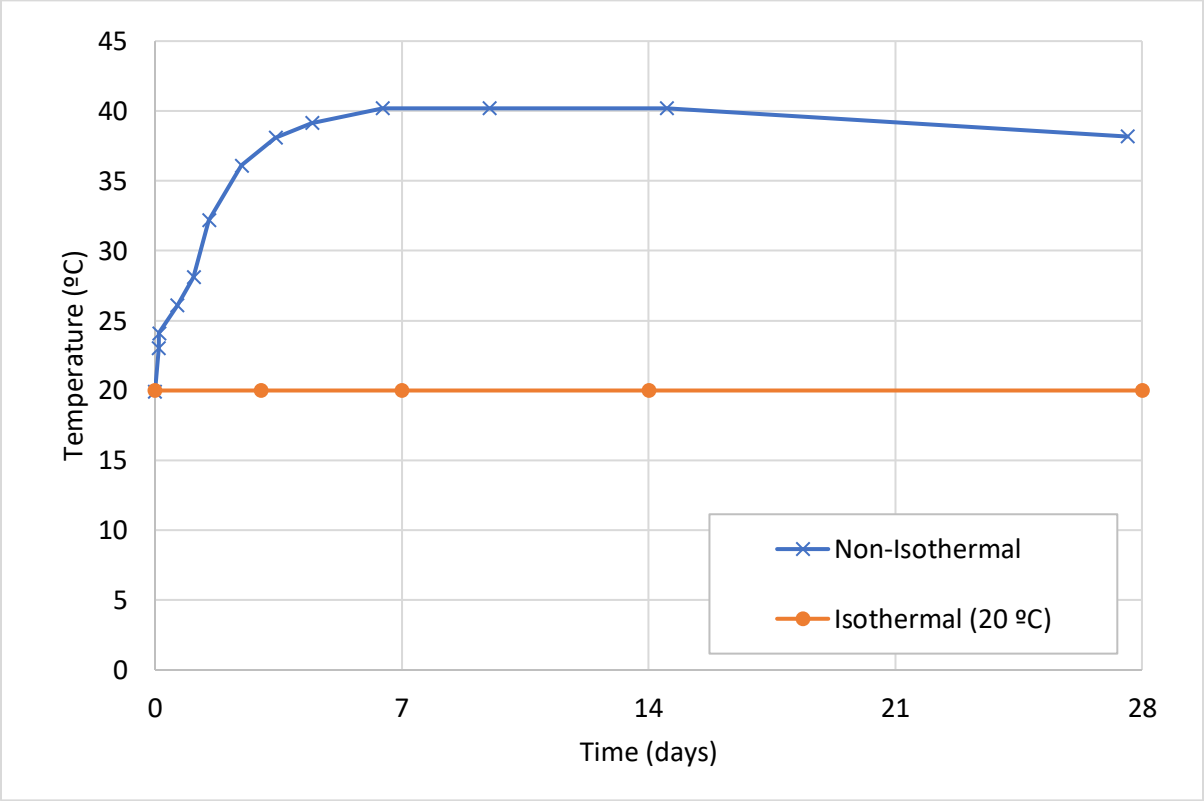

Figure 6-4. Adopted CPB mass temperature profiles based on field measurements.

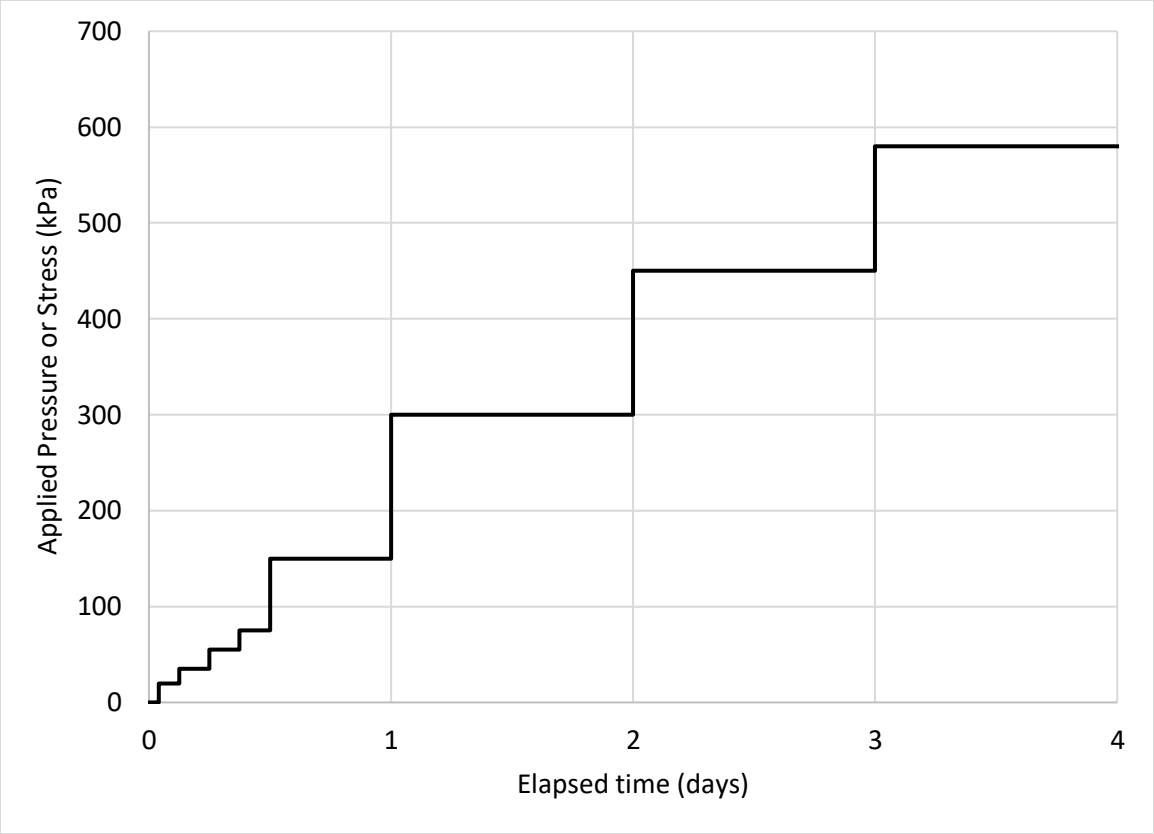

Figure 6-5. Evolution of applied curing stress vs curing time

Furthermore, different sets of transducers were employed to monitor the evolution of various parameters in order to gain deeper insight into the coupled effect of thermal loading and mechanical loading on the geotechnical response of CPB in presence of NPs impacts. The sensors were strategically situated at various sections of the columns, integrated with a data acquisition system (made by Xi'an Yima Opto-electrical Technology Co.) or a data logger to facilitate continuous and unbroken data recording. Pore water pressure (DMTY) and earth pressure (DMKY) transducers were utilized to monitor the evolution of the pore water pressure and total stress, respectively. Detailed information about these sensors is presented in Table 6-6. In conjunction with the aforementioned transducers, a series of advanced 5TE sensors were also judiciously deployed, to monitor the electrical conductivity (EC) and temperature within the CPB column. These high precision 5TE sensors were selected for their accuracy, with a tolerance of ±10% for EC measurements and a mere ±1°C for temperature readings. EC and temperatures provide valuable information about the progress of the cement hydration. The evaluation of EC

was performed by the application of an alternating current between a calibrated pair of electrodes embedded within the sensor, leading to the measurement of the resultant electrical resistance. Such fluctuations in EC stand as an empirically robust indicator of ionic movement within cement-based materials. This dynamic is fundamentally tethered to the intricate chemical evolution of cement hydration, thus offering invaluable insights into the material's transformational phase behavior and mechanical properties.

Table 6-6. Detailed specifications of pore water pressure and total pressure sensors used in the CPB model

Sensor	Total earth pressure sensor	Pore water pressure sensor
Manufacture	Dan street Nanjing Electronic Technology Co.	
Model Type	DMTY	DMKY
Capacity	1 MPa	1 MPa
Accuracy	±0.3%	±0.3%
Output signal	0 to 5V	0 to 5V

6.3.4 Testing program and microstructural analysis

6.3.4.1. Uniaxial Compressive Strength (UCS) test

Specimens, extracted from various points in the column's height, were subjected to Uniaxial Compressive Strength (UCS) tests in conformity with the ASTM-C109 standards. Upon reaching specified curing intervals—for example, 1, 3, 7, 28 days—the plug CPB column was deconstructed, and a suite of cores was extracted from disparate heights of the column using a coring apparatus following the procedure described in Section 2.3. Each core was segmented into smaller cubic samples (5 cm x 5 cm) that satisfied the specifications outlined by ASTM-C109, thereby rendering them suitable for UCS testing. To ensure the reliability and repeatability of the test results, the average UCS results were measured and reported from at least three identical samples.

6.3.4.2. Microstructural analysis and physical properties determination

Two techniques of microstructural analyses were combined to assess the microstructure (binder hydration products, pore structure) of the studied CPB. These techniques include thermal analysis (thermogravimetry (TG), differential thermogravimetry (DTG)), mercury intrusion porosimetry (MIP). In the preparation of samples for thermal analysis, a series of cement paste specimens were formulated with a water-to-cement ratio (w/c) of 1. Upon completion of the requisite curing period, the specimens were meticulously dried in a temperature-controlled oven at 45°C over a span of four days, ensuring complete evaporation of free water. Subsequently, the samples were ground into a fine powder, ready for TG/DTG (thermogravimetric/differential thermogravimetric) analyses conducted with a state-of-the-art thermogravimetric analyzer, SDT 2960 simultaneous DSC-TGA. The thermal protocol involved heating the specimens at a calibrated rate of 10°C/min, escalating to a peak temperature of 1000°C, all under a nitrogen (N2) atmosphere flowing at a controlled rate of 100 mL/min. The thermal analysis enables us to assess the type and amount of cement hydration products formed in the CPB matrix.

For the Mercury Intrusion Porosimetry (MIP) analysis, the Micromeritics AutoPore III 9420 mercury porosimeter was deployed, delivering precise characterization of the porosity of CPB samples. MIP tests were performed on small CPB samples. Prior to the MIP tests, the sample were dried for 4 days at 45◦C. Drying at this temperature does alter the pore structure of CPB as shown in many previous studies (Add some references).

To ascertain the physical properties of CPB, samples were extracted from diverse sections of the columns at specified curing intervals. The initial phase encompassed the measurement of specific gravity, conducted in accordance with ASTM D854, a standardized guideline delineating the procedure for gauging the specific gravity of soil solids using a water pycnometer. This measurement subsequently facilitated the determination of particle density, a vital parameter for the subsequent calculation of void ratio. Following this, the bulk density was quantified through a process involving the careful filling of a container of known volume with the dried CPB material, leading to the calculation of mass per unit volume. Armed with the bulk density and particle density data, the total porosity was computed utilizing the mathematical relation: $n =$

$1 - \frac{\rho_b}{\rho_p}$, where ρ_b represents the bulk density (kg/cm³), and ρ_p signifies the specific gravity (kg/cm³). Lastly, the void ratio was deduced from the total porosity, employing the formula: $e = \frac{n}{1-n}$.

6.4. Results and discussion

6.4.1 Evolution of pore-water pressure

The results illustrated in Figure 6-6 detail the evolution of pore water pressure at the base of the CPB columns without NPs (control columns) and with NPs (Nano-CPB columns) exposed to both isothermal and non-isothermal curing temperatures.

This figure shows that, irrespective of the curing temperature, the CPB columns show an initial increase in the pore water pressure up to a peak followed by decrease in pore water pressure during the curing period for both columns. This initial increase in the pore water pressure is mainly caused by the increase in the self-weight of the CPB during the filling process of the column, i.e., of the mine cavity (stope). An increase of the backfill weight is obviously associated with an increase of the total stress, which leads to higher pore water pressure. The subsequent diminution in pore water pressure as the curing time increases is due to the self-desiccation of the CPB material. This self-desiccation is caused by the consumption of water by the cement hydration process (Ghirian 2016, Cui and Fall 2017, 2018a,b).

Furthermore, Figure 6-6 indicates that the field non-isothermal curing condition or higher curing temperature has a significant impact on the magnitude of the pore water pressure within the CPB columns. After one day of curing, i.e., when the CPB temperature reached 28°C (Figure 6-4), the pore water pressure values in the CPB column cured under field thermal conditions became smaller than those in the CPB column cured at constant room temperature (20°C) and the difference in pore water pressure values increased as the curing time increased. Such a trend and difference can be elucidated by evaluating the influence of curing temperature on two distinct mechanisms pivotal to the mechanical performance of CPB: the binder hydration reaction, and microstructure refinement. Prior research, for instance, Tian and Fall (2021), deduced that

elevated curing temperatures expedite the binder hydration reaction. This leads to the formation of increased quantities of precipitated hydration compounds, notably calcium silicate hydroxide (C-S-H) and calcium hydroxide (CH). This hastened effect of curing temperature on binder hydration influences the evolution of pore water pressure in a twofold manner. Initially, heightened hydration rates can be perceived as a rapid depletion of pore water due to the inherent nature of the cement hydration reaction which consumes water. Subsequently, the microstructural refinement, marked by the creation of larger volumes of hydration compounds, results in a greater number of CPB matrix micropores and voids being occupied by these precipitates. This filling diminishes the interconnectivity of capillary pores and traps pore water molecules, thereby curtailing the hydrostatic pressure height within the CPB matrix, which, in turn, yields a reduced pore water pressure, as observed by Al-Moselly et al. (2022). In light of these insights, it becomes evident why the CPB column cured under non-isothermal field conditions demonstrated a swifter pore water pressure reduction compared to its counterpart cured under isothermal conditions.

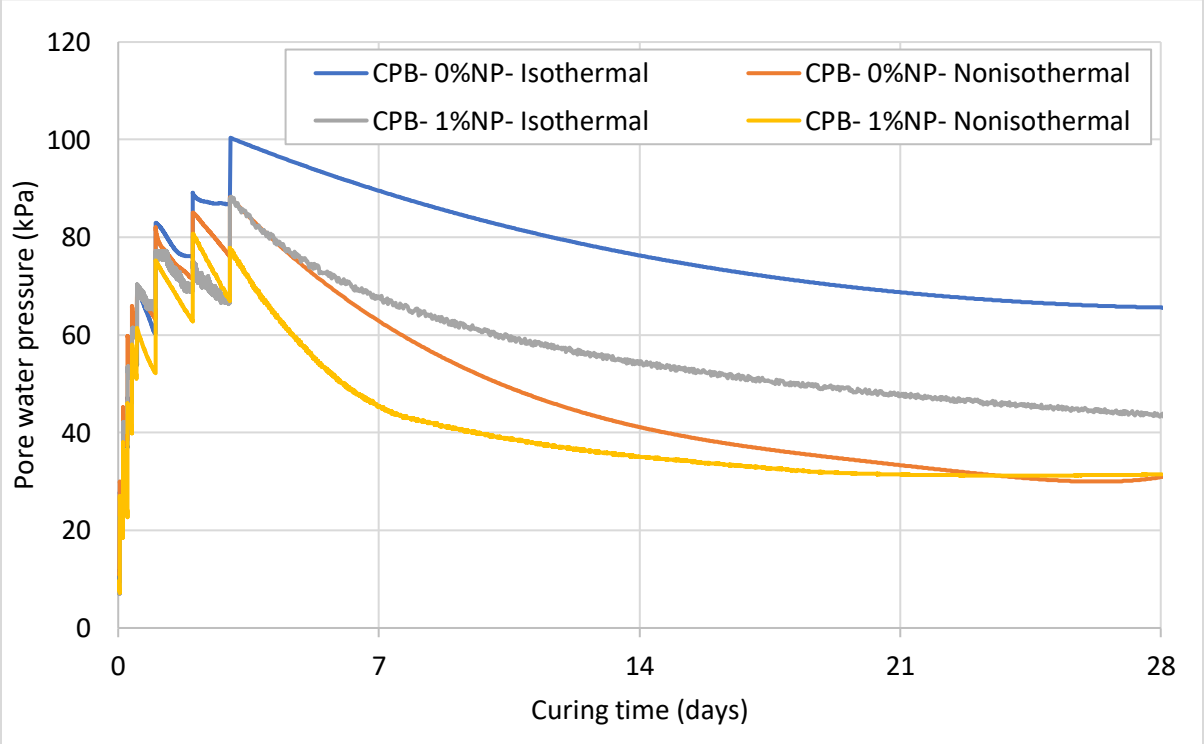

Figure 6-6. Pore water pressure evolution at the bottom of the CPB columns with and without NPs exposed to various thermal curing conditions (isothermal and non-isothermal conditions)

The aforementioned mechanism of higher temperature induced generation of a larger amount of hydration products is supported by the results of thermal analyses presented in Figure 6-7. This figure displays the thermal analysis outcomes of two analogous cement paste samples of CPB subjected to varying curing temperatures. One sample underwent a seven-day curing process at room temperature (specifically, 20°C), while the other was cured at 35°C over the same duration. Analysis from Figure 6-7 reveals that the sample exposed to the elevated curing temperature demonstrated a more pronounced weight loss during thermal analysis, manifesting as heightened peak values. These peaks are indicative of the formation of diverse hydration products. A more substantial weight loss or increased peak values signal the presence of a larger volume of hydration products within the sample. For instance, the peak discerned between 80°C and 120°C signifies the decomposition of specific hydration products like C-S-H, gypsum, and ettringite, as well as water evaporation (Jiang et al. 2019). In contrast, the peak spanning 400°C to 500°C delineates the disintegration of CH, and the subsequent peak between 650°C and 700°C points to the dehydration of calcite (Aldhafeeri and Fall 2017). From these observations, one can deduce that a higher curing temperature facilitates the production of an elevated quantity of hydration products.

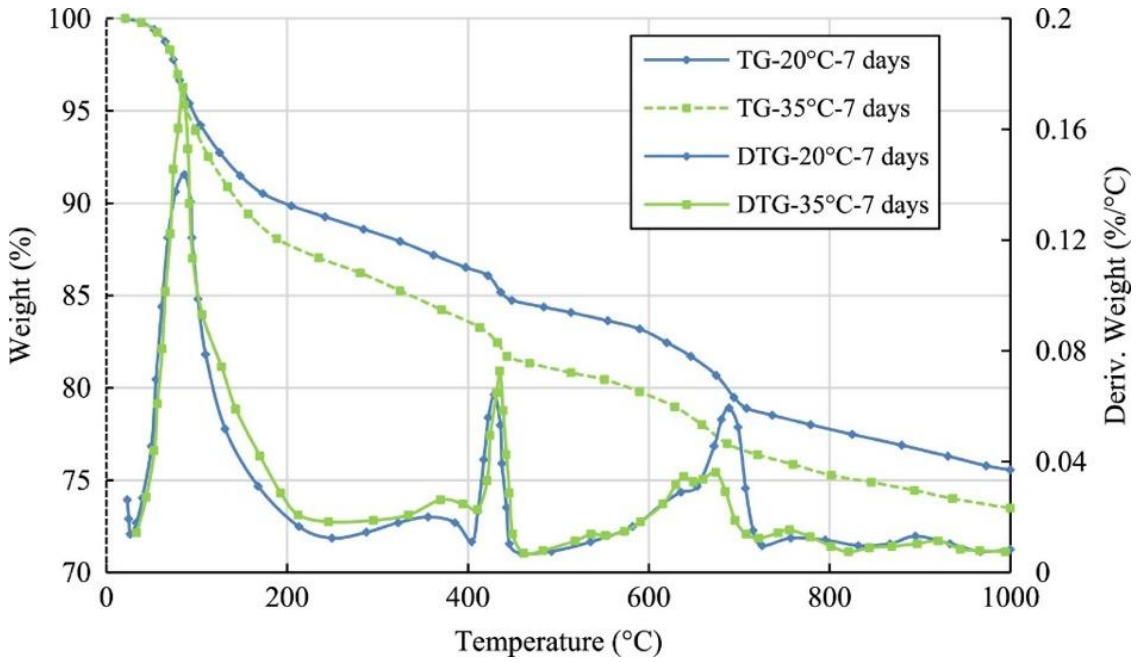

Figure 6-7. Results of thermal analysis depicting the effect of higher curing temperature on cement hydration process and quantity of generated hydration products

Moreover, Figure 6-6 shows that the evolution of pore water pressure in the columns is not only a function of temperature, but also of the presence or absence of NPs in the paste backfill. From the Figure 6-6, the CPB columns without and with NP subjected to non-isothermal field curing conditions display a similar trend in initial pore water pressure increase as well as in subsequent pore water pressure reduction. However, the column containing NPs demonstrated a swifter pore water dissipation than its control counterpart throughout the curing period. This enhanced dissipation rate can be attributed to the influence of NPs on various facets of the CPB mixture, encompassing binder hydration and microstructural refinement. Concerning the NPs' effect on binder hydration, previous research (Xiaoyan et al. 2012, Sato and Beaudoin 2015, Saremi and Fall 2023) suggests that nano-calcium carbonate can modify the cement hydration process in various ways. For instance, nano-calcium carbonate boosts the hydration process by offering additional nucleation sites for cement grains. This promotes the creation of more hydration products like C-S-H, leading to faster pore water consumption (Camiletti et al. 2013, Fu et al. 2022). A study by Saremi and Fall (2023) on the role of nano-calcium carbonate in CPB strength development revealed an increase in hydration product formation with nano-calcium carbonate particles, as shown in Figure 6-8. Based on this figure, it is evident that the cement paste augmented with NPs exhibits a pronounced weight reduction across multiple decomposition phases (two out of three main decomposition peaks). Notably, the phase spanning 100°C to 200°C is primarily attributed to the disintegration of water molecules as well as hydration products, including notable constituents such as ettringite, gypsum, and C–S–H, as mentioned earlier. Additionally, the third salient decomposition phase, which manifests between 600°C and 700°C, is predominantly linked to calcite decomposition. Pertinently, when considering the second decomposition peak, associated with the presence of CH in the studied cement pastes, it is imperative to highlight that nano-calcium carbonate particles possess pozzolanic properties (Shaikh and Supit 2014, Cosentino et al. 2020). These particles can engage in a reaction with CH, culminating in the formation of supplemental C-S-H compounds. Such a reaction inherently diminishes the overarching CH content in the cement paste infused with nano calcium carbonate (Roshani and Fall 2020b). This observation aligns congruently with the pronounced weight reduction observed during the initial decomposition phase, indicating an elevated presence of C-

S-H in the nanoparticle-enhanced cement paste. Given this decomposition mechanism, it becomes rational to infer that cement paste formulated without the inclusion of NPs displayed an elevated weight loss during the second predominant decomposition peak. Consequently, the instrumental role of NPs in catalyzing binder hydration—thereby resulting in an augmented yield of hydration products—becomes unequivocally manifest. This phenomenon further substantiates the accelerated dynamics observed in pore water pressure dissipation.

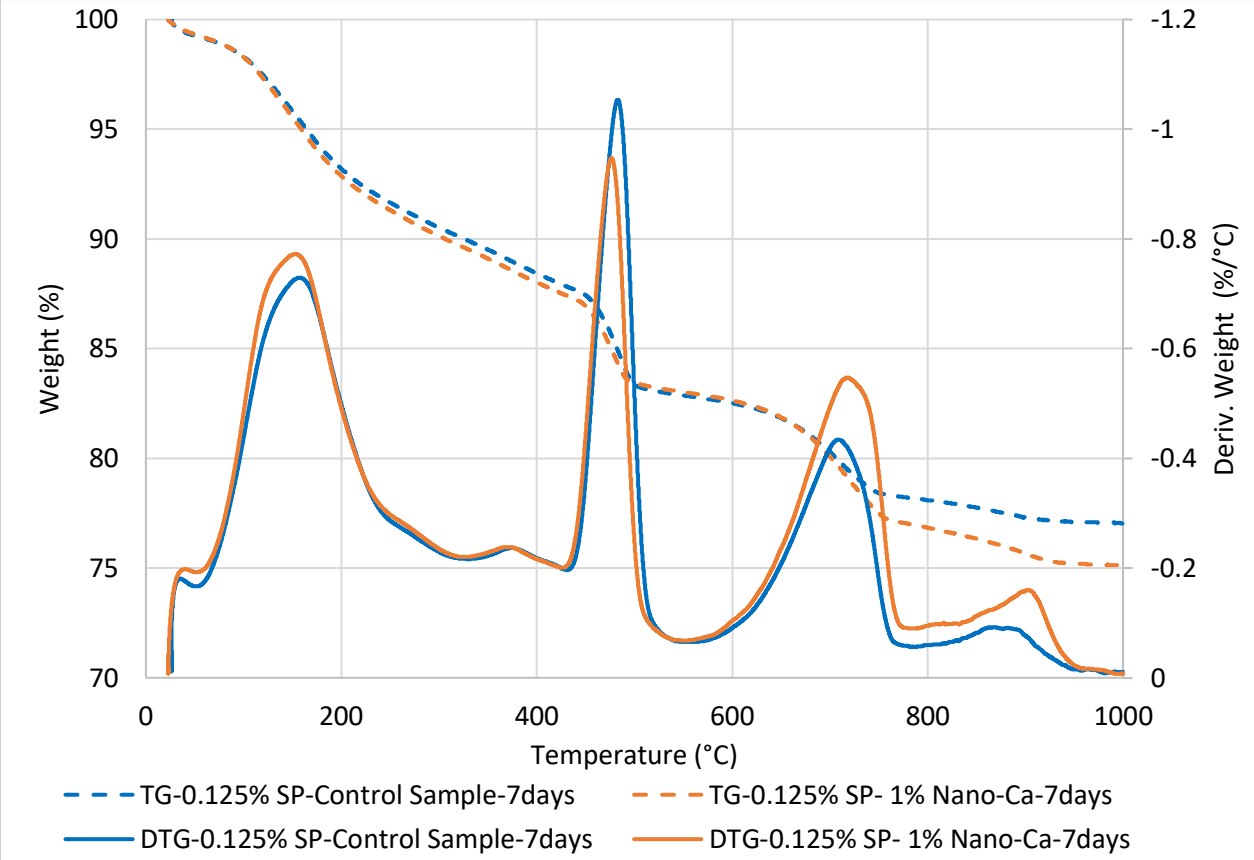

Figure 6-8. Results of thermal analysis conducted on cement paste prepared with addition (1%) and without (control) addition of nano-calcium carbonate supporting the beneficial impact of NPs on generation of higher amounts of hydration products compared to control sample.

Beyond the influence of NPs on binder hydration, numerous studies have emphasized that NPs can positively enhance the physical attributes of cementitious mixtures due to their filler effect (Camiletti et al. 2013, Oey et al. 2013, Ren et al. 2021, Cao et al. 2022, Fu et al. 2022). Additionally, Figure 6-9 showcases evidence of microstructural refinement in paste backfill attributed to the inclusion of nano-calcium carbonate particles. As illustrated in the figure, the CPB sample blended

with a 1% NPs content showed a significantly reduced cumulative porosity compared to the control sample, i.e., sample prepared without NPs. This can be attributed to the filling capacity of the NPs in the filler matrix.

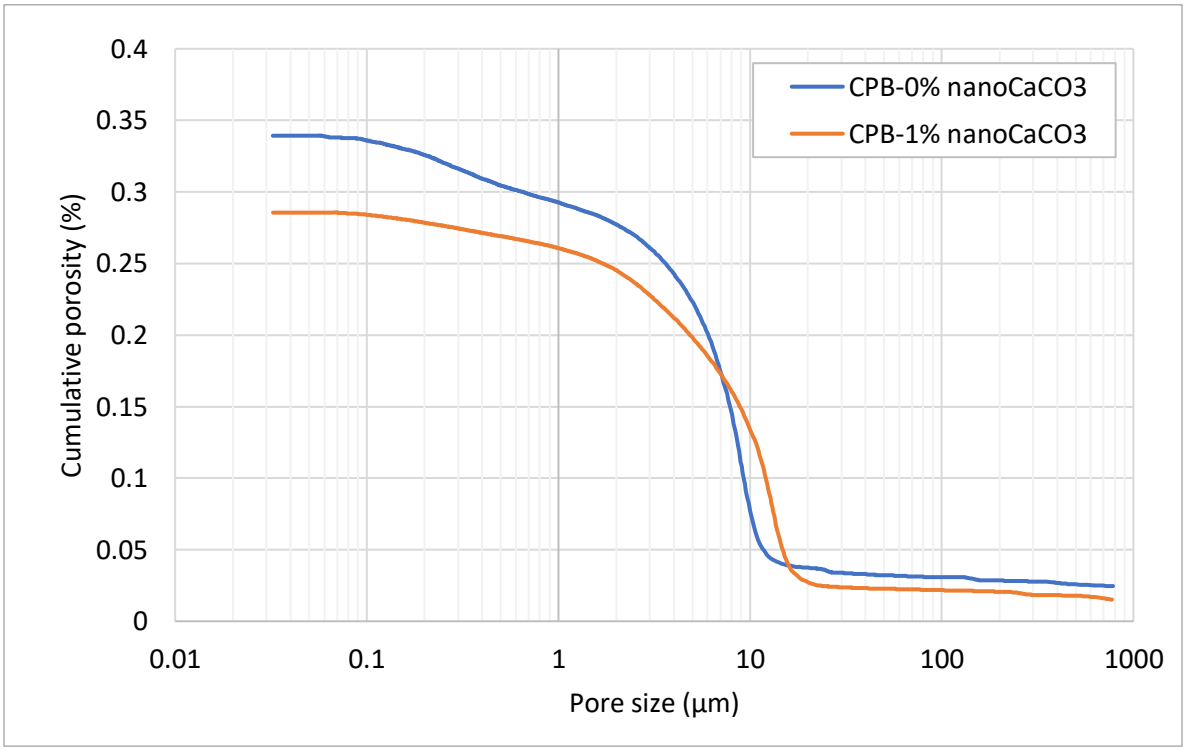

Figure 6-9. Results of MIP test on CPB samples made with and without nano-calcium carbonate

6.4.2 Evolution of compressive strength of the CPB columns

Figure 6-10 displays the influence of non-isothermal field curing conditions on the UCS of CPBs without NP obtained from distinct heights of the plug CPB columns at specific curing intervals, such as 1, 3, 7, and 28 days. As observed from this figure, regardless of their positioning within the column or the curing temperature (either isothermal or non-isothermal), all samples exhibited an upward trend in UCS values with advancing curing time. This augmentation in strength is predominantly linked to binder hydration progress, i.e., to the formation of more cement hydration products for longer curing time (Bullard et al. 2011, Xiapeng et al. 2019, Liu and Fall 2022). As previously noted, the cement hydration products formed due to the ongoing hydration process play a crucial role in cementing solid (tailings) particles, subsequently enabling effective transmission of shear stress throughout the paste backfill framework. Put simply, a

continued precipitation of hydration products filling the micropores within the backfill matrix suggests the potential for increased compressive strength. Supporting this, thermal analysis results from Fang and Fall (2021) on identical cement pastes cured for intervals of 7 and 28 days clearly indicated that samples cured for extended durations showcased greater weight loss during thermal analysis, pointing to an increased presence of hydration products in those samples.

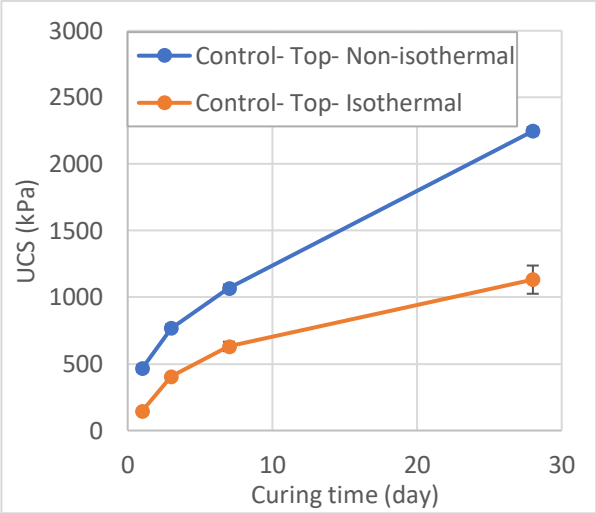

(a)

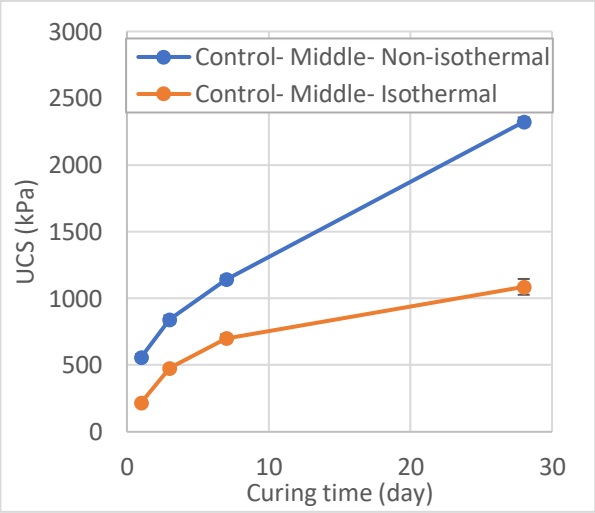

(b)

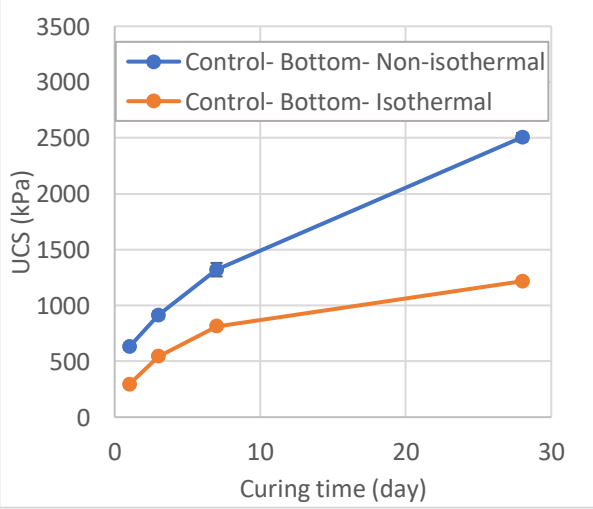

(c)

Figure 6-10. Impact of non-isothermal (higher temperatures) curing conditions on evolution of compressive strength at different heights of the plug backfill column (control = CPB without NPs). a): top of the column; b): middle of the column; c): bottom of the column (see Figure 6-2)

Furthermore, Figure 6-10 reveals that samples obtained from the column cured under non-isothermal conditions, i.e., higher temperatures, exhibit a more rapid strength acquisition pace and higher strength compared to their counterparts from the isothermally cured column. As highlighted in preceding sections, the advantageous effect of curing CPB at elevated temperatures on binder hydration is believed to be the primary driver of this enhancement. To further substantiate this explanation, Figure 6-11 shows the findings from void ration and porosity analyses on CPB samples procured from both isothermally and non-isothermally cured columns. This figure indicates that samples cured under non-isothermal conditions manifest a notably sharper decline in void ratio values than those cured under steady room temperature (isothermal setting). This can be ascribed to the formation of an increased volume of hydration products, as previously elucidated. Corroborating this, samples subjected to non-isothermal conditions displayed a swifter elevation in dry density, attributable to the hastened binder hydration, which in turn precipitates greater quantities of hydration products.

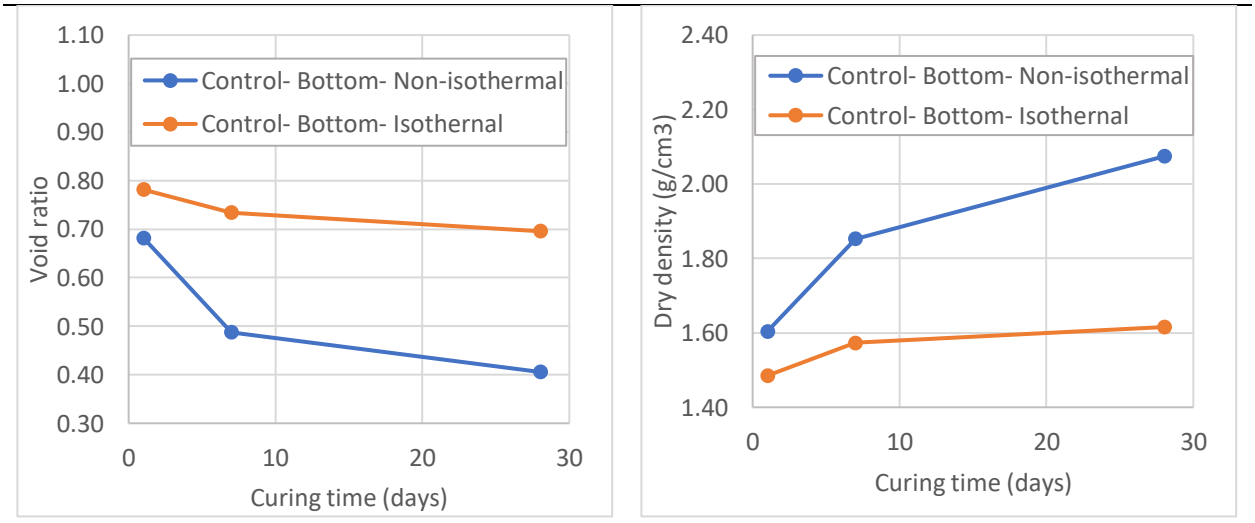

Figure 6-11. Beneficial effect of higher curing temperature on evolution of different physical properties at the bottom of the plug backfill column, a) void ratio, b) dry density

Additional evidence of pore refinement owing to the influence of non-isothermal curing temperatures can be found in a study undertaken by Cui and Fall (2016). According to their findings, curing CPB under non-isothermal conditions leads to the development of a more refined pore structure. This outcome is attributed to the fact that curing at elevated temperatures facilitates the generation of greater quantities of hydration products, thereby contributing to a more intricate and consolidated microstructure.

Furthermore, an examination of Figure 6-10 reveals that samples retrieved from the lower portions of both columns possess higher compressive strength in comparison to those extracted from the middle and upper levels of the column. This distinctive behavior can be rationalized by considering two concurrent phenomena occurring during the curing phase.

Firstly, the presence of heavier solid particles within the CPB mixture leads to a logical anticipation that these denser constituents would settle at a quicker rate. This settling results in the accumulation of these heavier particles at the lower regions of the column, where they are inherently capable of sustaining higher compressive loads. Furthermore, as a consequence of the pressure gradient exerted upon the column due to externally applied curing stress, the elevated pressure localized at the column's base serves to intensify the packing density of the backfill matrix situated in that specific lower section. This amplification of packing density underscores the synergistic interplay between external curing stress and geomaterial distribution within the columnar structure. This observation aligns with the findings of the pore structure (void ratio, porosity) analysis depicted in Figure 6-12, further reinforcing the understanding of how particle distribution and applied curing stress within the CPB matrix affects the overall compressive strength. According to the findings presented in Figure 6-12, samples obtained from the bottom of the columns demonstrated less void ratio and porosity compared to those taken from the higher levels.

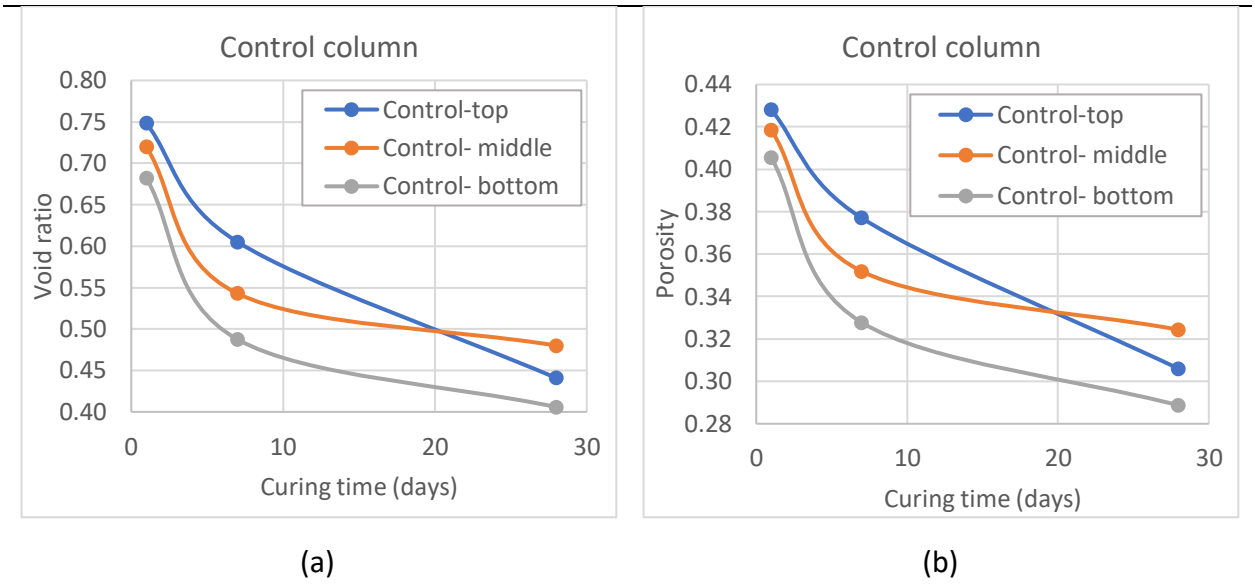

Figure 6-12. Results of physical properties measurements at different sections of the plug backfill column exhibiting the effect of curing stress and height on evolution of (a) void ratio, and (b) porosity

The second phenomenon contributing to the higher compressive strength at the bottom of the columns is the effect of curing stress on the hydration reaction. Results from prior studies have clearly indicated that curing CPB under applied stress could lead to the generation of greater quantities of hydration products (Fang and Fall 2020, Al-Moselly et al. 2022, Saremi and Fall 2023). For a more comprehensive understanding of how applied pressure might result in the production of a larger amount of cement hydration products, Figure 6-13 portrays the results of thermal analysis conducted on two identical cement samples. One was subjected to 150 kPa curing stress, and the other was cured without applied pressure. From this thermal analysis, it is evident that the cement sample cured under 150 kPa of applied pressure experienced a higher level of weight loss during the heating process compared to the control sample. In addition, the stress-cured sample shows higher endothermic peaks in the 450-550°C temperature range than the unstressed sample. In other words, the stress-cured sample contains more cement hydration products than the unstressed sample. These observed differences in weight losses and the endothermic peaks of the studied samples can be interpreted as variations in specific hydration products burned at particular temperature ranges, such as CSH, CH, and ettringite. In essence, a sample with a greater volume of hydration products would show more weight loss, and particularly higher peaks 450-550°C temperature range due to the destruction of CH. Therefore,

curing the CPB under applied pressure results in more hydration products, leading to stronger bonding between solid particles and a higher level of packing density for the samples that endured more pressure during their curing time. Considering that samples taken from the bottom of the column faced greater pressure due to the column's self-weight and applied pressure, the improved UCS test results in these samples, compared to those from the middle and top of the column, become explicable. This analysis provides an insightful explanation for the observed variations in compressive strength across different sections of the column.

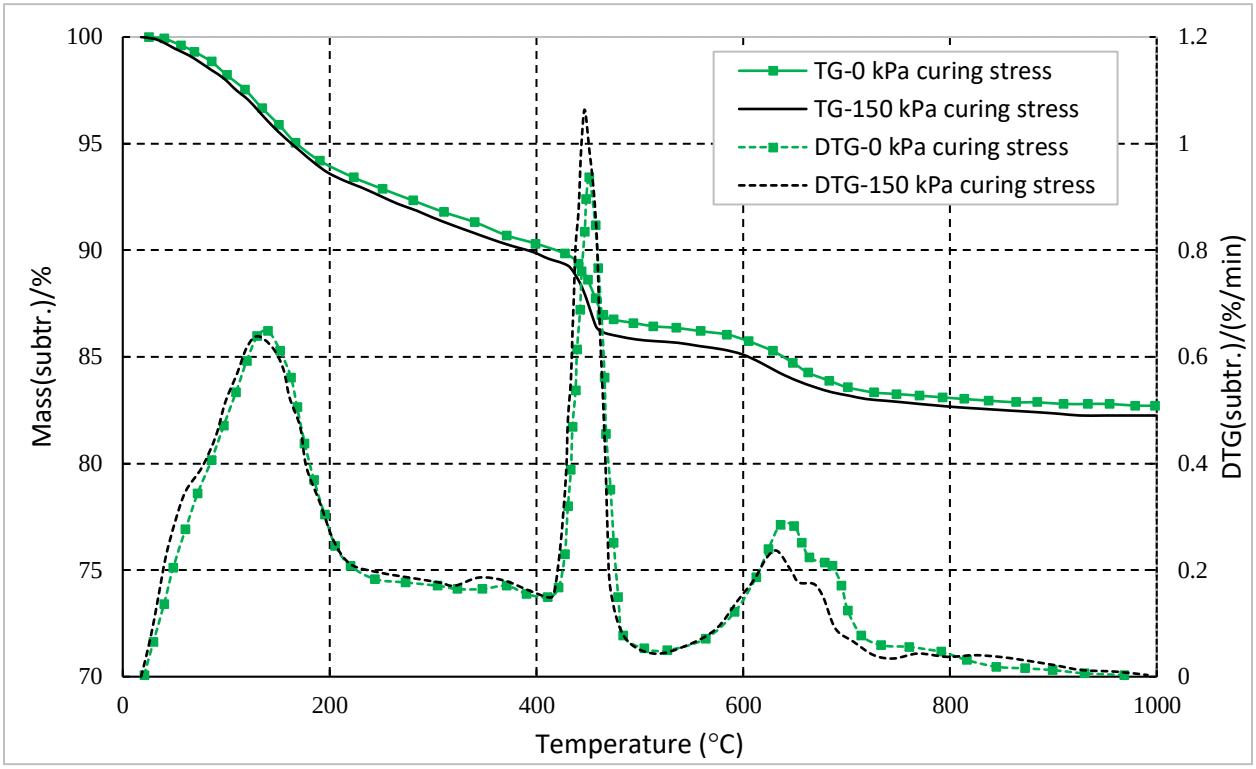

Figure 6-13. Results of TG/DTG analysis depicting the favorable impact of curing stress on binder hydration progress by generating higher amounts of hydration products.

The results of the UCS development of the columns studied indicated that not only do curing time, self-weight pressure and curing temperature have a significant influence on the strength development of the CPB plug in the field, but that the presence or absence of NPs also plays an important role, as demonstrated in Figure 6-14, which illustrates the outcomes of UCS tests performed on samples extracted from various heights of both the nano-CPB plug column and the

control column (CPB without NPs). These columns were subjected to field temperature (non-isothermal curing) and mechanical (backfill self-weight pressure) curing conditions.

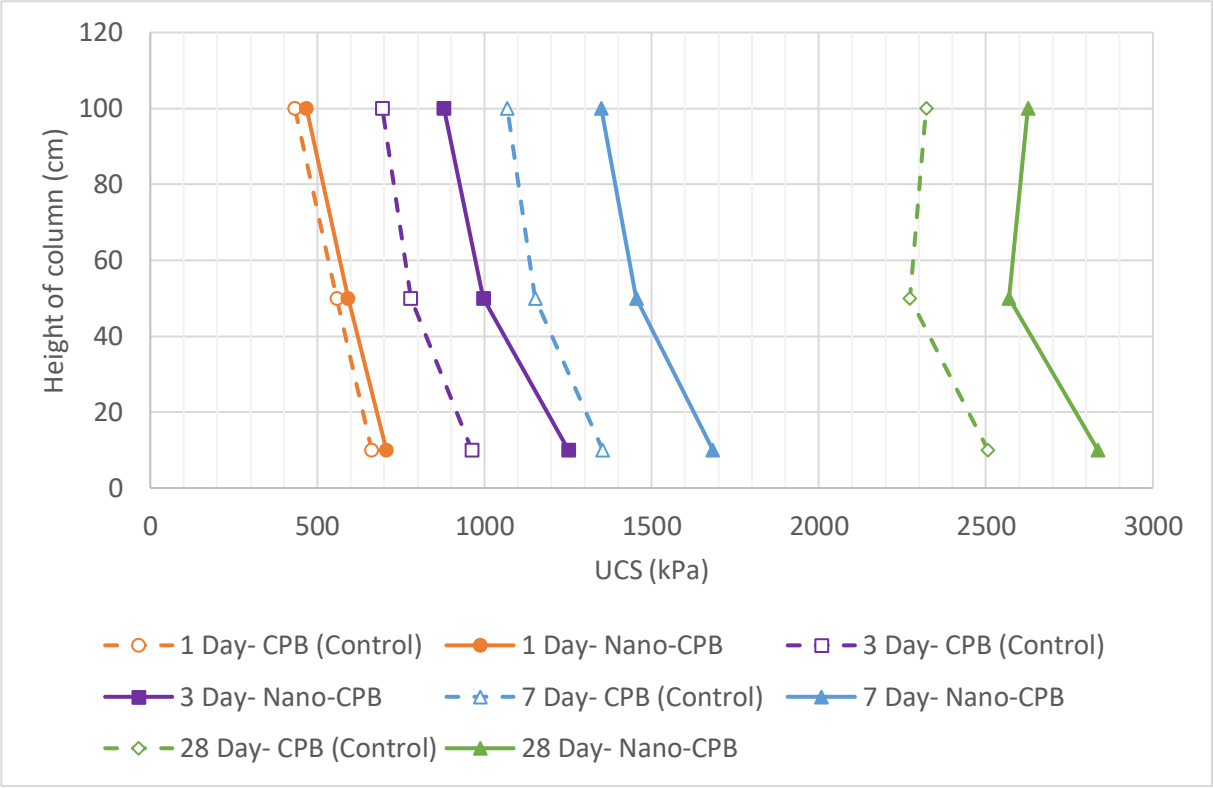

Figure 6-14. Evolution of compressive strength across diverse vertical sections of columns subjected to field overburden pressure and non-isothermal curing conditions: a comparative analysis between control (without NPs) and nano-modified columns.

Additionally, it may be discerned that the columns prepared with the integration of NPs consistently exhibited a higher compressive strength in contrast to the control column across the entire curing timeframe. As delineated in prior sections, this observation can be attributed to the propitious impact of NPs on both the binder hydration process and the overall physical properties of the CPB. As substantiated in Figure 6-8 the inclusion of NPs appears to be the pivotal factor in the observed weight loss during heating in the cement paste containing NPs, compared to the control cement paste. This finding provides evidence for the generation of greater quantities of hydration products. Moreover, as depicted in Figure 6-9, the integration of NPs led to a lower cumulative porosity in comparison to the control sample. This is indicative of how the filler effect

of NPs contributed to enhancing the packing density of the CPB mixture, thereby optimizing its structural characteristics.

Additional empirical evidence corroborating the impact of NPs inclusion on the mechanical performance of CPB is provided through the temporal analysis of electrical conductivity (EC) within the CPB column, as illustrated in Figure 6-15. The sensor embedded within the NP-augmented column consistently registered diminished EC values throughout the curing process in comparison to the control column containing 0% NPs. This phenomenon, as previously mentioned, can be attributed to the dual role of NPs including, first, their filler effect, and second, their contribution in accelerating the cement hydration. These combined effects contribute to a more refined pore structure (Figure 6-9) and a reduced packing density within the CPB matrix (Saremi and Fall 2023). Consequently, the modified pore architecture leads to decreased ion mobility within the pore fluid, attributable to the reduced interconnectivity of pores and the elongation of the ionic flow path. These factors collectively rationalize the observed lower EC values in columns treated with 1% nano-CaCO3 compared to the control (0% NP) column. (Ghirian 2016, Haruna and Fall 2020, Al-Moselly et al. 2022).

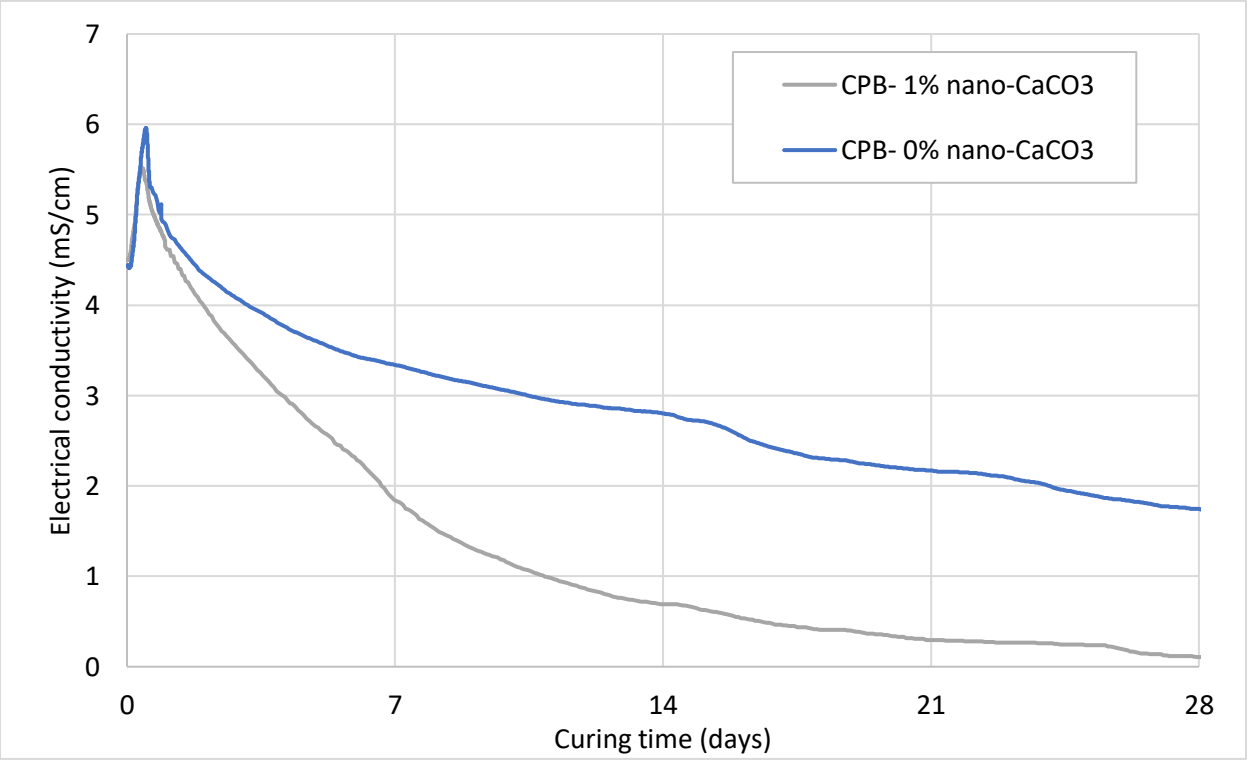

Figure 6-15. Effect on NPs on evolution of EC in the studied CPB columns

6.4.3 Evolution of total stress

Figure 6-16 illustrates the temporal evolution of the total pressure (total stress) exerted at the base of the columns without (control) and with NPs, subjected to both isothermal and non-isothermal curing temperatures. It is important to note that the total stress values detected by the sensors comprise not only the pressure applied at the top of the CPB column, but also the self-weight of the CPB. Moreover, the total stress presented here is directly connected to the self-weight of the backfill plug in real-world field conditions.

An analysis of the depicted figure exposes a consistent trend: irrespective of the curing temperature and the presence of nanoparticles in the backfill column, the total stress within the backfill column or plug shows a gradual increase in tandem with the applied stress on the column's top surface. This stress mirrors the force exerted by the backfill mass as it fills the stope. The progressive augmentation of total stress in the plug, observed during this initial phase, aligns with findings from numerous field investigations and modeling studies focused on backfill masses (e.g., Belem et al. 2004, Helinski et al. 2010, Doherty et al. 2015, Cui and Fall 2017). This affirmation underscores the efficacy of the developed column setups in accurately replicating the field behavior of CPB plugs.

From Figure 6-16, it becomes also evident that during the initial filling phase of the stope, a discernible trend emerges. Specifically, there is a gradual increase in the disparity between the measured total stress and the self-weight stress of the CPB plug. In simpler terms, the total stresses within the CPB plug progressively diminish relative to the stress attributed to the self-weight of the plug as the curing time advances during the backfill stope filling process. Furthermore, as depicted in Figure 6-16, following the initial rise in total stress during the stope-filling phase to form the plug, there is a subsequent decline in total pressure as the curing time advances. This trend holds true regardless of the specific temperature conditions applied during the curing process and the presence or absence of nanoparticles in the CPB material. Additionally, the disparity between the total stress measured at the bottom of the CPB column and the stress attributed to self-weight widens with increasing curing time, with the self-weight stresses exhibiting higher values. The observed reduction in measured total stresses in comparison to the stresses attributed to the self-weight of the CPB plug, along with the declining total stress as CPB

curing time increases, regardless of curing temperature or the presence of nanoparticles, can be primarily attributed to the synergistic effects of two key factors.

The first factor is the advancement of binder hydration over curing time. The advancing hydration of the binder corresponds to increased water consumption, causing a decline in pore water pressure (see Figure 6-6) and, consequently, a reduction in total stress. The phenomenon of generating additional binder hydration products and the associated increase in water consumption over curing time has been illustrated and discussed in previous sections.

The second factor is related to the development of arching within the CPB column. The arching effect, commonly delineated in geotechnical literature as the "soil arching phenomenon," denotes the complex redistribution of stress within a granular medium when encapsulated or confined by another material and subjected to external loadings. This intricacy arises predominantly due to the onset of shear stresses at the interface of the juxtaposed materials. These stresses are engendered by differential coefficients of friction between the two materials, leading to a non-uniform stress distribution (Zhao et al. 2019). Such a phenomenon is pivotal in understanding the load-bearing capacities and stress-strain behavior of granular assemblies, especially when they interact with surrounding matrices under varied loading conditions. Put differently, this mechanism operates within a confined space, such as a mine cavity filled with CPB, as illustrated by the aluminum column filled with CPB in this investigation. In this scenario, the load is not evenly distributed throughout the material; rather, it is transferred to the surrounding stable medium via interface shear, as discussed by Helinski et al. (2010) and Cui and Fall (2017). To elaborate further, in our study, the stress transfer from the CPB material to the adjacent aluminum column took place through interface shear. This arching phenomenon reduced the vertical stress experienced by the CPB plug beneath the loaded area.

Moreover, upon closer examination of Figure 6-16, a noticeable discrepancy emerges between the columns subjected to isothermal curing conditions and those exposed to non-isothermal field conditions. It becomes apparent that, both during the initial stope filling phase (plug construction) and after the completion of plug formation, the total pressures recorded at the base of the column subjected to isothermal curing conditions consistently surpass those measured at the base of the column cured under non-isothermal field conditions, regardless of

the curing time. In other words, the higher field curing temperature reduced the total stress developed in the backfill plug. This phenomenon can be ascribed to the predominant impact of non-isothermal (elevated) field curing temperatures on accelerating binder hydration. This acceleration, in turn, intensifies the rate of pore water consumption, thereby increasing the self-desiccation rate. The accelerated kinetics of hydration under non-isothermal conditions have been thoroughly expounded upon in previous sections of this study. Substantiating evidence includes observations from pore water pressure dissipation monitoring (see Figure 6-6) and microstructural refinement (see Figure 6-11). Furthermore, a higher initial backfill temperature contributes to increased arching, effectively reducing the stress level in the CPB column. This can be elucidated by the fact that more rapid binder hydration at a higher initial temperature leads to a more pronounced consolidation of the CPB, enhancing interface adhesion (Nasir and Fall, 2010). This heightened consolidation is evidently associated with greater relative displacement along the aluminum/CPB interface, resulting in increased interface shear stress. Moreover, the temperature-induced improvement in interface adhesion translates to higher interface shear strength (Nasir and Fall, 2010), indicating that the interface possesses the capacity to withstand elevated shear stresses. The collective body of evidence presented herein affirms the intricate interplay of temperature, stress, cement hydration kinetics, and structural characteristics in determining the mechanical behavior of CPB, underscoring the necessity for judicious consideration of these variables in both theoretical modeling and practical applications.

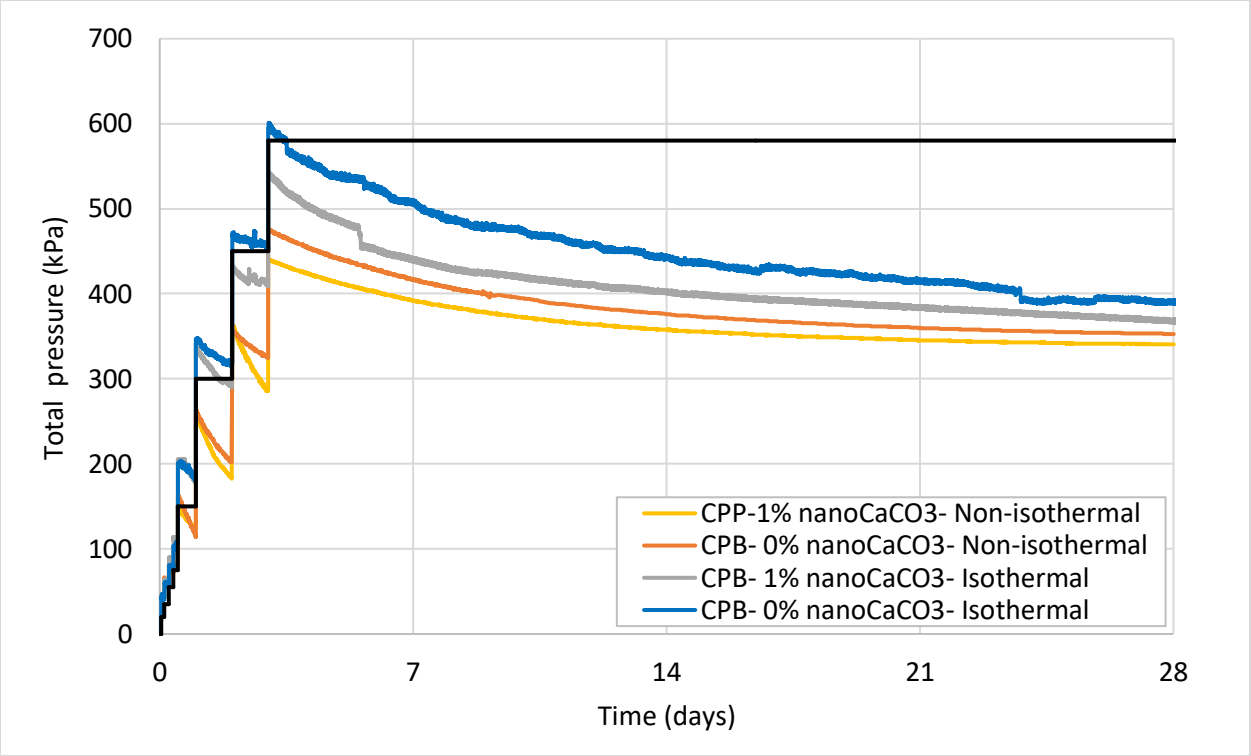

Figure 6-16. Evolution of total pressure at the bottom of the CPB with and without NPs

Figure 6-16 further clarifies that both the values and the temporal evolution of total stress within the CPB plug are influenced not only by curing temperature but also by the presence or absence of nanoparticles. Irrespective of the curing temperature, CPB columns containing nanoparticles exhibit lower total pressure values and a more rapid decline in total pressure over time once the initial filling of the column, i.e., the construction of the plug, is completed. This observed distinction can be primarily attributed to the multifaceted roles played by nanoparticles (NPs) within the CPB matrix. Most crucially, NPs act as catalysts, accelerating binder hydration by providing additional nucleation sites for the accumulation of cement hydration products. This, in turn, expedites the rate of pore water pressure dissipation and enhances the arching effect due to greater consolidation and increased interface shear strength, as discussed previously (Cyr et al., 2006; Li et al., 2015). In summary, the introduction of NPs into the CPB matrix exerts a marked influence on a range of physicochemical parameters, culminating in accelerated transitions and mobilizations that, collectively, account for the more rapid reduction in total stress in the CPB plug.

The findings elucidated in this section carry significant implications for augmenting the stability of backfilled stopes, optimizing backfill design, curtailing backfill costs, and increasing mine productivity. Notably, the research underscores that the non-isothermal field curing temperatures and/or the incorporation of nanoparticles (NPs) into the CPB plug substantially enhances the arching effect within the CPB plug, thereby effectively reducing stress levels. This stress reduction holds substantial practical importance, particularly in relation to the cost of CPB, where up to 75% is associated with binder consumption (Grice, 2001). Arching facilitates a more efficient and optimal utilization of cement, as the diminished stress in the backfill mass alleviates the necessity for excessive cement content to support the applied load. To illustrate, the arching effect could empower a CPB with an unconfined compressive strength of 500 kPa to withstand a backfill height exposure exceeding 100 meters. Conversely, in the absence of arching, such conditions would mandate a strength of 2 MPa, leading to heightened cement requirements and a subsequent increase in the overall cost of CPB operations (Kuganathan, 2005). Furthermore, the findings highlight that field temperatures and/or the presence of nanoparticles (NPs) reduce total stress and expedite its decline within the CPB plug. This impact significantly affects the stability of barricades, essential structures at the base of backfilled stopes, crucial for preventing the influx of fresh CPB into operational platforms. Barricade stability, a key factor for mining safety and continuity, is closely linked to the magnitude and decline rate of total stress within the backfill. Lower total stress and a faster decline rate correlate with increased barricade stability and earlier opening, crucial for mining efficiency. Economically, reduced total stress and faster dissipation are highly significant, contributing to shorter mining cycles and increased operational efficiency. Notably, the incorporation of NPs and higher curing temperatures emerges as pivotal factors in minimizing mandatory suspension durations, ultimately enhancing productivity in mining operations, leading to substantial financial gains.

6.5. Summary and conclusion

The main objective of this experimental study is to investigate the influence of non-isothermal curing conditions in the field and the incorporation of calcium carbonate nanoparticles on the

geotechnical performance of CPB columns subjected to mechanical conditions (vertical stresses) of real CPB plugs in the field. The ensuing findings are as follows.

- A realistic CPB plug model was devised to emulate real CPB plug field scenarios, considering the mechanical and thermal stresses experienced by backfill plug masses during both deposition and post-deposition phases. This physical model comprises fully instrumented columns equipped with a comprehensive thermal and mechanical loading system. It facilitates the continuous monitoring and evaluation of crucial geotechnical parameters (e.g., pore water pressure, total stress, strength, microstructure) under diverse field thermal and mechanical (vertical stress) loading conditions.
- The introduction of nanoparticles (NPs) into the CPB mixture has a profound impact on various geotechnical aspects, including mechanical strength, pore water pressure, total pressure development, and microstructure of the CPB plug. These effects are observed regardless of the curing conditions. CPB plugs enriched with NPs demonstrate superior geotechnical performance across key parameters: reduced pore water pressure and a more rapid decline over time, heightened strength, accelerated development of mechanical strength, lower total stresses, quick dissipation of total stresses, an improved arching effect, and a more refined pore structure. These enhancements primarily arise from the dual functionality of NPs: their filler effect, which reduces the size of capillary pores, and their role in enhancing the cement hydration process. The NPs contribute to this enhancement by serving as additional nucleation sites, facilitating a rapid hydration process, leading to an increased production of hydration by-products and stronger self-desiccation.

The results indicate that CPB columns cured at non-isothermal field temperatures (elevated temperatures) perform better than those cured under conventional isothermal conditions, exhibiting lower pore water pressure, faster dissipation of pore water pressure, greater and faster increase in compressive strength, faster reduction in total soil pressure, improved arching effect and notable microstructural improvement. This observed superiority is mainly attributed to the fact that high temperatures accelerate the binder hydration process. This acceleration not

only leads to greater production of hydration by-products, but also accelerates the consumption of pore water.

In conclusion, the outcomes of this research offer a thorough understanding of the impacts of simulated field curing conditions, particularly non-isothermal curing temperatures and field-overburden pressures, on the geotechnical performance of CPB plugs enhanced with nano-calcium carbonate particles. These insights are essential for the optimal design of CPB plugs. This optimization aims to enhance the geotechnical efficiency of CPB plug while balancing backfill costs and mining productivity.

6.6. References

Al-Moselly, Z., Fall, M., and Haruna, S. 2022. Further insight into the strength development of cemented paste backfill materials containing polycarboxylate ether-based superplasticizer. Journal of Building Engineering, **47**: 103859. Elsevier.

Aldhafeeri, A., Fall, M. (2017). Sulphate induced changes in the reactivity of cemented tailings backfill. International Journal of Mineral Processing 166 (10):13-23.

Belem, T., Aatar, O. El., Bussière, B., Benzaazoua, M., Fall, M., Yilmaz, E. 2006. Self-weight consolidation of column of cemented pastefill. 7th Seminar on paste and thickened tailings, April 2006, Irlande, 13p.

Belem T., Harvey A., Simon R., Aubertin M. (2004). Measurement and prediction of internal stresses in an underground opening during its filling with cemented fill. Proceedings of 5th international symposium on ground support in mining and underground construction. Perth, Australia, pp. 28-30

Benkirane, O., Haruna, S., and Fall, M. 2023a. Strength and microstructure of cemented paste backfill modified with nano-silica particles and cured under non-isothermal conditions. Powder Technology, **419**: 118311. doi:10.1016/j.powtec.2023.118311.

Benkirane, O., Haruna, S., and Fall, M. 2023b. Mechanical and microstructural characteristics of cemented paste tailings modified with nano-calcium carbonate and cured under various thermal conditions. International Journal of Mining, Reclamation and Environment, **37**(4): 277–296. Taylor & Francis. doi:10.1080/17480930.2023.2172661.

Bullard, J.W., Jennings, H.M., Livingston, R.A., Nonat, A., Scherer, G.W., Schweitzer, J.S., Scrivener, K.L., and Thomas, J.J. 2011. Mechanisms of cement hydration. Cement and Concrete Research, **41**(12): 1208–1223. Pergamon. doi:10.1016/J.CEMCONRES.2010.09.011.

Camiletti, J., Soliman, A.M., and Nehdi, M.L. 2013. Effect of nano-calcium carbonate on early-age properties of ultra-high-performance concrete. Magazine of Concrete Research, **65**(5): 297–307. Thomas Telford Ltd.

Cao, M., Yuan, X., Ming, X., and Xie, C. 2022. Effect of High Temperature on Compressive Strength and Microstructure of Cement Paste Modified by Micro- and Nano-calcium Carbonate Particles. Fire Technology, **58**(3): 1469–1491. doi:10.1007/s10694-021-01211-0.

Cosentino, I., Liendo, F., Arduino, M., Restuccia, L., Bensaid, S., Deorsola, F., and Ferro, G.A. 2020. Nano CaCO3 particles in cement mortars towards developing a circular economy in the cement industry. Procedia Structural Integrity, **26**: 155–165. doi:10.1016/j.prostr.2020.06.019.

Cui, L., and Fall, M. 2016. Mechanical and thermal properties of cemented tailings materials at early ages: Influence of initial temperature, curing stress and drainage conditions. Construction and Building Materials, **125**: 553–563. Elsevier. doi:10.1016/J.CONBUILDMAT.2016.08.080.

Cui, L, Fall M. (2017). Modeling of pressure on retaining structures for fill mass. Tunnelling and Underground Space Technology 69:94-107.

Cui, L, Fall M., 2018a. Multiphysics modeling and simulation of strength development and distribution in cemented tailings backfill structures. International Journal of Concrete Structures and Materials, 12 (1): 1-22.

Cui, L., and Fall, M. 2018b. Modeling of self-desiccation in a cemented backfill structure. International Journal for Numerical and Analytical Methods in Geomechanics, **42**(3): 558–583. doi:10.1002/nag.2756.

Cui, L., Fall, M. (2016). Multiphysics model for consolidation behaviour of cemented paste backfill. ACSE International Journal of Geomechanics 17(3): 23p; 04016077-23.

Cyr, M., Lawrence, P., and Ringot, E. 2006. Efficiency of mineral admixtures in mortars: Quantification of the physical and chemical effects of fine admixtures in relation with compressive strength. Cement and Concrete Research, **36**(2): 264–277. Pergamon. doi:10.1016/J.CEMCONRES.2005.07.001.

Doherty J.P., Hasan A., Suazo G.H., Fourie A. (2015). Investigation of some controllable factors that impact the stress state in cemented paste backfill. Canadian Geotechnical Journal, 52 (12): 1901-1912

Fall, M., Célestin, J.C., Pokharel, M., and Touré, M. 2010. A contribution to understanding the effects of curing temperature on the mechanical properties of mine cemented tailings backfill. Engineering Geology, **114**(3): 397–413. doi:10.1016/j.enggeo.2010.05.016.

Fall, M., Célestin, J.C., Sen, H.F, 2010. Potential use of polymer-pastefill as waste containment barrier materials. Journal of Waste Management 30: 2570-2578.

Fang, K., Fall, M. 2019. Chemically induced changes in shear behaviour of interface between rock and tailings backfill undergoing cementation. Rock Mechanics and Rock Engineering 2 (9), 3047-3062.

Fang, K., and Fall, M. 2020. Shear Behavior of the Interface Between Rock and Cemented Backfill: Effect of Curing Stress, Drainage Condition and Backfilling Rate. Rock Mechanics and Rock Engineering, **53**(1): 325–336. doi:10.1007/s00603-019-01909-2.

Fang, K., and Fall, M. 2021. Shear Behaviour of Rock–Tailings Backfill Interface: Effect of Cementation, Rock Type, and Rock Surface Roughness. Geotechnical and Geological Engineering, **39**(3): 1753–1770. doi:10.1007/s10706-020-01586-x.

Fu, Q., Zhang, Z., Zhao, X., Xu, W., and Niu, D. 2022. Effect of nano calcium carbonate on hydration characteristics and microstructure of cement-based materials: A review. Journal of Building Engineering, **50**: 104220. doi:10.1016/j.jobe.2022.104220.

Ghirian, A. 2016. Coupled thermo-hydro-mechanical-chemical (THMC) processes in cemented tailings backfill structures and implications for their engineering design. Dissertation, University of Ottawa, Ontario, Canada

Grice T. (2001). Recent mine developments in Australia. Proceeding of the 7th International Symposium on Mining with Backfill (MINEFILL), pp. 351-357

Haruna, S., and Fall, M. 2020. Strength development of cemented tailings materials containing polycarboxylate ether-based superplasticizer: experimental results on the effect of time and temperature. Canadian Journal of Civil Engineering, **48**(4): 429–442.

Helinski, M., Fahey, M., and Fourie, A. 2010. Behavior of Cemented Paste Backfill in Two Mine Stopes: Measurements and Modeling. Journal of Geotechnical and Geoenvironmental Engineering, **137**(2): 171–182. American Society of Civil Engineers. doi:10.1061/(ASCE)GT.1943-5606.0000418.

Jiang, H., Yi, H., Yilmaz, E., Liu, S., and Qiu, J. 2020. Ultrasonic evaluation of strength properties of cemented paste backfill: Effects of mineral admixture and curing temperature. Ultrasonics, **100**: 105983. doi:10.1016/j.ultras.2019.105983.

Jiang, H. Fall, M., Li, Y., Han J. (2019). An experimental study on compressive behaviour of cemented rockfill. Construction and Building Materials 213:10-19.

Kong, D., Su, Y., Du, X., Yang, Y., Wei, S., and Shah, S.P. 2013. Influence of nano-silica agglomeration on fresh properties of cement pastes. Construction and Building Materials, **43**: 557–562. doi:10.1016/j.conbuildmat.2013.02.066.

Koohestani, B., Belem, T., Koubaa, A., and Bussière, B. 2016. Experimental investigation into the compressive strength development of cemented paste backfill containing Nano-silica. Cement and Concrete Composites, **72**: 180–189. Elsevier. doi:10.1016/J.CEMCONCOMP.2016.06.016.

Kuganathan K (2005). Geomechanics of mine fill. Potvin, Thomas, Fourie (Eds.), Handbook on Mine Fill, Australian Centre of Geomechnics, p. 23.49

Li, W., Huang, Z., Zu, T., Shi, C., Duan, W.H., and Shah, S.P. 2015. Influence of Nanolimestone on the Hydration, Mechanical Strength, and Autogenous Shrinkage of Ultrahigh-Performance Concrete. Journal of Materials in Civil Engineering, **28**(1): 04015068. American Society of Civil Engineers. doi:10.1061/(ASCE)MT.1943-5533.0001327.

Liu, S., and Fall, M. 2022. Fresh and hardened properties of cemented paste backfill: Links to mixing time. Construction and Building Materials, **324**: 126688. doi:10.1016/j.conbuildmat.2022.126688.

Nasir, O., and Fall, M. 2009. Modeling the heat development in hydrating CPB structures.

Nasir O., Fall M. (2010). Coupling binder hydration, temperature and compressive strength development of underground cemented paste backfill at early ages Tunn Undergr Sp Tech, 25 (1) (2010), pp. 9-20

Oey, T., Kumar, A., Bullard, J.W., Neithalath, N., and Sant, G. 2013. The Filler Effect: The Influence of Filler Content and Surface Area on Cementitious Reaction Rates. Journal of the American Ceramic Society, **96**(6): 1978–1990. John Wiley & Sons, Ltd. doi:10.1111/JACE.12264.

Orejarena, L., Fall, M., 2008. Mechanical response of a mine composite material to extreme heat load. Bulletin of Engineering Geology and Environment 67(3):387-396.

Pengyu, Y., and Li, L. 2015. Investigation of the short-term stress distribution in stopes and drifts backfilled with cemented paste backfill. International Journal of Mining Science and Technology, **25**(5): 721–728. doi:10.1016/j.ijmst.2015.07.004.

Ren, Z., Liu, Y., Yuan, L., Luan, C., Wang, J., Cheng, X., and Zhou, Z. 2021. Optimizing the content of nano-SiO2, nano-TiO2 and nano-CaCO3 in Portland cement paste by response surface methodology. Journal of Building Engineering, **35**: 102073. doi:10.1016/j.jobe.2020.102073.

Roshani, A., and Fall, M. 2020a. Flow ability of cemented pastefill material that contains nano-silica particles. Powder Technology, **373**: 289–300. doi:10.1016/j.powtec.2020.06.050.

Roshani, A., and Fall, M. 2020b. Rheological properties of cemented paste backfill with nano-silica: Link to curing temperature. Cement and Concrete Composites, **114**. Elsevier Ltd. doi:10.1016/J.CEMCONCOMP.2020.103785.

Sagade, A. 2023. Fresh and Hardened Properties of Cemented Paste Backfill with Ternary Binder. Thesis, Université d'Ottawa / University of Ottawa.

Sanchez, F., and Sobolev, K. 2010. Nanotechnology in concrete – A review. Construction and Building Materials, **24**(11): 2060–2071. doi:10.1016/j.conbuildmat.2010.03.014.

Saremi, A., and Fall, M. 2023. Strength and suction development of nano-cemented paste tailings materials. Cleaner Materials, **8**: 100190. doi:10.1016/j.clema.2023.100190.

Sato, T., and Beaudoin, J.J. 2015. Effect of nano-CaCO3 on hydration of cement containing supplementary cementitious materials. https://doi.org/10.1680/adcr.9.00016, **23**(1): 33–43. Thomas Telford Ltd. doi:10.1680/ADCR.9.00016.

Shaikh, F.U.A., and Supit, S.W.M. 2014. Mechanical and durability properties of high volume fly ash (HVFA) concrete containing calcium carbonate (CaCO3) nanoparticles. Construction and Building Materials, **70**: 309–321. doi:10.1016/j.conbuildmat.2014.07.099.

Sheshpari, M. 2015. A review of underground mine backfilling methods with emphasis on cemented paste backfill. Electronic Journal of Geotechnical Engineering, **20**(13): 5183–5208.

Sui, W., Zhang, D., Cui, Z.C., Wu, Z., and Zhao, Q. 2015. Environmental implications of mitigating overburden failure and subsidences using paste-like backfill mining: a case study. International Journal of Mining, Reclamation and Environment, **29**(6): 521–543. Taylor & Francis. doi:10.1080/17480930.2014.969049.

Tian, X., and Fall, M. 2021. Non-isothermal evolution of mechanical properties, pore structure and self-desiccation of cemented paste backfill. Construction and Building Materials, **297**: 123657. doi:10.1016/j.conbuildmat.2021.123657.

Walske, M.L., McWilliam, H., Doherty, J., and Fourie, A. 2016. Influence of curing temperature and stress conditions on mechanical properties of cementing paste backfill. Canadian Geotechnical Journal, **53**(1): 148–161. NRC Research Press. doi:10.1139/cgj-2014-0502.

Wang, K., Tanesi, J., and Ardani, A. 2014. Effects of nanomaterials on the hydration kinetics and rheology of Portland cement pastes.

Wang, Y., Fall, M., and Wu, A. 2016. Initial temperature-dependence of strength development and self-desiccation in cemented paste backfill that contains sodium silicate. Cement and Concrete Composites, **67**: 101–110. Elsevier. doi:10.1016/J.CEMCONCOMP.2016.01.005.

Wu, D., Fall, M., Cai, S-J, 2012. Coupled modeling of temperature distribution and evolution in cemented tailings backfill structures that contains mineral admixtures. Journal of Geotechnical and Geological Engineering 30(4): 935-961.

Wu, D., Fall, M., Cai, S-J, 2014. Numerical modelling of thermally and hydraulically coupled processes in hydrating tailings backfill columns. International Journal of Mining, Reclamation and Environment 28(3):173-199.

Xiaoyan, L., Ch, L., Aihua, L., and Xinrui, W. 2012. Effect of Nano-CaCO3 on Properties of Cement Paste. Energy Procedia, **16**(2012): 991–996.

Xiapeng, P., Fall, M., and Haruna, S. 2019. Sulphate induced changes of rheological properties of cemented paste backfill. Minerals Engineering, **141**: 105849. doi:10.1016/j.mineng.2019.105849.

Xu, W., Chen, W., Tian, M., and Guo, L. 2021. Effect of temperature on time-dependent rheological and compressive strength of fresh cemented paste backfill containing flocculants. Construction and Building Materials, **267**: 121038. doi:10.1016/j.conbuildmat.2020.121038.

Yilmaz, E. 2018. Stope depth effect on field behaviour and performance of cemented paste backfills. International Journal of Mining, Reclamation and Environment, **32**(4): 273–296. Taylor & Francis. doi:10.1080/17480930.2017.1285858.

Yilmaz, E., and Fall, M. 2017. Introduction to Paste Tailings Management. *In* Paste Tailings Management. *Edited by* E. Yilmaz and M. Fall. Springer International Publishing, Cham. pp. 1–5.

Zhao, X., Fourie, A., and Qi, C. 2019. An analytical solution for evaluating the safety of an exposed face in a paste backfill stope incorporating the arching phenomenon. International Journal of Minerals, Metallurgy, and Materials, **26**(10): 1206–1216. doi:10.1007/s12613-019-1885-7.

CHAPTER 7. Thechnical Paper IV: Self-Desiccation Behaviour of Nano-Cemented Tailings Backfill Plug: Insights from Thermo-Mechanical-Chemical Column Experiments

Amirreza Saremi, Mamadou Fall

Published in Journal of Materials Research and Technology, Volume 30, May–June 2024, Pages 5952-5962

https://doi.org/10.1016/j.jmrt.2024.04.189

7.1. Abstract

This paper examines the influence of various factors, including the addition of nano-calcium carbonate particles (chemical processes, C) to CPBs, non-isothermal field curing temperatures (thermal factor, T), and field vertical curing stress (mechanical factor, M), on the self-desiccation capacity of CPB plugs. The assessment of self-desiccation involves the determination of pore water pressure (PWP) and volumetric water content (VWC) in the examined CPBs. Thermo-mechanical-chemical (TMC) column experiments were conducted to investigate the interaction among these factors and their collective impact on the evolution of PWP and VWC within the CPB plug. The findings underscore that each factor, both individually and in combination, significantly affects the magnitude and progression of self-desiccation in CPB plugs. Notably, the factors of elevated field temperature and the introduction of nano-calcium carbonate (NC) to the CPB exert the most substantial influence on the extent and enhancement of self-desiccation, whereas the impact of field curing stress in isolation is comparatively much weaker. The integration of nano-calcium carbonate, especially under non-isothermal conditions and concurrent field stress, emerges as a key contributor to enhanced PWP and VWC dissipation rates. The role of non-isothermal field curing temperature is underscored as a significant contributing factor in the self-desiccation of CPB plugs. The results presented in this paper will contribute to a more cost-effective design of CPB plugs and the improved optimization of CPB mixtures with nano-calcium carbonate particles.

Keywords: Cemented paste backfill, Tailings, Mine, Nanoparticles, Plug, Non-isothermal temperature, Overburden pressure

7.2. Introduction

Cemented paste backfill (CPB) technology represents an innovative and sustainable approach to tailings management (Grice 1998; Belem et al., 2006; Orejarena and Fall, 2008; Ercikdi et al. 2009a,b; Yilmaz 2011; Jiang et al. 2019; Aldhafeeri and Fall, 2017). CPB consists of a composite mixture of water, tailings and a hydraulic binding agent (Hassani et al. 2001; Tariq and Yanful 2014; Wu et al. 2016; Ghirian and Fall 2017; Yilmaz and Fall 2017; Haruna and Fall, 2020; Yang et al. 2020). Primarily used to backfill mine workings, CPB offers an environmentally friendly alternative that addresses both the geotechnical and environmental challenges associated with traditional mine waste management. By diverting tailings from surface deposits to backfilled mine workings, CPB significantly reduces the risk of environmental contamination and dam failure. In addition, the material contributes to the mechanical stabilization of underground excavations, improving the structural integrity of the mining operation. This stabilization is particularly beneficial in mitigating the problems of ground subsidence and wall collapse, which are common challenges in traditional mining practices (Benvenuti et al. 1997; Akcil and Koldas 2006). Beyond these benefits, CPB also has a pronounced impact on mine operational productivity (Yilmaz et al. 2003; Wang et al. 2004; Huynh et al. 2006; Sheshpari 2015; Yilmaz 2017; Wu et al. 2020; Al-Moselly et al. 2022).

As a generally accepted practice, underground mining cavities (stopes) are typically backfilled using a two-layer approach with fresh paste backfill material. This process involves the placement of a primary plug followed by the application of residual backfill, also referred to as the main or final pour (Figure 7-1). To ensure that the CPB plug remains confined within the designated stope and to prevent unintended overflow into adjacent areas, the implementation of a temporary retaining structure (barricade) is indispensable (Figure 7-1). The design of such a barricade is non-trivial; it must be engineered to withstand the exerted loads or pressures exerted by the fresh CPB throughout the backfilling operation and curing process. Therefore, the robust design of this temporary barricade structure is of paramount importance, not only for the safety of personnel and equipment but also for maintaining the overall structural integrity of the mining operations. The pressure acting on the barricade is mainly a function of the pore water pressure within the hydrating CPB plug mass. Key field factors that significantly affect the magnitude and evolution

of pore water pressure and hence the pressure applied to barricades - in other words, barricade safety - include the drainage and self-desiccation capabilities of CPB plug (Wu et al., 2014). For example, if a barricade is designed with adequate drainage capabilities, the build-up of hydrostatic pressure behind it can be significantly reduced due to the dissipation of pore water pressure. Similarly, the onset of self-desiccation due to water consumption by binder hydration leads to a similar reduction in pore water pressure and promotes the transformation of CPB from a fluid state to a more solid material (Wu et al. 2014). Therefore, a thorough study of these influencing factors is essential to optimize both barricade construction and CPB formulation. In addition, engineering solutions/techniques that accelerate the dissipation of pore water pressure or amplify the effects of self-desiccation can be highly beneficial to the stability of the barricade and CPB plug, and to the overall productivity of mining operations. Accelerated pore pressure reduction, particularly when accompanied by the development of negative pore water pressure (suction) due to self-desiccation, correlates with reduced downtime in mining operations. This quickening of pressure equilibration allows the CPB backfill structure to achieve the necessary mechanical strength in a shorter timeframe, thereby enabling the timely removal of temporary barricades and the resumption of excavation activities (Ghirian and Fall 2013, Saremi and Fall 2023).

A pragmatic approach to accelerating the dissipation of pore water pressure in CPB is to use chemical additives that catalyze binder hydration. This approach has a dual advantage. Firstly, accelerated hydration of the binder leads to faster production of hydration products, which serve as the main bonding agents between solid particles in the microstructure of the backfill. This allows the design strength of the backfill to be reached more quickly, enabling the backfill structure to become self-supporting in a reduced timeframe. Secondly, binder hydration intrinsically consumes free water as part of its reaction mechanism. Consequently, enhancing this hydration process indirectly accelerates the rate of pore water pressure dissipation (Ghirian and Fall 2016a, Al-Moselly et al. 2022).

In recent years, numerous studies have concluded that the addition of nanoparticles to cementitious materials can significantly improve the hydration of the binder contained in these materials (e.g, Camiletti et al. 2013, Cao et al. 2019, Cao et al. 2022, Fu et al. 2022a, Benkirane et

al. 2023). Moreover, previous studies (e.g., Koohestani et al. 2016, Roshani and Fall 2020, Benkirane et al. 2023, Saremi and Fall 2023) on the effect of different types of nanoparticles (e.g., nano-silica (SiO_2), nano-calcium carbonate ($CaCO_3$), nano-iron oxide (Fe_2O_3), and nano-aluminum oxide (Al_2O_3)) on CPB properties have shown that nano-calcium carbonate (Nano-$CaCO_3$) has the most significant impact on the enhancement of binder hydration and strength development in small CPB samples. These results suggest that the addition of nano-calcium carbonate (NC) to the CPB plug could potentially improve its self-desiccation capacity. However, the effect of NC on the self-desiccation of the CPB plug is not known.

Moreover, once constructed underground, the CPB plug experiences simultaneous exposure to both mechanical (M) and thermal (T) loads during its hardening phase or during the binder hydration process (chemical factor, C) (Fall and Ghirian, 2014), as depicted in Figure 7-1. CPB structures typically comprise substantial high-rise geotechnical formations, often reaching several tens of meters in height. The significant mass of the CPB introduces considerable time-dependent total pressure and stress within the plug, thereby influencing the cement hydration process and, consequently, the self-desiccation process (Ghirian and Fall, 2013). Additionally, the temperature of the surrounding rocks naturally rises with depth due to the geothermal gradient (Nasir and Fall 2009). Furthermore, the hydration of the binder generates notable amounts of internal heat within the CPB structure (Fang and Fall 2018, 2019). The hydration rate of the binder in CPB is directly influenced by both external and internal heat sources, consequently impacting the self-desiccation process. These conclusions suggest that the self-desiccation behavior of CPB plug containing nanoparticles cannot be solely attributed to the cement type or the mere presence of nanoparticles (chemical factors, C). Instead, it is subject to the combined effects of field curing temperatures (T factor) and stresses (M factor) acting on the CPB plug. Essentially, the complex interplay among nanoparticles, thermal and mechanical processes, and their interactions governs the onset and progression of self-desiccation within the CPB plug containing nano-calcium carbonate particles (NC). However, to date, there exists a noticeable gap in research addressing the synergistic impacts of field curing temperature and vertical curing stress (CPB self-weight pressure) on the self-desiccation of CPB plugs incorporating NC. No studies have

been carried out to evaluate and understand the self-desiccation of nano-CPB plugs cured under conditions close to those encountered in the field.

Hence, the main goal of this study is to perform thermo-mechanical-chemical (TM) column experiments, specifically designed to systematically examine the self-desiccation of field CPB plugs incorporating NC particles. These experiments will involve exposure to curing conditions, including temperatures and stresses, that replicate non-isothermal curing and CPB self-weight pressures experienced in real-world field scenarios. The assessment of self-desiccation will be quantified by monitoring the evolution of pore water pressure and volumetric water content within the CPB plug.

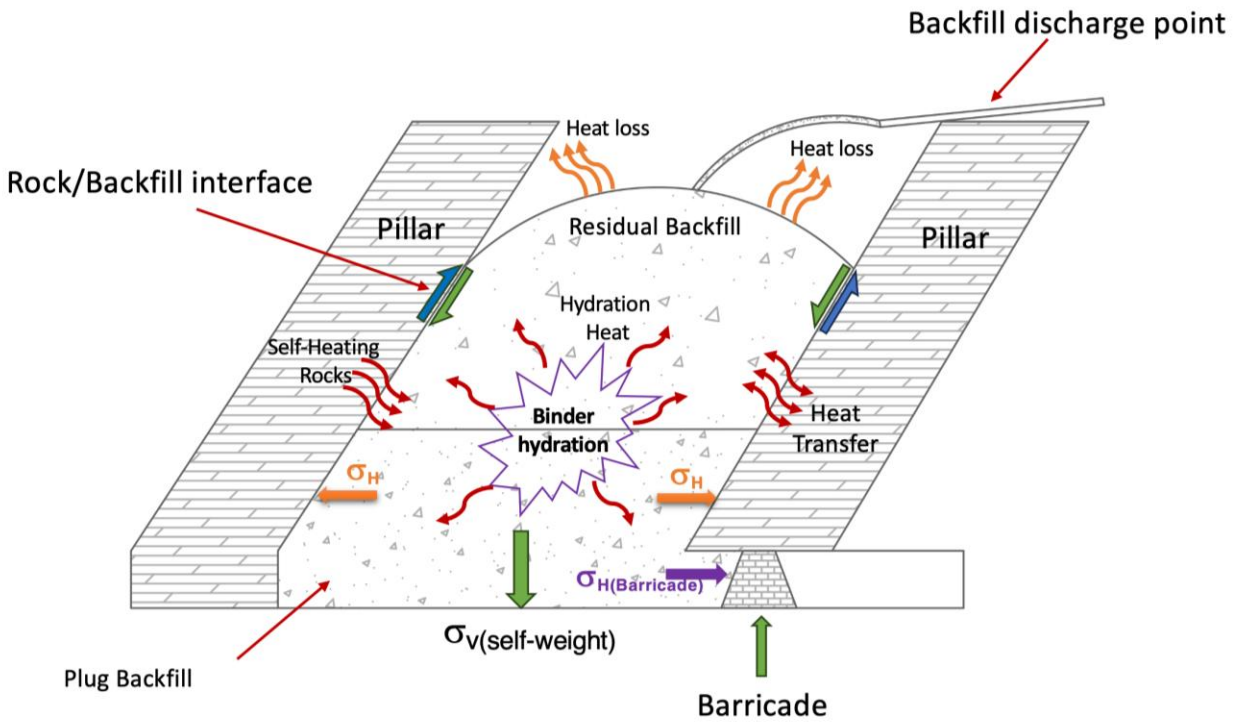

Figure 7-1 Schematic representation of a backfilled stope, illustrating the interaction between various field factors with CPB plug, residual backfill, and adjacent environment

7.3. Experimental Program

7.3.1 Materials

7.3.1.1. Tailings

To prepare the fresh CPB mixture, synthetic silica tailings (ST) were selected, which are primarily composed of quartz (Table 7-1), a mineral known for its non-reactive nature. STs have a high silica content (SiO_2; 99.8%), making them a chemically inert material. The rationale behind this choice was to eliminate potential uncertainties in the analysis and interpretation of the study's results. Specifically, the non-reactive properties of ST reduce the risk of unintended chemical reactions that may occur with natural tailings, which could in turn interfere with the binder hydration process and ultimately affect the findings. Regarding the physical characteristics of the ST, Figure 7-2 showcases the grain size distribution curve of the selected tailings, alongside the average grain size distribution of nine Canadian mine tailings. A comparative analysis of these curves reveals an acceptable degree of similarity, underscoring the representativeness of the ST for field conditions. Table 7-1 and Table 7-2 provide the ST's physical and chemical properties, respectively.

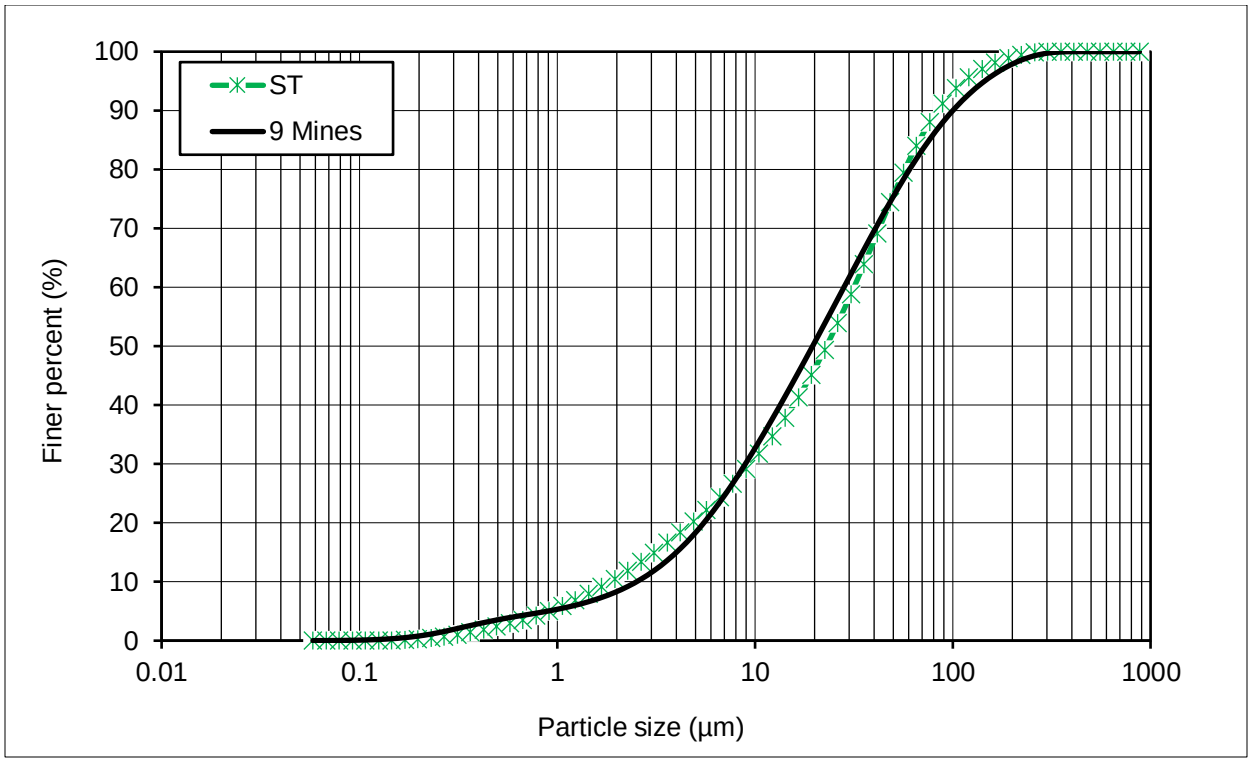

Figure 7-2. Grain size distribution of silica tailings (ST) versus mean distribution from nine Eastern Canadian mines.

Table 7-1. Composition breakdown of minerals in the silica tailings (ST)

Tailings	Mineral											
	Quartz	Albite	Dolomite	Calcite	Chlorite	Magnetite	Pyrite	Talc	Pyrrhotite	Spinel	Others	Total
Content (%)	99.8	-	-	-	-	-	-	-	-	-	0.2	100.0

ST: silica tailings

Table 7-2. Comparison of physical properties for ST and the average of nine tailing types.

Element	G_s	D_{10}	D_{30}	D_{50}	D_{60}
Unit	-	µm	µm	µm	µm
ST	2.7	1.9	9.0	22.5	31.5
Average of 9 types of tailings	-	1.8	9.1	20.0	30.8

G_s: specific gravity.

7.3.1.2. Nanoparticles

In light of the advantageous effects of nano-calcium carbonate particles on various mechanical properties of CPB, as described in prior studies (Saremi and Fall, 2023)—such as improvements in compressive strength and microstructural refinement—this particular nanomaterial was selected for investigation in the current experimental study. Data concerning the physical and chemical properties of the NCs, utilized in this study are outlined in Table 7-3.

Table 7-3. Characterization of the utilized Nano-Calcium Carbonate (Nano-$CaCO_3$).

Nano-$CaCO_3$	
Appearance	White powder
$CaCO_3$ (%)	≥98
HCl insoluble (%)	≤0.1
Particle size (nm)	20–50
Fe (%)	≤0.08
Mn (%)	≤0.006

7.3.1.3. Binder, mixing water, and superplasticizer

Ordinary Portland Cement Type 1 (PCI), the most prevalent cement type employed in both mining and construction industries, was utilized as the hydraulic binder. Additionally, tap water served as the mixing agent for mixing the silica tailings and the binder to create the fresh CPB mixture. The use of PCI is a strategic choice because its characteristics are well-documented and it is commonly used in similar applications, making the study's results easily translatable to real-world scenarios. The standardized nature of PCI ensures the reliability and replicability of the experiment's outcomes. Tap water was selected for its accessibility and to replicate the conditions often encountered in practical mining applications. The use of tap water eliminates additional variables that could arise from using mine process wastewater, thereby providing a more accurate description of the behaviour of the CPB plug.

The incorporation of a polycarboxylate ether-based superplasticizer addresses a critical challenge in the effective application of nanoparticles (e.g., NCs) in CPB formulations. Given the natural tendency of NCs to agglomerate due to their high surface energy and strong interparticle forces,

achieving homogenous dispersion within the mixture becomes imperative. Otherwise, these agglomerated NCs would not effectively contribute to the hydration process or serve their role as fillers in the microstructure of the CPB (Saremi and Fall 2023). By utilizing a proven dispersing agent like a polycarboxylate ether-based superplasticizer (MasterGlenium 7500), uniform distribution of NCs in the fresh CPB mixture will be ensured. This serves a dual purpose: it enhances hydration kinetics by facilitating more nucleation sites, and it contributes to the microstructural integrity by filling in micro voids. As a result, both the mechanical and hydraulic properties of the CPB should benefit, leading to more robust and optimized backfill structures.

7.3.2 Sample preparation

The preparation of the fresh CPB mixture was conducted to ensure uniformity and homogeneity, following a three-step procedure:

1. **Dry mixing of solid components:** The silica tailings and the predetermined amount of PCI were initially mixed for 5 minutes using a mechanical mixer. This step was aimed at achieving a uniform distribution of the solid particles.
2. **Preparation of the liquid solution:** The requisite quantities of superplasticizer (SP) and NCs were added to water. The solution was then stirred for 3 minutes to obtain a homogenous liquid, facilitating an optimal dispersion of the NCs and SP within the mixture.
3. **Final mixing:** The derived homogenous liquid solution was subsequently added to the dry mix of PCI and tailings, initiating the final stage of mixing that continued for an additional 10 minutes. The outcome of this final step was the ready-to-use fresh CPB mixture.

As outlined above, the direct addition of NC particles into the mixer was avoided. This is because adding NC particles directly into the mixer would lead to the formation of weak and unhydrated nanoparticles due to agglomeration. Such agglomerated particles tend to occupy the voids between the CPB particles, ultimately diminishing the mechanical strength of the CPB (Saremi and Fall, 2022). This agglomeration issue arises from the high reactivity of NCs and the strong Van der Waals forces between them, making NCs more prone to agglomeration compared to

other pozzolanic materials. To address this challenge, additives were initially mixed with water before being introduced into the dry mixture of tailings-cement and subsequently combined through mixing.

To acquire a detailed insight into the impact of NC on the behavior of CPB, a reference or control column devoid of NCs was also prepared. This control was created using the same mix ratios as the experimental columns but excluded NCs, serving as a foundational benchmark for subsequent comparative evaluations. Data outlining the compositions of the CPB columns is presented in Table 7-4.

Table 7-4. Mix composition of the prepared nano-CPB column and control column

Sample nomenclature	Binder Content (%)	PCI in the Binder (%)	SP (%)	W/C ratio	NC content (%)	Solid Content (%)
PCI-CPB (control)	4.5	100	0.125	7.8	0	74
PCI-CPB-NC	4.5	100	0.125	7.8	1	74

PCI, Portland cement type I; ST, silica tailings; W/C ratio, mass of water divided by the mass of binder. NC. Content (%) = Mass of NCx100/Mass of binder; Binder Content = Mass of binderx100/ (Mass of dry tailings + Mass of binder); NC, Nano-Calcium Carbonate, Solid Content (%) = (Mass of solid/Mass of the whole CPB)

7.3.3 Physical framework set up and monitoring

To fulfill the objectives of this research, a new physical apparatus has been engineered, designed to simulate a plug under various field conditions that a backfill plug structure would encounter during placement and post-placement in a mine stope, such as curing stress (M), non-uniform thermal (T) conditions and binder hydration progress (C). This custom-built setup employs aluminum sheeting, chosen for its mechanical resilience against the pressures exerted by an air-driven piston located at the column's apex, as illustrated in Figure 7-3. Beyond its mechanical characteristics, aluminum's excellent thermal conductivity ensures even heating of the cured backfill sample in accordance with the selected thermal loading regimen. Consequently, the rationale for selecting aluminum as the principal material for this apparatus is further elaborated upon.

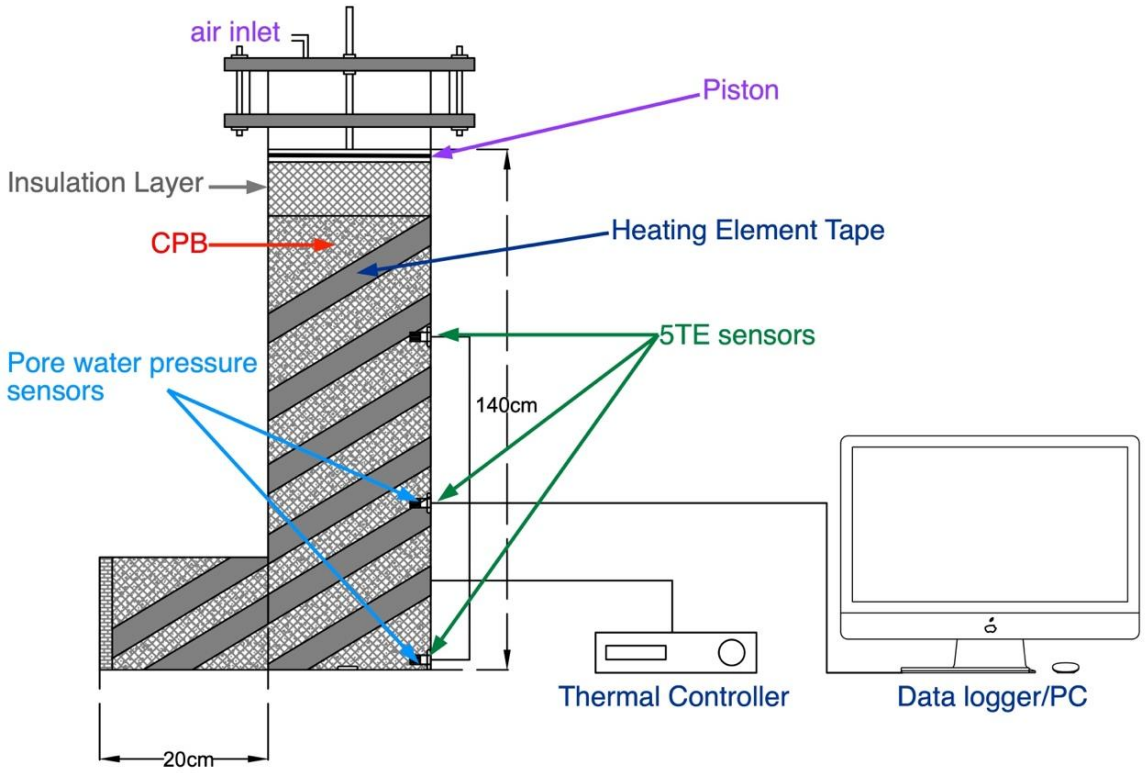

Figure 7-3. Diagram of the engineered plug backfill physical model with sensor arrangement details.

Pertaining to the implementation of non-isothermal curing temperatures, a specialized heating element tape from Omega Sensing Solutions ULC was employed to envelop the columns, capable of generating temperatures up to 760 ºC. This heating system enables non-isothermal temperatures to be applied to the CPB column during curing, simulating the curing temperatures of the CPB mass in the field. The thermal loading pattern, illustrated in Figure 7-4, was thus adopted to mimic the temperature variations typically encountered in a mine backfill structure. This temperature profile (non-isothermal) represents the time-dependent temperature evolution within the lower part (plug) of a CPB mass in field conditions, as detailed in Nasir and Fall (2009). The temperature was measured at a point 2.5 meters above the bottom of a backfill structure with dimensions of 20 meters in height and 10 meters in width (Nasir and Fall, 2009). Details concerning the selected thermal loading pattern are depicted in Figure 7-4.

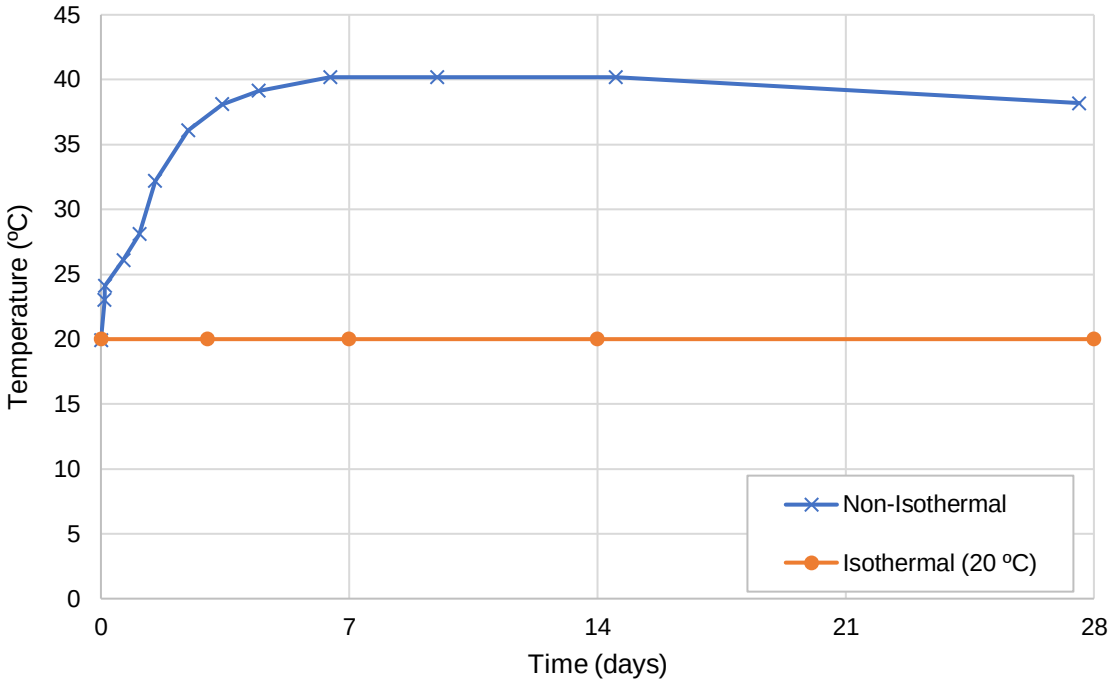

Figure 7-4. Non-isothermal and isothermal (20°C) temperature profiles over time applied to CPB columns.

As depicted in Figure 7-3, the designed column incorporates an air-driven piston, facilitating the curing of the CPB under an applied stress. This system's introduction primarily aims to replicate and study the CPB plug's behavior under the self-weight load typically encountered in real-world backfill structures. This system enables us to reproduce the desired field pressure scenario without the need for a physically inaccessible column. Complementing this, Figure 7-5 illustrates the specific vertical loading pattern exerted atop the CPB column. Notably, the peak pressure applied to the column reaches 600 kPa, corresponding to a 34.8 m high backfill structure, given a CPB bulk density of 17.2 kN/m^3. To reproduce actual field conditions, applied pressures were progressively increased, mimicking the sequential backfilling process of a stope as generally observed in real mine backfilling operations.

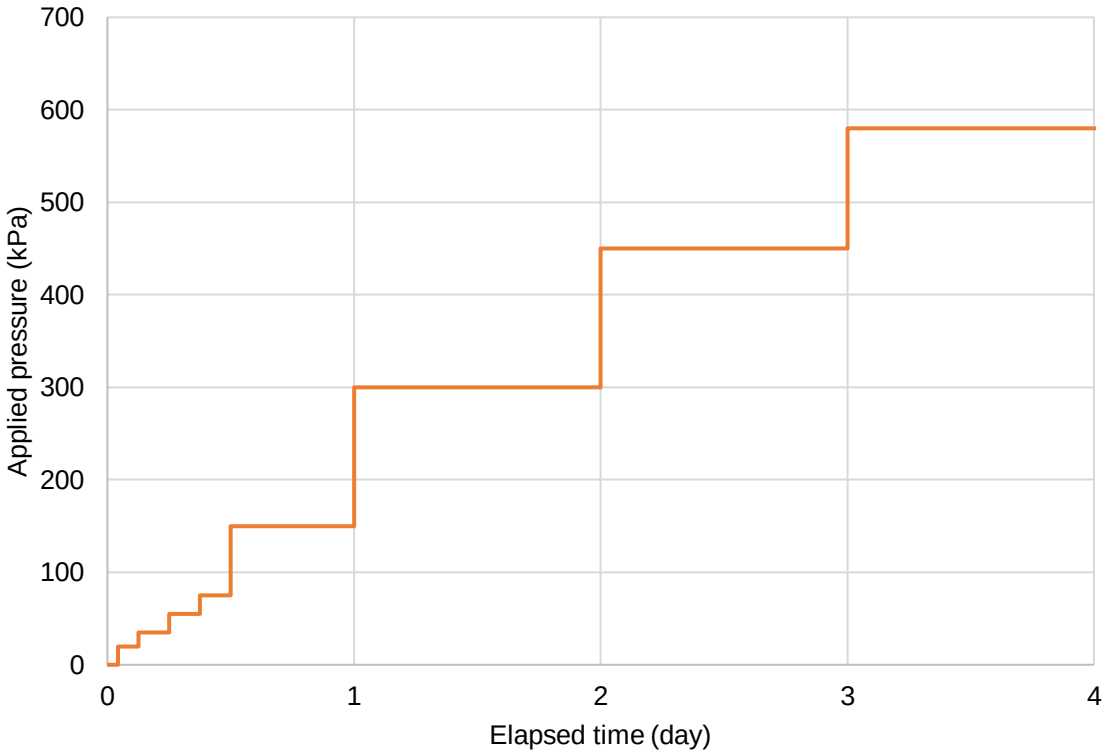

Figure 7-5. Variation of applied curing stress over a four-day period.

A principal objective of this research is to assess the combined effects of thermal and mechanical loadings in the presence of NCs on the self-desiccation capacity of CPB plug, where the self-desiccation is analyzed through the evolution of positive pore water pressure and VWC within the CPB columns. To achieve this, a combination of different sensors, specifically chosen for their ability to accurately track changes in these parameters, was employed. These sensors provided continuous data acquisition on the PWP and VWC, among other factors. PWP sensors (DMKY miniature PWP gauge), described in Table 7-5, were used to monitor the PWP in the CPB columns. This PWP sensor can measure a maximum pressure of 1 MPa with an accuracy of 0.3%. Utilizing the strained full-bridge circuit principle, the DMKY series strain-type pore water pressure gauge operates efficiently. Within the sensor, a high-precision full-bridge strain gauge is affixed to the sensing membrane. As water pressure applies force to the membrane's surface, it undergoes deformation, which is then transmitted to the strain gauge. Subsequently, the collected strain change information is processed, enabling the determination of the corresponding water pressure. To collect and store the data recorded by the sensors, a data acquisition system

developed by Xi'an Yima Opto-electrical Technology Co was used. 5TE sensors were also installed in the column to measure key parameters, such as volumetric water content (VWC) and temperature (Figure 7-3). The 5TE sensor employs high-frequency oscillation and signal filtering techniques to achieve excellent accuracy while minimizing the influence of porous medium texture. By utilizing capacitance/frequency domain technology, the 5TE accurately determines volumetric water content (VWC) by measuring the dielectric constant of the surrounding media. Operating at a frequency of 70 MHz, the sensor effectively reduces the impact of salinity and soil texture variations, ensuring reliable performance across a wide range of soil types. Additionally, the 5TE incorporates an onboard thermistor for precise temperature measurement. The volumetric water content measurement range is between 0% – 100%, that of the temperature is -40°C – 60°C with an accuracy of ± 1°C. These sensors were placed throughout the CPB columns and connected to a data logger that recorded the data continuously.

Table 7-5. Specifications of pore water pressure sensor utilized in the model

Sensor	Pore water pressure sensor
Manufacture	Dan street Nanjing Electronic Technology Co.
Model Type	DMKY
Capacity	1 MPa
Accuracy	±0.3%
Output signal	0 to 5V

7.3.4 Microstructural analysis and determination of physical attributes

To gain a more in-depth understanding of the mechanisms responsible for changes in the self-desiccation capacity of the CPB plugs studied under TMC curing and loading conditions, several microstructural and physical tests were carried out. These tests helped to analyze the changes in CPB characteristics, such as porosity, void ratio, dry density and microstructure, including mineralogical composition and pore structure.

Thermal analysis techniques, including thermogravimetry (TG) and differential thermogravimetry (DTG), were applied to assess the mineralogical changes within the cement matrix of CPB due to binder hydration, both in samples with NCs and those without. To prepare for TG/DTG, cement

paste samples with a water-to-cement (w/c) ratio of 1 were dried at 45°C for four days to remove free water. After drying, the samples were powdered for analysis using a thermogravimetric analyzer capable of simultaneous DSC-TGA, which heated the samples at a rate of 10°C per minute to a maximum of 1000°C under a nitrogen flow of 100 ml/min.

Mercury intrusion porosimetry (MIP) was used to determine the main characteristics of CPB pore structure, such as pore size distribution. MIP tests were carried out using an AutoPore III 9420 mercury porosimeter, which measures pore volume distribution in materials by means of mercury intrusion or extrusion. Prior to MIP testing, all samples were oven-dried at 45°C until they reached a constant mass. Drying at this temperature did not appear to cause cracking. The samples were then reduced to cubic pieces approximately 0.5 to 1 cm in size.

Additionally, a diverse set of tests were conducted on samples extracted from various heights within the columns and at different times during curing to determine the physical properties of CPB (e.g., void ratio, porosity, dry density). The sampling involved a coring process. The extracted samples were then measured for specific gravity according to the ASTM D854 standard using a water pycnometer. This measurement is crucial for calculating the particle density of the CPB, which is essential for determining the void ratio. The bulk density of the samples was found by placing the dry CPB material in a known volume and calculating its mass relative to this volume. From the bulk density and particle density values, the overall porosity could be computed using the formula: $n = 1 - (\rho_b / \rho_p)$, where ρ_b is the bulk density and ρ_p is the particle density, both expressed in kg/cm^3. The void ratio was then derived from the porosity with the equation: $e = n / (1 - n)$.

7.4. Results and discussion

7.4.1 Coupled effect of nanoparticles, field curing temperature, and mechanical stress on self-desiccation development of CPB plug

Figure 7-6 and Figure 7-7 depict the outcomes of the coupled impact of nanoparticles, NC, (chemical process, **C**), non-isothermal field curing temperature (thermal process, **T**), and field

mechanical curing stress (mechanical process, **M**) on the development and evolution of pore water pressure (PWP) and volumetric water content (VWC) in CPB columns.

These figures clearly illustrate that, regardless of the presence or absence of nanoparticles within the CPBs, there is a notable rapid increase in both PWP and VWC during the first few days, reaching a peak value after three days, followed by a gradual decrease. The observed pattern aligns well with findings from various field studies on CPB masses (e.g. Thompson et al. in 2012, Doherty et al. in 2015, and Wang et al. in 2023). This consistency validates and supports the effectiveness of the TMC-Column testing and monitoring setup developed in this study to reproduce realistic field loading conditions for CPB plug, supporting its usefulness for subjecting laboratory CPB columns to realistic field loading scenarios.

This initial rise in both PWP and VWC is attributed to the increase in pressure applied at the top of the CPB column, mimicking the progressive increase in the self-weight of the backfill mass during stope filling (Figure 7-5). The augmentation in backfill self-weight is obviously linked to an increase in hydrostatic pore pressure within the backfill mass (Cui and Fall, 2016, 2017). In addition, subjecting the CPB material to stress in the initial hours of curing results in the rearrangement of the solid particles (i.e. tailings and cement) and acceleration of the release of additional free water, leading to a higher PWP measurement (Ghirian and Fall 2016; Chen et al. 2021). This gradual decrease in both PWP and VWC over time following the peaks is due to water consumption by cement hydration. As the cement hydration process advances, it absorbs available free water within the backfill matrix to facilitate its progression (Ghirian 2016, Al-Moselly et al. 2022). This absorption is vital for generating hydration products, such as calcium-silicate-hydrate (C-S-H), calcium hydroxide (CH) and ettringite (Kjellsen and Detwiler 1992, Sinthaworn and Nimityongskul 2011). Consequently, this phenomenon is a key factor influencing the dissipation of pore water pressure within the backfill plug and structure.

Analysis of the results presented in Figure 7-6 and Figure 7-7 also indicates that nano-calcium carbonate (NC) particles significantly enhance and accelerate the self-desiccation capacity of the CPB plug. CPBs with NC show lower PWP and VWC values, as well as a faster decrease in PWP and VWC than CPBs without NC. For example, after 7 days of curing, PWP values at the bottom of the CPB column with NC were measured at 43 kPa, while PWP values at the bottom of the CPB

column without NC were recorded at 60 kPa. In other words, the PWP in the CPB with NC was about 30% lower than in the CPB without NC. This finding suggests that, in the field, the CPB plug incorporating NCs would apply less pressure on the barricades and lead to faster barricade opening. This is beneficial for the safety of the working environment and the productivity of the mine.

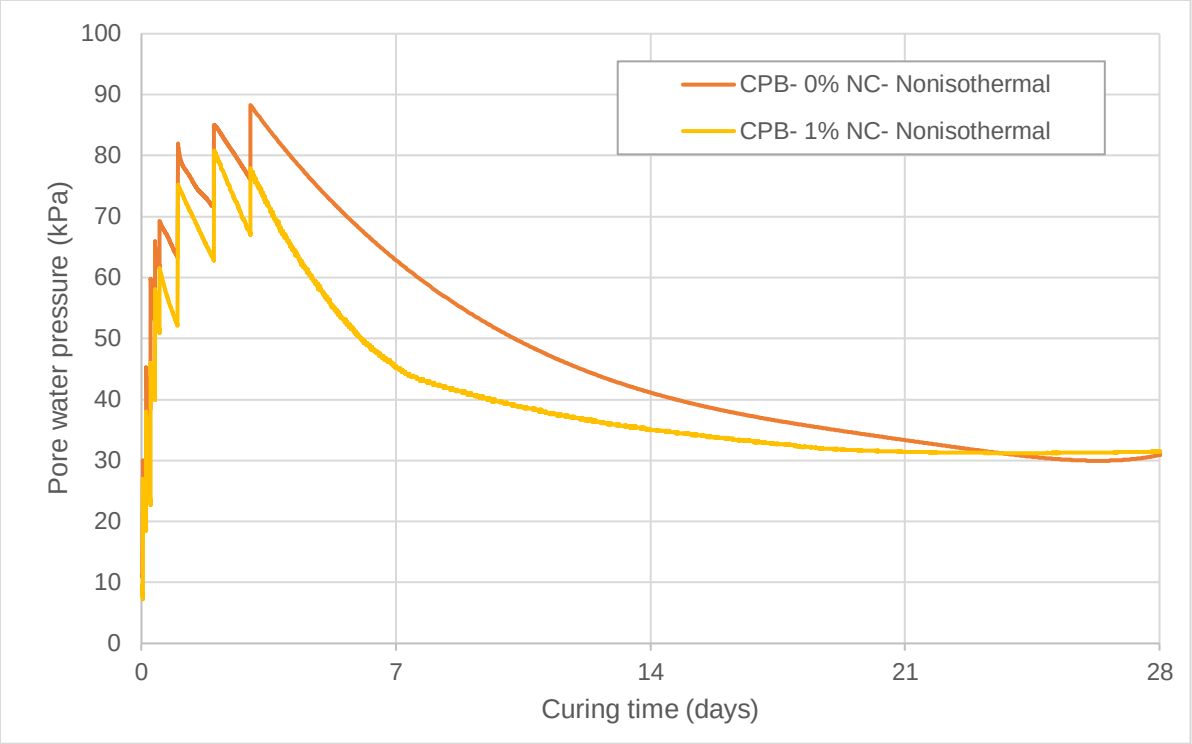

Figure 7-6. PWP evolution at the bottom of the CPB columns with 1%NC (Nano-CPB-TMC) and without NC (CPB-0%NC-TMC) subjected to coupled thermo-mechanical loading conditions during curing

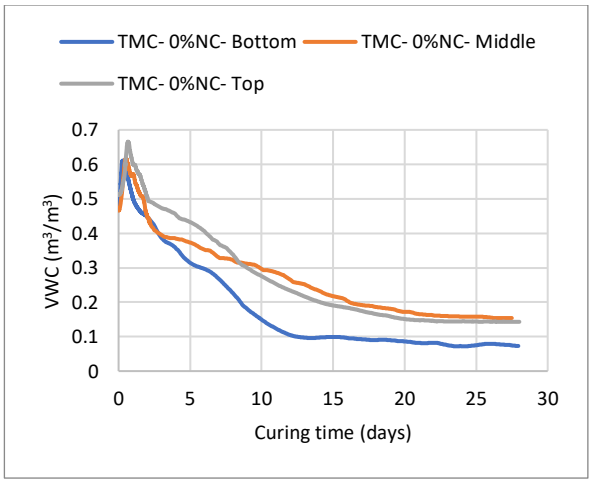

(a) VWC dissipation at different levels of control CPB column

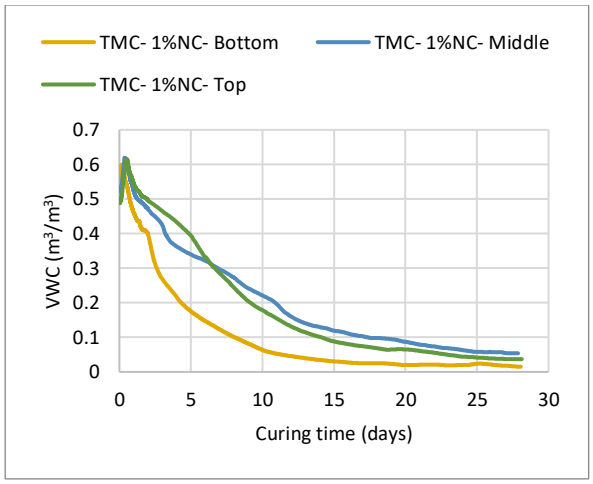

(b) VWC dissipation at different levels of nano- CPB column

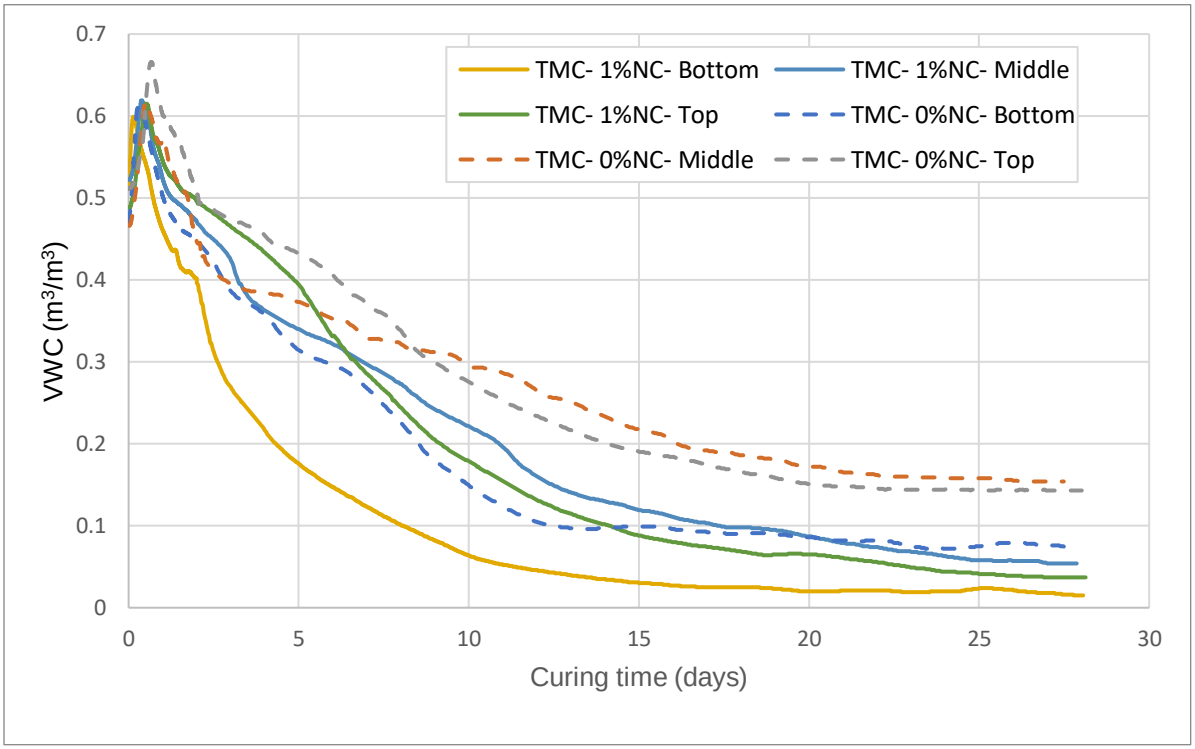

c) Comparative illustration of VWC dissipation within the nano-modified CPB plug and control (without NC) column cured under field thermo-mechanical conditions

Figure 7-7. VWC evolution at different levels of the CPB columns with 1%NC and without NC (control) subjected to field coupled thermo-mechanical loading conditions during curing

The significant influence of the NC particles on self-desiccation in CPB columns is closely tied to their ability to enhance the cement hydration process, thereby generating more cement hydration products (Camiletti et al. 2013; Roshani and Fall 2020a; Fu et al. 2022; Benkirane et al.

2023; Saremi and Fall 2023). This enhancement is directly correlated with the increased consumption of pore water, resulting in a reduction in pore water pressure or water content.

The mechanism by which NCs enhance the cement hydration reaction has been largely demonstrated and explained in several previous studies (e.g., Fu et al. 2022; Wang et al. 2016; Sato and Beaudoin, 2011) and can be succinctly summarized as follows: (i) Firstly, the introduction of NC initiates nucleation, disrupting the silicon-rich layer surrounding cement particles and facilitating the formation of hydration products. In addition, it facilitates the adsorption of Ca^{2+} ions released during hydration of cement particles, reducing their concentration around the particles and further accelerating the hydration process. (ii) Secondly, NC undergoes a reaction with C_3A and CH, resulting in the production of hydrated calcium carboaluminate characterized by a unique backbone structure and increased permeability. This reaction not only increases the concentration gradient around cement particles, but also accelerates ion diffusion, thus promoting cement particle hydration (Fu et al. 2022). The formulas for the reactions of NC with C_3A in cement and CH in cement hydration products to generate monohydrated calcium carboaluminate and semihydrated calcium carboaluminate are as indicated below (Fu et al. 2022):

$CaCO_3+11H_2O+3CaO\cdot Al_2O_3 \rightarrow 3CaO\cdot Al_2O_3\cdot CaCO_3\cdot 11H_2O0.5$

$CaCO_3+11.5H_2O+3CaO\cdot Al_2O_3+0.5Ca(OH)_2 \rightarrow 3.5CaO\cdot Al_2O_3\cdot 0.5CaCO_3\cdot 12H_2O$

In addition, the size of the NCs plays a crucial role; smaller NCs result in a greater number of unsaturated bonds on the surface, higher curing temperatures increase the atomic activity of the NC surface, thus promoting both nucleation and chemical reactivity. Substantiating this explanation are the outcomes of thermal analyses performed on CPB cement paste samples with and without NC additives, as depicted in Figure 7-8. In this figure, the TG/DTG analysis results of 7-day cement paste samples, containing 1% NC and 0% NC, both prepared with 0.125% superplasticizer, are presented. The analyses reveal that the sample with NC additives exhibits more hydration products, evident from its elevated endothermic peaks and weight loss within the 100° to 170°C temperature range. This suggests that CPBs containing nano-$CaCO_3$ yield more C-S-H gel and ettringite (Shaikh and Supit 2014, Cosentino et al. 2020), aligning with the suction and monitoring VWC results in Figure 7-6 and Figure 7-7, respectively. Furthermore, the observed

higher peak or lower weight loss at 400-450°C in the sample without NC particles indicates a higher content of calcium hydroxide or Portlandite (CH) than the sample with NC, as illustrated in Figure 7-8. This diminished CH content in the presence of NC is agreement with aforementioned assertion that NC reacts with C_3A and CH, leading to the generation of hydrated calcium carboaluminate characterized by a unique backbone structure and increased permeability (e.g., Sanchez and Sobolev, 2010; Seifan et al. 2020; Fu et al. 2022).

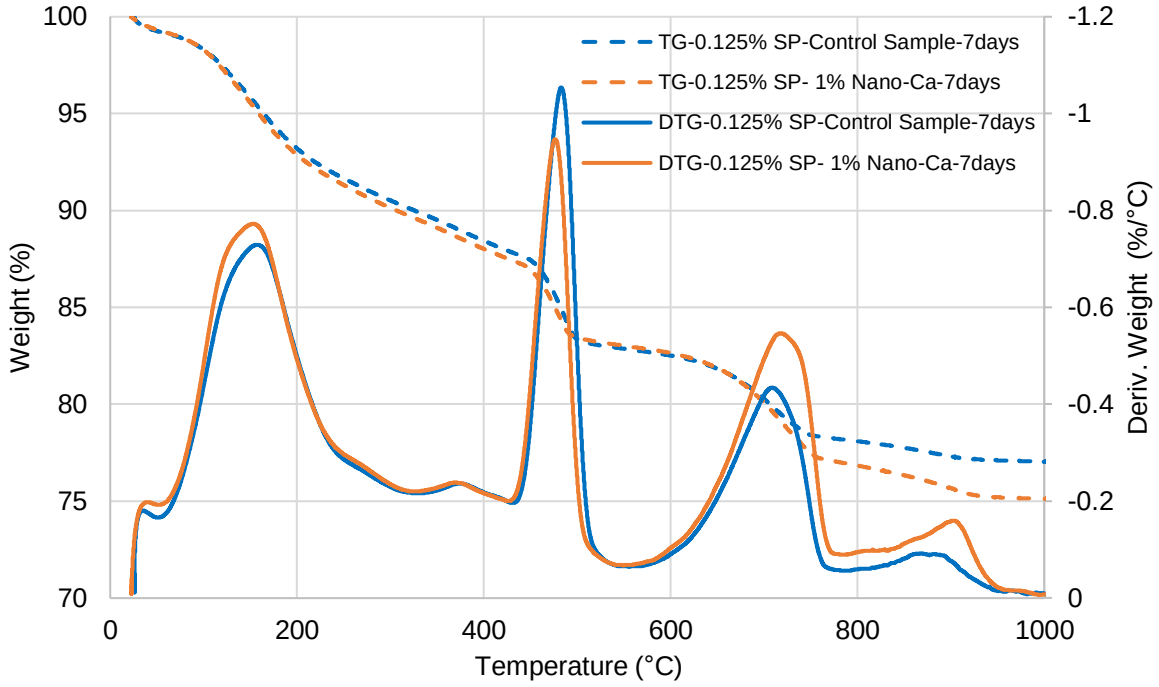

Figure 7-8 .TG/DTG diagrams of 7-day-old cement pastes of CPB with 1%NC and without NC (cement pastes contain 0.125% superplasticizer (SP)).

Moreover, upon analyzing Figure 7-7, it becomes apparent that, regardless of the presence or absence of NC, the lower sections of the columns exhibit lower values of volumetric water content (VWC) than the middle and upper levels. To elucidate, self-desiccation is notably more pronounced at the lower parts of the undrained columns compared to the middle and upper portions. This discrepancy can be ascribed to the impact of curing stress on the cement hydration reaction. Previous studies have demonstrated that subjecting CPB material to stress during curing can result in the production of increased quantities of hydration products (Al-Moselly et al. 2022, Saremi and Fall 2023). The greater quantity of hydration products implies a heightened consumption of water, or in simpler terms, a more pronounced self-desiccation. To support this

statement and to gain a better insight into the impact of curing stress on plug self-desiccation, the results obtained by monitoring the evolution of VWC in the CPB column with NC cured under vertical stress conditions (Figure 7-5) and at room temperature (20°C) are compared with those obtained by monitoring the evolution of VWC in a cylindrical CPB sample (20 cm x 10 cm) with the same composition cured under standard laboratory conditions, i.e. without stress and at room temperature. The comparison is illustrated in Figure 9. The results presented clearly show that the application of vertical stresses during curing, like those encountered in the field, accelerates the decrease in water content in the CPB, i.e. enhances self-desiccation. For example, 7-day VWC values were recorded at 0.541 and 0.584 m^3/m^3, in stress-cured and stress free-cured CPB, respectively. In other words, there was a 7% reduction in VWC due to curing stress. This reduction is attributable to the enhanced hydration of the cement due to the stresses applied during curing, as described above.

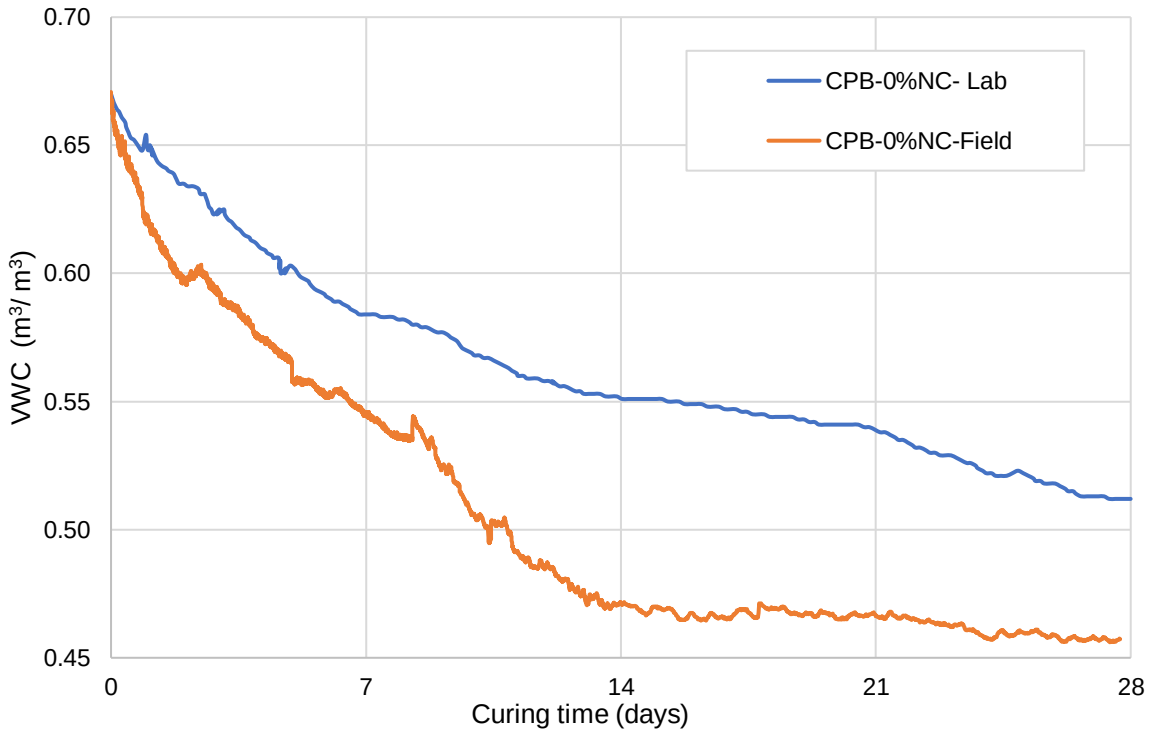

Figure 7-9. Comparative evolution of VWC in two CPB samples subjected to field mechanical loading (CPB-0%NC-Field) versus stress-free standard laboratory (CPB-0%NC-Lab) conditions at room temperature (20°C) during curing

This correlation between higher curing stress and increased hydration products is substantiated experimentally by the thermal analysis (TG/DTG) presented in Figure 7-10, which involved two identical cement paste samples of CPB. One of the samples underwent curing under a stress of 150 kPa, while the other was cured under stress-free conditions. The thermal analysis results unequivocally indicate that the cement sample exposed to 150 kPa of curing stress experienced a higher level of weight loss during the heating process compared to the control sample. Furthermore, the sample subjected to curing stress displays elevated endothermic peaks within the temperature range of 450-550°C compared to the specimen cured without stress, indicating a more substantial presence of cement hydration products. In essence, curing CPB under stress leads to the production of more hydration products, resulting in intensified self-desiccation for CPBs subjected to increased pressure during their curing duration. Given that the lower segments of the undrained column experienced elevated pressure from both the column's self-weight and applied pressure, it becomes comprehensible why self-desiccation is more pronounced at these depths compared to the middle and upper portions of the column.

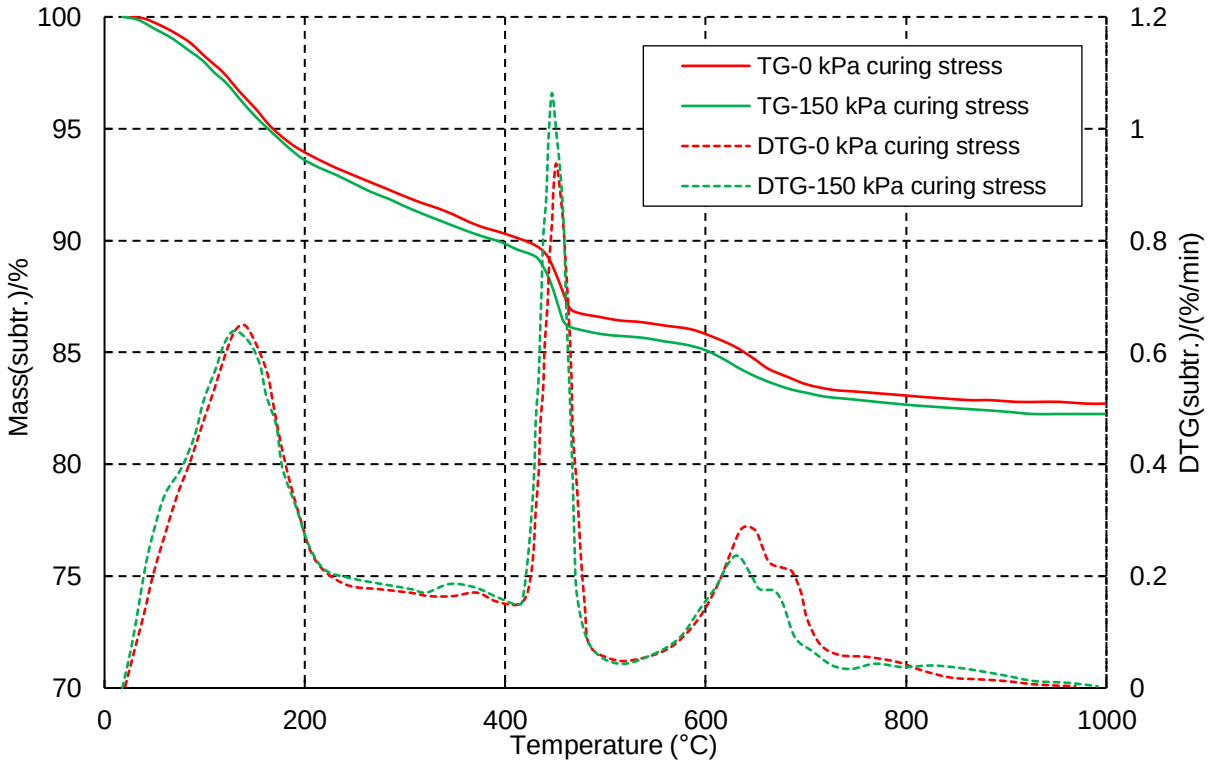

Figure 7-10. TG/DTG diagrams of cement pastes of CPB cured under stress (150 kPa) and under stress-free conditions.

The findings outlined in this section provide insights into the effects of NC (a chemical factor, **C**) on the extent and progression of self-desiccation in CPB plug undergoing non-isothermal curing temperatures (thermal) and curing stresses (mechanical) designed to replicate real-world field conditions. They also clarified the contribution of the mechanical factor (curing stress) to the magnitude and advancement of the observed self-desiccation. However, the contribution of the coupled thermo-mechanical factor and the individual effect of non-isothermal field curing temperatures to the scale and development of self-desiccation in CPB plugs has yet to be fully elucidated. These aspects are addressed in the following sections.

7.4.2 Contribution of the thermo-mechanical factors to the evolution of self-desiccation of CPB plug

To elucidate the contribution of the coupled thermo-mechanical factors - specifically, the simultaneous elevation of backfill temperature (Figure 7-4) and height (resulting in an increase in vertical stress, Figure 5) - to the extent and progression of self-desiccation in the CPB plug (shown previously), the results obtained from monitoring the volumetric water content evolution in the CPB column with NC cured under thermo-mechanical conditions are compared with those observed in a cylindrical CPB sample (20 cm x 10 cm). The cylindrical sample shares the same composition as the column but is cured under standard laboratory conditions, lacking the application of pressure (stress) and temperature designed to simulate field conditions during curing. In simpler terms, both the CPB column and the CPB cylinder undergo the same chemical factor (C), but they experience distinct thermo-mechanical loading conditions during the curing process. More explicitly, the CPB column is subjected to thermo-mechanical coupling (TMC) factors during curing, while the CPB cylinder is exclusively exposed to the chemical factor (C). The comparative results are illustrated in Figure 7-11.

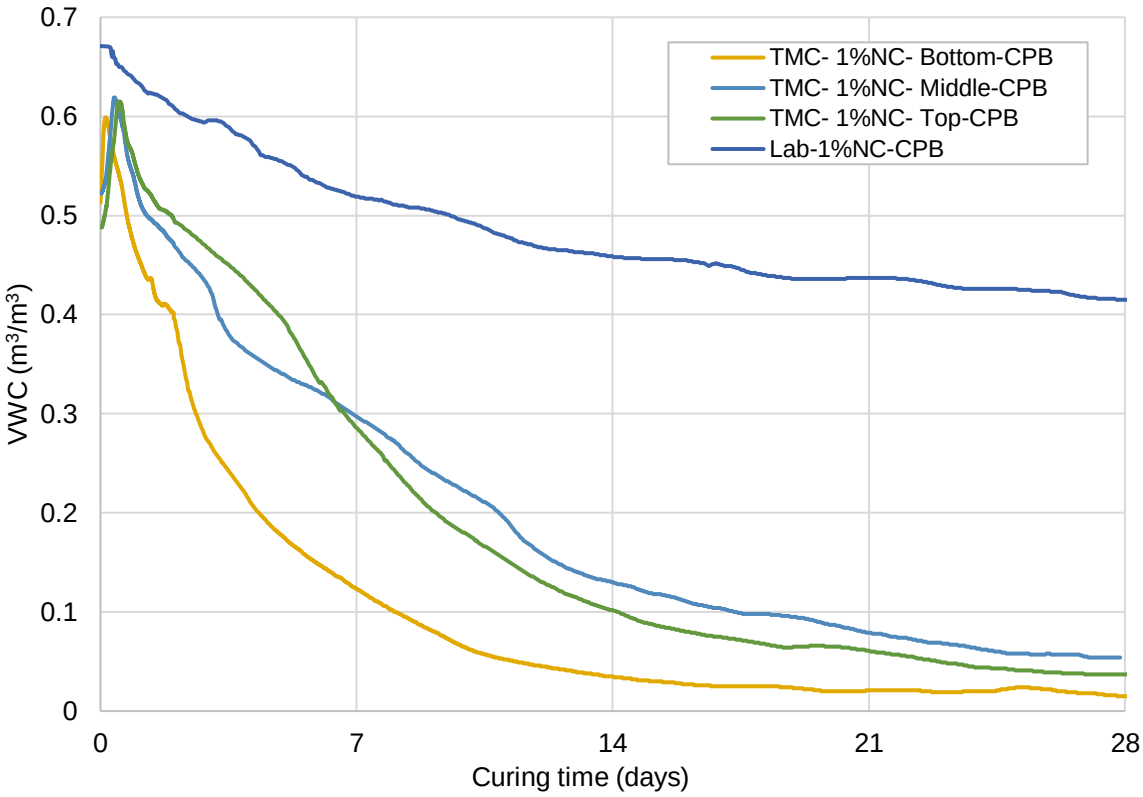

Figure 7-11. Comparative evolution of VWC of CPB exposed to field non-isothermal temperature and field curing stress versus CPB cured under standard laboratory condition.

This figure shows a significantly swifter decline in VWC and markedly lower VWC values in the NC-CPB column exposed to thermo-mechanical conditions during curing, as opposed to NC-CPB samples (Lab-1%NC-CPB) cured under standard laboratory conditions. In other words, the coupled effect of non-isothermal backfill temperature and vertical backfill stress on the rate and extent of self-desiccation is substantial. To illustrate, after 7 days of curing, the VWC value at the bottom of the NC-CPB column was 0.11 m^3/m^3, while the VWC value in the NC-CPB cylinder was 0.52 m^3/m^3. In other words, the VWC value in the NC-CPB column was almost five times lower than that in the cylinder. This finding underscores that the conventional method of curing CPB samples under stress- and temperature-free laboratory conditions fails to capture the true field behavior of the CPB plug, especially concerning self-desiccation. This more intense and faster self-desiccation of the NC-CPB column is due to the synergistic effects of high temperatures and stress applied during curing on cement hydration. Both factors significantly impact binder hydration kinetics (Wu et al. 2014; Cui and Fall, 2018). The application of stress and temperature

during CPB curing enhances and accelerates the cement hydration process, resulting in the formation of a greater amount of hydration products. These products not only fill the pores of the CPB material matrix and refine its pore structure, but also necessitate water consumption. This greater refinement of the pore structure of CPB material in the column, due to the precipitation of more hydration products compared to CPB in the cylinder, is confirmed experimentally by the results of the determination of the evolution of physical characteristics (void ratio and dry density) of CPB at different depths in the column and of CPB in the cylinder, presented in Figure 7-12. This figure shows that the CPB samples extracted from the column have much lower void ratio values and higher dry density values, reflecting their finer, denser porous structure compared to the CPB cylinder samples. For example, CPB samples extracted from the base of the column subjected to field thermal and stress curing conditions showed a 39% reduction in void ratio and a 16% increase in dry density compared to their laboratory-hardened counterparts. This underscores the simultaneous impact of thermal and mechanical factors, shedding light on the enhanced self-desiccation in the examined samples. However, a critical inquiry remains: to what extent does the thermal factor individually contribute to this impact? The subsequent sections will examine the isolated effect of the thermal factor on the self-desiccation development within the CPB.

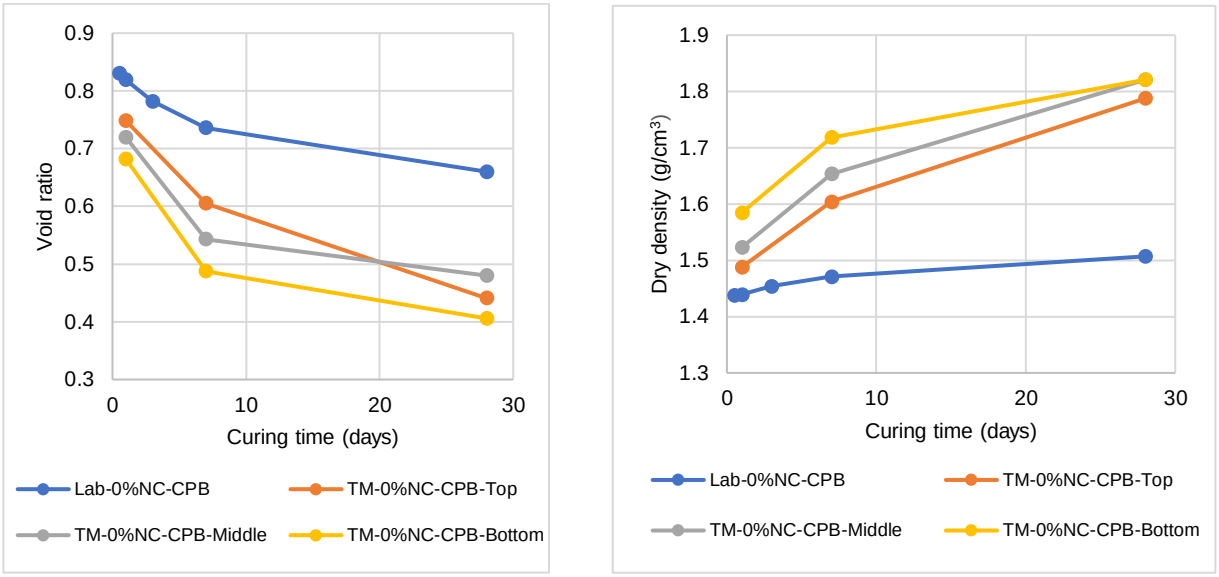

(a) (b)

Figure 7-12. Comparative evolution of the physical properties of CPBs exposed to field non-isothermal temperature and field curing stress (thermo-mechanical factors) versus CPB cured under standard laboratory (Lab-0%NC-CPB) condition: a) void ratio, b) dry density

7.4.3 Contribution of the non-isothermal field temperature to the evolution of self-desiccation of CPB plug

To clarify the contribution of the thermal factor, i.e. the non-isothermal field curing temperature, to the magnitude and advancement of self-desiccation in the CPB plug, the results obtained by monitoring the evolution of PWP and VWC in NC-CPB columns subjected to coupled thermo-mechanical loading during curing are compared with those obtained by monitoring the evolution of PWP and VWC in NC-CPB columns subjected only to mechanical stress (vertical stress, Figure 7-5) during curing. These comparisons are shown in Figure 7-13 (PWP comparison) and Figure 7-14 (VWC comparison).

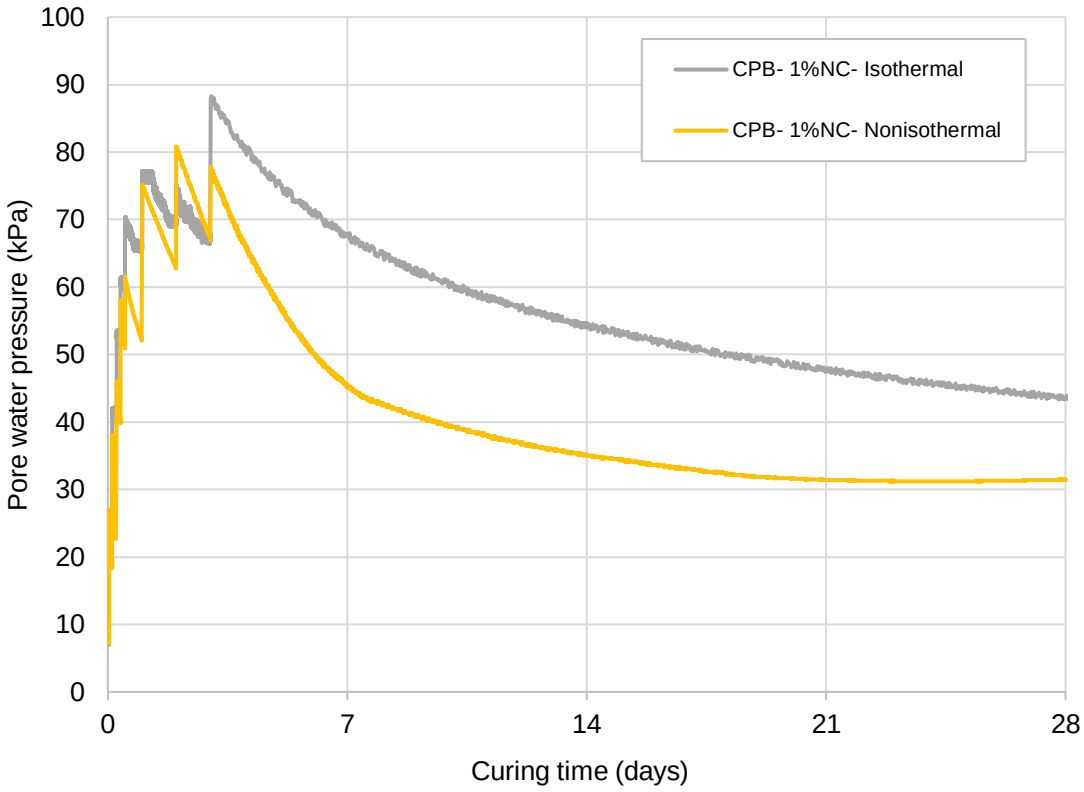

Figure 7-13. PWP monitoring results at the bases of nano-CPB columns exposed to thermo-mechanical loadings (CPB-1%NC-Non-isothermal) and mechanical-only loadings (CPB-1%NC-Isothermal) during curing.

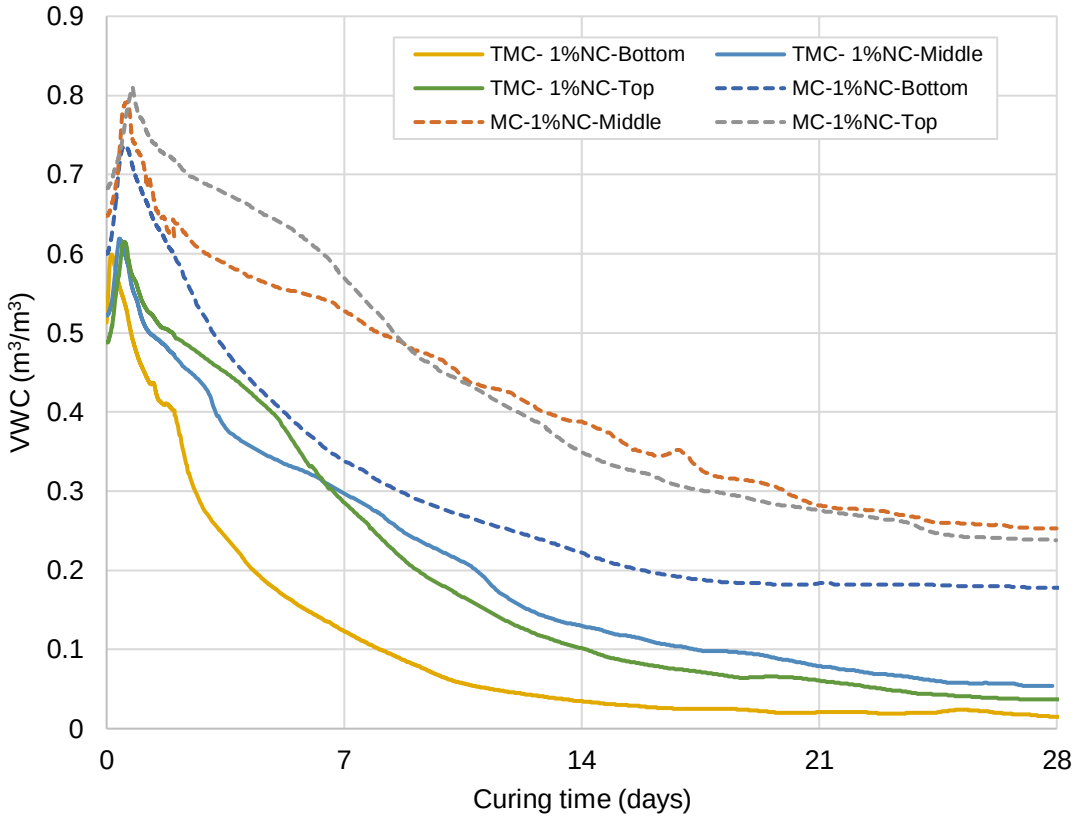

Figure 7-14. VWC monitoring results at different levels of nano-CPB columns exposed to thermo-mechanical loadings (TMC-1%) and mechanical-only loadings (MC-1%) during curing.

These figures show that NC-CPB columns exposed to coupled thermo-mechanical loading during curing exhibit lower maximum values of PWP (Figure 7-13) and VWC (Figure 7-14). For instance, when considering the bottom of the column under combined thermo-mechanical loading, the 7-day pore water pressure (7-day-PWP) and volumetric water content (7-day-VWC) values were recorded at 44 kPa and 0.103 m^3/m^3, respectively. In contrast, for the bottom of the column exposed solely to mechanical loading, the corresponding 7-day-PWP and 7-day-VWC values stood at 67 kPa and 0.318 m^3/m^3. This indicates a substantial 35% reduction in the 7-day water pressure value and an even more pronounced 68% reduction in the 7-day VWC value, both attributed to the elevated curing temperature experienced in the field. Furthermore, after the maximum values, the NC-CPB column exposed to coupled thermo-mechanical loading shows faster PWP dissipation, as well as much lower PWP and VWC. This means that the non-isothermal field curing temperature has a significant impact on the self-desiccation of the CPB plug. This is because a higher curing temperature accelerates the chemical reactions of cement hydration, leading to

the formation of more hydration products. In other words, more water will be consumed, and at a faster rate in CPB cured at higher temperatures (Bentz, 2008; Haruna and Fall 2020). Clearly, higher and faster water consumption would lead to lower values and a faster decrease in PWP and VWC. The influential role of high curing temperatures in improving binder hydration is demonstrated by the thermal analysis results presented in Figure 7-15. This figure shows the results of thermal analysis (DT/DTG) performed on two CPB cement paste specimens of the same composition subjected to different curing temperatures. While one specimen was cured at room temperature (20°C) for 7 days, its counterpart was cured at a temperature of 35°C for 7 days. Figure 15 clearly shows that the 35°C-specimen exhibits greater weight loss and higher peaks in the 80°C-120°C and 400°C- 500°C temperature ranges. This means that more cement hydration products (e.g., C-S-H, ettringite, CH) are formed in the sample cured at an elevated temperature. Indeed, the peak visible between 80°C and 120°C is characteristic of the thermal decomposition of products, such as C-S-H, gypsum and ettringite, as well as water volatilization (Haiqiang et al. 2016, Chen et al. 2021). Conversely, the peak covering the range from 400°C to 500°C indicates CH disintegration, and the following peak emerging between 650°C and 700°C signifies the calcite dehydration event (Fall et al. 2010, Ghirian and Fall 2016b). This formation of more cement hydration products in the sample cured at elevated temperature is further confirmed by the results of MIP tests carried out on two 7-day CPB samples cured at 20°C and 35°C, as shown in Figure 7-16. This figure shows a finer pore structure in the CPB cured at 35°C, which corresponds to the precipitation of more hydration products in the samples cured at a higher temperature.

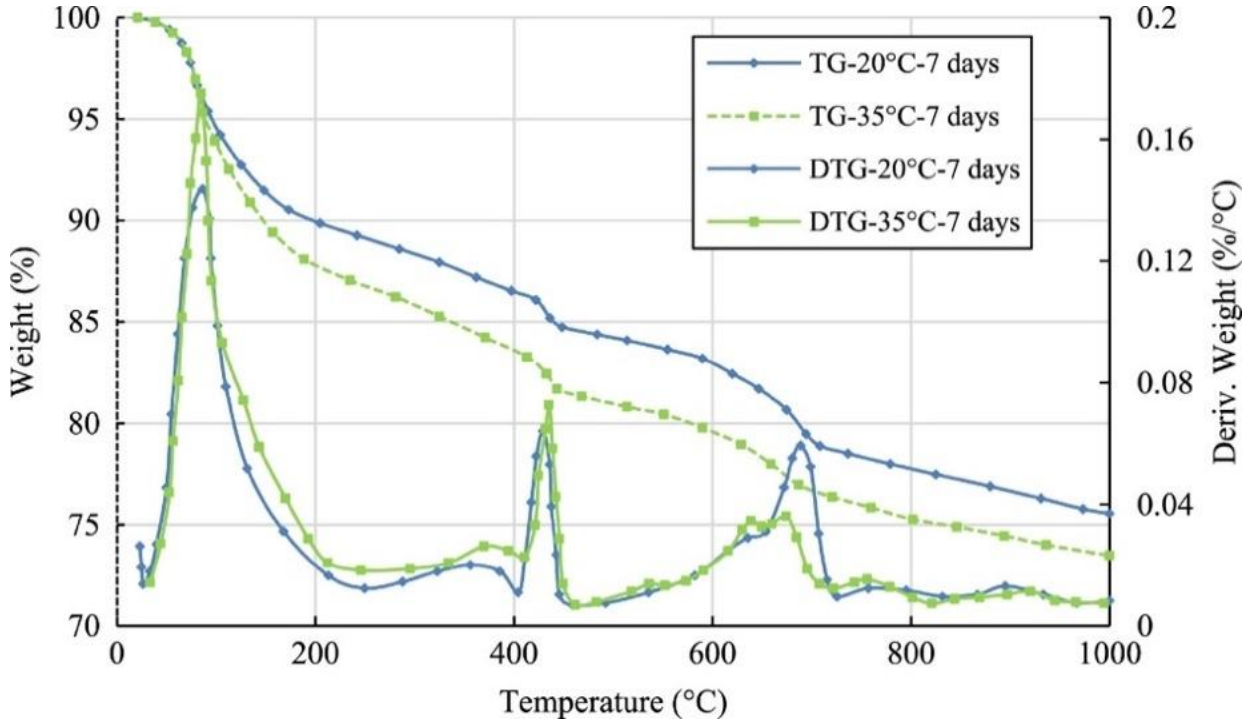

Figure 7-15. Results of thermal analysis highlighting the influence of high curing temperatures on cement hydration and the production of hydration products.

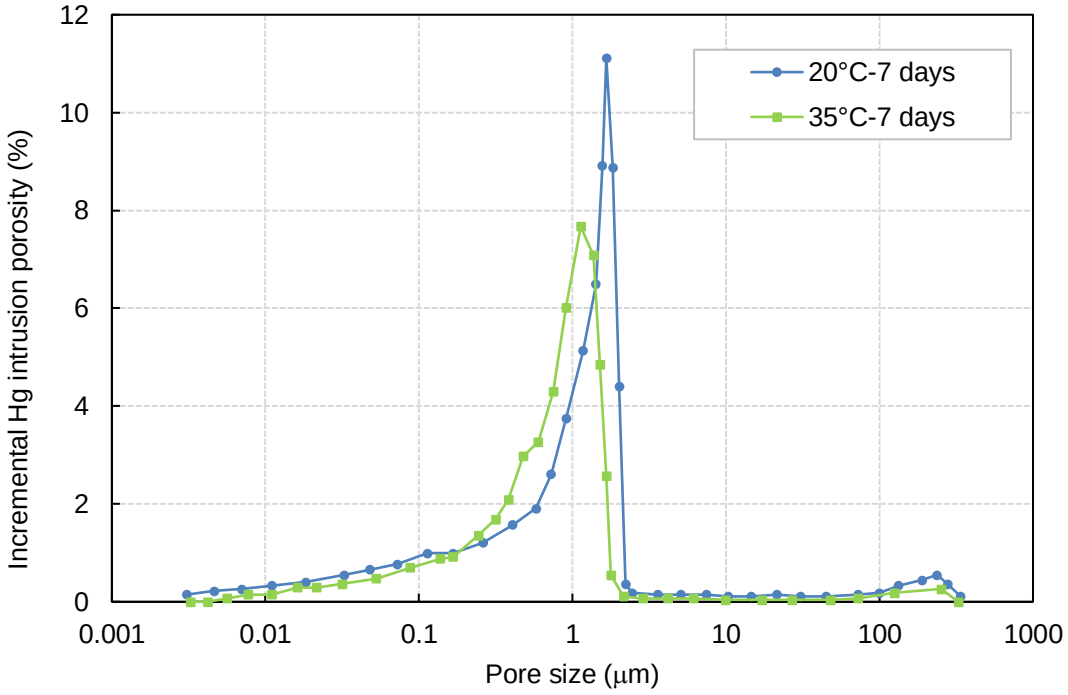

Figure 7-16. Effect of elevated temperature on the pore size of CPB

The results presented and discussed in section 3.1 indicated that the 7-day-VWV value of CPB decreased by 7% due to the individual effect of curing stress, whereas it is found in this section that due to the individual effect of curing temperature, the 7-day-VWC value of CPB decreased substantially by 68%. This means that the elevated field curing temperature of CPB plug has a much greater influence on its self-desiccation capacity than the field curing stress. This result is consistent with the findings of previous studies on cement hydration, which indicate that temperature has a greater effect on the cement hydration process than stress (e.g, Zhou and Baudoin, 2003). These findings underscore the importance of considering the influence of field backfill curing temperature during the design phase of the CPB plug and barricades. Neglecting to consider field backfill temperature factors can result in either an overly conservative or potentially unsafe design for CPB plugs and/or barricades.

7.5. Conclusions and discussions

Column thermo-mechanical-chemical (TM) experiments, specially designed to examine the self-desiccation of CPB plugs in the field, were carried out. These experiments involve exposing the CPB column with and without NC to curing conditions, including temperatures and stresses, that mimic the non-isothermal curing and self-weight pressures of CPBs.

A new physical apparatus has been developed and built. This apparatus is equipped with a set of sensors, a pneumatic loading system and heater band elements, all devised to simulate the realistic stress and temperature conditions of backfill curing in the field.

The results obtained indicate that the interactions of the factors investigated, i.e. calcium nano-carbonate (NC) particles (C factor), non-isothermal field curing temperature (T factor) and field mechanical curing stress (M factor) significantly affect the extent and evolution of CPB plug self-desiccation. Moreover, these factors, when considered individually, have a notable impact on CPB plug self-desiccation. However, the magnitude of the individual impact of each factor on self-desiccation is different. The factors, high field temperature and addition of NC to the CPB, have the most significant effect on the extent and enhancement of self-desiccation in the CPB plug, while the individual impact of field curing stress is the weakest.

The results show that higher non-isothermal field curing temperatures increase and accelerate CPB plug self-desiccation due to the acceleration of cement hydration by higher temperatures. The results underline the paramount importance of taking field curing temperatures into account when assessing pore water pressure and VWC development in the CPB plug, i.e. when evaluating plug self-desiccation. These considerations are essential for improving the efficiency of CPB, ensuring their stability and guaranteeing the stability of the associated barricades. Such dynamics prove advantageous for early barricade openings.

In addition, this research highlights the key role played by NCs in the decline of VWC and the rate of dissipation of pore pressure. It turns out that NC nanoparticles significantly enhance and accelerate the self-desiccation capacity of the CPB plug exposed to thermal and mechanical curing conditions mimicking field conditions.

The results presented in this article are expected to improve the cost-effectiveness of the CPB plug and barricade design. In addition, the results will also contribute to the optimization of CPB mixes, adding a new layer of efficiency to the overall mine backfilling process.

7.6. References

Aldhafeeri, A., Fall, M. (2017). Sulphate induced changes in the reactivity of cemented tailings backfill. International Journal of Mineral Processing 166 (10):13-23.

Akcil, A., and Koldas, S. 2006. Acid Mine Drainage (AMD): causes, treatment and case studies. Journal of Cleaner Production, **14**(12): 1139–1145. doi:10.1016/j.jclepro.2004.09.006.

Al-Moselly, Z., Fall, M., and Haruna, S. 2022. Further insight into the strength development of cemented paste backfill materials containing polycarboxylate ether-based superplasticizer. Journal of Building Engineering, **47**: 103859. Elsevier.

Belem, T., Aatar, O. El., Bussière, B., Benzaazoua, M., Fall, M., Yilmaz, E. (2006). Characterisation of self-weight consolidated paste backfill. 7th Seminar on paste and thickened tailings, April 2006, Irlande, 13p.

Benkirane, O., Haruna, S., and Fall, M. 2023. Mechanical and microstructural characteristics of cemented paste tailings modified with nano-calcium carbonate and cured under various thermal conditions. International Journal of Mining, Reclamation and Environment, **37**(4): 277–296. Taylor & Francis. doi:10.1080/17480930.2023.2172661.

Bentz, D.P. 2008. A review of early-age properties of cement-based materials. Cement and Concrete Research, **38**(2): 196–204. doi:10.1016/j.cemconres.2007.09.005.

Benvenuti, M., Mascaro, I., Corsini, F., Lattanzi, P., Parrini, P., and Tanelli, G. 1997. Mine waste dumps and heavy metal pollution in abandoned mining district of Boccheggiano (Southern Tuscany, Italy). Environmental Geology, **30**(3): 238–243. doi:10.1007/s002540050152.

Camiletti, J., Soliman, A.M., and Nehdi, M.L. 2013. Effect of nano-calcium carbonate on early-age properties of ultra-high-performance concrete. Magazine of Concrete Research, **65**(5): 297–307. Thomas Telford Ltd.

Cao, M., Ming, X., He, K., Li, L., and Shen, S. 2019. Effect of macro-, micro-and nano-calcium carbonate on properties of cementitious composites—A review. Materials, **12**(5): 781. MDPI.

Chen, S., Wu, A., Wang, Y., and Wang, W. 2021. Coupled effects of curing stress and curing temperature on mechanical and physical properties of cemented paste backfill. Construction and Building Materials, **273**: 121746. Elsevier. doi:10.1016/J.CONBUILDMAT.2020.121746.

Cosentino, I., Liendo, F., Arduino, M., Restuccia, L., Bensaid, S., Deorsola, F., and Ferro, G.A. 2020. Nano CaCO3 particles in cement mortars towards developing a circular economy

in the cement industry. Procedia Structural Integrity, **26**: 155–165. doi:10.1016/j.prostr.2020.06.019.

Cui, L, Fall M., 2018. Multiphysics modeling and simulation of strength development and distribution in cemented tailings backfill structures. International Journal of Concrete Structures and Materials, **12** (1): 1-22.

Cui, L, Fall M. 2017. Modeling of pressure on retaining structures for fill mass. Tunnelling and Underground Space Technology **69**:94-107.

Cui, L., Fall, M. 2016. Multiphysics model for consolidation behaviour of cemented paste backfill. ACSE International Journal of Geomechanics **17**(3): 23p; 04016077-23.

Doherty, J. P., Hasan, A., and Suazo, G. H., 2015 Fourie Investigation of some controllable factors that impact the stress state in cemented paste backfill. Canadian Geotechnical Journal 52:1901-1912.

Ercikdi, B., Cihangir, F., Kesimal, A., Deveci, H. and Alp, I. 2009a. Utilization of industrial waste products as pozzolanic material in cemented paste backfill of high sulphide mill tailings', J Hazard Mater, 168(2-3), 848-56.

Ercikdi, B., Kesimal, A., Cihangir, F., Deveci, H. and Alp, İ. 2009b. Cemented paste backfill of sulphide-rich tailings: Importance of binder type and dosage', Cement and Concrete Composites, 31(4), 268-274.

Fall, M., Célestin, J.C., Pokharel, M., and Touré, M. 2010. A contribution to understanding the effects of curing temperature on the mechanical properties of mine cemented tailings backfill. Engineering Geology, **114**(3): 397–413. doi:10.1016/j.enggeo.2010.05.016.

Fang, K., and Fall, M. 2019. Chemically induced changes in shear behaviour of interface between rock and tailings backfill undergoing cementation. Rock Mechanics and Rock Engineering 2 (9), 3047-3062.

Fu, Q., Zhang, Z., Zhao, X., Xu, W., and Niu, D. 2022. Effect of nano calcium carbonate on hydration characteristics and microstructure of cement-based materials: A review. Journal of Building Engineering, **50**: 104220. doi:10.1016/j.jobe.2022.104220.

Ghirian, A. 2016. Coupled thermo-hydro-mechanical-chemical (THMC) processes in cemented tailings backfill structures and implications for their engineering design.

Ghirian, A., and Fall, M. 2013. Coupled thermo-hydro-mechanical–chemical behaviour of cemented paste backfill in column experiments. Part I: Physical, hydraulic and thermal processes and characteristics. Engineering Geology, **164**: 195–207. doi:10.1016/j.enggeo.2013.01.015.

Ghirian, A., and Fall, M. 2016. Strength evolution and deformation behaviour of cemented paste backfill at early ages: Effect of curing stress, filling strategy and drainage. International

Journal of Mining Science and Technology, **26**(5): 809–817. Elsevier. doi:10.1016/J.IJMST.2016.05.039.

Ghirian, A., and Fall, M. 2017. Properties of cemented paste backfill. Paste Tailings Management,: 59–109. Springer International Publishing. doi:10.1007/978-3-319-39682-8_4/FIGURES/50.

Grice, T. 1998. Proceedings of 2nd Annual Summit – Mine Tailings Disposal Systems. Australasian Institute of Mining and Metallurgy, Melbourne.

Haiqiang, J., Fall, M., and Cui, L. 2016. Yield stress of cemented paste backfill in sub-zero environments: Experimental results. Minerals Engineering, **92**: 141–150. doi:10.1016/j.mineng.2016.03.014.

Hassani, F. P., Ouellet, J., and Hossein, M. (2001). Strength development in underground high sulphate paste backfill operation. CIM bulletin, 57-62.

Haruna, S., and Fall, M. 2020. Strength development of cemented tailings materials containing polycarboxylate ether-based superplasticizer: experimental results on the effect of time and temperature. https://doi.org/10.1139/cjce-2019-0809, **48**(4): 429–442. NRC Research Press 1840 Woodward Drive, Suite 1, Ottawa, ON K2C 0P7. doi:10.1139/CJCE-2019-0809.

Huynh, L., Beattie, D. A., Fornasiero, D., Ralston, J. 2006. Effect of polyphosphate and naphthalene sulfonate formaldehyde condensate on the rheological properties of dewatered tailings and cemented paste backfill. Minerals engineering, 19(1), 28-36.

Jiang, H. Fall, M., Li, Y., Han J. (2019). An experimental study on compressive behaviour of cemented rockfill. Construction and Building Materials 213:10-19.

Kjellsen, K.O., and Detwiler, R.J. 1992. Reaction kinetics of portland cement mortars hydrated at different temperatures. Cement and Concrete Research, **22**(1): 112–120. doi:10.1016/0008-8846(92)90141-H.

Koohestani, B., Belem, T., Koubaa, A., and Bussière, B. 2016. Experimental investigation into the compressive strength development of cemented paste backfill containing Nano-silica. Cement and Concrete Composites, **72**: 180–189. Elsevier. doi:10.1016/J.CEMCONCOMP.2016.06.016.

Li, W., and Fall, M. 2016. Sulphate effect on the early age strength and self-desiccation of cemented paste backfill. Construction and Building Materials, **106**: 296–304. Elsevier. doi:10.1016/J.CONBUILDMAT.2015.12.124.

Liu, X., Fang, T., and Zuo, J. 2019. Effect of Nano-Materials on Autogenous Shrinkage Properties of Cement Based Materials. Symmetry, **11**(9): 1144. Multidisciplinary Digital Publishing Institute. doi:10.3390/sym11091144.

Nasir, O., and Fall, M. 2009. Modeling the heat development in hydrating CPB structures. Computers and Geotechnics, **36**(7): 1207–1218. doi:10.1016/j.compgeo.2009.05.008.

Oey, T., Kumar, A., Bullard, J.W., Neithalath, N., and Sant, G. 2013. The Filler Effect: The Influence of Filler Content and Surface Area on Cementitious Reaction Rates. Journal of the American Ceramic Society, **96**(6): 1978–1990. John Wiley & Sons, Ltd. doi:10.1111/JACE.12264.

Orejarena, L., Fall, M., 2008. Mechanical response of a mine composite material to extreme heat load. Bulletin of Engineering Geology and Environment **67**(3):387-396.

Ren, Z., Liu, Y., Yuan, L., Luan, C., Wang, J., Cheng, X., and Zhou, Z. 2021. Optimizing the content of nano-SiO2, nano-TiO2 and nano-CaCO3 in Portland cement paste by response surface methodology. Journal of Building Engineering, **35**: 102073. doi:10.1016/j.jobe.2020.102073.

Roshani, A., and Fall, M. 2020. Rheological properties of cemented paste backfill with nano-silica: Link to curing temperature. Cement and Concrete Composites, **114**. Elsevier Ltd. doi:10.1016/J.CEMCONCOMP.2020.103785.

Saremi, A., and Fall, M. 2023. Strength and suction development of nano-cemented paste tailings materials. Cleaner Materials, **8**: 100190. doi:10.1016/j.clema.2023.100190.

Sanchez, F., Sobolev, K., 2010. Nanotechnology in concrete – a review. Constr. Build. Mater., 24 (2010), pp. 2060-2071

Sato T., Beaudoin J.J. (2011). Effect of nano-CaCO3 on hydration of cement containing supplementary cementitious materials. Adv. Cement Res., 23 (1) (2011), pp. 33-43

Seifan M., Mendoza S., Berenjian, A., 2020. Mechanical properties and durability performance of fly ash based mortar containing nano and micro-silica additives. Construct Build Mater, 252 (2020), Article 119121

Shaikh, F.U.A., and Supit, S.W.M. 2014. Mechanical and durability properties of high volume fly ash (HVFA) concrete containing calcium carbonate (CaCO3) nanoparticles. Construction and Building Materials, **70**: 309–321. doi:10.1016/j.conbuildmat.2014.07.099.

Sheshpari, M. 2015. A review of underground mine backfilling methods with emphasis on cemented paste backfill. Electronic Journal of Geotechnical Engineering, **20**(13): 5183–5208.

Sinthaworn, S., and Nimityongskul, P. 2011. Effects of temperature and alkaline solution on electrical conductivity measurements of pozzolanic activity. Cement and Concrete Composites, **33**(5): 622–627. doi:10.1016/j.cemconcomp.2011.02.012.

Tariq, A., and Yanful, E. K. 2013. A review of binders used in cemented paste tailings for underground and surface disposal practices. Journal of environmental management, 131, 138-149.

Tian, X., and Fall, M. 2021. Non-isothermal evolution of mechanical properties, pore structure and self-desiccation of cemented paste backfill. Construction and Building Materials, **297**: 123657. doi:10.1016/j.conbuildmat.2021.123657.

Thompson, B.D., Grabinsky, M.W., and Bawden, W.F, 2012. In situ measurements of cemented paste backfill at the Cayeli Mine. Canadian Geotechnical Journal **1**(1):755-772.

Wang, Y., Na, Q., Yang, J., Zhang, L., Zhang J., J. Li, and Jin, F, 2023. Monitoring of barricade pressure during the entire backfilling process for a high iron mine stope. Case Studies in Construction Materials **19**: e02456.

Wang C., Liu J.C., Zhang C., Zhang C., Li Z.Y., Yin D.D.(2016). Influence and mechanism of nano-CaCO3 on properties and structures of cement-based materials. J. Hunnan Univ.: Nat. Sci. ED., 43 (6) (2016), pp. 22-28

Wang, X., Li, J., Xiao, Z., Xiao, W. 2004. Rheological properties of tailing paste slurry. J. Central South Univ. Technol. 11, 75-79.

Wu, D., Sun, G., & Liu, Y. 2016. Modeling the thermo-hydro-chemical behavior of cemented coal gangue-fly ash backfill. Construction and Building Materials, 111, 522-528.

Wu, D., Hou, W., Liu, S., and Liu, H. 2020. Mechanical Response of Barricade to Coupled THMC Behavior of Cemented Paste Backfill. International Journal of Concrete Structures and Materials, **14**(1): 39. doi:10.1186/s40069-020-00413-0.

Wu, D., Fall, M., and Cai, S-J, 2014. Numerical modelling of thermally and hydraulically coupled processes in hydrating tailings backfill columns. International Journal of Mining, Reclamation and Environment **28**(3):173-199.

Yang, L., Yilmaz, E., Li, J., Liu, H., and Jiang, H. (2018). Effect of superplasticizer type and dosage on fluidity and strength behavior of cemented tailings backfill with different solid contents. Construction and Building Materials, 187, 290-298.

Yilmaz, E., and Fall, M. 2017. Paste tailings management. *In* Paste Tailings Management.

Yilmaz, E. 2017. Stope depth effect on field behaviour and performance of cemented paste backfills. International Journal of Mining, Reclamation and Environment, 1-24.

Yilmaz, E. (2011). Advances in reducing large volumes of environmentally harmful mine waste rocks and tailings. Gospodarka Surowcami Mineralnymi, 27(2), 89–112.

Yilmaz, E., Kesimal, A., Deveci, H., Ercikdi, B. 2003. The factors affecting the performance of paste backfill: physical, chemical and mineralogical characterization. In First Engineering Sciences Congress for Young Researcher (MBGAK'03), Istanbul.

Zhou, Q, Beaudoin, JJ (2003) Effect of applied hydrostatic stress on the hydration of Portland cement and C3S. Adv Cem Res 15(1):9–16

CHAPTER 8. Synthesis and Integration of Results

8.1. Introduction

In this culminating chapter, the synthesis of findings from the comprehensive analysis conducted throughout this doctoral research elucidates the impact of nanoparticle (NPs) on the geotechnical behavior of CPB. In the first paper of this dissertation which serves as a cornerstone, the effects of four distinct nanoparticle types—namely nano-silica (SiO_2), nano-calcium carbonate ($CaCO_3$), nano-iron oxide (Fe_2O_3), and nano-aluminum oxide (Al_2O_3)on the engineering properties of small-scale CPB specimens cured under controlled laboratory conditions were assessed. The initial investigation reveals that amongst the studied NPs, nano-calcium carbonate significantly increases the mechanical integrity through improve in compressive strength and self-desiccation process.

Building upon this foundational research, subsequent studies, articulated in the second and third papers, delve into the dynamics of nano-enhanced CPB under field-simulated conditions.The influence of overburden pressure and non-isothermal curing temperaturesfactors that more closely mimic in-situ field conditions are examined to elaborate their impact on the geotechnical performance of upscaled CPB columns.

Lastly, the fourth paper provides insight into the complex interactions and impact of thermo-mechano-chemical (TMC) processes on evolution of self-desiccation within the CPB plug columns. This crucial interrelation is essential in determining the evolution of pore pressure within the nano-enhanced CPB matrix, offering critical insights into the long-term structural comportment of CPB as a sustainable solution in mine waste management. Table 8-1 demonstrate a summary of the experimental programs conducted for each of the technical papers developed during this PhD study.

Table 8-1. Summary of studied factors and experimental program conducted in this PhD research

Technical Paper	Chapter	Np Types	Np Content	Field Overburden Pressure	Curing Temperature	Coupled TMC Processes	UCS Test	Microstructural Tests	Monitoring Experiments
1	3	☒	☒				☒	MIP, XRD, TG/DTG	EC, VWC, Suction,
2	4		☒	☒			☒	MIP, TG/DTG, Void/Porosity, Dry Density	EC, VWC, PWP, TEP,
3	5		☒	☒	☒	☒	☒	MIP, TG/DTG, Void/Porosity, Dry Density	EC, VWC, PWP, TEP,
4	6		☒	☒	☒	☒		MIP, TG/DTG, Void ratio,	VWC, PWP, EC,

NP: Nanoparticles; UCS: Unconfined Compression Test; TMC: Thermal, Mechanical, and Chemical; MIP: Mercury Intrusion Porosimetry; TG/DTG: Thermogravimetry, and derivative thermogravimetry; XRD: X-ray diffraction; EC: Electrical conductivity; VWC: Volumetric Water Content; PWP: Pore Water Pressure; TEP: Total Earth Pressure; ☒ : Conducted

8.2. Effect of Nanoparticles' Type on mechanical performance of Cemented Paste Backfill

In the fourth chapter of this dissertation, which examines the outcomes of the first paper, the influence of four distinct nanoparticle (NPs) types on the compressive strength and self-desiccation processes of small-scale CPB samples over different curing periods is analyzed. The

research involved preparing samples with a consistent dosage of different NPs: nano-silica (SiO_2), nano-calcium carbonate ($CaCO_3$), nano-iron oxide (Fe_2O_3), and nano-aluminum oxide (Al_2O_3). Results indicate that the type of NP and its dispersion method critically determine its effectiveness as a supplementary additive, with the potential to significantly improve the geotechnical properties of CPB, particularly in enhancing compressive strength and promoting self-desiccation in the backfill matrix, as demonstrated in Figure 8-1.

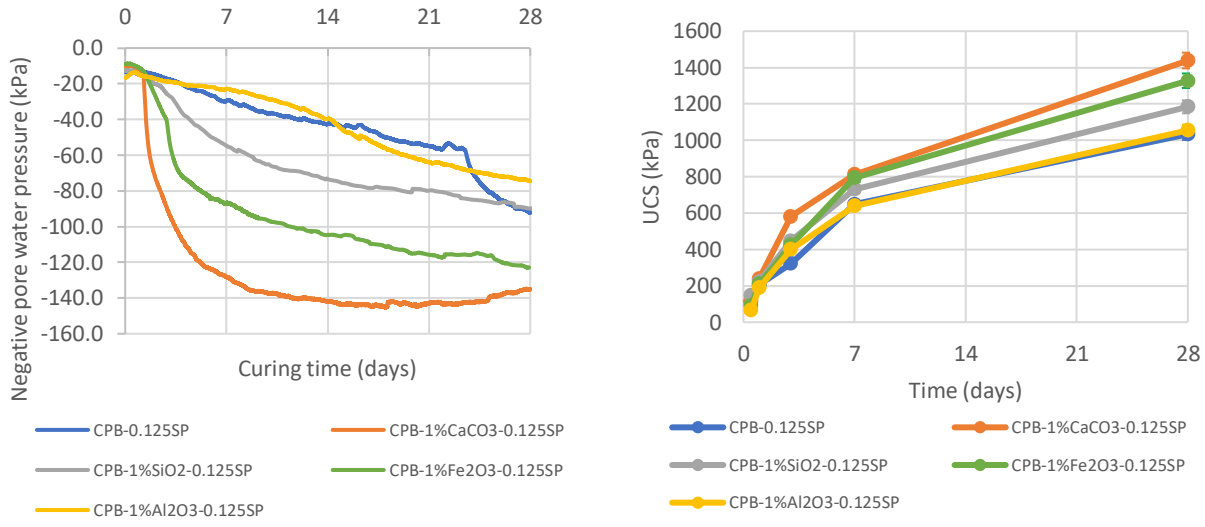

(a) (b)

Figure 8-1. Effect of NPs on (a) strength; and (b) suction development of CPB

The observed enhancements in CPB properties with the addition of nanoparticles are attributed to several mechanisms within the fresh CPB matrix. Firstly, when properly dispersed, NPs can serve as a filler due to their high specific surface area (SSA) (Camiletti et al. 2013, Koohestani et al. 2016, Cao et al. 2019). This characteristic enables them to occupy micro pores within the CPB microstructure, leading to a denser matrix with a significantly reduced pore volume and void ratio compared to control samples without NPs.

Secondly, NPs have been found to actively participate in cement hydration, acting as nucleation sites for cement grains (Roshani and Fall 2020a, Fu et al. 2022, Benkirane et al. 2023b). This accelerates the hydration kinetics and increases the formation of critical hydration by-products such as calcium silicate hydrate, calcium hydroxide, and ettringite. These by-products are crucial in creating bonds between the particles within the paste matrix, thereby improving compressive

strength (Ghirian and Fall 2013, Al-Moselly et al. 2022, Alainachi et al. 2022). Additionally, by accelerating hydration and promoting more precipitation of hydration products within the capillary pores, NPs play a pivotal role in the development of the self-desiccation, leading to the consumption of water within the matrix and contributing to the overall durability of the CPB (Benkirane et al. 2023a). To corroborate this observation, the results from volumetric water content (VWC) monitoring of CPB columns cured under field-adapted conditions (as depicted in Figure 8-2) distinctly show that the nano-enhanced CPB column experienced a quicker reduction in VWC over time relative to the NP-free CPB column, even when both were subjected to similar curing conditions. This accelerated VWC consumption in the nano-enhanced columns underscores the efficacy of nanoparticles in improving the hydration process and subsequent water usage within the CPB matrix.

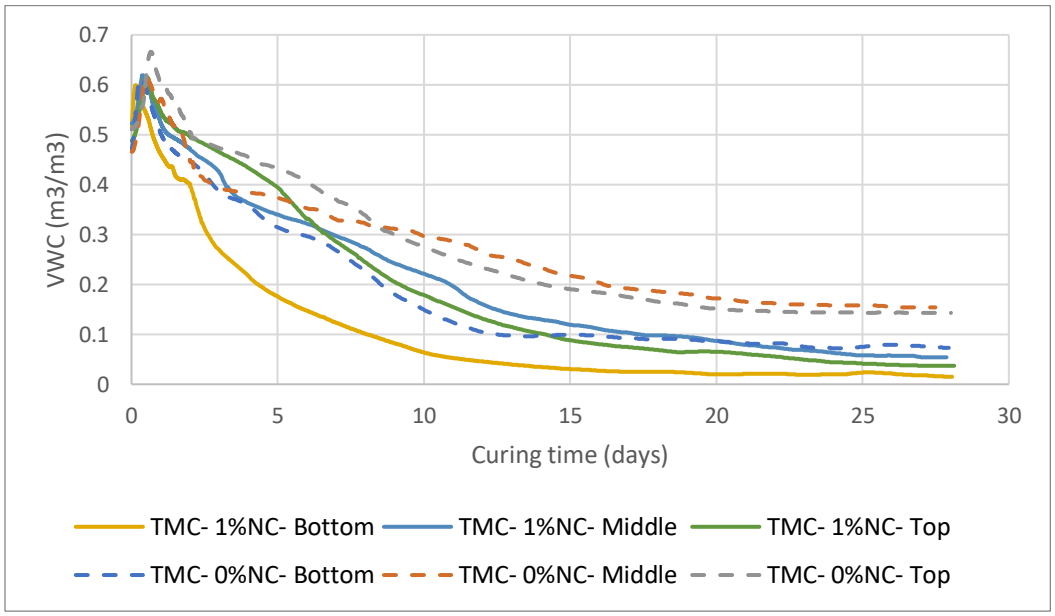

Figure 8-2. Evolution of VWC within different levels of CPB columns (with and without nano-calcium carbonate (NC)) cured under field-adapted conditions

8.3. Role of Multiphysics processes on mechanical performance of Nano-CPB plug

The Multiphysics processes are important in determining the behavior of paste backfill structures, including Thermal (T), Mechanical (M), and Chemical (C) interactions. It is vital to acknowledge the influence of these factors on the mechanical performance of CPB plugs, as

evidenced by the findings of this Ph.D. study. These processes interact synergistically to affect the strength development, stability, and durability of CPB structures, ultimately influencing their suitability and reliability in mining operations.

8.3.1 Thermal process

As elaborated in previous chapters, the thermal influences on CPB performance can be categorized into internal and external sources (Nasir and Fall 2009, Fang and Fall 2018). Internally, the exothermic reactions, particularly the heat emanating from binder hydration, constitute the primary sources of thermal variation (Chen et al. 2021). Externally, the thermal gradient established between the surrounding environment and the backfill structure facilitates heat transfer and creates external thermal variations (Fang and Fall 2018, Roshani and Fall 2020b). A key objective of this study, as outlined in the first chapter, is to examine the effects of thermal loading on the mechanical properties of CPB samples enhanced with NPs. To achieve this, a thermal loading regime, replicating temperature gradients observed in actual mining environments, was applied to the CPB columns under investigation.

The experimental results substantiate that thermal loading on the CPB column positively influences mechanical and hydraulic characteristics, including the rate of compressive strength development, the dissipation of pore water pressure, and subsequently total earth pressure. Figure 8-3 illustrates that CPB samples cured under conditions that mimic field-adapted thermal temperatures demonstrate more rapid compressive strength gain and swifter total earth pressure dissipation resulted by faster dissipation of pore water pressure and development of arching effect when compared to samples cured at a constant ambient room temperature.

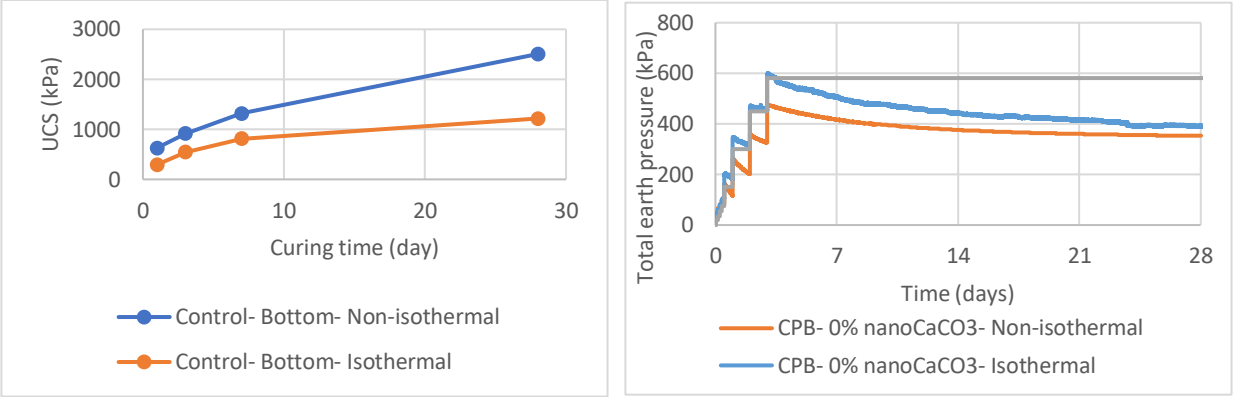

(a) (b)

Figure 8-3. Effect of thermal loading on evolution of a) compressive strength, b) total earth pressure

These improvements are largely attributable to the effect of curing temperature on binder hydration processes, which can either speed up or decelerate this progression (Fall et al. 2010, Chen et al. 2021, Cao et al. 2022). Microstructural analyses have verified that CPB samples subjected to elevated curing temperatures predominantly exhibit a higher quantity and quality of hydration products such as calcium silicate hydrate (C-S-H), gypsum, and ettringite. This supports the observed superior compressive strength and more efficient dissipation of total earth pressure in CPB samples cured under non-isothermal conditions resulted by faster dissipation of pore water pressure.

The impact of NPs has been conclusively demonstrated: CPB columns containing NPs and subjected to non-isothermal curing temperatures showed enhanced performance relative to NP-free CPB samples cured under the same conditions. This superior performance is credited to the mechanisms induced by the NPs, which include microstructural refinement through pore filling and accelerated cement hydration by providing additional nucleation sites, thus contributing to the overall improved geotechnical properties of the nano-enhanced CPB (Roshani and Fall 2020b, Benkirane et al. 2023a).

8.3.2 Mechanical process

Another pivotal factor affecting the behavior of backfill structures is the mechanical parameters, which include the self-weight of the paste backfill, the mechanical interactions at the CPB/rock mass interface, and the stress applied by the movement of equipment. To address

another primary goal of this study, the physical framework established allowed for the curing of CPB columns under a loading pattern that simmulate backfill discharge plan, including the pressure exerted on the backfill corresponding to an equivalent height of 34.8 meters (600 Kpa of pressure). This simulation is crucial in understanding the stress response of CPB in conditions that closely mirror those found in actual mining operations.

The compressive strength tests performed on samples extracted from various levels of the studied CPB column indicate that samples from the lower sections exhibited an elevated unconfined compressive strength (UCS). This can be attributed to the fact that the bottom of the column experince the greatest curing stress, a sum of the pressure applied from above and the intrinsic self-weight of the CPB (Nujaim et al. 2020). This heightened stress level contributed to a more compact microstructure, as evidenced by physical property measurements indicating lower void ratio and reduced porosity. Moreover, corroborating previous studies, this increased curing stress favorably influences the production of more hydration by-products (Ghirian and Fall 2016, Cui and Fall 2016), which are crucial in enhancing the interparticle bonds within the CPB matrix, thereby improving its overall mechanical strength.

Additionally, it has been observed that samples from the lower levels of the column achieve strength more rapidly than those from higher levels during the initial stages of curing (Figure 8-4). This phenomenon is due to the fluid state of fresh CPB, which results in the highest stress concentration at the bottom of the column (Nujaim 2020). However, as curing progresses, the rate of strength gain in samples from the top of the column begins to surpass those at the bottom, further from the point of applied pressure. This shift in strength development is attributed to the transition of the CPB from a fluid to a solid state, as the binder hydration process advances over time.

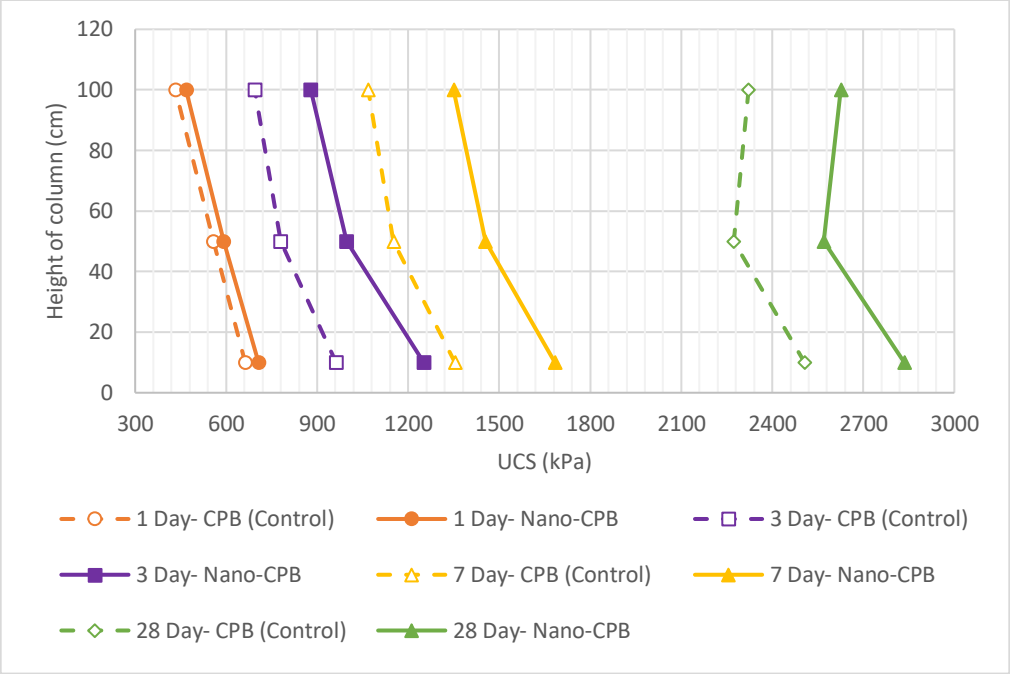

Figure 8-4. Evolution of compressive strength within different sections of Nano-CPB and control columns subjected to field overburden pressure over curing time

8.4. References

Alainachi, I., Fall, M., and Majeed, M. 2022. Behaviour of Backfill Undergoing Cementation Under Cyclic Loading. Geotechnical and Geological Engineering, **40**(9): 4735–4759. doi:10.1007/s10706-022-02181-y.

Al-Moselly, Z., Fall, M., and Haruna, S. 2022. Further insight into the strength development of cemented paste backfill materials containing polycarboxylate ether-based superplasticizer. Journal of Building Engineering, **47**: 103859. Elsevier.

Benkirane, O., Haruna, S., and Fall, M. 2023a. Strength and microstructure of cemented paste backfill modified with nano-silica particles and cured under non-isothermal conditions. Powder Technology, **419**: 118311. doi:10.1016/j.powtec.2023.118311.

Benkirane, O., Haruna, S., and Fall, M. 2023b. Mechanical and microstructural characteristics of cemented paste tailings modified with nano-calcium carbonate and cured under various thermal conditions. International Journal of Mining, Reclamation and Environment, **37**(4): 277–296. Taylor & Francis. doi:10.1080/17480930.2023.2172661.

Camiletti, J., Soliman, A.M., and Nehdi, M.L. 2013. Effect of nano-calcium carbonate on early-age properties of ultra-high-performance concrete. Magazine of Concrete Research, **65**(5): 297–307. Thomas Telford Ltd.

Cao, M., Ming, X., He, K., Li, L., and Shen, S. 2019. Effect of macro-, micro-and nano-calcium carbonate on properties of cementitious composites—A review. Materials, **12**(5): 781. MDPI.

Cao, M., Yuan, X., Ming, X., and Xie, C. 2022. Effect of High Temperature on Compressive Strength and Microstructure of Cement Paste Modified by Micro- and Nano-calcium Carbonate Particles. Fire Technology, **58**(3): 1469–1491. doi:10.1007/s10694-021-01211-0.

Chen, S., Wu, A., Wang, Y., and Wang, W. 2021. Coupled effects of curing stress and curing temperature on mechanical and physical properties of cemented paste backfill. Construction and Building Materials, **273**: 121746. Elsevier. doi:10.1016/J.CONBUILDMAT.2020.121746.

Cui, L., and Fall, M. 2016. Mechanical and thermal properties of cemented tailings materials at early ages: Influence of initial temperature, curing stress and drainage conditions. Construction and Building Materials, **125**: 553–563. doi:10.1016/j.conbuildmat.2016.08.080.

Fall, M., Célestin, J.C., Pokharel, M., and Touré, M. 2010. A contribution to understanding the effects of curing temperature on the mechanical properties of mine cemented tailings backfill. Engineering Geology, **114**(3): 397–413. doi:10.1016/j.enggeo.2010.05.016.

Fang, K., and Fall, M. 2018. Effects of curing temperature on shear behaviour of cemented paste backfill-rock interface. International Journal of Rock Mechanics and Mining Sciences, **112**: 184–192. Pergamon. doi:10.1016/J.IJRMMS.2018.10.024.

Fu, Q., Zhang, Z., Zhao, X., Xu, W., and Niu, D. 2022. Effect of nano calcium carbonate on hydration characteristics and microstructure of cement-based materials: A review. Journal of Building Engineering, **50**: 104220. doi:10.1016/j.jobe.2022.104220.

Ghirian, A., and Fall, M. 2013. Coupled thermo-hydro-mechanical-chemical behaviour of cemented paste backfill in column experiments. Part I: Physical, hydraulic and thermal

processes and characteristics. Engineering Geology, **164**: 195–207. doi:10.1016/J.ENGGEO.2013.01.015.

Ghirian, A., and Fall, M. 2016. Strength evolution and deformation behaviour of cemented paste backfill at early ages: Effect of curing stress, filling strategy and drainage. International Journal of Mining Science and Technology, **26**(5): 809–817. doi:10.1016/j.ijmst.2016.05.039.

Koohestani, B., Belem, T., Koubaa, A., and Bussière, B. 2016. Experimental investigation into the compressive strength development of cemented paste backfill containing Nano-silica. Cement and Concrete Composites, **72**: 180–189. Elsevier. doi:10.1016/J.CEMCONCOMP.2016.06.016.

Nasir, O., and Fall, M. 2009. Modeling the heat development in hydrating CPB structures. Computers and Geotechnics, **36**(7): 1207–1218. Elsevier. doi:10.1016/J.COMPGEO.2009.05.008.

Nujaim, M. 2020. Geomechanical behaviour of waste rock barricades and cemented paste backfills : experiments and modelling. phdthesis, Université de Lorraine ; Université du Québec à Abitibi-Témiscamingue.

Nujaim, M., Belem, T., and Giraud, A. 2020. Experimental Tests on a Small-Scale Model of a Mine Stope to Study the Behavior of Waste Rock Barricades during Backfilling. Minerals, **10**(11): 941. Multidisciplinary Digital Publishing Institute. doi:10.3390/min10110941.

Roshani, A., and Fall, M. 2020a. Flow ability of cemented pastefill material that contains nano-silica particles. Powder Technology, **373**: 289–300. doi:10.1016/j.powtec.2020.06.050.

Roshani, A., and Fall, M. 2020b. Rheological properties of cemented paste backfill with nano-silica: Link to curing temperature. Cement and Concrete Composites, **114**: 103785. doi:10.1016/j.cemconcomp.2020.103785.

CHAPTER 9. Conclusions and Recommendations

9.1. General conclusions

The experimental study presented herein has culminated in a series of significant findings with respect to the geotechnical performance of Cemented Paste Backfill (CPB) and CPB plug augmented with nanoparticles (NPs). These findings are enumerated as follows:

- The incorporation of NPs into CPB mixes has been demonstrably effective in enhancing various geotechnical attributes. Notably, this enhancement includes an accelerated rate of strength gain and notable microstructural improvements. The underlying mechanism for these improvements is predominantly attributed to the substantial specific surface area (SSA) of the NPs. This characteristic not only facilitates the NPs' role as a filler material but also markedly accelerates the hydration process of cement.
- Among the NPs examined, nano-calcium carbonate emerged as the most effective in terms of promoting strength development, microstructural refinement, and fostering self-desiccation processes in CPB.
- The study underscores the pivotal role of NPs dispersion in unlocking their potential benefits for CPB's geotechnical performance. Effective dispersion techniques should be integral when utilizing nanomaterials as supplementary cementitious materials (SCMs). In the absence of proper dispersion, the addition of nanoparticles can inadvertently diminish CPB's compressive strength, thus acting as a counterproductive factor.
- The influence of field overburden pressure on CPB has been a topic of particular interest. It has been established that applied stress can significantly modify CPB plug's behavior, notably enhancing its strength development and self-desiccation . This is attributed to the beneficial impact of applied pressure on microstructural densification and the acceleration of cement hydration reactions. Moreover, the synergistic effect of NPs combined with field-adapted pressure has shown superior performance in various parameters (such as Unconfined Compressive Strength (UCS), pore pressure dissipation, evolution of total/effective stress, and physical properties) compared to control CPB plug devoid of nanoparticles and subjected to no stress.
- The study also sheds light on the critical role of non-isothermal curing temperatures on CPB plug. It has been observed that curing CPB plug under these conditions markedly enhances binder hydration, leading to an increase in the UCS of all CPB samples when compared to those cured at ambient conditions.

These findings not only contribute to the existing body of knowledge in geotechnical engineering but also offer practical implications for the improvement of CPB in mining waste management applications.

9.2. Recommendations

Based on the outcomes of this research, the following recommendations are proposed to guide future scholarly inquiry and experimental endeavors:

- Given the singular focus on one type of binder in this study, future investigations could broaden the scope to assess the impact of nanoparticles (NPs) on diverse binder systems to generalize the findings and optimize CPB formulations.
- It would be beneficial for subsequent research to explore the synergistic effects of utilizing multiple types of NPs concurrently, to discern their collective influence on the geotechnical properties of CPB.
- To acquire a comprehensive understanding of the durability and mechanical integrity of CPB, the long-term mechanical behavior of large-scale nano-enhanced CPB columns should be monitored and analyzed beyond the standard 28-day curing period.
- It is crucial to evaluate the environmental ramifications of nano-modified CPB, with particular emphasis on its ecological footprint, and leaching behavior.
- While this study concentrated on the effects of elevated curing temperatures, there is a niche for research into the behavior of CPB with NPs when subjected to sub-zero temperatures, which could have significant practical implications in colder climates.
- The robustness of nano-CPB against aggressive chemical environments, such as those involving sulfate attacks, warrants further investigation to delineate the protective efficacy of NPs in such scenarios.
- Comprehensive studies aimed at delineating the cost-benefit and carbon footprint-benefit analysis of integrating NPs into CPB preparations are recommended. The cost-benefit analysis should include an evaluation of potential economic savings and implications for large-scale application in the mining industry, while the carbon footprint-benefit analysis should comprise an assessment of potential carbon footprint improvements and implications for mine cemented backfill operations.
- It would be beneficial for future studies to develop coupled THMC models for CPB plug with nanoparticles. These models will result in the development of simulation tools that enable to design and predict the geotechnical performance of nano-CPB plug in any field scenarios.

CHAPTER 10. Appendix A: Thermal loading monitoring

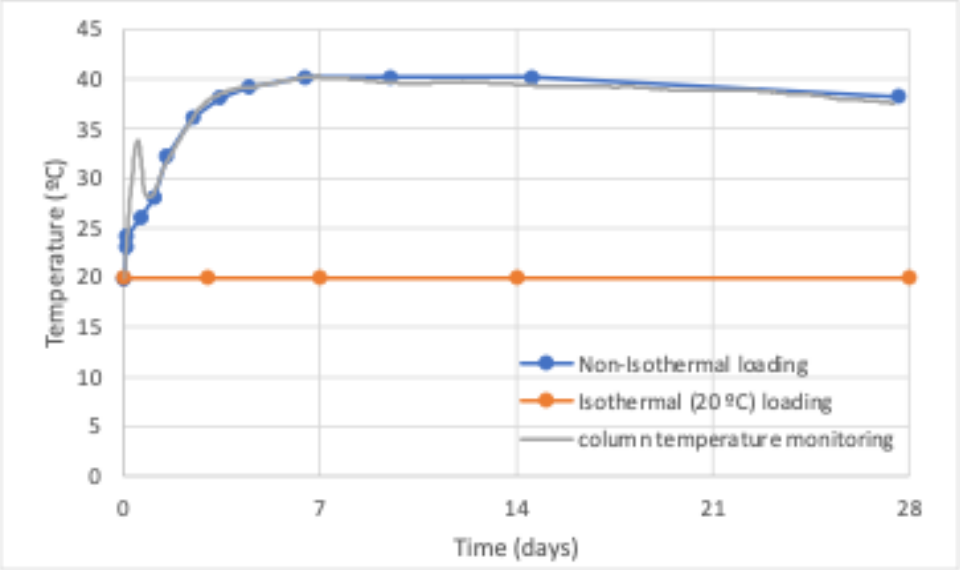

Figure 10-1: Column temperature monitoring versus the applied curing temperature (iso/non-iso thermal curing temperature)